CONCURRENT OPTIMIZATION USING PROBABILISTIC ANALYSIS OF DISTRIBUTED MULTIDISCIPLINARY ARCHITECTURES FOR DESIGN UNDER UNCERTAINTY

A Dissertation
Presented to
The Academic Faculty

by

Sayan Ghosh

In Partial Fulfillment
of the Requirements for the Degree
Doctor of Philosophy in the
School of Aerospace Engineering

Georgia Institute of Technology
December, 2016

CONCURRENT OPTIMIZATION USING PROBABILISTIC ANALYSIS OF DISTRIBUTED MULTIDISCIPLINARY ARCHITECTURES FOR DESIGN UNDER UNCERTAINTY

Approved by:

Professor Dimitri N. Mavris,
Committee Chair
School of Aerospace Engineering
Georgia Institute of Technology

Professor Graeme J. Kennedy
School of Aerospace Engineering
Georgia Institute of Technology

Professor Brani Vidakovic
School of Industrial and Systems
Engineering
Georgia Institute of Technology

Professor Lakshmi N. Sankar
School of Aerospace Engineering
Georgia Institute of Technology

Professor Daniel P. Schrage
School of Aerospace Engineering
Georgia Institute of Technology

Date Approved: 20 October 2016

To my grandparents, the late Mrs. Purnima Mullick, the late Mr. Provanshu Kumar Mullick, the late Mrs. Bela Rani Ghosh, and the late Dr. Phani Bhusan Ghosh.

ACKNOWLEDGMENTS

I would like to express my heartfelt gratitude to Professor Dimitri Mavris for taking me under his guidance for my PhD. Dr. Mavris has not only supported me academically towards the successful completion of my thesis but also has mentored me into becoming a professional researcher and engineer. I consider it a privilege to be a student under the guidance of someone as distinguished as Dr. Mavris.

I would like to thank Dr. Brani Vidakovic, Dr. Graeme J. Kennedy, Dr. Daniel P. Schrage, and Dr. Lakshmi N. Sankar, the distinguished members of my committee for their time and invaluable advice. I really appreciate the effort they have taken to review and provide me with their guidance.

I would also like to thank Dr. Jimmy Tai, Dr. Michelle Kirby, and Dr. Taewoo Nam for their guidance and encouragement at different phases of my graduate studies. I would like to extend my special thanks to Dr. Chung Lee for introducing me to the world of *uncertainty*. The valuable discussion with him during the early phase of my graduate program has guided and helped me to choose my research area for this thesis as well as my professional career.

I am deeply grateful to Dr. Sanjeev Sharma and Mr. Simon Coggon at Airbus, Filton, UK. They have introduce me to the current industrial challenges involving uncertainty and multidisciplinary design which has helped me in the formulation of the research objective for this thesis.

I would like to thank all my friends and colleagues at Aerospace Systems Design Laboratory. A special thanks to Mario Lee, Alek Gavrilovski, David Rancourt, Ryan Jacobs, Justin Kizer, Michael Steffens, and Miguel Walter for their help and constructive criticism of my proposal and thesis.

Last but not the least, I would like to extend my sincere gratitude to my family for their constant encouragement, support and unconditional love. I acknowledge the sacrifice that my parents, Mrs. Shreela Ghosh and Mr. Timir Ranjan Ghosh, have made and continue to make in their life for my personal and academic success. I would like to thank my wife Paulami, for her selfless support and motivation. Thank you for being part of this arduous journey and my life.

TABLE OF CONTENTS

LIST OF TABLES

LIST OF FIGURES

SUMMARY

Uncertainty-based Multidisciplinary Optimization (UMDO) relies on propagation of uncertainties across several disciplines. A typical aircraft design process involves collaboration of multiple and diverse teams involving high-fidelity disciplinary tools and experts. Therefore, traditional methods such as "All-In-One" (AIO), which integrates all the disciplines and treats the entire multidisciplinary analysis process as a black box becomes infeasible for uncertainty propagation and analysis. If all the disciplines cannot be tightly integrated, then it is helpful to use a method that conducts uncertainty propagation in each discipline independently and combines their results to evaluate the system level uncertainty.

Distributed UMDO methods based on Collaborative Optimization (CO), Concurrent Subs-Space Optimization (CSSO), Analytical Target Cascading (ATC), etc. use the strategy of decomposition and coordination to carry out distributed uncertainty analysis and optimization by preserving disciplinary autonomy. However, there are shortcomings in these methods which lead to inaccurate quantification of uncertainty at the system level. One such disadvantage is the inability to handle statistical dependencies among coupling variables. In most cases, the statistical dependencies manifest due to the underlying functional relationship between the variables. Most of the existing distributed UMDO methods in literature assume that the coupling variables are independent of each other. Although under certain conditions this assumption is valid, nonetheless it may lead to inaccurate estimation of uncertainty quantification at system level if the dependencies of coupling variables are significant and if the system level metric is sensitive to the dependencies. Another limitation

in the existing distributed UMDO literature is related to interdisciplinary compatibility. One of the common strategies to achieve interdisciplinary compatibility is by moment matching method. In most of the existing distributed UMDO methods only marginal distribution of coupling variables are considered in the moment matching, which works well when coupling variables are statistically independent. However, when coupling variables are dependent, this strategy does not guarantee that interdisciplinary compatibility is satisfied for every instantiation of uncertain variables. Also, most of these methods assume that the uncertain coupling variables have fixed functional form of probability density function, most commonly a Gaussian density function. This assumption breaks down when the local uncertainties in disciplines are non-Gaussian and disciplines are non-linear functions of input variables which may lead to non-Gaussian disciplinary responses.

To overcome these limitations, Probabilistic Analysis of Distributed Multidisciplinary Architectures (PADMA) has been developed. PADMA is a bi-level distributed uncertainty-based multidisciplinary analysis (UMDA) method which allows each discipline to carry out uncertainty propagation independently and concurrently. It is a non-iterative method in which dependence and interdisciplinary compatibility is handled by evaluating the probability of Event of Interdisciplinary Compatibility (EIC). Probability of EIC is evaluated using conditional probability density functions of disciplinary metrics. A quantile copula regression method has also been developed which is used to build probabilistic model of multivariate disciplinary metrics. In quantile copula regression, the conditional probability density functions are modeled by regressing multiple levels of quantiles of disciplinary metric, allowing a comprehensive representation of overall conditional distribution without any assumption of functional form of probability density function. Also, quantile copula regression models the dependencies between disciplinary metrics using copula functions when disciplines have multiple

outputs. Finally, a distributed UMDO method, Concurrent Optimization using Probabilistic Analysis of Distributed Multidisciplinary Architectures (CO-PADMA), has been developed using PADMA and quantile copula regression. CO-PADMA is a bi-level distributed UMDO method which allows distributed analysis and optimization, while handling the dependencies and interdisciplinary compatibility, to find optimum design and quantify the uncertainty of system metrics accurately. The advantages of the methods developed in this thesis have been demonstrated by their application to analytical and physics-based problems.

CHAPTER I

INTRODUCTION

An inherent property of a complex system design is uncertainty [1]. Uncertainty arises due to fidelity of analysis model, experimental data, interdisciplinary interfaces, operating conditions, immature technologies and so on. Uncertainty can be also be due to future requirements and other market factors like fuel cost, market demands, etc. Moreover, uncertainties evolve over time during any design process. For example, as the design progresses, more information and data becomes available from high fidelity models or experiments leading to reduction in uncertainties of model. Also, as the requirement changes with time, constraints can be relaxed or tightened to influence the uncertainties. Aircraft are one such complex system. It is important to consider uncertainty in the aircraft design process to avoid an expensive redesign process or performance penalty.

Aircraft design requires simultaneous design of its multiple systems like wing, fuselage, etc.; its subsystems like control surfaces, panels, etc; and its components like actuators, hydraulics, etc. This requires analysis from various disciplines like aerodynamics, structure, control, mission analysis, etc. The performance of the aircraft not only depends on each subsystem independently, but also on the complicated inter-dependencies among its subsystems and components. Typically, the effects of the inter-dependencies among these disciplines and subsystems are not evident and failure to incorporate these in the design process may lead to the necessity for redesign which can be expensive and time consuming. To address these issues, various multidisciplinary design analysis and optimization (MDO) methods have been developed to carry out the design process while handling the iteration among the disciplines.

Besides, the complexity of these interdisciplinary interactions increases when there are uncertainties in the design. In order to accurately quantify the uncertainty on the system level metric, it is important to capture the uncertainties associated with the interactions among disciplines, in addition to quantifying uncertainties in each discipline independently. This challenge can be addressed by setting up an integrated analysis of all the critical subsystems and disciplines which can be used to evaluate system level metrics like reliability, robustness, etc. and identifying the configuration which satisfies the stakeholder's requirement with optimal performance. This requires uncertainty quantification and management in a MDO setting, which is also referred here as Uncertainty-based Multidisciplinary Design Optimization (UMDO).

Traditional deterministic multidisciplinary analysis (MDA) methods [2], such as All-In-One (AIO), build an integrated workbench, linking all the disciplines involved in the design process. These methods treat integrated MDA environment as a black box to carry out analysis and design. Similarly, uncertainty analysis can be carried out for multidisciplinary systems using various techniques of uncertainty propagation and by treating the integrated MDA environment as a black box. However, in a complex and coupled system like aircraft, there is a huge computational burden to run a multidisciplinary analysis (MDA) for one design because it involves several iterations to converge to a design which satisfies interdisciplinary compatibility. Therefore, carrying out uncertainty analysis using these integrated methods are not always practical. Also, as the high-fidelity analysis gets involved in the design process, it may not be feasible to integrate the discipline into a single integrated workbench.

An aircraft design typically involves collaboration of multiple and diverse teams of engineers from different disciplines or subsystems [3]. As the complexity increases, it becomes increasingly difficult to design and manage distributed design [4, 5]. This has a direct consequence of cost overrun and delay for the aircraft manufacturer. For example, there has been a delay of two years in developing the Boeing 787,

with a cost overrun of $10 billion [5, 6] due to the difficulties in coordination among the suppliers. Similarly, Airbus delayed the delivery of A380 by two years with cost overrun of 2 billion euros [7, 8] due to lack of coordination among distributed disciplinary boundaries.

As will be discussed in this chapter, there are computational and organizational challenges to carry out the UMDO process in an industrial setting. In a typical aerospace industry, multiple teams and experts are involved in the design process using their own design and analysis tools, and they are often globally dispersed. Therefore, a distributed UMDO process is desirable to carry out concurrent and collaborative uncertainty-based design to support the system level design while complying with the disciplinary organization structure in the industry, and maintaining disciplinary autonomy.

With the distributed UMDO process as the focus of the current work, the challenges associated with distributed UMDO methods will be discussed and subsequently the research objective will be stated in the following sections.

1.1 Motivation

The aerospace industry has played a major role in civil transportation, space travels, nation's defense strategy, warfare, etc. since the invention of *Wright Flyer* by Wright Brothers in 1903. It plays an important role in making the world well connected and readily accessible for international trade and travel. In addition to generating GDP of $606 billion in 2014, the industry provides employment for 58 million people worldwide in aviation and related tourism, out of which 8.7 million people work directly in the aviation industry [9]. Based on historical trends, it is anticipated that world GDP will grow at the rate of 3.1% annually over next 20 years with a forecast of growth of 4.9% of passenger traffic and 4.7% of air cargo traffic [10]. With the increase in civil traffic, it is projected that commercial air traffic is expected to increase to about

47,500 aircraft by 2036, out of which more than 90% will be with new generation technology [11], as shown in Figure 1.

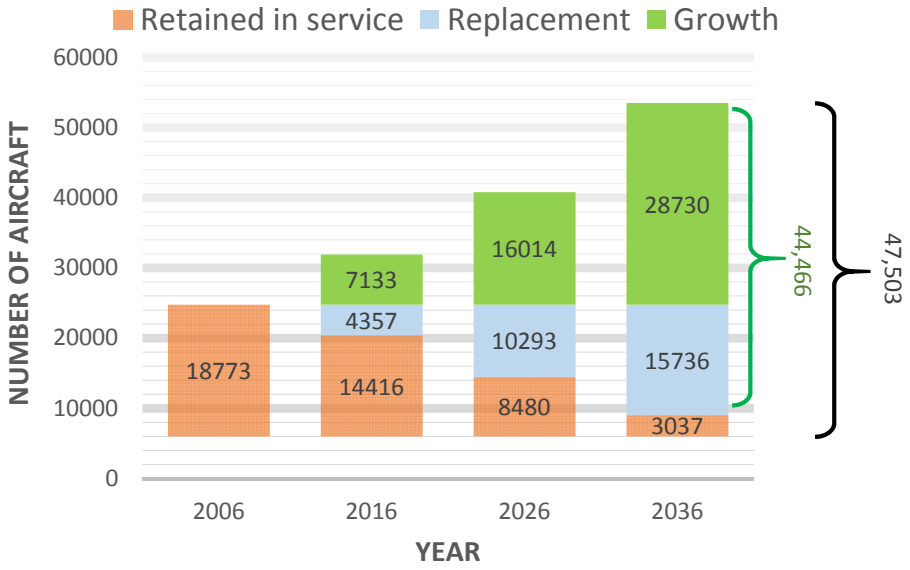

Figure 1: Expected number of commercial aircraft by 2036 [11]

As the number of civil aircraft is expected to double in the next 20 years, there is a need to replace aging aircraft with more efficient and environmentally responsible aircraft. Also, key factors like future fuel price, economic growth, environmental regulations, infrastructure limitation, emerging markets, changes in other modes of transportation, technology changes, etc are going to play a major role in designing new aircraft. For example, NASA Environmentally Responsible Aviation (ERA) program has set up targets for emission, noise and fuel burn as stated in Table 1. Similarly, the Advisory Council for Aeronautics Research in Europe (ACARE) has established its Vision 2020, that targets an overall reduction of CO_2 emissions by 50%.

To achieve market demand of efficient aircraft in future while maintaining the additional requirements like lower maintenance costs, environmental regulations, etc. there is a strong need to include advanced technology in the newer aircraft, redesign of the existing aircraft configuration (derivative aircrafts), and to explore unconventional design etc. For example, recent fleets of Boeing 787, Airbus 380, Bomabardier

Table 1: NASA ERA system-level goals [12]

Technology benefits[a]	N+1 (2015)	N+2 (2020)	N+3 (2025)
Noise (cum. below stage 4)	-32 dB	-42 dB	-52 dB
LTO NOx (below CAEP6)	-60%	-75%	-80%
Cruise NOx[b]	-55%	-70%	-80%
Aircraft fuel burn[b]	-33%	-50%	-60%

[a]N+1 and N+3 values are referenced to a Boeing 737-800 with CFM56-7B engines, and N+2 values are referenced to a Boeing 777-200 with GE90 engines

[b]Relative to 2005 best in class

C-Series, etc., feature as much as 70% content in advanced material like composites, leading to as much as 15% of weight savings [11]. Aerodynamic technologies like Natural Laminar Flow (NLF) [13], Active Flow Control (AFC) [14], etc. are possible approaches to improving aerodynamic performance of aircraft. Similarly, technologies like open rotors [15], advanced gear turbofan [16], etc. are evolving to improve the propulsive performance. Recently aircraft manufactures have also redesigned and manufactured efficient derivative aircrafts like Boeing 737 Next Generation, A320neo, A330ceo, A350-1000 XWB, etc. to fulfill the growing demand to satisfy customer constraints and future regulations. Research is also being carried out on unconventional configurations like Blended Wing Body [17], Strut Braced Wing [18], Truss Braced Wing [19], etc. to improve the performance over the traditional tube and wing configurations.

Use of advanced technologies or advanced concepts introduce a lot of uncertainties in the design process. This is due to the fact that these technologies or concepts are still under development or they have not been integrated into the aircraft system yet. With the expansion of the global market for civil aircraft and the necessity to address other stringent environmental, financial, social and operational requirements under these uncertainties, the complexity of the design process for new vehicles is increasing. There is a need to move from traditional deterministic design methods to uncertainty based design techniques to handle these evolving requirements while

minimizing the risk, cost and design time. Uncertainty based design can give the decision makers tools to carry out trade-off analysis between various elements of design, take mitigating action to manage uncertainties, and allow resource allocation in appropriate technologies or design to avoid any future adverse situation. With the advancement in computational power, modeling techniques, computational methods, and numerical methods, advanced design methods have opened the doors to new opportunities and challenges in the uncertainty-based design process.

1.2 Aircraft Design Process: The Paradigm Shift

While the aerospace industry is expanding, there has been a *paradigm shift* in the design process within the design community with system *affordability* being the focus [20]. In "*Design for Affordability*" the decisions in the design process is not only dictated by the aircraft's capabilities, effectiveness and other characteristics but also by cost associated with the design. This requires a robust decision-making process which balances the benefits and costs of the system.

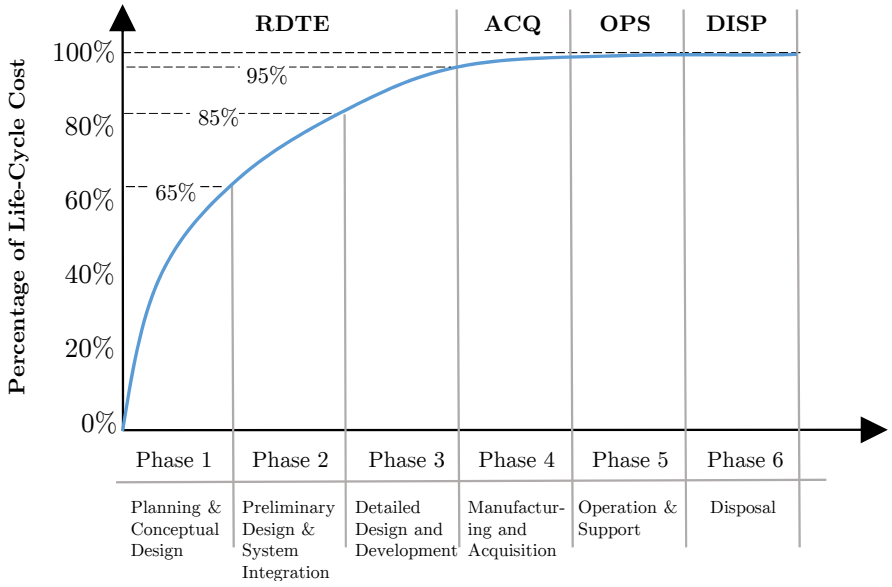

Figure 2: Life Cycle Cost during the Aircraft Life Cycle Phases [21]

One of the major activities of a design process is making decision on allocation

of resources like money, personnel, and infrastructure after carrying out trade study and analyses so that an appropriate design is selected that satisfies the goals, product objectives, customer needs and technical requirements [22, 23] while controlling the costs. In traditional design methods, the major part of aircraft life cycle cost is allocated in the early design stages as shown in Figure 2.

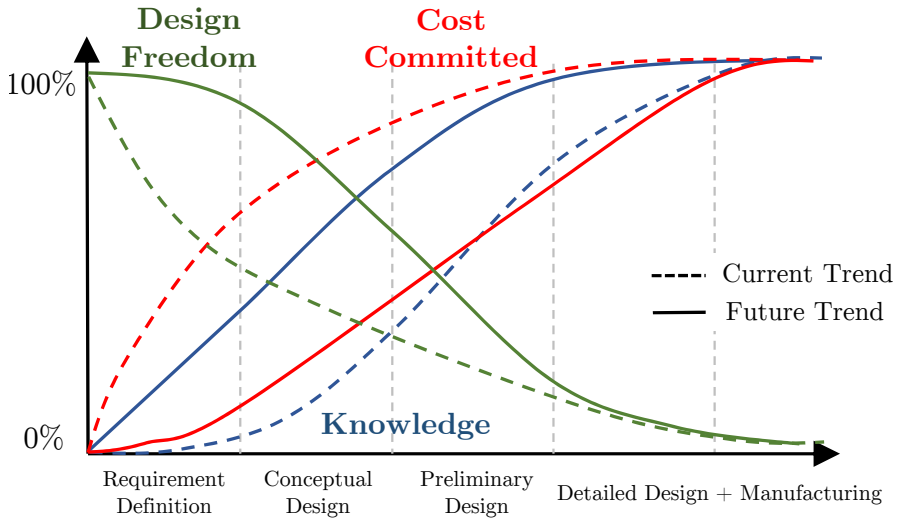

Figure 3: Paradigm shift in aircraft design process

The National Science Foundation 1996 Strategic Planning Workshop [24] emphasized a paradigm shift change in aerospace engineering which allows design freedom at later stages of the design process and helps to avoid expensive redesign. Conceptually, the paradigm shift is shown in Figure 3 by comparing the current design process to a theoretical future design process. There are three main elements of the paradigm shift; *design knowledge*, *design freedom* and *cost commitment*. It is desirable to commit the largest part of cost and resources available for a project towards the later phase of the aircraft design process. Also, it is beneficial to have more design freedom available in the later phase of design. The availability of more knowledge in the early phase of the aircraft design allows the flexibility of the cost commitment and greater design freedom towards the later phase. This paradigm shift requires new methods to generate data, information and knowledge, support synthesis and analysis, and

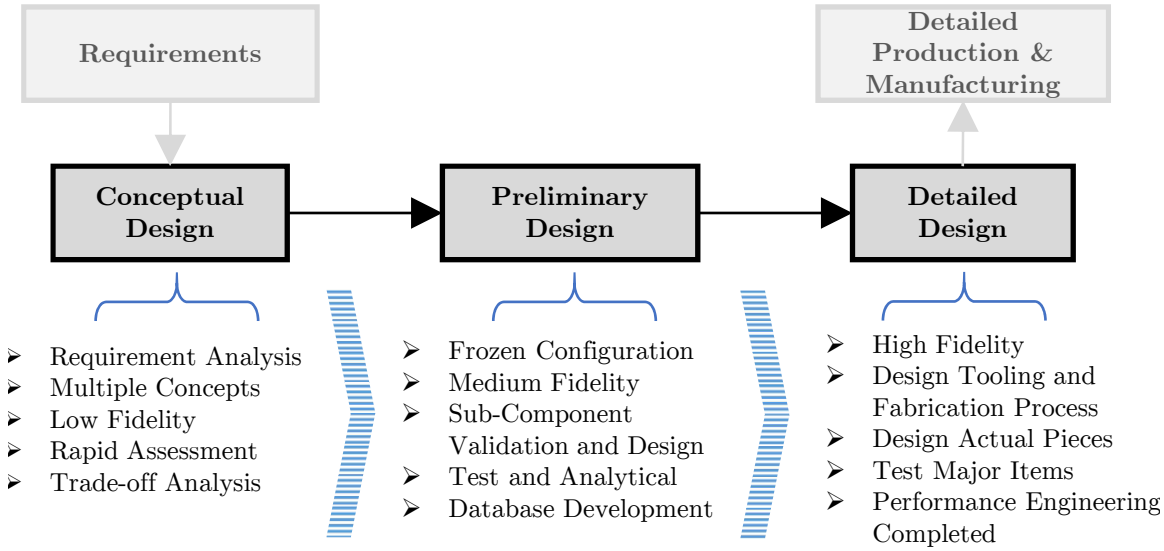

Figure 4: Phases of aircraft design process

facilitate the decision-making process early in the design phase. Uncertainty-based design is one such method to gain knowledge and information during the early design decision process.

There are three main phases in an aircraft design process [22]; Conceptual, Preliminary, and Detailed as shown in Figure 4. The change of design phase is generally linked with the level of details in representation and analyses. The main purpose of conceptual design is to explore a large number of design alternatives, carry out trade studies, identify and select a feasible and viable design concept which can be further developed and refined during the preliminary design phase. In the conceptual phase the development of overall aircraft configuration is driven by the design requirement, which can be revised or relaxed according to the requirements. This is the most important phase considering the number of concepts explored, investigation of technologies, feasibility study, and mapping between the requirements and configurations. The analyses in this phase are not very detailed but it is important to consider the interaction among various disciplines, subsystems, and technologies. However, there is a dearth of data, information and knowledge regarding the problem, requirements,

constraints, technologies to be considered, tools and models to be used, and so on. For example, most of the models and tools used in this phase are lower order/fidelity models or empirical models which are based on historical data. Therefore, accounting for the uncertainties in the design process is one of the critical aspects in the conceptual design phase.

Once the final design configuration is down-selected in the conceptual design phase, the design process moves to the preliminary design phase. It is in this phase that high-fidelity tools are introduced to carry out analysis on higher details to optimally size various subsystems and components to obtain a design that meets the requirements and the constraints. During this phase, specialists and experts in the area of aerodynamics, structures, control system, landing gear, etc. become involved in carrying out design and analysis. Other non-conventional disciplines such as economics, maintainability, reliability and safety are also introduced during this phase. The final goal of the preliminary design phase is to come up with a full-scale development proposal for the detailed design phase. Although more information and knowledge is available in this phase, uncertainty is still prevalent during this phase.

The detailed design phase starts with the design of actual pieces to be fabricated based on information and knowledge available from the preliminary phase. This is the most expensive part of the design process which involves a large number of designers supported by Computer Aided Design (CAD) and Computer Aided Manufacturing (CAM) tools. The smallest possible pieces which are not considered during preliminary design like flap, tracks, brackets, clips, doors, etc, including the pieces involved in hydraulic, electrical, pneumatic, fuels and other system are designed in this phase.

1.3 Uncertainty in Design

Uncertainty as defined by Booker et al. [25] is defined as "*What is not known precisely*" while precision is defined as "*Abilities in making good predictions, being exact,*

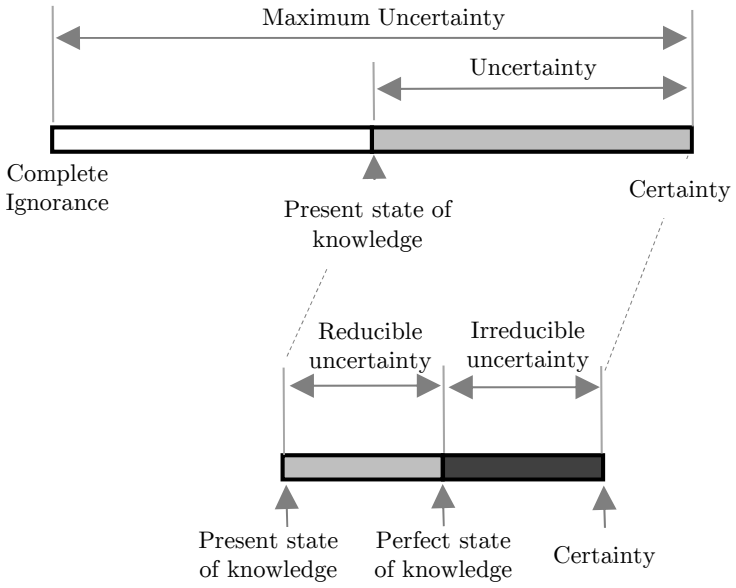

Figure 5: Definition of uncertainty [26]

being correct, maintaining control, operating within specifications, and representing the physical world". Nikolaidis et al.[26] defines uncertainty as the gap between the current state of knowledge and certainty, where certainty is defined as "*the condition in which a decision maker knows everything needed in order to select the action with the most desirable outcome*". The uncertainty can be further classified into reducible and irreducible uncertainty as shown in Figure 5.

In the aircraft design process uncertainty can be due to fidelity of analysis model, experimental data, interdisciplinary interfaces, operating conditions, immature technologies and so on [27, 28, 29, 30, 31, 32]. Moreover, the uncertainties evolve over time as shown in Figure 6. For example, in the conceptual design phase, uncertainty is more prevalent compared to the preliminary and detailed design phases. This is primarily because of two reasons. The first reason is the *model form uncertainty*, which is associated with the accuracy of low fidelity models used in the conceptual design phase. The second reason is the *parameter uncertainty*, which is associated with the parameters or variables which are not known accurately early in the design phase. For example, aerodynamics analysis of a wing in the conceptual design phase requires

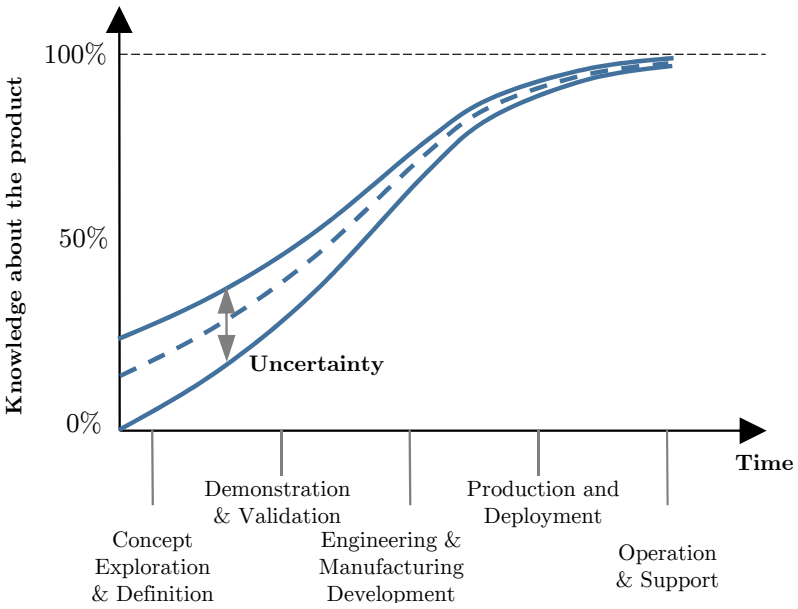

Figure 6: Evolution of uncertainty [20]

lift curve slope (Cl_α) of airfoils. This is not accurately known until the late preliminary or detailed design phases when the shape of the wing has been fixed. Thus, Cl_α have to be considered as an uncertain parameter during aerodynamic analysis in the conceptual design phase. Uncertainty can also arise due to future requirements and other market factors like fuel cost, market demands, etc. As the requirements change with time, constraints can be relaxed or tightened to influence the uncertainties.

Typically, it takes a decade to design a new aircraft, a production time of 20 to 30 years with the service life of the aircraft being 25 to 45 years [11]. As the designers have very limited knowledge and information at beginning of the design process of a new system, the uncertainty is at a maximum. Freezing a design configuration without considering these uncertainties early in the design process may lead to performance degradation, requirement and constraint violation. This may cause an expensive redesign leading to cost overrun and delay.

To overcome this issue the designers need to account for uncertainty early in the design stage such that appropriate decisions can be taken to avoid expensive redesign process later in design stages. As the design progresses and more information and

data gets accumulated, the designer's present knowledge moves towards certainty thus reducing the uncertainty. In the early phase of design, availability of more knowledge and consideration of uncertainty when making a decision reduces the risk of not achieving the target of the system and avoids costly redesign. Therefore, for a lengthy product life cycle, it is important to carry out *uncertainty management* early in the design process to make critical design decisions for investment in future technologies, engine, airframe configuration, etc. One such recently developed approach is called *Probabilistic Certificate of Correction* which is used as metric to make decisions under uncertainty at all the stages of design process.

1.3.1 Probabilistic Certificate of Correction (PCC)

Probabilistic Certificate of Correction (PCC) has been developed as part of DARPA Adaptive Vehicle Make program with the goal of reducing the design and integration time for a complex system [33]. In a complex system, there are many requirements, constraints and regulatory threshold which needs to be fulfilled at the system level. To ensures that the final product or the system is able to perform at the level of customers satisfaction, a certification process is carried out on a physical benchmark test. The certification process generally involves a verification process, which ensures that the right processes were used to build the product and a validation process, which ensures that the product meets the customers requirements. In the current design process, the verification and validation process is carried out by comparing a virtual prototype with the physical prototype. Since, the physical prototypes are not available early in the design process, chances of finding the error and incompatibilities are delayed. This significantly increases the risk of redesign of system, leading to program cost overruns.

To overcome this challenge, virtual prototype metric called Probabilistic Certificate of Correctness (PCC) [34] has been developed which incorporates:

- **Probability of satisfying requirements:** Gives the expected behavior as an estimated probability as computed with a statistical sampling technique.

- **Confidence in the probability of satisfying requirements:** Gives a statistical confidence in the estimated probability; related directly to the number of samples and the approach taken for estimating the probability of satisfying a requirement.

- **Systematically modeled and verified set of assumptions:** Eliciting and building assumptions into a simulation model facilitates a comprehensive approach to model verification, error reduction, inconsistencies, and in appropriate applications of a model.

PCC estimates the probability that the physical prototype will satisfy the certification or acceptance test by using the behavior of virtual prototype with known confidence and verified model assumptions. PCC is estimated by rigorously accounting all sources of uncertainty including model verification, manufacturing tolerances, human factors, confidence in the stochastic sampling, etc.

The core idea of PCC is to quantify uncertainty by using modeling and simulations to minimize the variation in the product development process for a given set of requirement. Instead of applying certification process at the late design state, PCC can be applied in the early design phases. For example, one of the common approach of product development process is V-cycle system engineering process [36] as shown in Figure 7a. In the V-cycle process, the testing and integration of hardware with the physical prototype is done later in the design process. Therefore, most of decisions on redesign or rework on the system, subcomponent or design process is delayed. The traditional V-cycle process can be improved by adding the PCC metric in each milestone gates as shown in Figure 7b. Using PCC metric with virtual prototype enables finding the errors and problems earlier in design phase and reduces the load

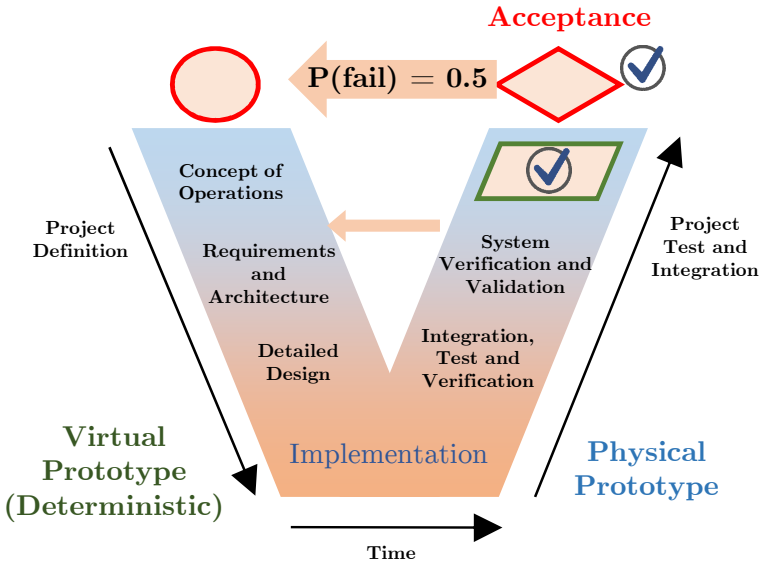

(a) Traditional V-Cycle

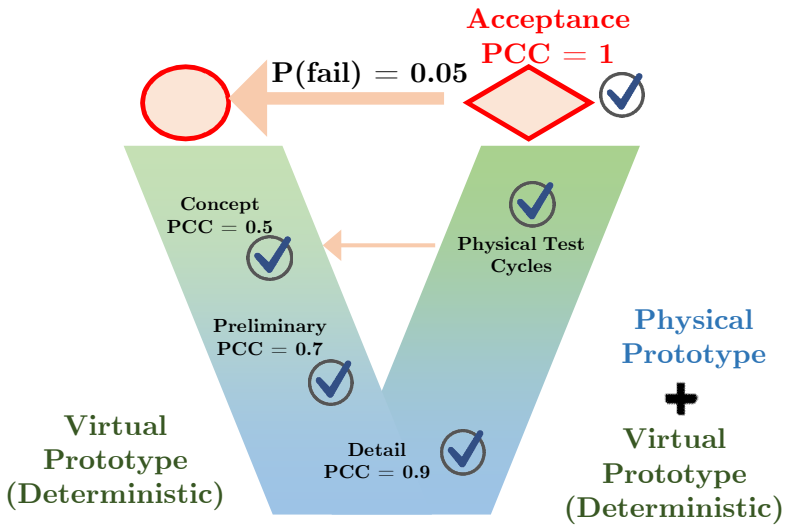

(b) V-Cycle with PCC

Figure 7: Reduction in redesign process using PCC in early stages of design [35]

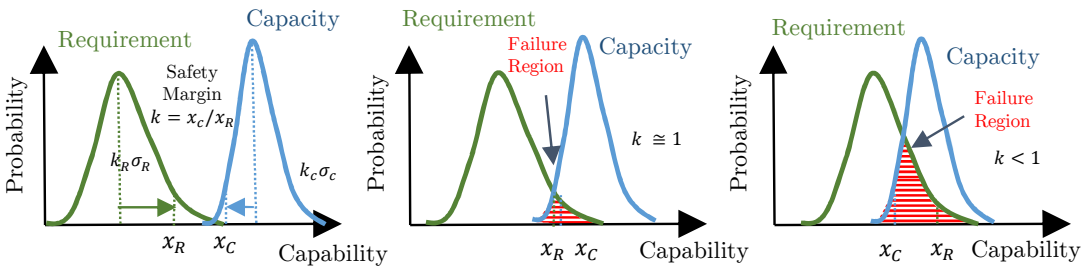

Figure 8: Use of safety margin

on the expensive rework or redesign at the end of physical certification phase.

Approaches like PCC allows decision making under uncertainty early in the design process to reduce the risk of expensive redesign process during the later phases. The core machinery of such methods lies in accounting for various sources of uncertainty and appropriately quantify the effect on the system level metrics of interest. This requires a rigorous and quantitative approach of *Uncertainty Quantification and Management* at different stages of design process to account for uncertainty in making appropriate decisions.

1.4 Uncertainty Quantification and Management

The existence of uncertainty in the aircraft design process is well known among designers. The traditional way of handing these uncertainties in a deterministic design process has been the use of *safety factor* or *safety margin*. However, these safety factors are generally based on historical data and expert judgment. Also, use of safety factors is a qualitative approach and does not quantify the actual reliability of the system. For example, as shown in Figure 8, a safety margin has been applied to both requirement and the capacity. Since, the uncertainty on the requirement (shown here as probability density function) has not been considered in the deterministic process, the actual reliability of the system is not known, which can lead to over design of system or result in low reliability.

Unlike qualitative approaches like safety factors, *uncertainty quantification* methods refer to *a quantitative process of assessment or evaluation of uncertainty based upon models, data, expertise, etc* [37]. An uncertainty quantification, typically involves:

- Mathematical model of the system
- Identifying the sources of uncertainties affecting the system
- Decision-making criteria motivating the uncertainty quantification like robustness, reliability, safety, optimization etc.

The mathematical model can be represented as a function (Equation 1) linking the inputs (fixed and uncertain variables) and the output variables of interest upon which decision criteria is applied.

$$\mathbf{z} = G(\mathbf{x}, \mathbf{u}) \tag{1}$$

The fixed variables (denoted here as $\mathbf{x}$) are generally comprised of design variables, scenario variables or the fixed parameters of the system. The uncertain variables (denoted here as $\mathbf{u}$) are generally comprised of all types of uncertainties like parameter uncertainty, model form uncertainty, data form uncertainty, etc. The output variables of interest (denoted here as $\mathbf{z}$) can be scalar, or a vector if there are multiple criteria for decision making. The mathematical model function (G) can represent a *deterministic* physics model (like Computational Fluid Dynamics (CFD) or Finite Element Model (FEM)) or an *intrinsically stochastic* or *non-deterministic* model (model for failure rates at component or system level in risk analysis).

Depending upon the field of research and requirement there can be different goals for uncertainty quantification [27]:

Understand To understand the influence of the uncertainties and rank them based on importance and sensitivity to guide any additional measurement, modeling or experiments.

Accredit To give credit to a model to reach an acceptable fidelity and accuracy for its use by carrying out calibration, estimation of the parameters of the model inputs, simplifying the system model physics, and finally validation.

Select To compare relative performance and optimize the choice of system, architecture, technologies, concepts, etc.

Comply To demonstrate compliance of the system with requirements, constraints and regulatory threshold.

1.4.1 Steps for Generic Uncertainty Quantification and Management (UQM) Methodology

Irrespective of research, a generic uncertainty quantification methodology is shown in Figure 9 which consists of the following steps:

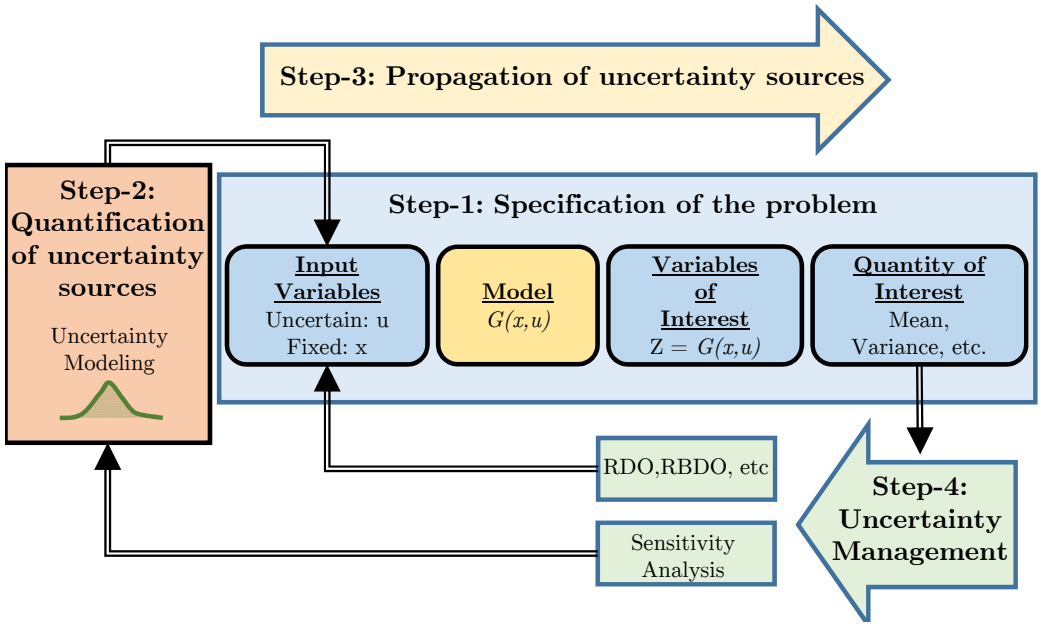

Figure 9: Generic Uncertainty Quantification (UQ) methodology

1. **Specification of the problem**: Specify the model G (analytical, complex computer code or experimental process) and identify the fixed variables $\mathbf{x}$, the uncertain variable $\mathbf{u}$, and output variables of interest $\mathbf{z}$.

2. **Characterize and quantify source of uncertainties**: This can be decomposed into two steps

   (a) **Uncertainty source characterization**: Characterize each source of uncertainties into reducible (aleatory) and irreducible (epistemic) uncertainty based on the current state of knowledge

   (b) **Uncertainty source quantification**: Various mathematical theories for uncertainty can be used to model uncertainty such as Probability Theory [38], Possibility Theory [39], Dempster Shafer Evidence Theory[40], Random Intervals [41], etc. Uncertain variables are quantified based on experimental data or expert's opinion using direct method like statistical fitting [42] or using indirect methods from data generated from separate models [43].

3. **Propagation of uncertainties**: Propagate the uncertainties in input $\mathbf{u}$ to uncertainties on variable of interest $\mathbf{z}$ through the model. Various uncertainty propagation techniques can be applied based on the computational complexity of the model like analytical formula, geometrical approximations, Monte Carlo sampling strategies, metamodel-based techniques, etc.

4. **Uncertainty Management**: The design variables are adjusted and modified such that the uncertainties can be managed and the goal of the uncertainty quantification can be achieved. Robust Design Optimization (RDO) and Reliability-Based Design Optimization (RBDO) are two typical methodologies applied in this step. Sensitivity analysis is another integral part of this step.

Sensitivity analysis [44, 45] evaluates the contribution of different uncertainty sources on the output of the model and ranks them according to their influence. This allows decision makers to carry out resource allocation to manage the critical uncertainty sources to reduce the overall uncertainty on system metric.

As discussed and shown in Figure 9 uncertainty quantification and management methodology is an iterative process. Multiple iterations are required to change the design variables appropriately to achieve the required goals (robustness or reliability). Generally an optimizer is used to carry out uncertainty management (RDO or RBDO), which increases the computational requirement by orders of magnitude higher than a deterministic optimization.

1.5 Uncertainty-Based Multidisciplinary Design Optimization (UMDO)

Research on uncertainty-based design can be found in literature as old as 1950's [46, 47] but was restricted by computational requirements. Although, with the advancement in computational power various methods and algorithms have been developed in last few decades, most of these methods were restricted to single disciplinary uncertainty analysis [48, 49, 50]. For example, aerospace engineering uncertainty-based designs were mainly focused in the area of structure [51], aerodynamics [52, 53], aeroelasticity [54] and control [55, 56]. As an aircraft system consists of multiple disciplines, uncertainty-based disciplinary design is not sufficient. An uncertainty-based multidisciplinary design optimization (UMDO) methodology is required to carry out uncertainty assessment to evaluate over all system reliability and robustness to support the design decision process.

To carry out the UMDO process on a complex system like aircraft, the model defined by the function $G(\mathbf{x}, \mathbf{u})$ in the UQM methodology described by Equation 1 has to be replaced with a full multidisciplinary analysis (MDA) function consisting

of all the critical disciplines to evaluate system level metrics. Propagation of uncertainty through multidisciplinary framework becomes complicated due to coupling when compared to uncertainty propagation in a single discipline. Due to coupling of the disciplines, the cross propagation of uncertainties is difficult to manage and can become a computationally expensive process. Therefore, a holistic approach is required to carry out design under uncertainty for a multidisciplinary system to improve the overall system design by exploiting the coupling between disciplines.

UMDO process is an extension of the deterministic MDO process to quantify uncertainties at system level due to uncertainties at discipline level and their interactions. The UMDO process allows generation of a robust and reliable design by using the synergistic effect of interdisciplinary coupling and interactions. Due these benefits, UMDO has attracted wide research interest and has been an active field of research in many areas. For example, Zang [3] has addressed various needs and opportunities for uncertainty-based multidisciplinary designs for aerospace vehicles in a NASA white paper. Various UMDO approaches have been successfully applied in the field of aerospace and they have demonstrated the benefit of this advanced design method [57, 20, 29, 58, 50, 27, 59, 60]. Many research works have been published in various elements of the UMDO process such as uncertainty classification and quantification, multidisciplinary uncertainty cross propagation and analysis, approximation methods for reducing calculation burden, optimization under uncertainty, and multidisciplinary organization of UMDO problems. The application of many of these methods on aerospace vehicles has been reviewed by Yao et al. [61].

1.5.1 Need for Distributed UMDO

As discussed in the previous section, it is crucial to bring in information, knowledge and data early in the design process for better decision making. From the MDO perspective, this requires bringing in high-fidelity mathematical models for disciplinary

analysis early in the design stage. Typically, these high-fidelity analyses require experts and sometimes teams to carry out design analysis. For example, carrying out aerodynamic analysis using Computational Fluid Dynamics (CFD) requires fine tuning of various parameters depending upon the type of problem and setting, which can only be handled by an expert in CFD methods. Therefore , a distributed UMDO architecture is preferred because it is not always feasible to integrate the high-fidelity analysis models into a single monolithic and integrated UMDO architecture.

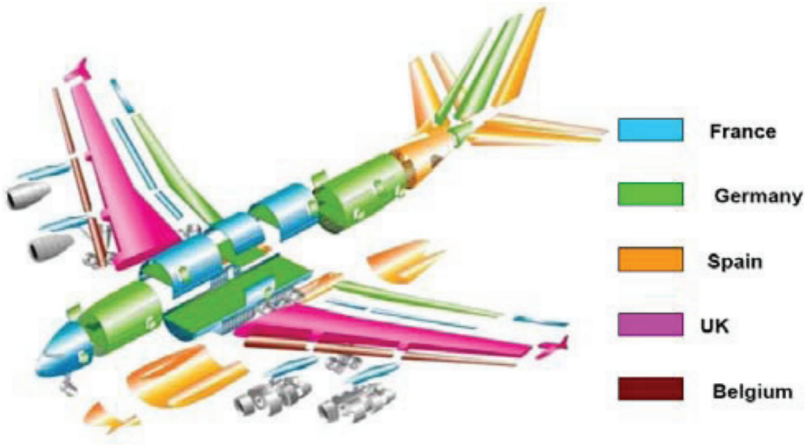

Figure 10: Multinational collaboration at Airbus [62]

Also, from an industrial design perspective, there are other challenges in engineering and design such as market globalization, short delivery time, evolution of customer requirements, supply chain management, complex industrial chain creation and so on [62]. This necessitates a tighter integration of diverse knowledge, multiple disciplines and collaboration of engineers and experts. On the other hand, market globalization demands decentralization and distribution of design, development and manufacturing work into multiple teams, often located at different global locations [63]. Also, large industries tends to transfer parts of their design work to multiple suppliers and contractors [64]. In Figure 10, the distribution of work completed by multiple companies from different countries in development of an Airbus aircraft has been depicted. This leads to a paradox of "*integration vs distribution*" [62] from an

industrial design perspective. A *collaborative engineering* [65] approach is generally adopted by industries to overcome this paradox by coordinating the activities of multiple teams, design groups and experts based on information flow, available resources, and other constraints.

Typically, the teams, design groups and experts have their own domain specific design methods and tools to work on their part of the design problem. For example, some of the advanced CFD or FEM analysis and design tools have intrinsically embedded *adjoint solver* to calculate derivatives [66], which are much more efficient for optimization compared to a gradient-based optimizer applied externally on a system level. Similarly, for uncertainty analysis, a discipline level expert generally has better knowledge, experience and tools to carry out uncertainty quantification on a discipline level rather than on the system level. For example, some of the advanced structural design tools come with an intrinsic uncertainty propagation method like Polynomial Chaos Expansion (PCE) [67] which are computationally efficient at the disciplinary level than on the system level. Therefore, a distributed UMDO process supports collaborative engineering by decomposing a complex problem into sub-problems, which can be solved independently by different entities, teams and experts, each using their domain specific analysis and design tools.

In conclusion, there are two main motivations of distributed UMDO architecture from an industrial perspective; *concurrency* and *autonomy*. Concurrency is achieved by allowing each discipline to use its computational and human resources to work on the analysis and design problem. Autonomy is accomplished by granting freedom to each discipline to make their own design decisions using their own design and analysis tools for their part of the over all problem. Distributed UMDO architecture helps to manage design under uncertainty of a complex system by decomposing the problem into a manageable sub-uncertainty-based optimization problem at disciplinary or subsystem level, with certain coordination strategy. Keeping these needs and benefits

of collaborative engineering in mind, distributed UMDO architecture is the focus of the current research.

1.6 Research Objective

As discussed in this chapter, as the global market for civil aviation continues to grow, requirement such as regulations, cost, performance, and so on are getting stringent. There is a huge pressure on design engineers in terms of time and overall life cycle cost for design and development of newer, more efficient aircraft. With the paradigm shift from performance-based design to affordability-based design, it has been the focus to bring in more information and knowledge earlier in the design phase. This changed the perspective of the design process from disciplinary-based design to over all system design so that the synergism of mutually interacting phenomena of subsystems and disciplines can be exploited to design systems and subsystems coherently. To support these, various MDO techniques have been developed in the last few decades to support the decision maker to assess the impact of interdisciplinary couplings on system level metrics and to carry out design trade off early in the design phase.

Although advanced MDO methods have been developed, most of them are applicable for deterministic design. Since uncertainty is the integral component of complex system design, there has been a need for incorporating uncertainty in the design and decision making process. This has led to the development of uncertainty-based multidisciplinary design optimization (UMDO) methodology to quantify and manage uncertainty in a multidisciplinary system. Although there are many challenges in managing complex system designs under uncertainty with the UMDO process, two important ones are computational and organizational challenges. This has led to the current focus of research on distributed UMDO process.

Based on the challenges associated with the distributed UMDO process, the overall research objective of the current work is as follows:

Research Objective: : *Develop an Uncertainty-based Multidisciplinary Design and Optimization (UMDO) methodology to accurately quantify the effect of uncertainties from disciplines to system level metrics of interest and provide an environment for Uncertainty Quantification and Management (UQ&M) in a distributed multidisciplinary setting.*

With this objective, a detailed background on overall UMDO procedure and existing methods for distributed UMDO methodologies is presented in Chapter 2. In Chapter 3, the challenges and the gaps in the existing distributed UMDO method are discussed and the research questions are formulated. The hypothesis to the research questions are discussed and tested in Chapters 4, 5, and 6. Finally, the overall contribution of this dissertation, limitations and future work are summarized in Chapter 7.

CHAPTER II

BACKGROUND

In this chapter, deterministic MDO is briefly introduced to set up the foundation for an uncertainty-based multidisciplinary optimization (UMDO) procedure. This is followed by a description of general UMDO procedure, methods and techniques for uncertainty modeling, analysis, propagation, and uncertainty-based optimization. Then a background on existing distributed UMDO architectures are discussed.

2.1 Multidisciplinary Design Optimization (MDO): A Brief Background

As discussed in the previous chapter, decisions made in the early phase, particularly in the conceptual design phase and early preliminary design phase, have tremendous impact on life cycle cost and development time of aircraft systems. To gain more knowledge at an earlier stage to support informed decision making, accurate and physics-based analyses with the use of mathematical modeling need to be carried out. For example, to carry out aerodynamic analysis mid-fidelity models like vortex lattice method or high-fidelity methods like Computational Fluid Dynamics (CFD) can give better insight into the problem compared to historical data-based empirical methods. Traditionally, high-fidelity tools and models are generally used in the preliminary design stage but there is a huge benefit in moving these analyses upstream to a conceptual design stage. The challenge of using mathematical models and tools early in the design phase comes from the characteristics of the aircraft system itself. As defined by Ackoff [68], a system is defined as

A system is a set of two or more interrelated elements of any kind that satisfies the following conditions:

- The properties or behavior of each element of the set has an effect on the properties or behavior of the set taken as a whole.
- The properties and behavior of each element, and the way they affect the whole, depend on the properties and behavior of at least one other element in the set. Therefore, no part has an independent effect on the whole and each is affected by at least one other part.
- Every possible subgroup of elements in the set has the first two properties: each has a non-independent effect on the whole. Therefore, the whole cannot be decomposed into independent subsets. A system cannot be subdivided into independent subsystems.

An aircraft is a complex system consisting of many such elements or contributing analyses (CAs) that contribute to the performance of the entire system. The CAs consist of disciplinary analyses, processes, or subsystems in the design of the complex system. For example, an aircraft system consists of multiple complex and heterogeneous elements like wing, tail, fuselage, landing gear, engine, etc. which require analyses from disciplines like aerodynamics, structures, propulsion, etc. The main driver of the complexity of the design process is the complex non-linear interdisciplinary interaction among various CAs leading to coupling [69, 70]. An optimum aircraft cannot be obtained by combining the optimal solutions from each discipline or optimally designed components and technologies. For example, increasing the fan

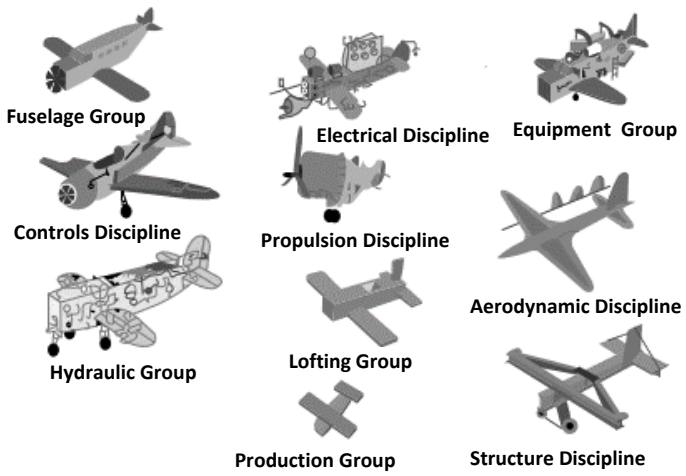

Figure 11: Optimal design from a disciplinarian's view [71]

diameter of an engine would reduce the noise level. But, it will generate weight and drag penalty resulting in an increase in fuel consumption. Also, carrying out disciplinary design without considering the coupling effect from other disciplines can lead to incompatible system design. For example, if the structure and aerodynamic disciplines are assigned to designing the wing independently, the structure discipline will tend towards shorter wing span to reduce the wing weight, whereas aerodynamic discipline will tend towards a larger wing span to improve aerodynamic performance. Although, disciplinary performance from each discipline (weight and aerodynamic performance) can improve the system level performance, like range, but this leads to interdisciplinary incompatibly (large span versus short span). A pictorial example of interdisciplinary incompatibility among multiple disciplines is shown in Figure 11.

Therefore, a trade-off is required among discipline-driven designer to generate an interdisciplinary compatible and feasible solution with optimal system level performance as shown in Figure 12. As Moir [72] mentioned,“ *the success or failure in the Aerospace and Defense sector is determined by the approach taken in the development of systems and how well or otherwise the systems or their interactions are modeled, understood and optimized.*”; therefore it is necessary to move from a discipline or

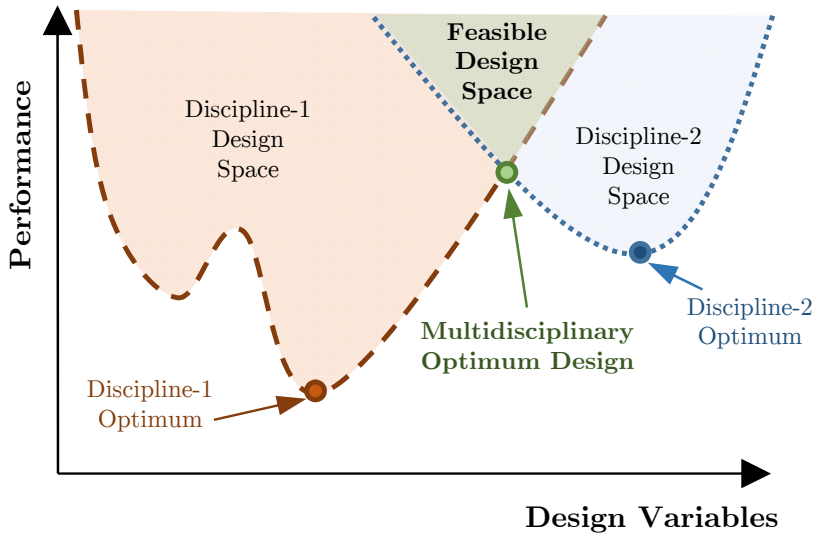

Figure 12: Disciplinary trade-off for interdisciplinary compatible and optimal system

component-based design to a Multidisciplinary Design Optimization (MDO) procedure, which handles the coupling and interdisciplinary compatibility among multiple disciplines while carrying out a system level optimization.

MDO can be defined as "*an evolving methodology, i.e. a body of methods, techniques, algorithms, and related application practices, for design of engineering systems coupled by physical phenomena and involving many interacting subsystems and parts*"[1]. The initial development work on MDO can be seen in work done by Schmit and Haftka [73, 74, 75, 76, 77] in the field of structural optimization. Some of the earliest applications of MDO on wing design involving multiple disciplines like aerodynamics, structures, and controls disciplines can be found in [78, 79, 80] which has been further extended to complete aircraft systems in [81, 82, 83, 84, 85, 86]. Currently, the MDO applications have also involved non-traditional disciplines like manufacturing[87], subsystem[88], emission[89], noise[90], economics[91], etc. Various benefits of industrial level MDO application can be found in Agte et al. [92]. Although, MDO has been embraced in almost all phases of aircraft design [93], its

[1]Defined by AIAA MDO Technical Committee (info.aiaa.org/tac/adsg/MDOTC/default.aspx)

greatest impact and benefit is recognized at conceptual design phase.

A general mathematical formulation for a MDO process is as follows:

$$\begin{aligned}
\text{minimize} \quad & f_o(\mathbf{x}, \mathbf{y}) + \sum_{i=1}^{N} f_i(\mathbf{x}_0, \mathbf{x}_i, \mathbf{y}_i) && && \text{(2a)}\\
\text{with respect to} \quad & \mathbf{x}, \hat{\mathbf{y}}, \mathbf{y}, \bar{\mathbf{y}} && &&\\
\text{subject to} \quad & c_o(\mathbf{x}, \mathbf{y}) \geq 0 && && \text{(2b)}\\
& c_i(\mathbf{x}_0, \mathbf{x}_i, \mathbf{y}_i) \geq 0 && \text{for } i = 1, \ldots, N && \text{(2c)}\\
& c_i^c = \hat{\mathbf{y}}_i - \mathbf{y}_i = 0 && \text{for } i = 1, \ldots, N && \text{(2d)}\\
& \mathcal{R}_i(\mathbf{x}_0, \mathbf{x}_i, \mathbf{y}_i, \hat{\mathbf{y}}_{j \neq i}, \bar{\mathbf{y}}_i) = 0 && \text{for } i = 1, \ldots, N && \text{(2e)}\\
& \mathbf{x}^L \leq \mathbf{x} \leq \mathbf{x}^U && && \text{(2f)}
\end{aligned}$$

where $\mathbf{x}$ is vector of design variables, $\mathbf{y}$ is vector of coupling variables, $\bar{\mathbf{y}}$ is vector of state variables used by a specific disciplinary analysis, f is the objective function, c is the design constraints, c^c is the interdisciplinary compatibility constraints, $\mathcal{R}$ is the residual form of the governing equation in disciplinary analysis and N is the number of disciplines. Variables with $()_0$ are the functions or variables shared by more than one discipline, $()_i$ are the functions or variables that apply to only i^{th} discipline, $\hat{()}$ are independent copies of variables distributed to other disciplines. Four important constraints in MDO problems are:

- *Disciplinary analysis constraints* are the equality constraint implicit in disciplinary analysis given by Equation 2e.
- *Design constraints* are linear or nonlinear constraints generally based on design requirements and are given by Equation 2b and Equation 2c.
- *Interdisciplinary compatibility constraints* are the auxiliary constraints introduced to relax interdisciplinary coupling, given by Equation 2d.

- *Side constraints* specify the design space range of design variables, given by Equation 2f.

One of the main aspects of implementing MDO is the *architecture*. An MDO architecture defines how different contributing analyses (CAs) or the disciplinary analysis models are coupled, how constraints are handled, use of approximation models, use of optimization strategy, information and data transfer, coordination strategy, and so on for a given problem such that the overall optimization is carried out to achieve the optimal design fulfilling all the constraints and requirements. Most of the MDO architecture can be categorized into two groups; *monolithic* or *single level* and *distributed* or *multi-level*.

- **Monolithic or single level architecture:** A single system-level optimizer is used to carry out optimization and for determining the state of the system. For example, Equation 2 is equivalent to the procedure for single level All-In-One (AIO) approach.

- **Distributed or multi-level architecture:** The optimization problem is decomposed or partitioned, typically among the CAs, where each CA solves the sub-problems containing small subsets of the variables and constraints.

Distributed architecture can be further decomposed into bi-level and multi-level architecture, and hierarchical and non-hierarchical. Review of MDO architectures can be found in Martins et al. [2].

Selection of appropriate architecture is very important as it influences the solution time and optimal design. Typically, selection of MDO architecture depends on factors like level of fidelity and complexity of CAs, organizational structure and so on. Sobieszczanski and Haftka [94] suggested three approaches to carry out the MDO process depending upon complexity of model and organizational structure. The first approach is for the situation when two or three disciplines are highly coupled. In this

case, a single analysis can analyze all the coupled disciplines in a monolithic fashion. This has led to creation of new disciplines like *aeroelasticity*, *thermoelasticity*, *structural control*, etc. This can minimize the complexities arising due to organizational structure and MDO itself. In the second approach, simple analysis tools are integrated into a single and modular monolithic MDO environment. This is generally possible at the conceptual design phase when the analysis tools are simple and does not require experts. The third approach is applied while using high-fidelity models and complex simulation models which are hard to integrate into a single monolithic architecture. This approach requires distributed architecture which applies decomposition methods and global sensitivity techniques so that the overall optimization process can be carried out with minimum changes to the disciplinary codes. A brief background of four commonly used distributed MDO architecture; Collaborative Optimization (CO), Concurrent SubSpace Optimization (CSSO), Bi-Level Integrated System Synthesis (BLISS), and Analytical Target Cascading (ATC), is discussed in Appendix I.

2.2 General Uncertainty-Based Multidisciplinary Design Optimization (UMDO) Process

The UMDO process is an extension of the deterministic MDO process to handle uncertainties in a multidisciplinary environment. There are two main blocks of the UMDO process as shown in Figure 13.

1. **Uncertainty System Modeling**: This is the first step of the UMDO process which mathematically describes the optimization problem under uncertainty. This is done by *system modeling* and *uncertainty modeling*.

    - ***System modeling***: This step consists of building mathematical models and tools of various subsystems and disciplines associated with the system. This step also includes formulation of optimization problem such as design

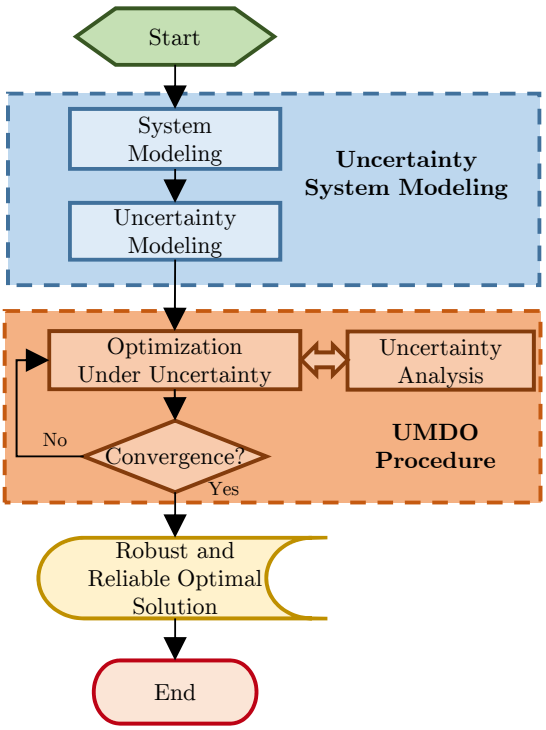

Figure 13: General UMDO process flowchart [61]

variables, optimization objectives, constraints, design space, etc. similar to deterministic optimization.

- ***Uncertainty modeling***: In this step, the uncertainty sources are identified and modeled using various mathematical theories.

2. **UMDO Procedure**: This procedure focuses on building efficient formulation to manage the interaction and information transfer between multiple disciplines to carry out the design process under uncertainty. This is done by *uncertainty analysis and propagation* and *optimization under uncertainty*.

   - ***Uncertainty Analysis and Propagation***: This process handles uncertainty analysis in each discipline, cross propagation of uncertainties between disciplines, and maintenance of interdisciplinary compatibility to quantify uncertainty at system level.

- ***Optimization under Uncertainty***: Similar to deterministic optimization, this step carries out design space exploration to find a robust and reliable solution while incorporating uncertainties.

The following section discusses mathematical details of uncertainty modeling, uncertainty propagation and analysis, optimization under uncertainty and UMDO procedure.

2.2.1 Uncertainty Modeling

One of the first and important steps for design under uncertainty is uncertainty modeling. Uncertainty modeling includes identification and classification of uncertainty sources using appropriate taxonomy based on the area of study and modeling and representation of the uncertainties using suitable mathematical tools. Uncertainty modeling may also include sensitivity analysis to screen out the sources which have unsubstantial effects on design so that the UMDO process could be simplified.

2.2.1.1 Uncertainty Classification

As discussed in Chapter 1, one of the commonly used taxonomies categorizes uncertainty into two types: *aleatory* and *epistemic*. Aleatory uncertainty is the inherent uncertainty in the system or the environment under consideration and it cannot be reduced even by gathering more information or data. Aleatory uncertainty is also known as *variability*, *type A*, *stochastic uncertainty* or *irreducible uncertainty*. Epistemic uncertainty is the uncertainty arising due to lack of knowledge and can be reduced by gaining more knowledge, data or information about the system under consideration. Epistemic uncertainty is also know as *subjective*, *type B*, *cognitive uncertainty* or *reducible uncertainty* [95, 96]. This taxonomy is commonly used in many fields of research including risk assessment, decision analysis, scientific computing and modeling, and simulation [97].

Different fields of research have developed their own taxonomies of uncertainties based on their application. For example, in economics uncertainty is classified as *fundamental* and *ambiguity* [98], in decision making uncertainty is classified into *risk* and *uncertainty (ignorance)* [99], in policy and risk analysis uncertainty is classified into *quantity* and *model form uncertainty* [100] while physical science mainly classifies uncertainty as *error* [101]. Similarly in engineering, controls and dynamical systems uncertainty is classified as *structured* and *unstructured* [102], civil engineering classifies uncertainties into *abstracted*, *non-abstracted*, and *unknown* [103], in mechanical engineering uncertainty is classified into *imprecision*, *probabilistic uncertainty* and *possibility* [104], and so on. In aerospace engineering, one of the common taxonomy in vehicle synthesis and design uncertainty is classified as *input*, *model parameter*, *measurement* and *operational* uncertainties [57]. Another taxonomy from the aerospace system design point of view classifies uncertainties into *operational/environmental*, *system level* and *discipline level* [105].

Thunnissen [28] provided a generalized categorization for uncertainty in design and development of a complex system, in which uncertainty is classified into *ambiguity*, *epistemic*, *aleatory* and *iterations*. Ambiguity is the uncertainty related to imprecision or vagueness due to the use of imprecise terms and expressions in general communication and linguistics. Aleatory and epistemic uncertainty are defined in the same way as discussed before. Epistemic uncertainties can be further classified into different categories as shown in Figure 14. Interaction uncertainty is due to the unanticipated iterations between teams and disciplines. This is particularly linked with information transfer and coupling variables in MDO environments.

2.2.1.2 Uncertainty Modeling

One of the key elements of uncertainty-based design and UMDO is the mathematical modeling of uncertainties. Uncertainty can be mathematically represented by its

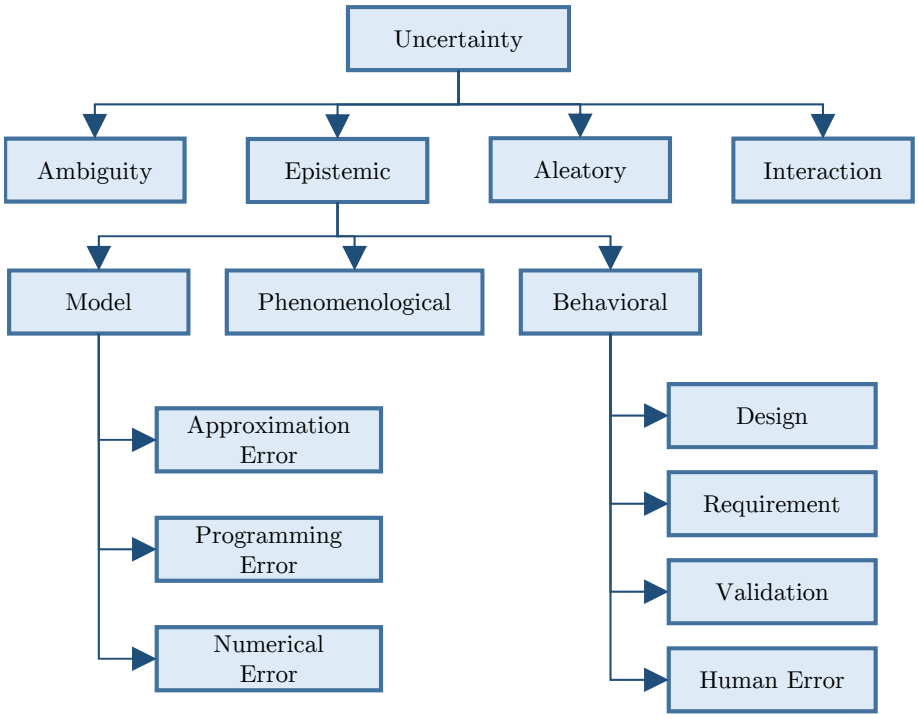

Figure 14: Classification of uncertainties in complex system design [28]

range or set and some measure within the range or set. Depending on the theory of measure, uncertainty can be modeled by different approaches. The choice of the theory or approaches to modeling uncertainties depends upon the type of uncertainty and available information. Some of the commonly used theories to model uncertainties are briefly discussed here.

- **Probability Theory:** Modern probability theory was introduced by Kolmogorov [106] who combined the notion of sample space with measure theory. In probability theory uncertainty is represented by random variables and probability measure is used to represent the magnitude of uncertainty. For a discrete random variable X, a sample space is defined as the set of all possible outcomes denoted by $\Omega = (x_1, \ldots, x_n)$. For each element of sample space $X \in \Omega$, a

probability $f(x)$ is assigned to each sample such that

$$f(x) \in [0,1] \text{ for all } x \in \Omega \tag{3a}$$

$$\sum_{x \in \Omega} f(x) = 1\,. \tag{3b}$$

The function $f(x)$ also called *probability mass function*, which is a mapping from sample space to probability space, i.e. $f : \Omega \to [0,1]$. For an event set $E \in \Omega$, the probability of X being in the event E is given as

$$\mathrm{P}(X \in E) = \int_{x \in E} f(x)dx \tag{4}$$

Similarly, for a continuous random variable $X \in \mathbb{R}$ defined in real space, *cumulative distribution function* (CDF) or simply *distribution function* $F(x)$ is defined by $F(x) = \mathrm{P}(X \leq x)$, where P is the probability and x is a particular realization of random variable. If $F(x)$ is absolutely continuous, then differentiating $F(x)$ with respect to x yields *probability density function* (PDF) $f(x)$.

Similarly, probability for more than one continuous variable is given by joint distribution and density function. For example, for two random variables X and Y, joint PDF $f(x,y)$ has following properties

$$f(x,y) \in [0,1] \text{ for all } (x,y) \in \Omega \tag{5a}$$

$$\int_{-\infty}^{\infty}\int_{-\infty}^{\infty} f(x,y)dxdx = 1 \tag{5b}$$

$$\mathrm{P}[(X,Y) \in E] = \int\int_{(X,Y)\in E} f(x,y)dxdx \tag{5c}$$

which can be further extended to more than two variables. For given joint distribution $P(X,Y)$ of two variables X and Y, distribution of individual variable ($\mathrm{P}(X)$ or $\mathrm{P}(Y)$) can be evaluated by *marginalizing* over the distribution of other variable i.e. integrating over the domain of other variable as $f_x(x) = \int_y \mathrm{P}(x,y)dy$ or $f_y(y) = \int_x \mathrm{P}(x,y)dx$, where $f_x(x)$ and $f_y(y)$ are called *marginal distributions* of X and Y, respectively. Similarly, *conditional distribution* $\mathrm{P}(Y|X)$ is defined as distribution of Y when X is known to be of particular

value and vice versa for $\mathrm{P}(X|Y)$. The joint distribution, marginal distributions and conditional distributions are related as

$$\mathrm{P}(X, Y) = \mathrm{P}(X|Y)\mathrm{P}(Y) = \mathrm{P}(Y|X)\mathrm{P}(X) \tag{6}$$

which can be reformulated to represent *Bayes' theorem* [107]

$$\mathrm{P}(Y|X) = \frac{\mathrm{P}(X|Y)\mathrm{P}(Y)}{\mathrm{P}(X)} \tag{7}$$

Typically, the probability distribution over random variables is defined by some parametric models (like Gaussian distribution, Uniform distribution, Poisson distribution, Exponential distribution, etc.) or by non parametric model (like Kernel density estimates, Mixture models, etc.) [38, 108]. These models are a function of some parameters $\boldsymbol{\theta}$ which has to be estimated based on evidence or data. The parameters $\boldsymbol{\theta}$ can be estimated by parametric estimation methods like methods of moment, *Maximum Likelihood Estimation* (MLE) method, *Maximum a Posteriori* (MAP) method, etc. [38, 108]. These methods can be broadly classified into two schools of philosophies of probability theory: *Frequentist* [38] and *Bayesian* [109] approach. In frequentist approach, an event's probability is the limit of its relative frequency in a large number of trials. For statistical inference of unknown parameters, frequentist approach assumes the parameter to have a fixed but unknown value which has to be inferred from trails. For example, n_t is the total number of trials and n_E is number of trials when event E occurred, then $\mathrm{P}(E) \approx n_E/n_t$. According to frequentist approach, as the number of trials approaches infinity the relative frequency converges to true probability, i.e. $\mathrm{P}(x) = \lim_{n_t \to \infty} n_x/n_t$.

Whereas, in Bayesian approach, probability is interpreted as degree of belief or by state of knowledge. Unlike frequentist approach, a probability is assigned to a hypothesis for a parameter. The statistical inference in Bayesian approach

is based on Bayes' theorem, where some prior subjective probability can be updated in light of some new evidence as

$$\mathrm{P}(\boldsymbol{\theta}|\mathbf{D}) \propto \mathrm{P}(\mathbf{D}|\boldsymbol{\theta})\mathrm{P}(\boldsymbol{\theta}) \tag{8}$$

where $\mathrm{P}(\boldsymbol{\theta})$ is called *prior* probability, $\mathrm{P}(\mathbf{D}|\boldsymbol{\theta})$ is called *likelihood* function and $\mathrm{P}(\boldsymbol{\theta}|\mathbf{D})$ is called the *posterior* probability. Therefore, Bayesian approach allows subjectivity or prior knowledge to be taken into account when sufficient data is not available.

Typically aleatory uncertainties are modeled using probability theory if sufficient information is available. For epistemic uncertainty, when subjectivity or prior information is important, Bayesian approach of probability is preferred [110].

- **Evidence Theory:** *Evidence theory* is also known as *Dempster-Shafer theory* (D-S theory) developed by Dempster and Shafer [111]. In evidence theory, the metrics to measure uncertainty are *belief* and *plausibility*, which are determined from known evidence and information for a proposition. Instead of assigning a precise probability for a proposition, this metric defines the ranges, i.e. lower and upper bounds of the probability based on the evidence.

  Let Σ be the universal set consisting of all the possible set of system and P_Ω (or 2^Σ) be the power set. Evidence theory defines a mass assignment function m such that

$$m : P_\Omega \to [0, 1] \tag{9a}$$

$$\sum_{E \in P_\Omega} (m(E)) = 1 \tag{9b}$$

  which assigns positive mass to the elements of power set P_Ω. Mass assignment can be used to bind the precise probability through belief and plausibility, $\mathrm{Bel}(E) \geq \mathrm{P}(E) \geq \mathrm{Pl}(E)$. The belief $\mathrm{Bel}(E)$ is the sum of mass of all the subsets

of A, which represents the amount of all the evidence supporting the fact that the actual state belongs to A. Plausibility $\mathrm{Pl}(E)$ is the sum of mass of all the sets that intersect with A, which represents the amount of all the evidence that does not rule out the fact that the actual state belongs to A.

$$\mathrm{Bel}(E) = \sum_{B|B\subseteq E} m(B) \tag{10a}$$

$$\mathrm{Pl}(E) = \sum_{B|B\cap E\neq\phi} m(B) \tag{10b}$$

Both metrics are related to each other as

$$\mathrm{Pl}(E) = 1 - \mathrm{Bel}(E) \tag{11a}$$

$$\mathrm{Bel}(E) + \mathrm{Bel}(\bar{E}) \leq 1 \tag{11b}$$

$$\mathrm{Pl}(E) + \mathrm{Pl}(\bar{E}) \geq 1 \tag{11c}$$

where $\bar{E}$ is the complement of E.

Evidence theory can be used to represent both aleatory and epistemic uncertainty. Theoretically, as the availability of information or data increases, the uncertainty representation by evidence theory approaches probability theory. Evidence theory also allows combination of data from multiple sources by using the rules of combination of evidence. Some of the drawbacks of the evidence theory is that it is difficult to interpret and it might be difficult to get information from experts. Also, there are associated computational burdens in terms of uncertainty propagation. More details on Evidence theory can be found in Dempster [40].

- **Possibility Theory:** Possibility Theory introduced by Zadeh [112] extends the concept of fuzzy set to represent uncertainties. In possibility theory, information is available through *possibility distribution* r which expresses the degree the analyst considers at which an event can occur. The subjective knowledge is

modeled with a pair (χ, r) to characterize the uncertain variable x, where χ is the set of possible values of x and r is the possibility distribution such that $r :\rightarrow [0,1]$ $\forall x \in \chi$ and $\sup\{r(x) : x \in \chi\} = 1$. The possibility distribution function r defines a measure of confidence assigned to each element of χ. Similar to evidence theory, possibility theory uses two metrics which define the measure of likelihood for subset of χ: *possibility* and *necessity*. For a subset E, possibility and necessity are defined as

$$\text{Pos}(E) = \sup(r(x) : x \in E) \tag{12a}$$

$$\text{Nec}(E) = 1 - \text{Pos}(\bar{E}) \tag{12b}$$

where $\bar{E}$ is complement of E. $\text{Pos}(E)$ measures the amount of information that does not refute that E contains the instantiation x of the uncertain variable X. $\text{Nec}(E)$ measures the amount of uncontradicted information that supports the affirmation that E contains the instantiation x of the uncertain variable X.

Possibility theory, like evidence theory, can be used to model both aleatory and epistemic uncertainty. Drawbacks of the possibility theory is that it is difficult to interpret and it might be difficult to get information from experts. Also, there are associated computational burdens in terms of uncertainty propagation. More details on Possibility theory can be found in Dubois and Prade [39].

- **Interval Analysis:** Interval analysis [113, 41] is a commonly used method to represent rounding errors and measurement errors in mathematical computation. In interval analysis uncertainty on a variable is represented by a pair of numbers, i.e. maximum and minimum values that the variable is expected to take. Uncertainty propagation is typically carried out using optimization methods or by using interval arithmetic rules. Though interval analysis is an intuitive and straightforward approach, it is unable to consider additional information related to expert's subjectivity or current state of knowledge.

Comparison Selection of mathematical framework to model uncertainty depends upon many factors like available knowledge, available data, ease of implementation, interpretation and understanding, computational requirements for uncertainty propagation process, etc. Though interval analysis seems to be a very intuitive option, it does not allow for any additional information other than the ranges of uncertainties. Evidence theory and possibility theory capture more information and may need relatively less information than probability theory to model uncertainty. Also, both these theories allow a better approach in handling the epistemic uncertainty. However, evidence theory and possibility theory are not commonly used in industrial settings. Also, mathematical methods for uncertainty propagation are typically computationally expensive and still an open area of research. On the other hand, probability theory is one of the well developed theories and it is commonly used in the engineering and scientific community. Uncertainty propagation methods using probability theories are well developed and there are many approaches to overcoming computational burdens to carry out uncertainty propagation. Though there are issues in handling epistemic uncertainty, Bayesian approach helps in overcoming them. Bayesian approach also allows combination and updating of uncertainty with increase in availability of information. Although, choice of uncertainty modeling is very subjective, in the current work probability theory is used because it is well developed, well understood and because of its familiarity among engineers and the scientific community.

2.2.1.3 Uncertainty Identification and Sensitivity Analysis

During the conceptual and preliminary design of an aircraft, a large number of uncertainty sources can exist. Carrying out uncertainty propagation by taking into account all the sources may lead to a huge computational burden due to dimensionality issues. Therefore, it is beneficial to identify the sources of uncertainty that cause significant

uncertainty in the output of the system and screen out the ones which do not have significant impact. Sensitivity Analysis (SA) is the study of how the variation in the model output can be apportioned, qualitatively or quantitatively between variations in model inputs [114]. Sensitivity analysis is typically used before carrying out uncertainty propagation to identify and rank the most influential input uncertainties. Screening out the uncertainty sources based on rank and influence decreases computational cost and model complexity for uncertainty propagation. It also allows allocation of resources on the sources having higher impact on the output so that uncertainty can be managed and reduced.

Most of the sensitivity analysis can be categorized into two groups: *local* and *global* [44]. Local methods are typically involved in taking partial derivative with respect to uncertain variable around a design. Adjoint methods and *Automated Differentiating* falls under this category. Global methods explore the entire uncertainty space and its impact on output. Some of the commonly used global methods are variance decomposition methods (Sobol' Indices [115], ANalyse Of VAriance [116]), linear relationship measures (Correlation Coefficients, Partial Correlation Coefficients, Standardized Regression Coefficient), etc.

2.2.2 Uncertainty Analysis and Propagation

Uncertainty analysis is a procedure to quantify uncertainties on system output by propagating the uncertainties from various sources through the system model. The uncertainty propagation method can be broadly classified into two groups: *intrusive* and *non-intrusive*. In intrusive methods, the mathematical model and the governing equation of the system are reformulated so as to incorporate the uncertainty directly into the system modeling. One of the commonly used approaches for intrusive methods is *Polynomial Chaos Expansion* (PCE) method [67]. In intrusive PCE methods, the coefficient of the expansion is defined by substituting the stochastic process with

its polynomial chaos expansion in the original governing equations. This leads to a coupled system of deterministic equations which can be solved by modifying the existing analysis codes.

Non-intrusive approaches on the other hand treats the deterministic system or simulation model as a black box and does not need any modification of existing simulation codes. Non-intrusive propagation approaches based on probability theory can be broadly classified into six categories.

2.2.2.1 Simulation based methods

In these methods, the input uncertainty space is repeatedly sampled and output of the analysis is evaluated for each sample. Monte Carlo Simulation (MCS) [117] is one such method used to carry out uncertainty propagation. For example, sample mean or expected value of output can be evaluated as $E[Y] = \sum_{i=1}^{N} f(u_i)$, where f is the analysis function, u is the uncertain variable, and N is the number of samples. The error associated with the estimation is proportional to $1/\sqrt{N}$ and does not depend on the dimension of u. If sufficiently large number of samples are used, MCS method can give statistical analysis with fairly accurate results. Therefore, the result of MCS is used as a benchmark for evaluating any other uncertainty propagation technique. Since the MCS method can easily become computationally expensive, other efficient sampling-based methods such as Importance Sampling [118], Adaptive Sampling[119], etc are also used as an alternative.

2.2.2.2 Local Expansion methods

Local expansion methods like Taylor series expansion locally approximates the analysis function and associated moments due to uncertain inputs. For example, a function can be approximated around a local point u_0 as $f(u) = f(u_0) + \sum_{i=1}^{k} \partial f(u_0)/\partial u_i (u_i - u_0(i))$. Based on this approximation, mean and standard deviation can be estimated

as

$$\mu_Y \simeq f(u_0) \tag{13a}$$

$$\sigma_Y \simeq \sqrt{\sum_{i=1}^{k} \left(\frac{\partial f(u_0)}{\partial u_i}\right)^2 \sigma_{u_i}^2 + \sum_{i=1}^{k} \sum_{j=i+1}^{k} \left(\frac{\partial f(u_0)}{\partial u_i}\right) \left(\frac{\partial f(u_0)}{\partial u_j}\right) \mathrm{cov}(u_i, u_j)} \tag{13b}$$

where $\mathrm{cov}(u_i, u_j)$ is the covariance between u_i and u_j. Although these methods are computationally efficient the accuracy of these methods decrease as the function becomes non-linear and the range of input uncertainties increase. Also, these methods require partial derivatives that may be difficult to evaluate for complex models.

2.2.2.3 Reliability methods

Reliability methods are mainly used to estimate the reliability of a system with respect to a given constraint $g(\mathbf{x}) \leq 0$, where the function g is called *limit state function*. The main purpose of reliability analysis is to estimate the probability of failure given by $p_f = \int_D p(\mathbf{x}) d\mathbf{x}$, where D is the region defined by $g(\mathbf{x}) > 0$. Two widely used reliability methods for engineering problems are *First Order Reliability Method* (FORM) and *Second Order Reliability Method* (SORM) [120]. In both these methods, the original non-Gaussian random variable $\mathbf{x}$ are transformed into an uncorrelated Gaussian random variable $\mathbf{u}$ with zero mean and unit variance in the standard normal space using *Rosenblatt transformation* [121], where the transformation is denoted as $\mathbf{x} = T(\mathbf{u})$. Then, the probability of failure is redefined as $p_f = \int_{D_u} \phi(\mathbf{u}) d\mathbf{u}$, where D_U represents the failure region in $\mathbf{U}$ space defined by limit state function $G(\mathbf{u}) = g(T(\mathbf{u})) = 0$. Next, the *Most Probable Point* (MPP), most likely failure point, design point or check point) which is of maximum probability density on the limit state function as shown in Figure 15a is evaluated using an optimization problem

$$\text{minimize} \qquad \beta = ||\mathbf{u}|| \tag{14a}$$

$$\text{with respect to} \qquad \mathbf{u}$$

$$\text{such that} \qquad G(\mathbf{u}) = 0 \tag{14b}$$

Finally, the limit state function is approximated using first or second order approximation at MPP and the probability of failure is estimated using the approximated limit state function. For example, FORM fits a tangent hyperplane at MPP and the probability of failure is given by $p_f \approx \Phi(-\beta)$ as shown in Figure 15b. Similarly, SORM assumes a quadratic function at MPP to evaluate probability of failure.

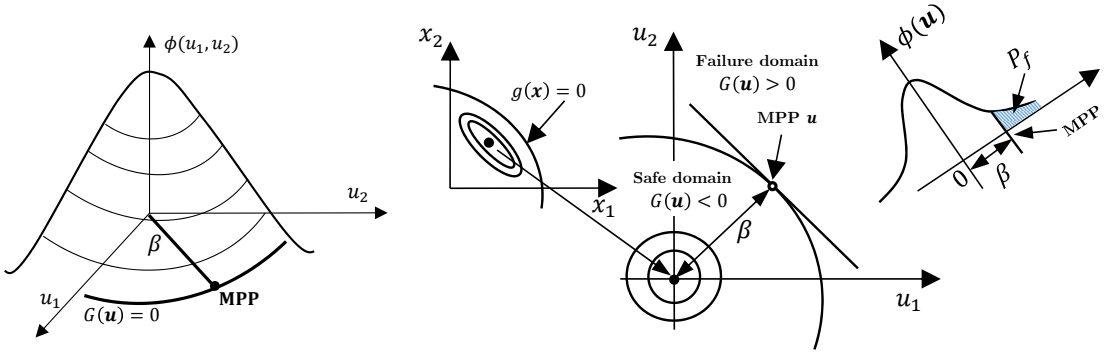

(a) MPP (b) FORM

Figure 15: Most Probable Point (MPP) and First Order Reliability Method (FORM)

2.2.2.4 Numerical Integration-Based Methods

These methods evaluate the statistical moments of output of an analysis by using approximation of multidimensional integral by appropriate quadrature formula [122]. These methods can be used to evaluate any statistical moments of an output. For example, the expected value of the output $y = f(u)$ is given by

$$E(y) = \int_{\Omega} f(u)f(u)du \simeq \sum_{i=1}^{N} f(u^i)w_i \tag{15}$$

where $p(u)$ is the probability density function of u, u^i are the quadrature points or collocation points and w_i are the quadrature coefficients. Quadrature points are generally chosen randomly or according to Gaussian quadrature where the Gaussian quadrature are roots of a polynomial q which is orthogonal to the probability density function $\int_{\Omega} q(u)p(u)w(u)du = 0$. Two commonly used numerical integration-based methods are *full factorial numerical integrations* [123] and *sparse grid approach* [124].

2.2.2.5 Functional Expansion Methods

These methods approximate the function on the entire domain of analysis rather than locally as in local expansion methods. Two commonly used methods are *Polynomial Chaos Expansion* (PCE) [125] and *Stochastic Collocation* (SC)[126]. In PCE, function is approximated using polynomial orthogonal basis as

$$y = f(\mathbf{u}) = a_0 + \sum_{i=1}^{\infty} a_i P_1(u_i) + \sum_{i=1}^{\infty} \sum_{j=1}^{i} P_2(u_i, u_j) + \dots \tag{16}$$

where P_i are orthogonal basis functions of degree i. The choice of polynomial function depends upon the type of distribution of uncertain variables $\mathbf{u}$. The expansion is generally truncated depending on some degrees d and approximation can be rearranged as $f(\mathbf{u}) \simeq \sum_{i=1}^{d} \alpha_i \Psi_i(\mathbf{u})$. The coefficient of the polynomial is estimated through orthogonal spectral projection or by regression method. If appropriate polynomials are used, then the moments of outputs are defined directly as the function of the coefficients.

Similarly, in SC the expansion is based on the *Lagrange interpolation polynomial* and the expansion is given as

$$Y(\mathbf{u}) \simeq \sum_{j_1=1}^{m_1} \sum_{j_2=1}^{m_2} \cdots \sum_{j_k=1}^{m_k} f(u_1^{j_1}, \dots u_k^{j_k})(L_1^{j_1}(u_1, u_1^{j_1}) \otimes \cdots \otimes L_k^{j_k}(u_k, u_k^{j_k})) \tag{17}$$

where $L_1^{j_1}$ is j_1^{th} Lagrange polynomial term for the interpolation in the u_1 direction and $\otimes$ is the tensor product.

2.2.2.6 Surrogate Modeling-Based Methods

Similar to functional expansion methods, surrogate models build the approximate functional forms of analysis function in the domain of interest but unlike PCE or SC the surrogate modeling does not depend on the distribution of input uncertainties. Surrogate models or metamodels can be built using a relatively small number of samples compared to MCS using *Design of Experiment* (DoE) [23] techniques. Depending

on the usage and complexity of the analysis function surrogate modeling techniques can be chosen from several families such as *Response Surface Method* (RSM) [127], *Artificial Neural Network* (ANN), *Support Vector Regression* (SVR), *Radial Basis Function* (RBF), *Gaussian Processes* (GPs), [108] etc. Since, these surrogate models are algebraic functions, it can be used in place of the original analysis function to carry out MCS to propagate uncertainties in a computationally efficient manner.

2.2.3 Optimization under Uncertainty

In a typical aircraft design process, two important criteria or goals for design under uncertainties are *robustness* and *reliability*. The following definitions are used in the current work:

Robustness: *"The degree of tolerance of the system to be insensitive to variations in both the system itself and the environment"* [3].

Reliability: *"The probability that a component (or a system) will perform its intended function without failure for a specified period of time under stated operating conditions"* [26].

The uncertainty management methodologies applied to achieve these goals are called *Robust Design Optimization* and *Reliability Based Design Optimization*. The choice of the methodology depends upon the impact of an adverse event and the frequency of the adverse event as shown in Figure 16.

2.2.3.1 Robust Design Optimization (RDO)

Robust Design Optimization (RDO) method was originally formulated by Japanese engineer Genichi Taguchi. He developed this method to improve the quality of manufactured products such that the product's performance is insensitive to the variation in the variables beyond the control of designer [128]. RDO is a systematic and efficient method to optimize design which is insensitive to variations. Based on the original idea, the mathematical formulation of the RDO method is stated as follows

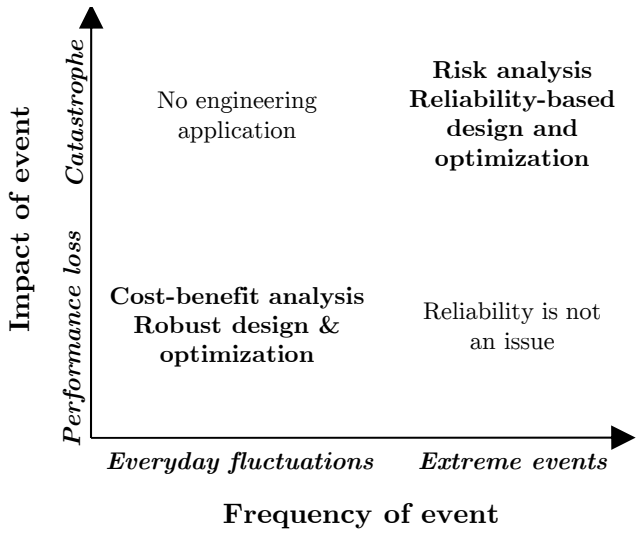

Figure 16: Scenario for uncertainty management methodologies [3]

[129]:

$$\begin{aligned} \text{minimize} \quad & F(\mu_f(\mathbf{x},\mathbf{u}),\sigma_f(\mathbf{x},\mathbf{u})) && \text{(18a)} \\ \text{with respect to} \quad & \mathbf{x} \\ \text{such that} \quad & \mathbf{g}(\mathbf{x},\mathbf{u}) \leq 0 && \text{(18b)} \\ & \mathbf{x}^L \leq \mathbf{x} \leq \mathbf{x}^U && \text{(18c)} \end{aligned}$$

where $\mathbf{x}$ and $\mathbf{u}$ are the design and the uncertain variables, μ_f and σ_f are the mean, and the standard deviation of the variable of interest is given by function $f(\cdot)$, and $F(\cdot)$ is the reformulated objective function with respect to μ_f and σ_f. One of the simplest forms of $F(\cdot)$ is the weighted sum of μ_f and σ_f given as

$$F(\mu_f(\mathbf{x},\mathbf{u}),\sigma_f(\mathbf{x},\mathbf{u})) = k\frac{\mu_f(\mathbf{x},\mathbf{u})}{w_{\mu_f}} + (1-k)\frac{\sigma_f(\mathbf{x},\mathbf{u})}{w_{\sigma_f}} \tag{19}$$

where k is the weighing factor, and w_{μ_f} and w_{σ_f} are scaling factors. The graphical illustration of RDO is shown in Figure 17.

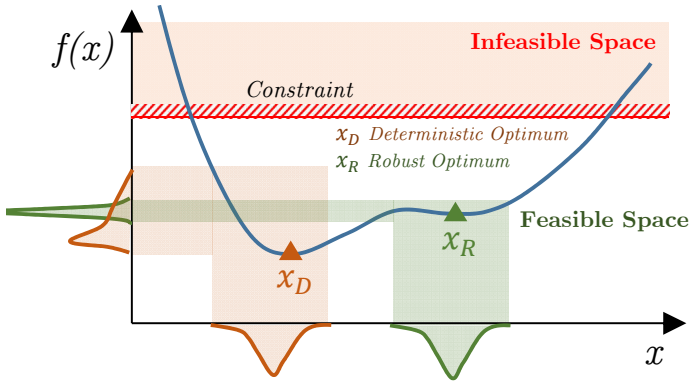

Figure 17: Graphical illustration of Robust Design Optimization (RDO)

2.2.3.2 Reliability-Based Design Optimization (RBDO)

The main focus of Reliability-Based Design Optimization (RBDO) is to obtain an optimal design while meeting the reliability constraints. It is a methodology to optimize design such that the system is reliable with a small chance of failure under a predefined acceptable level [130, 131]. The mathematical formulation of RBDO method is stated as follows:

$$\begin{aligned} \text{minimize} \quad & \mu_f(\mathbf{x}, \mathbf{u}) && \text{(20a)} \\ \text{with respect to} \quad & \mathbf{x} \\ \text{such that} \quad & P(\mathbf{g}(\mathbf{x}, \mathbf{u}) \leq 0) \geq \mathbf{R} && \text{(20b)} \\ & \mathbf{x}^L \leq \mathbf{x} \leq \mathbf{x}^U && \text{(20c)} \end{aligned}$$

where $P(\cdot)$ is the probability of the events described in the function within the parenthesis, and $\mathbf{R}$ is the acceptable level of reliability. The graphical illustration of RDO is shown in Figure 18.

In scenarios, where both robustness and reliability are the criteria of the design, both RDO and RBDO can be combined to formulate *Reliability-Based Robust Design*

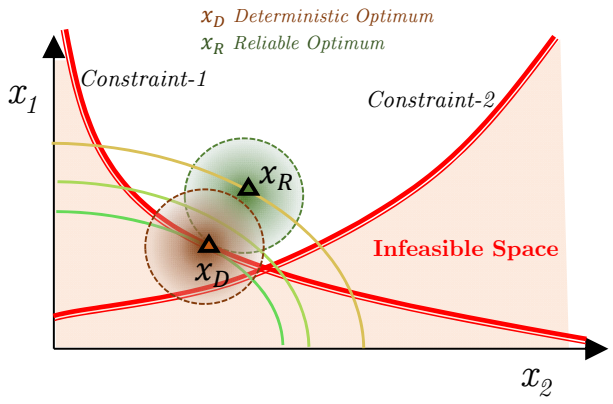

Figure 18: Graphical illustration of Reliability-Based Design Optimization (RDO)

Optimization (RBRDO) [130]. The mathematical formulation is given as:

$$\begin{aligned} \text{minimize} \quad & F(\mu_f(\mathbf{x},\mathbf{u}),\sigma_f(\mathbf{x},\mathbf{u})) && \text{(21a)} \\ \text{with respect to} \quad & \mathbf{x} \\ \text{such that} \quad & P(\mathbf{g}(\mathbf{x},\mathbf{u}) \leq 0) \geq \mathbf{R} && \text{(21b)} \\ & \mathbf{x}^L \leq \mathbf{x} \leq \mathbf{x}^U && \text{(21c)} \end{aligned}$$

2.2.4 UMDO Procedure

A general mathematical framework for a UMDO procedure is given as:

$$\begin{aligned} \text{minimize} \quad & \Upsilon[f(\mathbf{x},\mathbf{u},\mathbf{y})] = \Upsilon_0[f(\mathbf{x},\mathbf{u},\mathbf{y})] + \sum_{i=1}^{N} \Upsilon_i[f(\mathbf{x}_0,\mathbf{x}_i,\mathbf{u}_i,\mathbf{y}_i)] && \text{(22a)} \\ \text{with respect to} \quad & \mathbf{x} \\ \text{such that} \quad & \Theta[g_j(\mathbf{x}_0,\mathbf{x}_i,\mathbf{u}_i,\mathbf{y}_i) \leq 0] > R_{ieq_j} \qquad \text{for } j = 1,\ldots,n_g && \text{(22b)} \\ & \Theta[h_k(\mathbf{x}_0,\mathbf{x}_i,\mathbf{u}_i,\mathbf{y}_i) \leq 0] > R_{eq_k} \qquad \text{for } j = 1,\ldots,n_h && \text{(22c)} \\ & \mathbf{x}^L \leq \mathbf{x} \leq \mathbf{x}^U && \text{(22d)} \end{aligned}$$

$\mathbf{u}$ is the vector of uncertain variables, Υ is the measure of metric of interest like expected value, variance, extreme value, etc. of the variable of interest, Θ is the measure of reliability like probability, plausibility, etc. g_j and h_k are the inequality

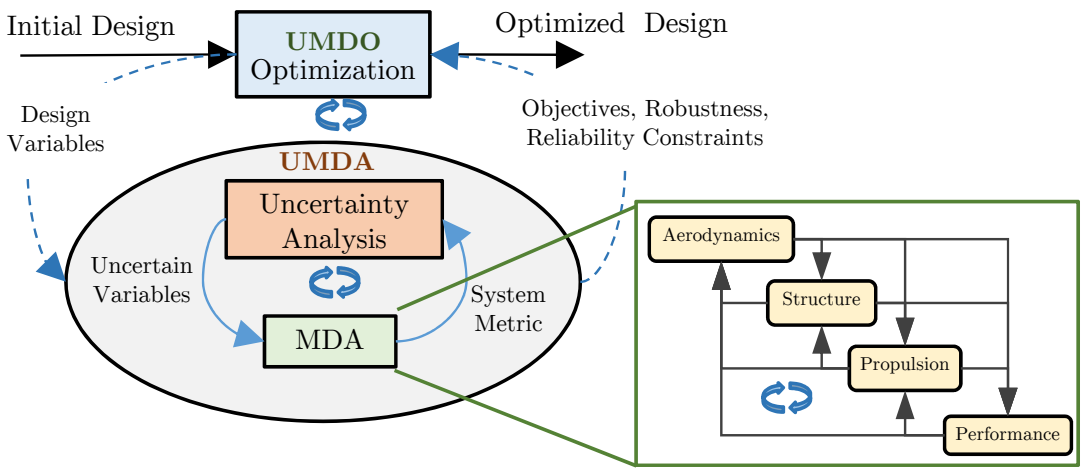

Figure 19: Double loop UMDO procedure

and equality constraints and R_{ieq_j} and R_{eq_k} are the required reliability level. All the other notations are similar to MDO procedure.

A traditional approach to carry out the optimization given in Equation 22 is to replace the model $G(\mathbf{x}, \mathbf{u})$ in Equation 1 by a fully integrated monolithic multidisciplinary analysis (MDA) process. This is also referred to as double-loop strategy as shown in Figure 19. In this strategy, uncertainty based multidisciplinary analysis (UMDA) is carried out by propagating uncertainties through a multidisciplinary system for a fixed setting of design variables in the inner loop. The outer loop carries out optimization process based on the outcomes of UMDA process. The entire process, including the outer loop, inner loop, and multidisciplinary analysis constitutes the uncertainty based design optimization (UDMO) procedure.

The traditional double-loop approach of UDMO procedure can become computationally challenging if high-fidelity disciplinary analyses are involved. Let's consider that the optimizer takes N_{opt} steps to converge to the optimum and at each step of optimization process, an UMDA is carried out using Monte Carlo Simulation (MCS) by propagating N_{MCS} samples of uncertainty variables through a deterministic MDA. Therefore, to carry out UMDO using the traditional double-loop method it requires

$N_{opt} \times N_{MCS}$ deterministic MDA function calls. Also, it should be noted that each deterministic MDA generally requires multiple iterations of disciplinary analyses to achieve interdisciplinary compatibility.

To overcome this computational problem, various UMDO processes have been proposed and can be classified into two categories [61]:

1. **Single level procedure:** In this method, the optimization loop and the uncertainty analysis are either decoupled or are executed in a sequential order or merged into a single equivalent deterministic optimization problem [132, 133, 134, 135, 136, 137]. The main benefit of these methods is that the existing MDO process can be used directly to enhance the efficiency. However single level procedure generally requires an integrated MDA. which can still lead to computational challenges for MDA with high-fidelity disciplinary analysis.

2. **Distributed procedure:** Also called as **decomposition and coordination-based procedure** or **multi-level procedure** for UMDO, applies an equivalent approach of distributed or a multi-level MDO architecture discussed in Section 2.1. In this approach, the overall problem is decomposed and distributed among the discipline or subsystem which carries out disciplinary or subsystem level uncertainty optimization problems, so that each sub-problem is within manageable control. In addition to reducing the computational burden on a single optimizer, the benefit of decomposition and coordination-based procedure is that it allows concurrency and autonomy among all the teams and disciplines.

2.2.5 Distributed UMDO Procedure

Based on the deterministic MDO architecture, many distributed UMDO procedures have been developed in which large scale computationally restrictive problems are decomposed and distributed into several manageable small scale uncertainty optimization problems. The main engine of this UMDO procedure is coordination strategy

by which a consistent optimum is achieved. Some of the commonly used distributed UMDO procedures are discussed here.

2.2.5.1 Collaborative Optimization (CO)-based UMDO Procedure

One of the first UMDO procedures based on Collaborative Optimization (CO) framework was proposed by McAllister et al. [138]. The optimization problem both at system and subsystem level is formulated using multi-objective mathematical formulation called *Decision Support Problem* (DSP). At system level, DSP carries out a robust optimization while minimizing mean and variance of system level metric while maintaining subsystem compatibility constraints. At subsystem level multi-objective compromise DSP is carried out with its first priority being minimization of discrepancy between the target specified by the system level and the local outputs. Second priority is given to optimization of local objectives which are not dealt with at system level. The uncertainty propagation at both levels are carried out using first order Taylor series expansion for mean and variance estimation. It is assumed that the variation of uncertainties are small and the sources of uncertainties are independent. It has been found that the method needs significant iteration to achieve system level compatibility due to equality constraint at system level optimization.

To overcome the problem with convergence caused by the compatibility equality constraints imposed on system level, Gu et al. [139] proposed a Robust Collaborative Optimization (RCO) framework based on an *Implicit Uncertainty Propagation* (IUP) method. In IUP method, the state variable is considered as an auxiliary design variable and its interval is estimated by calculating the *Global Sensitivity Equations* (GSE). Also, it models the uncertainties as an interval given by range of the uncertainties. Based on the IUP method, another RCO approach to handle probabilistic uncertainties has also been developed [140]. However, methods based on IUP relies on first order Taylor series expansion of state variables, which can generate errors

when disciplinary functions are non-linear. Also, IUP methods require repeated GSE calculation, which can be computationally expensive and sometimes it may not be available for certain design points.

To overcome the issues of IUP-based methods, a *Moment-Matching* RCO (MM-RCO) [141] was proposed in which mean and standard deviation of the state variables are also considered as auxiliary design variables in each of the disciplines rather than being estimated by IUP module. During the optimization process, the target for state variables are not only the mean but also the standard deviations. Also, additional interdisciplinary compatibility constraints on the state variable standard deviation are added at the system-level optimization. For example, Equation 23 shows the optimization problem at system level where the auxiliary variables at system level are shared design variable x^0_{sh} and mean and standard deviation of coupling variables $\mu^0_{y_{ij}}$ and $\sigma^0_{y_{ij}}$, respectively. The compatibility constraints are given by $J_i = 0$, which are the objective function for i^{th} subsystem.

System Optimization

$$\begin{aligned} \text{minimize} \quad & F = \mu_f + \kappa\sigma_f && \text{(23a)} \\ \text{with respect to} \quad & X^0_{sys} = [x_{sys}, x^0_{sh}, \mu^0_{y_{ij}}, \sigma^0_{y_{ij}}] \\ \text{such that} \quad & J_i = 0 \quad \forall i && \text{(23b)} \end{aligned}$$

The optimization problem at subsystem level is given as

i^{th} Subsystem Optimization

$$\begin{aligned} \text{minimize} \quad & J_i = ((x^0_{sh})_i - x^i_{sh})^2 + ((\mu^0_{y_{ij}})_i - \mu^i_{y_{ij}})^2 + ((\sigma^0_{y_{ij}})_i - \sigma^i_{y_{ij}})^2 && \text{(24a)} \\ \text{with respect to} \quad & X^i_{ss} = [x^i_{loc}, x^i_{sh}, \mu^i_{y_{ij}}, \sigma^i_{y_{ij}}] \\ \text{such that} \quad & \mu_{g_i} + \kappa\sigma_{g_i} \leq 0 && \text{(24b)} \end{aligned}$$

where the objective is to minimize the discrepancy with respect to the target given by system level (variables with superscript (^{0})) and the output of subsystem while satisfying the local reliability constraint. The design variables are subsystem local variables

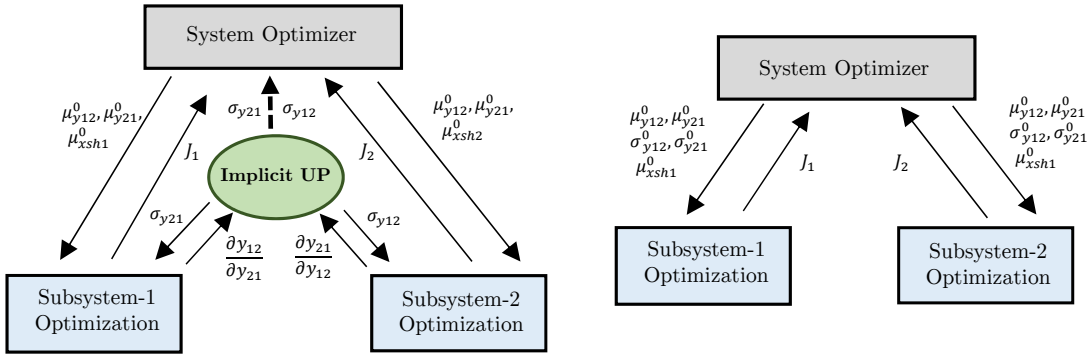

(a) RCO based on IUP (b) Moment Matching RCO

Figure 20: Design architectures of Robust Collaborative Optimization (RCO)

x^i_{sh}, local copy of shared variable x^i_{sh}, local copy of mean and standard deviation of coupling variable associated with each discipline i.e. $\mu^i_{y_{ij}}$ and $\sigma^i_{y_{ij}}$, respectively.

Although MM-RCO overcomes some of the issues of IUP-based RCO methods, it is assumed that it cannot handle the statistical dependency between the coupling variables. To overcome this issue, Ghosh et al. [142] developed a *Covariance Matching Collaborative Optimization* (CMCO) in which discrepancy with respect to correlations among coupling variables are also considered in addition to mean and standard deviation. CMCO assumes that ranges of uncertainty are small and the coupling variables follow multivariate Gaussian distribution.

In another approach based on CO, a novel dual surface based RCO [143] method was proposed where two response surfaces replace the mean and standard deviation estimation of the state variables and system metric. However, a large number of samples are required to build the response surface of mean and standard deviation which can make this process computationally very expensive. Additionally, errors associated with the response surface may also lead to large impact on the uncertainty estimation of system metric.

UMDO methods based on CO does not enforce disciplinary consistency explicitly at each iteration and sensitivities calculated from subsystems are not consistent until the system level optimizer has satisfied the compatibility constraints. This may lead to

inaccuracy of the uncertainty analysis and further influence optimization convergence.

2.2.5.2 Concurrent Subspace Optimization (CSSO)-based UMDO Procedure

Similar to CO, deterministic Concurrent Subspace Optimization (CSSO) framework has also been used for the UMDO procedure. One such method was proposed by Padmanabhan and Batill [144] in which CSSO architecture has been used to realize reliability-based optimization for an MDO problem. In this procedure, system level carries out reliability analysis using FORM method to obtain outputs of objective, intermediate variables, reliability constraints and their sensitivities with respect to deterministic and uncertain variable at the initial design point. This information is then used with first order Taylor series approximation models to build metamodels, which are used in the subspace optimization for estimation of non-local state variables and reliability constraints. These metamodels are then used by subspace optimizer which are executed concurrently to carry out their local optimization. Approximation models are then built using the data obtained from subspace optimization. Next, a *Coordination Procedure* (CP) is carried out with approximation model and the design solution is updated and passed to the system analysis and reliability analysis for next cycle. This process is repeated until convergence is achieved. The process flowchart is shown in Figure 21.

Game Theory-based Composite SubSpace Uncertainty Optimization (GBCSSUO) proposed by Yao et al. [145] integrates *Game Theory* with CSSO procedure and was applied successfully on a space system design problem [60] under uncertainty. In this procedure, approximation model of objectives and coupling variables are built using design of experiment techniques. In each subspace, optimization is carried out where mean and standard deviation of objectives are optimized while satisfying the local reliability constraints. During subspace optimization only accurate analysis tools

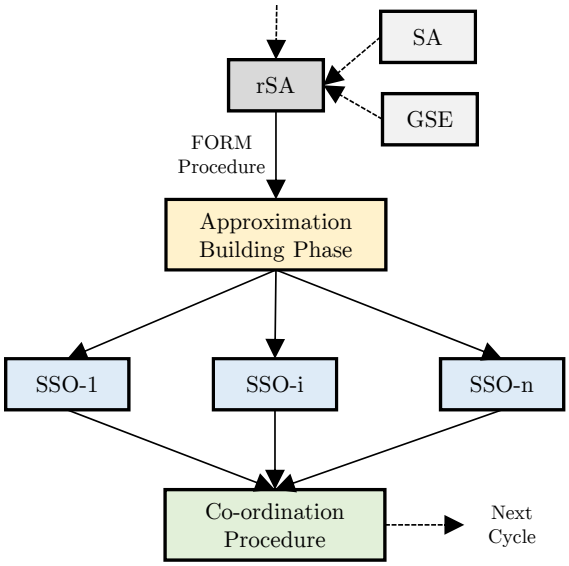

Figure 21: Flowchart of reliability-based CSSO method [144]

associated with the subspace are used, while non-local variables are estimated using approximation models to reduce the computational burden. In the coordination procedure, approximation models are used from each subspace to carry out system optimization. After each cycle, approximation models are updated at the new optimum, which is used for the next cycle. This process is repeated until convergence is achieved. Although the method is flexible in order to carry out system and subsystem optimization, this procedure ignores the cross propagation effect of uncertainties which can lead to inaccurate uncertainty analysis.

2.2.5.3 Analytical Target Cascading (ATC)-based UMDO Procedure

Since Analytical Target Cascading (ATC) is a multilevel MDO method (Figure 22a), the probabilistic version of ATC helps in carrying out uncertainty propagation in a multilevel distributed architecture. One of the earliest UMDO approaches using ATC was proposed by Kokkolaras et al. [146]. The method assumes that the initial uncertainty information is available at the bottom of the hierarchy. A bottom to top coordination strategy is used to propagate uncertainty from lower level to higher level elements in hierarchy. The *Advanced Mean Value* (AMV) method is used to propagate

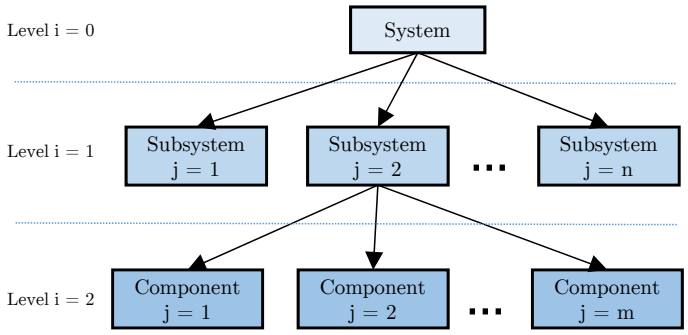

(a) Hierarchy in PATC

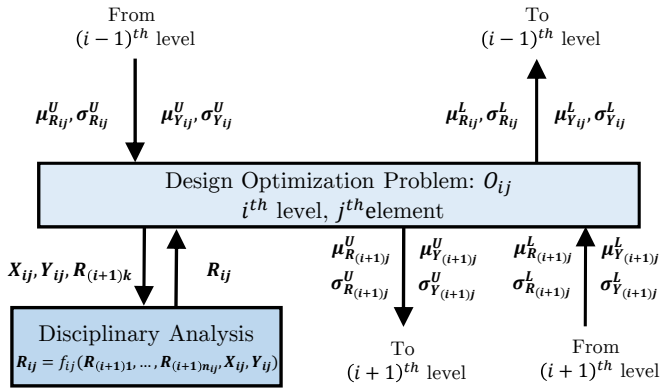

(b) Information flow an element in PATC

Figure 22: Probabilistic Analytical Target Cascading (PATC) architecture

uncertainty and quantify the outputs of each element. The mean and the standard deviation of the responses are then passed on to the parents of the component. The optimization problem is solved in each element, from lower level to upper level, in conjunction with the propagation of the uncertainties in each element. Once the top most level is reached, new targets are cascaded downwards, from top to bottom. With the new targets, elementary optimization is carried out from bottom to top again. The process is continued until convergence is achieved.

In the method proposed by Kokkolaras, coordination is carried out by only matching the mean values of coupling variables between the levels. This creates issues in accurate quantification of uncertainty leading to an inconsistent optimum. Based on the same process, moment-matching formulation of ATC [147] has been developed in

which standard deviations are also matched in addition to the mean values of coupling variables. The information flow for a i^{th} level element is shown in Figure 22b. Further, enhanced probabilistic ATC (EPATC)[148] has been developed, in which covariances are also matched to handle the dependencies of the coupling variables. It has been demonstrated that these improved methods of ATC can solve the same problems as that of the All-In-One (AIO) approach if the uncertainty can be characterized by only two moments and the joint distributions can be represented by joint Gaussian distribution.

CHAPTER III

PROBLEM DEFINITION

In the previous chapter, a brief background on general UMDA and UMDO procedure and state of the art methods on distributed UMDO methods have been discussed. While focusing on the research objective of developing an UMDO methodology to accurately quantify the effect of uncertainties from distributed disciplines on system level metrics of interest, some of the challenges associated with distributed UMDA and UMDO architectures in the existing methods are discussed in this chapter. Based on the gap analysis, the problem definition is carried out by stating the research questions.

3.1 Challenges in Distributed UMDA

A distributed uncertainty based multidisciplinary analysis (UMDA) requires propagation of uncertainties through the disciplines in a parallel, concurrent, independent or "decoupled" manner. This leads to handling of following challenges:

3.1.1 Dependencies among Uncertain Coupling Variables

Dependence is defined as a statistical relationship between two random variables. For example, two random variable X and Y are statistically dependent if their joint probability $P(X,Y)$ is not equal to the product of their probabilities $P(X)$ and $P(Y)$, i.e. $P(X,Y) \neq P(X)P(Y)$. If $P(X,Y) \geq P(X)P(Y)$ then X and Y are called positively dependent, else they are, negatively dependent when the inequality sign is reversed. The degree of dependence may be quantified by some suitable measure of association such as correlation coefficient.

To carryout any arithmetic on random variables it is important to quantify the

dependence among the random variables. For example, mean and variance of the sum of two dependent random variables X and Y with mean of μ_X and μ_Y and standard deviation of σ_X and σ_Y and correlation of ρ_{XY} is given as

$$\mu_{X+Y} = \mu_X + \mu_Y \tag{25a}$$

$$Var_{X+Y} = \sigma_X^2 + \sigma_Y^2 + 2\rho_{XY}\sigma_X^2\sigma_Y^2 \tag{25b}$$

If the magnitude of correlation is relatively small, then the third term on the right hand side of Equation 25b can be neglected. In such a case, assumption of independence among the random variables may be considered. However, if magnitude of correlation is significant, then assumption of independence among random variables will lead to inaccurate quantification of uncertainty for even a simple arithmetic such as $X+Y$. Similarly, in a multidisciplinary analysis under uncertainty, the dependence among disciplinary variables can affect the uncertainty quantification of system level metric. For example, consider a notional multidisciplinary problem of the aircraft weight estimation problem as shown in Figure 23a. At the system level, aircraft weight discipline estimates the take-off gross weights, W_{TOGW}. There are two subsystems, wing and empennage subsystem, which provides wing weight W_{WING} and empennage weight W_{EMPG} to the system level weight discipline. Now, consider that the material properties are uncertain (defined here as U) which affects both wing and empennage subsystems. For uncertainty propagation, Monte Carlo Simulation (MCS) can be used to sample U and for each sample of U a deterministic multidisciplinary analysis is carried out to estimate the uncertainty on W_{WING}, W_{EMPG}, and W_{TOGW}. A single sample of MCS run is notionally shown as star symbol in Figure 23a. Since, the source of uncertainty U is common for both wing and empennage subsystem, the coupling variables W_{WING} and W_{EMPG} will be dependent or correlated. For example, let's assume that the uncertain variable is the material density. A random draw of

U with higher material density will generate a heavier wing weight and heavier empennage weight and vice versa. This dependency is not lost while evaluating W_{TOGW} because of the integrated multidisciplinary environment where MDA is carried out for each sample of U.

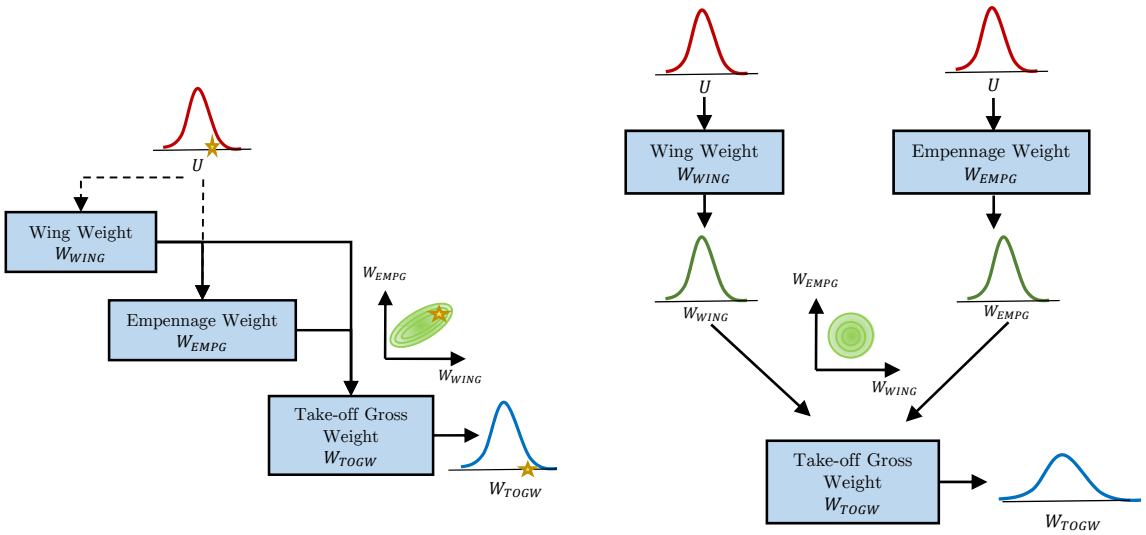

(a) Dependency maintained in integrated UMDA

(b) Dependency lost in distributed UMDA

Figure 23: Dependency of coupling variables

Now consider a distributed design in Figure 23b where uncertainty is propagated independently in wing weight and empennage subsystem. Since, the uncertainty on W_{WING} and W_{EMPG} is quantified in an independent or decoupled manner, the information of the association of these variables with respect to the uncertainty variable U is lost. With only marginal distribution of W_{WING} and W_{EMPG} available to the system level discipline, it has to assume independence between W_{WING} and W_{EMPG}. This leads to inaccurate quantification of uncertainty on system level metric W_{TOGW}. Therefore, handling of dependency is one of the challenging aspects of distributed UMDA.

3.1.2 Interdisciplinary Compatibility

This challenge is generally concerned with any equality constraints in distributed UMDA. However, it is most critical for interdisciplinary compatibility constraint. Without satisfying this constraint, a consistent solution cannot be achieved. In Section 2.1, the interdisciplinary constraint is stated by Equation 2d, which ensures that the coupling variables are consistent in all the disciplines. For example, consider a simple *deterministic* multidisciplinary problem with aerodynamics and weight as two disciplines, with weight W and lift to drag ratio L/D as coupling variables. W_A is the input and L/D_A is the output of aerodynamic discipline and L/D_W is the input and W_W is the output of weight discipline. Subscripts $()_A$ and $()_W$ refer to the variables associated with aerodynamic and weight discipline respectively. The interdisciplinary compatibility is satisfied when $W_A = W_W = W^*$ and $L/D_A = L/D_W = L/D^*$. A typical method to achieve this in a deterministic MDA is using Fixed Point Iteration (FPI) method. In FPI, a guess weight W^* is used as input to the aerodynamic discipline to evaluate L/D^*. This L/D^* is then used as an input to weight discipline to evaluate W'. If $W^* \neq W'$, the guess value of W^* is updated and the process is repeated until $W^* = W'$ within some specified tolerance.

Now, consider the same multidisciplinary problem under uncertainty, where uncertainties U are associated with aerodynamic and weight disciplines. To carry out uncertainty propagation in an integrated and coupled MDA framework a relatively simple method, *Sampling Outside Fixed Point Iteration* (SOFPI) can be used. In SOFPI, Monte Carlo sampling is used to sample uncertainty variables U and for each sample of U an FPI is carried out in a deterministic MDA framework. Since, the interdisciplinary compatibility is satisfied for each sample of U, the joint distribution is given by the converged samples of L/D^* and W^* is the true joint distribution of interdisciplinary compatible solutions.

To carry out uncertainty propagation in a distributed fashion, one of the common

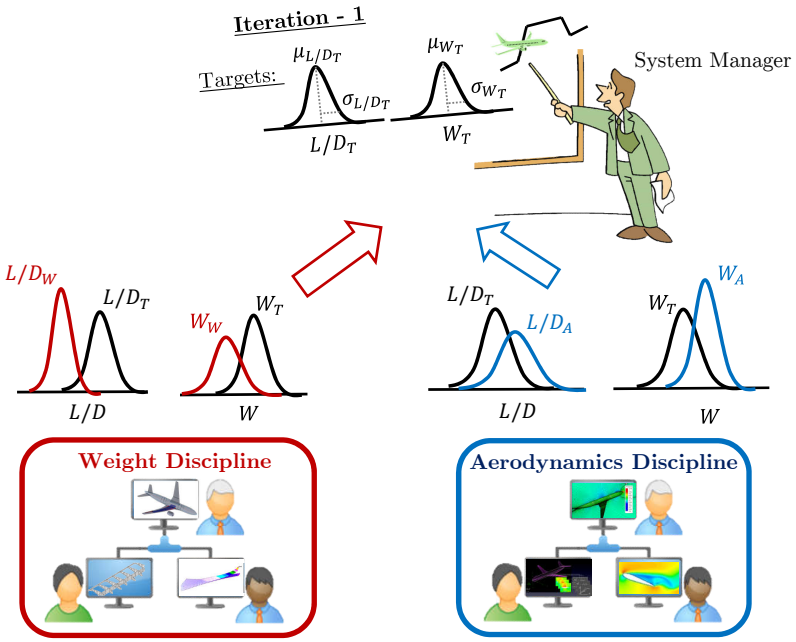

Figure 24: Handling of interdisciplinary compatibility by matching marginal distributions

state of the art approaches is *Moment-Matching* strategy (used at each step of optimization process in UMDO methods based on CO, ATC, etc.). In Moment-Matching matching strategy, the system designer sets target moments for each coupling variable (L/D_T and W_T) as shown notionally in Figure 24. Generally, the target moments are specified by the first few moments like mean and standard deviation. Each subsystem carries out uncertainty analysis independently and optimizes probability distribution of input variables to reduce the discrepancy between target moments and the moments of local coupling variables. For example, weight discipline minimizes $J_W = ||\mu_{W_T} - \mu_{W_W}||^2 + ||\sigma_{W_T} - \sigma_{W_W}||^2 + ||\mu_{L/D_T} - \mu_{L/D_W}||^2 + ||\sigma_{L/D_T} - \sigma_{L/D_W}||^2$ by optimizing the probability distribution of its input variable W_W by tweaking μ_{L/D_W} and σ_{L/D_W}. Each discipline reports the discrepancy J_W and J_A to the system level after finishing their optimization process. Based on the discrepancy information, the system designer provides new target moments of L/D_T and W_T to each subsystem for the next iteration of disciplinary optimization. This is repeated until the discrepancy

is less than the specified tolerance.

However, there are few shortcomings in the Moment-Matching strategy.

- Matching only few moments such as mean and standard deviation is not sufficient. Two probability distributions can have the same mean and standard deviation but can have a different probability density functions as shown in Figure 25a.

- Matching only the marginal distributions are also not sufficient. Different disciplines can have different dependencies between input and output coupling variables while having the same marginal distributions. Figure 25b shows two joint distributions of random variables y_1 and y_2. Both joint distributions have very similar marginals but their dependencies are different.

- Moment-matching strategy does not ensure that interdisciplinary compatibility is satisfied for each instantiation of uncertain variables. Although, other methods based on *approximate model sharing strategy* (used by distributed UMDO methods based on CSSO) may ensure compatibility for each instantiation of uncertain variables, most of these methods are not applicable when disciplinary analyses are stochastic or non-deterministic, i.e. disciplinary functions are not explicit functions of uncertain variables and outputs of the disciplinary analyses are random variables (defined by joint probability density) for a fixed deterministic value of input. This generally happens when aleatory uncertainties are present in the disciplinary analyses and act as noise or natural randomness. For example, if a wing aerodynamic discipline requires a physical experiment, then for a fixed wing design the aerodynamic performance evaluated by wind tunnel test can have uncertainty due to various experimental noises and errors. In a modeling and simulation environment, there can be implicit uncertainty due to numerical error, model form error, uncertainty associated with expert

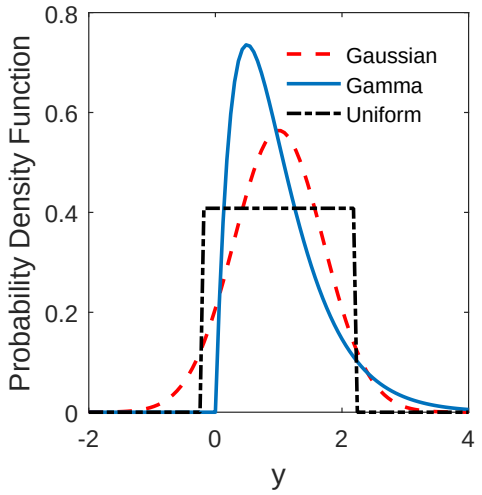

(a) Probability density functions with same mean and standard deviation

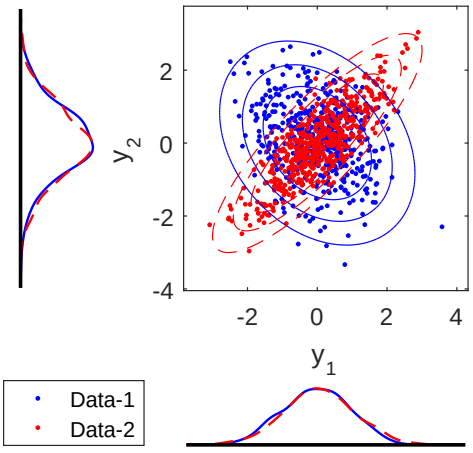

(b) Two joint distributions with same marginals but different dependency

Figure 25: Shortcomings of matching moments and marginal distribution for inter-disciplinary compatibility

judgment, etc. Under such scenarios, the disciplinary outputs cannot be modeled by explicit function of uncertain variables and approximate model sharing strategy cannot be used for UMDA.

Effect of dependency in UMDA: A numerical demonstration Consider a simple analytical problem with two disciplines given in Equation 26.

$$y_1 = x_1^2 + x_2 + x_3 - 0.2y_2 \tag{26a}$$

$$y_2 = \sqrt{y_1} + x_1 + x_3 \tag{26b}$$

where y_1 and y_2 are the coupling variables and x_1, x_2 and x_3 are the uncertain variables. The uncertain variables are assumed to have Gaussian distribution with mean $\mu_{x_i} = 1.0$ and standard deviation $\sigma_{x_i} = 0.1$. Uncertain variables x_1 and x_3 are assumed to be dependent with correlation ρ_{x_1,x_3}. The correlation is varied between $(-0.95, 0.95)$ and for each setting of ρ_{x_1,x_3} an integrated UMDA process is carried out to estimate the joint distribution of coupling variables. In each integrated UMDA

process, 500,000 samples of uncertain variables are used and for each instance of uncertain variables a deterministic MDA problem is solved to find the solution of coupling variables. Samples of converged coupling variables are then used to evaluate the correlation of coupling variables for each setting of ρ_{x_1,x_3}. Figure 26a shows the correlation of coupling variables ρ_{y_1,y_2} as a function of correlation of input uncertain variables ρ_{x_1,x_3}.

Consider a system metric of the form

$$f = y_2 - \alpha y_1 \tag{27}$$

where statistics on f is estimated by using the samples of converged solutions of the coupling variables and α is a parameter which is varied between 0.5 and 0.9. Figure 26b shows the trend of standard deviation of the system metric, σ_f as a function of ρ_{x_1,x_3} for different setting of α. As observed, only in the case of $\alpha = 0.9$, σ_f is not sensitive to the dependency of uncertain variables. Only in this scenario, distributed UMDA methods based on Moment-Matching such as CO and ATC-based UMDA methods are appropriate, which assumes independence in the coupling variables. However in all the other setting of α, σ_f is sensitive to the dependency of uncertainty variables. Under these scenarios, it is important to handle the dependency among uncertainty variables, which is not handled by the distributed UMDA methods based on Moment-Matching approach.

The challenges related to dependency and interdisciplinary compatibility leads to the first research question:

Research Question 1.0: *What is an appropriate method to accurately quantify the uncertainty on system metric and joint distribution of coupling variables while handling the dependency and interdisciplinary compatibility in a distributed multidisciplinary analysis under uncertainty?*

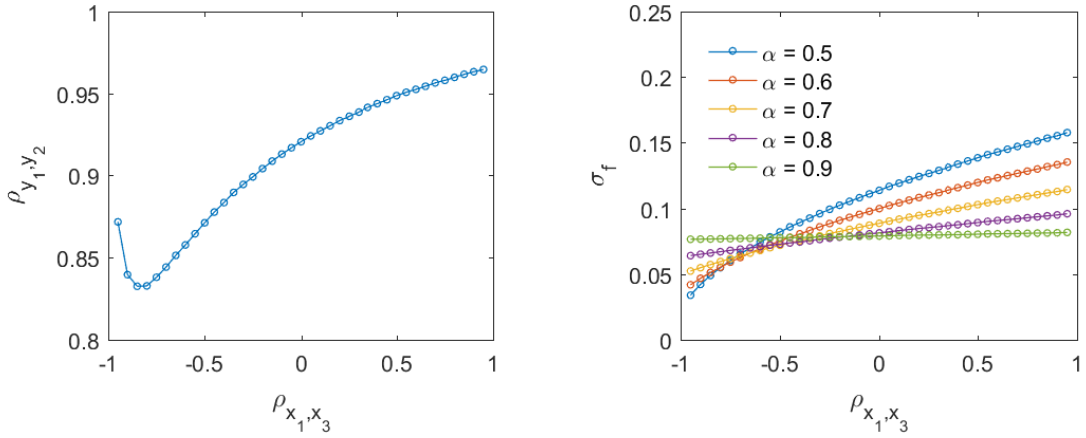

(a) Correlation of coupling variables ρ_{y_1,y_2} as a function of correlation of input uncertainty variables ρ_{x_1,x_3}

(b) Standard deviation of the system metric, σ_f as a function of ρ_{x_1,x_3} for different setting of α

Figure 26: Effect of dependency between uncertainty variables on the coupling variables and system metric

3.2 Challenges with Probabilistic Modeling of Disciplines

One of the commonly used approaches to improve the computational efficiency for design space exploration and optimization in a deterministic multidisciplinary analysis is to build deterministic surrogate models [23]. Deterministic surrogate models are built for disciplinary output as a function of input variables, $\mathbf{y}_i = \tilde{f}_i(\mathbf{x})$. This approach allows each discipline to carry out their analysis independently and build a deterministic surrogate of disciplinary output as a function of design variables and input coupling variables. System level uses these surrogates to execute a integrated single-level multidisciplinary analysis to achieve interdisciplinary compatible solutions and consistent system level metrics. Beside, these surrogate models are of simple algebraic forms, which makes them a computationally efficient option to carry out optimization and design space exploration in a multidisciplinary setting.

A similar approach is also used in UMDO, where each discipline build surrogates of disciplinary metrics as a function of input variables and uncertainty variables, $\mathbf{y}_i = \tilde{f}_i(\mathbf{x}, \mathbf{u}_i)$. Nevertheless, in many scenarios the disciplines may have inherent

aleatory uncertainties or noises such as numerical error, structural uncertainty, experimental uncertainty, interpolation uncertainty, etc. In some cases, expert judgment is also used to improve the disciplinary models. For example, safety factors used in engineering analysis are provided by the disciplinary experts based on their experiences and expert judgment. Generally, these factors are also uncertain and add up to the overall uncertainty of the discipline. Unlike parameter uncertainty, these uncertainties may not always have an explicit form and generally act like a noise. Therefore, instead of deterministic surrogate model of the form $\mathbf{y}_i = \tilde{f}_i(\mathbf{x}, \mathbf{u}_i)$, a non-deterministic model of the form $\mathbf{y}_i = \tilde{f}_i(\mathbf{x}) + \epsilon_i$ is more applicable, where ϵ_i is the inherent noise or uncertainty associated with the discipline.

Probabilistic modeling is one of the common approaches to model disciplinary function of the form $\mathbf{y}_i = \tilde{f}_i(\mathbf{x}) + \epsilon_i$. In probabilistic modeling, the uncertainty or the noise is defined by a certain probability distribution function and hence disciplinary output is given by conditional probability distribution for any given input variable setting. For example, assuming the uncertainty is defined by Gaussian distribution, conditional probability of disciplinary output is given as $\mathrm{P}(y|\mathbf{x}, \mathbf{w}) = \mathcal{N}(y|\mu(\mathbf{x}, \mathbf{w}), \beta^{-1})$, where $\mu(\mathbf{x}, \mathbf{w})$ is the function determining the mean for a given value of $\mathbf{x}$, $\mathbf{w}$ are the unknown parameters of the mean function, β is the unknown precision or inverse of variance of the uncertainty. Some of the commonly used probabilistic models are Bayesian regression, Gaussian Processes, Probabilistic Neural Network, etc [108].

Although many probabilistic models exist in statistics and machine learning literature, there are some limitations in these models when applied to probabilistic modeling of engineering disciplines for multidisciplinary analysis. The limitations which have the most effect on uncertainty quantification in an UMDA are *non-Gaussian noises*, *heteroskedasticity*, and *multivariate responses*. Generally, most of the probabilistic models assume that the uncertainty on output variables have Gaussian distribution. Although these assumptions are valid for most of the scenarios where

these uncertainties arise due to random noise, this may not be valid if some local disciplinary uncertainty causes non-Gaussian behavior in the disciplinary outputs. Although probabilistic models like the *Generalized linear model (GLM)* allows uncertainty distribution models other than Gaussian distribution, this approach assumes that uncertainty will follow the same distribution form in the entire space of $\mathbf{x}$. However, this assumption breaks down when the form of uncertainty distribution varies with $\mathbf{x}$.

Another challenge is to model *heteroskedasticity*, which refers to the situation when variance of output variables varies in the range of input variables. Most of the probabilistic models assume that the variance or precision of output variable is constant in the design space. Nonetheless, this is not always true for a typical disciplinary analysis. For example, consider an aerodynamic discipline which uses the Euler equation to carry out aerodynamic analysis. Since the Euler equation is valid for inviscid flow, uncertainty of the analysis will be small for smaller values of Mach number. However, as the Mach number increases, the uncertainty will rise due to the viscous effect of the flow condition.

Also, engineering subsystem or disciplinary analysis may have multiple responses and these responses are functionally dependent and in the presence of uncertainties these multiple responses are also statistically dependent on each other. Therefore, it is also important to model their dependencies in addition to their conditional distributions. An approach to extend the probabilistic modeling of a single response to multivariate responses is by using a parametric multivariate distribution function such as multivariate Gaussian distribution as $\mathrm{P}(\mathbf{y}|\mathbf{x},\mathbf{w}) = \mathcal{N}(\mathbf{y}|\boldsymbol{\mu}(\mathbf{x},\mathbf{w}),\boldsymbol{\Sigma})$, where $\mathbf{y} \in \mathbb{R}^{1\times n}$ is vector of n outputs and $\boldsymbol{\mu}(\mathbf{x},\mathbf{w})$ is multivariate regression of conditional mean and $\boldsymbol{\Sigma} \in \mathbb{R}^{n\times n}$ is a covariance matrix. The limitation of using multivariate Gaussian distribution is that it assumes that the marginal distribution for

each response is a Gaussian distribution. Limited options are available to model non-Gaussian marginal distributions using a parametric multivariate distribution function such as *Matrix gamma distribution*, *Multivariate t-distribution*, *Wishart distribution*, *Hotelling's T-squared distribution*, etc. Models using any of these parametric multivariate distribution functions have the limitation that the marginal distribution and dependence structures are fixed and the dependence information is coupled with the marginal distribution.

This leads to the second research question:

Research Question 2.0: *What is an appropriate probabilistic modeling technique to comprehensively model conditional probability of multivariate disciplinary response with heteroskedasticity and statistical dependence ?*

3.3 Challenges in Distributed UMDO

In a general procedure to carryout distributed UMDO, system optimizer carries out uncertainty-based design on system level metric, provides uncertainty information on the coupling variables to the subsystems, and maintains the interdisciplinary compatibility and design constraints. Each subsystem level optimizer carries out uncertainty-based design at subsystem level while considering the local uncertainties and maintaining its local reliability constraints. The uncertainty on non-local or coupling variables are handled through some coordination procedure. The coordination procedure also provides sensitivity information to the subsystem optimizer to determine the cost function for the optimization process. For example, if increasing the range is the purpose of a system level optimizer, an aerodynamic discipline will try to minimize "negative" of lift to drag ratio ($-L/D$) while a structural discipline will minimize "positive" of take-off gross weight (W_{TOGW}).

Two commonly used coordination procedures are *target matching strategy* and *approximate model sharing strategy* (both discussed in detail in Chapter 6). Methods

based on target matching strategy such as CO-based method, ATC-based methods, etc. can carry out distributed optimization under uncertainty; however handling of dependencies of coupling variable is limited. Although these methods can handle non-deterministic disciplines, they assume coupling variables have Gaussian distribution and represent the uncertainty on coupling variables by using the mean and standard deviation. A method based on approximate model sharing strategy such as a CSSO-based method, can handle the dependencies and non-Gaussian coupling variables. However, they are not applicable to non-deterministic disciplines, as they are limited by deterministic approximated models. The characteristics of distributed UMDO methods are compared in Table 2.

All the aforementioned characteristics such as handling of dependencies, interdisciplinary compatibility, non-Gaussian uncertainties and heteroskedasticity are important for accurate quantification of dependencies as well as uncertainty on coupling variables and system level metrics. Based on the limitation of existing distributed UMDO method the third research question is:

Research Question 3.0: *What is an appropriate procedure to carry out distributed optimization of a multidisciplinary system under uncertainty to accurately quantify the dependency and uncertainty on coupling variables and system metrics for non-deterministic disciplinary analyses ?*

Table 2: Characteristics comparison of distributed UMDO methods

	Distributed Optimization	**Dependency Handling**	**Non-Deterministic Discipline**	**Non-Gaussian Coupling variable**
Single level UMDO	✗	✓	●	✓
CO-based UMDO	✓	●	✓	✗
ATC-based UMDO	✓	●	✓	✗
CSSO-based UMDO	✓	●	✗	●

Note: Single level UMDO is not a distributed UMDO bethod, it is mentioned here as baseline comparison

● signifies methods have that specific characteristic but with limitation.

CHAPTER IV

PROBABILISTIC ANALYSIS OF DISTRIBUTED MULTIDISCIPLINARY ARCHITECTURES (PADMA)

In this chapter, Probabilistic Analysis of Distributed Multidisciplinary Architecturess (PADMA) methodology has been developed to answer the first research question.

Research Question 1.0: *What is an appropriate method to accurately quantify the uncertainty on system metrics and joint distribution of coupling variables while handling the dependency and interdisciplinary compatibility in a distributed multidisciplinary analysis under uncertainty?*

Hypothesis 1.0: *In a distributed multidisciplinary analysis under uncertainty, if accurate conditional probability density functions of disciplinary metrics are available from each discipline, then Probabilistic Analysis of Distributed Multidisciplinary Architectures (PADMA) can accurately quantify the uncertainty on system metrics and joint distribution of coupling variables by evaluating probability of Event of Interdisciplinary Compatibility (EIC).*

In the next section, a general overview of dependence of random variables and modeling of joint probability density function with probabilistic graphical model is discussed. Then, PADMA methodology is discussed in detail for both feed-forward and feedback couplings. This is followed by a discussion on the numerical procedure to carry out the PADMA method. The hypothesis is then validated by using numerical experiments on two problems, and results are compared with benchmark and state of the art method. In the last section, an overall summary of the chapter is discussed.

4.1 Approach Overview

In statistics two random variables, A and B are dependent if their joint probability is not equal to the product of their probabilities i.e $\mathrm{P}(A, B) \neq \mathrm{P}(A)\mathrm{P}(B)$. One of the common metrics to quantify dependency is correlation coefficients, ρ. Pearson's correlation coefficient is one of the commonly used correlation coefficient to model linear dependencies. For examples, consider n continuous random variables $\mathbf{x} = [x_1, \ldots, x_n]$ with Gaussian distribution with mean vector $\boldsymbol{\mu} = [\mu_{x_1}, \ldots, \mu_{x_n}]^T$, standard deviation $\boldsymbol{\sigma} = [\sigma_{x_1}, \ldots, \sigma_{x_n}]$. If a correlation coefficient matrix $\mathbf{R}$ is defined such that i^{th} column and j^{th} row contains the correlation coefficient of x_i and x_n i.e. $\mathbf{R}_{ij} = \rho_{ij}$ and $\boldsymbol{R}_{ij} = \boldsymbol{R}_{ji}$, then the joint distribution of $\mathbf{x}$ is given as $\mathbf{x} \sim \mathcal{N}(\boldsymbol{\mu}, \boldsymbol{\Sigma})$, where

$$\mathcal{N}(\boldsymbol{\mu}, \boldsymbol{\Sigma}) = \frac{1}{\sqrt{(2\pi)^n |\boldsymbol{\Sigma}|}} \exp\left(-\frac{1}{2}(\mathbf{x} - \boldsymbol{\mu})^{\mathrm{T}} \boldsymbol{\Sigma}^{-1} (\mathbf{x} - \boldsymbol{\mu})\right), \tag{28a}$$

$$\text{where } \boldsymbol{\Sigma} = \mathrm{diag}(\boldsymbol{\sigma}) \boldsymbol{R} \mathrm{diag}(\boldsymbol{\sigma}) \tag{28b}$$

where $\mathrm{diag}(\boldsymbol{\sigma})$ is a diagonal matrix with diagonal entries $\sigma_{x_1}, \ldots, \sigma_{x_n}$. However, Pearson's correlation coefficient is only sensitive to the linear relationship between random variables, and Equation 28 assumes a multivariate Gaussian dependency structure with Gaussian marginal distributions. Although other correlation coefficients and joint distribution functions exist for non-linear dependencies and non-elliptical dependency structures, they are limited.

A general form of joint density function is given by *general product rule* in probability theory [38]. Using general product rule for n continuous random variable $x_1, \ldots, x_n$, joint probability density function is given as

$$f_{\mathbf{x}}(x_1, \ldots, x_n) = f_{x_n}(x_n | x_{n-1}, \ldots, x_1) f_{x_{n-1}}(x_{n-1} | x_{n-2}, \ldots, x_1) \cdots f_{x_1}(x_1) \tag{29}$$

where the order of the variables is arbitrary and $f_{x_k}(x_k | x_{k-1}, \ldots, x_1)$ is the conditional probability density function of x_k given $x_{k-1}, \ldots, x_1$. This formulation does not assume any correlation or dependency structures. The dependencies are embedded

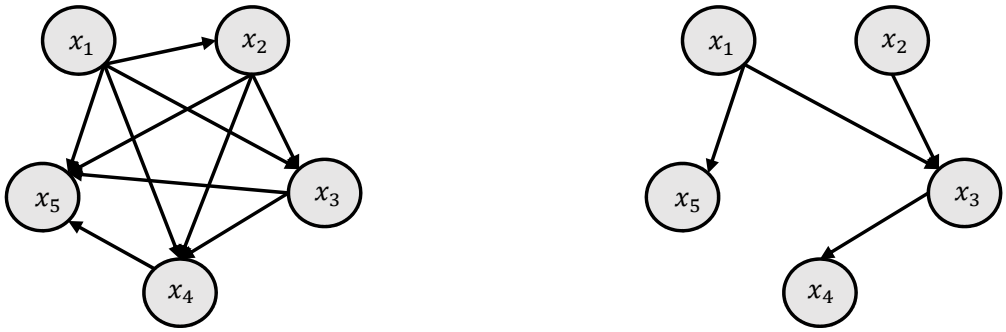

(a) Saturated BN (b) Unsaturated BN

Figure 27: A notional example of directed acyclic graph used by Bayesian Network (BN) representing variables and their dependencies

in the conditional probability density functions which define the overall dependency structure of the joint distribution. For a two random variable $x_1 \sim \mathcal{N}(\mu_{x_1}, \sigma_{x_1})$ and $x_2 \sim \mathcal{N}(\mu_{x_2}, \sigma_{x_2})$ and correlation coefficient ρ, one can retrieve Equation 28 by using $f_{x_2}(x_2) = \mathcal{N}(\mu_{x_1}, \sigma_{x_1})$ and $f_{x_1}(x_1|x_2) = \mathcal{N}\left(\mu_{x_1} + \frac{\sigma_{x_1}}{\sigma_{x_2}}\rho(x_2 - \mu_{x_2}),\ (1-\rho^2)\sigma_{x_1}^2\right)$ in Equation 29.

The general form of the joint density function is particularly appropriate for an engineering analysis problems under uncertainty where the functional relationship between the input and output variables are non-linear and the probability density function of input or output does not have a general parametric form. As in an engineering analysis with x as an input and y as an output, modeling joint distribution with Equation 29 as $f_{xy}(x, y) = f_y(y|x)f_x(x)$ allows greater flexibility as compared to assuming a fixed joint distribution function as in Equation 28.

In the domain of *Probabilistic Graphical Model* of *Machine Learning* [149], the general form of joint distribution given by Equation 29 forms the fundamental equation to model joint distribution of random variables. *Bayesian Network (BN)* [150] is one of the commonly used probabilistic graphical models which represent the dependencies among random variables using a directed acyclic graph and evaluate the joint distribution using the general form of joint distribution. In Bayesian Network,

the random variables are represented using a *node* and the conditional dependencies are depicted using *arrows*. For examples, Figure 27a shows a Bayesian Network of five random variables x_1, x_2, x_3, x_4, and x_5. Two arrows going into x_3 from x_1 and x_2 signify that x_3 is conditionally dependent on x_1 and x_2 with some conditional probability $f_{x_3}(x_3|x_1, x_2)$. In this case, x_3 is called *child* node and x_1 and x_2 are called *parent* nodes. The joint distribution of all the variables can be given by

$$\begin{aligned} f_{\mathbf{x}}(x_1, x_2, x_3, x_4, x_5) =& f_{x_5}(x_5|x_4, x_3, x_2, x_1) f_{x_4}(x_4|x_3, x_2, x_1) \times \\ & f_{x_3}(x_3|x_2, x_1) f_{x_2}(x_2|x_1) f_{x_1}(x_1) \end{aligned} \tag{30}$$

The graph in Figure 27a is also called a *saturated graph* as each node is connected to all the other nodes. In other words, each variable is *directly* dependent on all the other variables. However, in most realistic scenarios some variables are only directly dependent on only a few other variables. For example, Figure 27b shows an unsaturated graph where only a few variables are directly dependent on each other. Since in an unsaturated graph some variables have fewer parent nodes, *conditional independence* [151] can be applied to their conditional probabilities. For example, as x_5 only depends on x_1 in an unsaturated graph, the conditional probability of x_5 can be simplified as

$$f_{x_5}(x_5|x_4, x_3, x_2, x_1) = f_{x_5}(x_5|x_1) \tag{31}$$

Applying conditional independence to all the other variables, the joint probability function of all the variables in the unsaturated graph given in Figure 27b can be simplified as

$$f_{\mathbf{x}}(x_1, x_2, x_3, x_4, x_5) = f_{x_5}(x_5|x_1) f_{x_4}(x_4|x_3) f_{x_3}(x_3|x_2, x_1) f_{x_2}(x_2) f_{x_1}(x_1) \tag{32}$$

Applying the concept of conditional independence for any arbitrary unsaturated graph, the the general form of joint distribution given by Equation 29 can be simplified as

$$f_{\mathbf{x}}(x_1, \ldots, x_n) = \prod_{k=1}^{n} f_{x_k}(x_k|Parent(x_k)) \tag{33}$$

where $Parent(x_k)$ are the set of variables which are the parent nodes of x_k.

A variable in an unsaturated graph which is not directly linked or dependent on some other variable, can still have *indirect* dependence through the intermediate variables which lie in the *path* between the variables [1]. For example, consider the unsaturated graph in Figure 27b. Variable x_4 which is the child node of x_3 is not directly dependent on x_1. However, x_3 is the child node of x_4 and is directly dependent on it. Therefore, any change in x_1 will influence x_3 which will indirectly affect x_4.

In a multidisciplinary problem there exists both direct and indirect dependency. For example, consider a multidisciplinary problem under uncertainty shown in Figure 28b. The problem consists of three variables; wing area(S), drag (D), and thrust (T). Drag is conditionally dependent on wing area due to aerodynamics with conditional probability function $f_D(D|S)$. Thrust is conditionally dependent on drag through propulsion physics, with conditional probability function $f_T(T|D)$. Although, thrust is not directly dependent on wing area, it is indirectly dependent through the intermediate variable, drag. The joint density function of wing area, drag, and thrust using Equation 33 is given as

$$f_{SDT}(S, D, T) = f_T(T|D) f_D(D|S) f_S(S) \tag{34}$$

where $f_S(S)$ is the probability density function of wing area. The formulation of joint density function of random variables given by Equation 33 allows modeling of direct as well indirect dependencies of random variables and is the building block of the PADMA method developed in the following section.

4.2 PADMA Methodology

Probabilistic Analysis of Distributed Multidisciplinary Architectures (PADMA) is a distributed UMDA procedure, where each discipline carries out their uncertainty

[1] Under certain conditions absence of direct dependency between variables may lead to conditional independence. Please refer to concept of D-separation in the theory of Bayesian Network [150]

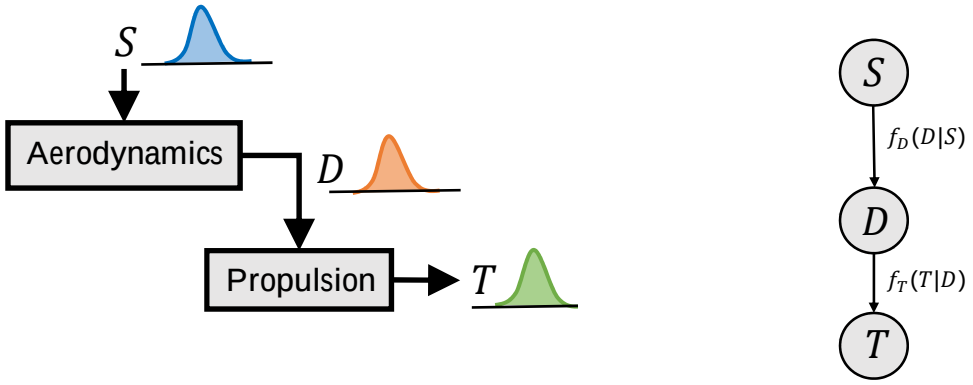

(a) Notional MDA problem under uncertainty (b) BN of MDA

Figure 28: A notional example of MDA problem under uncertainty and Bayesian Network (BN) of the disciplinary variables

propagation and analysis independently and concurrently. It consists of two levels, disciplinary level and system level. At the disciplinary level, each discipline carries out uncertainty propagation independently and concurrently and coordinates with the system level. At the system level, probability of interdisciplinary compatibility is evaluated to calculate the accurate joint probability distribution of coupling variables and system level metrics.

4.2.1 Handling Dependency in Distributed UMDA

In an UMDA with completely decoupled disciplines or subsystems, estimating marginal distributions of coupling variables is sufficient to accurately quantify the uncertainty on system metrics. However, if there is coupling between disciplines or if some variables are shared between disciplines, then it is important to estimate joint distribution of coupling variables to accurately quantify the uncertainty on system metrics. Joint distribution of coupling variables not only contains the information of marginal distribution of each variable, it also contains the dependency information among the variables.

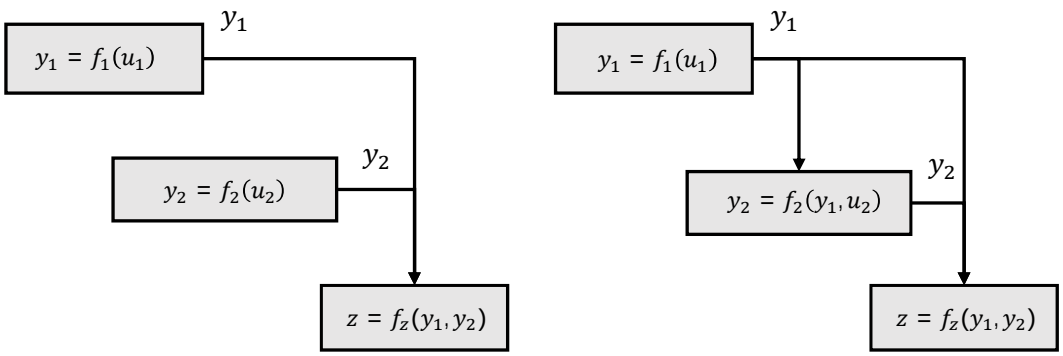

(a) Completely decoupled UMDA (b) Feed-forward coupled UMDA

Figure 29: Notional examples of completely decoupled and feed-forward coupled Uncertainty-based Multidisciplinary Analysis (UMDA)

$$y_1 = f_1(u_1) \tag{35a}$$

$$y_2 = f_2(u_2) \tag{35b}$$

$$z = f_z(y_1, y_2) \tag{35c}$$

For example, consider the notional example of completely decoupled UMDA problem in Figure 29a and given by Equation 35. The output of the first discipline is y_1 and and the output of the second discipline is y_2. u_1 and u_2 are uncertain variables associated with first and second discipline respectively. The disciplinary analyses may or may not be an explicit functions of uncertain variables, i.e. uncertain variables can either be parametric (or epistemic uncertainty) or random noise (aleatory uncertainty) or both. System level metric z is a function of y_1 and y_2. Since the first two disciplines are completely decoupled from each other, y_1 and y_2 are statistically independent to each other. Therefore, marginal distribution of y_1 and y_2 is sufficient to estimate accurate distribution of z. Uncertainty propagation can be carried out independently and concurrently by each discipline to estimate the marginal distributions of y_1 and y_2.

$$y_1 = f_1(u_1) \tag{36a}$$

$$y_2 = f_2(y_1, u_2) \tag{36b}$$

$$z = f_z(y_1, y_2) \tag{36c}$$

Now, consider the MDA problem with feed-forward coupling in Figure 29b and given by Equation 36. The only difference in this problem is that it has a feed-forward coupling from the first discipline to the second discipline. The output of the second discipline y_2 is now also a function of y_1. There is a functional relationship between y_1 and y_2 in the second discipline which leads to a statistical dependency due to the presence of uncertain variables u_1 and u_2. Therefore, to evaluate the uncertainty on system level metric z, accurate estimation of joint distribution of y_1 and y_2 is required.

A straightforward approach to carry out uncertainty propagation in feed-forward MDA is by propagating uncertainty through the first discipline to evaluate uncertainty on y_1, given by probability density function $f_{y_1}(y_1)$. The uncertainty on y_1 is then propagated through the second discipline to evaluate the uncertainty on y_2 and the joint distribution $f_{y_1,y_2}(y_1, y_2)$. $f_{y_1,y_2}(y_1, y_2)$ is then used to evaluate uncertainty on z. However, uncertainty propagation independently and concurrently in a distributed fashion is not a straightforward process because the second discipline needs the information on uncertainty on y_1, i.e. $f_{y_1}(y_1)$. Therefore, the second discipline has to wait until the first discipline finishes its uncertainty propagation process. This creates a sequential process, counteracting the benefit and the need for distributed UMDA.

However, the general form of joint probability distribution given by Equation 33 paves the path for a way to evaluate joint distribution of coupling variables in feed-forward UMDA while allowing each discipline to carry out concurrent and independent uncertainty propagation. According to Equation 33 the joint density function

of compatible solutions of coupling variables for feed-forward MDA given by Equation 36, can be evaluated as

$$f^*_{y_1,y_2}(y_1, y_2) = f_{y_1}(y_1) f_{y_2}(y_2|y_1) \tag{37}$$

As shown in Figure 30 the first term on the left hand side of the equation $f_{y_1}(y_1)$ can be evaluated by carrying out uncertainty propagation in the first discipline independently. The second term, which is the conditional density function $f_{y_2}(y_2|y_1)$, is evaluated by following process. At first, a probability density function on y_1 for is guessed for the second discipline. Let $g_{y_1}(y_1)$ be a guessed density function of y_1. The second discipline uses $g_{y_1}(y_1)$ to propagate the uncertainty independently and concurrently to evaluate the joint density of input and output variable as $g_{y_1,y_2}(y_1, y_2)$. Applying the *product rule* of probability theory, the conditional density function of y_2 given y_1 is given as

$$f_{y_2}(y_2|y_1) = \frac{g_{y_1,y_2}(y_1, y_2)}{g_{y_1}(y_1)} \tag{38}$$

Using this conditional density function evaluated by the second discipline and $f_{y_1}(y_1)$ evaluated by the first discipline, joint density function of y_1 and y_2 is estimated using Equation 37.

Extending the formulation for n disciplines, the joint probability density function of compatible solutions coupling variables in feed-forward UMDA under uncertainty is given as

$$f^*_{\mathbf{y_1},\ldots,\mathbf{y_n}}(\mathbf{y_1}, \ldots, \mathbf{y_n}) = \prod_{i=1}^{n} f_{\mathbf{y_i}|\mathbf{y_{.i}}}(\mathbf{y_i}|\mathbf{y_{.i}}) \tag{39}$$

where $\mathbf{y_i}$ represents output coupling variables of i^{th} discipline, $\mathbf{y_{.i}}$ represents input coupling variables to i^{th} discipline, and $f_{\mathbf{y_i}|\mathbf{y_{.i}}}(\mathbf{y_i}|\mathbf{y_{.i}})$ is conditional probability density of outputs of i^{th} discipline. To evaluate $f_{\mathbf{y_i}|\mathbf{y_{.i}}}(\mathbf{y_i}|\mathbf{y_{.i}})$, each discipline carries out uncertainty propagation with a guessed density function $g_{\mathbf{y_{.i}}}(\mathbf{y_{.i}})$ on input coupling variables and evaluates the joint distribution of input and output coupling variables

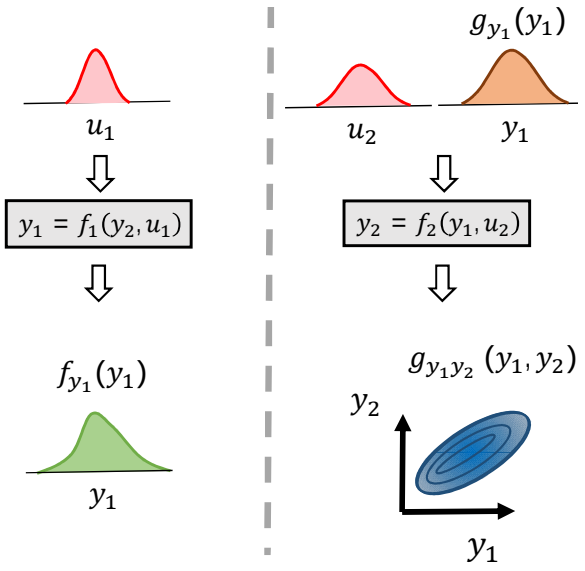

Figure 30: Distributed uncertainty analysis and propagation in feed-forward coupled MDA under uncertainty

$g_{\mathbf{y_i},\mathbf{y_{.i}}}(\mathbf{y_i}, \mathbf{y_{.i}})$. The conditional density function is then given as

$$f_{\mathbf{y_i}|\mathbf{y_{.i}}}(\mathbf{y_i}|\mathbf{y_{.i}}) = \frac{g_{\mathbf{y_i},\mathbf{y_{.i}}}(\mathbf{y_i}, \mathbf{y_{.i}})}{g_{\mathbf{y_{.i}}}(\mathbf{y_{.i}})} \tag{40}$$

4.2.2 Handling Interdisciplinary Compatibility in Distributed UMDA

When there is a feedback coupling in an UMDA, interdisciplinary compatibility is critical to accurately quantify the uncertainty on coupling variables. Interdisciplinary compatibility is defined as reaching a consistent solution of coupling variables which satisfies all the disciplinary relationships simultaneously. This is mathematically equivalent to a achieving a solution of system of coupled equations, where equations represent disciplinary analyses.

To understand the concept of interdisciplinary compatibility in feedback coupled UMDA let's consider a notional two discipline multidisciplinary problem as shown in Figure 31a and given by Equation 41.

$$y_1 = f_1(y_2, u_1) \tag{41a}$$

$$y_2 = f_2(y_1, u_2) \tag{41b}$$

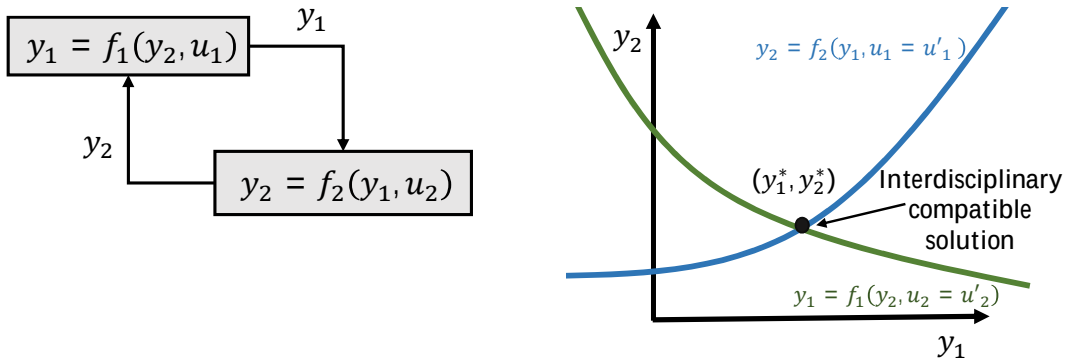

(a) Notional UMDA example with feedback coupling

(b) Notional interdisciplinary compatible solution in deterministic setting

Figure 31: Notional demonstration of deterministic multidisciplinary analysis

In this case, y_1 and y_2 are coupling variables and u_1 and u_2 are uncertainty variables. In a deterministic setting, the value of u_1 and u_2 are known precisely, say $u_1 = u'_1$ and $u_2 = u'_2$. Under such a case, the solution of a system of equations given by Equation 41 is the interdisciplinary compatible solution. Graphically, the intersection point (y_1^*, y_2^*) of notional disciplinary functions shown in Figure 31b is the interdisciplinary compatible solution.

In a non-deterministic scenario, the interdisciplinary compatible solution is given by a joint probability density function over the coupling variables, $f^*_{y_1,y_2}(y_1, y_2)$. A straightforward way to evaluate $f^*_{y_1,y_2}(y_1, y_2)$ is to sample u_1 and u_2 and evaluate the deterministic interdisciplinary compatible solution for each instance of u_1 and u_2. The joint probability density function $f^*_{y_1,y_2}(y_1, y_2)$ is evaluated by samples of all the deterministic solutions. One such method is Simulation Outside Fixed Point Iteration (SOFPI) where Fixed Point Iteration (FPI) is used to find the deterministic solutions for each instance of uncertain variables. This is pictorially demonstrated in Figure 32.

Methods like SOFPI are only applicable when the disciplinary functions can be explicitly determined as a function of uncertain variables. When the disciplinary

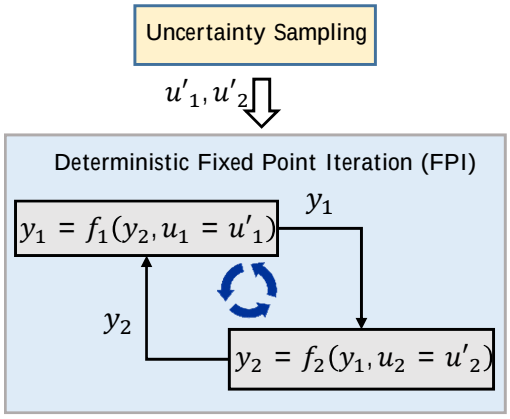

(a) Simulation Outside Fixed Point Iteration (SOFPI)

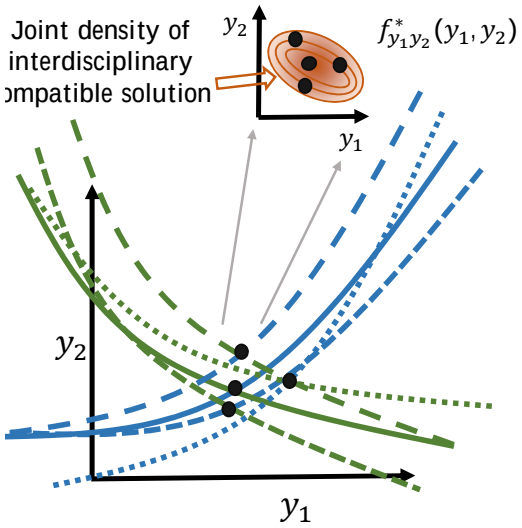

(b) Notional joint probability density of interdisciplinary compatible solutions

Figure 32: Notional demonstration of uncertainty-based multidisciplinary analysis for integrated architecture using Simulation Outside Fixed Point Iteration (SOFPI)

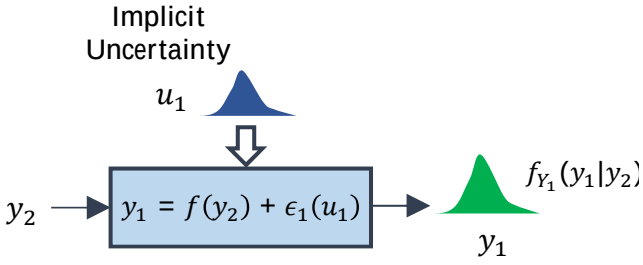

Figure 33: A non-deterministic function

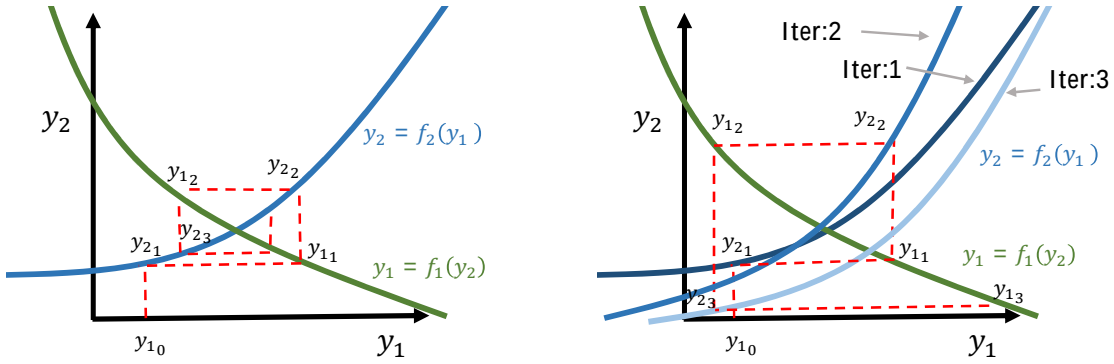

(a) FPI in deterministic case

(b) FPI in non-deterministic case

Figure 34: Notional Fixed Point Iteration (FPI) examples for deterministic and non-deterministic cases

functions are non-deterministic with implicit uncertainty, it cannot be represented by an explicit function of uncertain variables. Under such condition, the disciplinary model generates random output for a fixed value of input due to inherent uncertainty in the disciplinary analyses. In other words, the output of a disciplinary model for a fixed value of input is not a deterministic value but a conditional probability density function of the output as shown in Figure 33.

Under such a circumstance, any root solving algorithm such as fixed point iteration (FPI) will lead to convergence issues. For example, to solve a notional deterministic MDA (Figure 34a) using FPI, a guessed value for $y_1 = y_{1_0}$ is assumed. Note that i in $y_{1_{(i)}}$ represents the iteration number. Using $y_1 = y_{1_0}$ function f_2 is used to evaluate y_{2_1}. Next, function f_1 is used to evaluate y_{1_1} with y_{2_1} as input. This completes one iteration of FPI. If y_{1_1} is not same as y_{1_0}, convergence is not achieved; then FPI carries out another iteration to evaluate y_{2_2} and y_{1_2}. The process is repeated until convergence is achieved.

To understand FPI in an uncertainty scenario, consider a similar MDA problem with disciplinary uncertainty. For simplicity, it is assumed that only the second discipline f_2 is non-deterministic. As explained earlier, if f_2 is evaluated with the fixed value of y_1 multiple times, then each time it will generate a random sample of

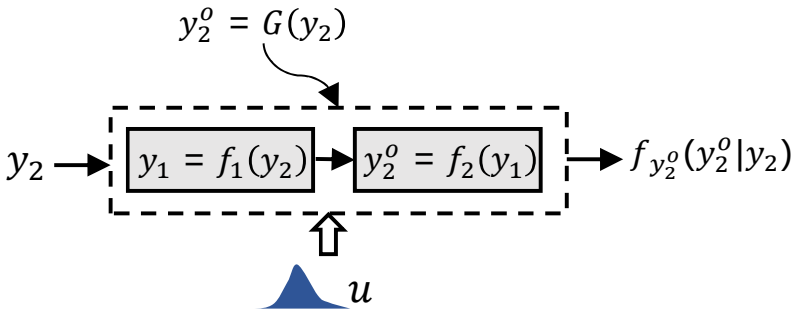

Figure 35: Integrated UMDA without feedback coupling used in Likelihood Approach for Multidisciplinary Analysis (LAMDA)

y_2. To carry out FPI, a guessed value for $y_1 = y_{1_0}$ is assumed and a random instance of f_2 is used to evaluate y_{2_1} with y_{1_0} as input. Next, the deterministic function f_1 is used to evaluate y_{1_1} with y_{2_1} as input. In the next iteration, another random instance of f_2 is used to evaluate y_{2_2} with y_{1_1} as input. This is carried on until convergence is achieved. But as seen in Figure 34b, due to non-deterministic behavior of f_2, it is infeasible to achieve convergence, i.e. $y_{1_i} = y_{1_{i-1}}$ or $y_{2_i} = y_{2_{i-1}}$ cannot be achieved.

Alternatively, a probabilistic approach can be used to find solutions which satisfy interdisciplinary compatibility. One such approach has been developed by Sankararaman and Mahadevan [152] and it is called Likelihood Approach for Multidisciplinary Analysis (LAMDA). In LAMDA, the entire UMDA is considered as a single function by removing all the feedback coupling links. For given values of coupling variables, uncertainty propagation is carried out through integrated UMDA without feedback coupling and the likelihood of interdisciplinary compatibility is evaluated. The likelihood information is then used to calculate the converged probability distribution of uncertain coupling variables.

For example, consider the coupled multidisciplinary analysis with two disciplines given by non-deterministic functions $y_1 = f_1(y_2)$ and $y_2 = f_2(y_1)$. Both disciplines are integrated into a single function given by $y_2^o = G(y_2) = f_2(f_1(y_2))$ as shown in Figure 35. $G(y_2)$ is non-deterministic, therefore for a given value of $y_2 = y_2^*$, it

will generate a probability distribution on y_2^o given by $f_{y_2^o}(y_2^o|y_2^*)$. Interdisciplinary compatibility is satisfied if $y_2^* = y_2^o$. Since, y_2^o is a random variable given by a conditional probability density, the likelihood that a given value of $y_2 = y_2^*$ will satisfy interdisciplinary compatibility is given as

$$L(y_2^*) \propto \mathrm{P}(y_2^o = y_2^*|y_2^*) = \int_{y_2^*-\epsilon/2}^{y_2^*+\epsilon/2} f_{y_2^o}(y_2^o|y_2^*)dy_2 \tag{42}$$

for some specified tolerance ϵ. The probability density of converged coupling variable is given as

$$f(y_2^*) = \frac{L(y_2^*)}{\int L(y_2)dy_2} \tag{43}$$

The probability distribution of y_1 can then be evaluated by propagating uncertainty through $y_1 = f_1(y_2)$ using the converged distribution of y_2 as input.

Although, LAMDA can evaluate the probability density of interdisciplinary compatibility solutions for non-deterministic disciplines, it requires propagation of uncertainty through an integrated UMDA. Therefore, the LAMDA method is not appropriate for distributed and concurrent multidisciplinary problems.

To achieve an interdisciplinary compatible solution in a distributed UMDA, let's look into a different view point of interdisciplinary compatibility using the example given in Equation 41. In a deterministic scenario with fixed value of uncertain variable $u_1 = u_1'$ and $u_2 = u_2'$, a setting $y_1 = y_1^*$ and $y_2 = y_2^*$ is considered to be interdisciplinary if the first discipline yields y_1^* as an output by taking y_2^* as input and the second discipline yields y_2^* as an output by taking y_1^* as input. Analogous to a deterministic setting, if $f^*_{y_1,y_2}(y_1, y_2)$ is the joint probability density of interdisciplinary compatible solutions with $f^*_{y_1}(y_1)$ and $f^*_{y_2}(y_2)$ as marginal density function of y_1 and y_2 respectively, then uncertainty propagation of y_2 with probability density function $f^*_{y_2}(y_2)$ through the first discipline will yield the $f^*_{y_1,y_2}(y_1, y_2)$ as the joint density function of input (y_2) and output (y_1). Also, uncertainty propagation of y_1 with probability density function $f^*_{y_1}(y_1)$ through the second discipline will yield same joint

density function, $f^*_{y_1,y_2}(y_1, y_2)$, of input (y_1) and output (y_2). This is shown pictorially in Figure 36

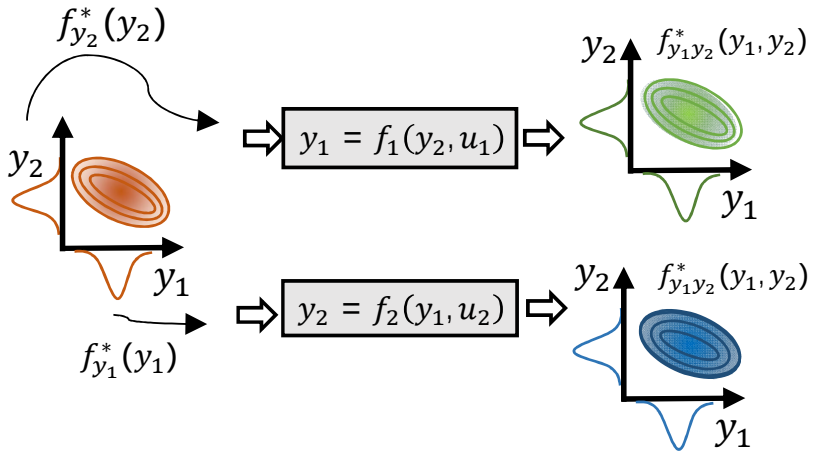

Figure 36: Another view point of interdisciplinary compatible solution under uncertainty

Since, the probability density of interdisciplinary compatible solutions of coupling variables are not known apriori, one can guess some probability density function of input coupling variable, and propagate that through its respective discipline concurrently and independently. For example, as shown in Figure 37, $g^{(1)}_{y_2}(y_2)$ is a guessed probability density function over y_2 and is propagated through the first discipline to evaluate joint distribution of $g^{(1)}_{y_1,y_2}(y_1, y_2)$. Concurrently, $g^{(2)}_{y_1}(y_1)$ is a guessed probability density function over y_1 and is propagated through the second discipline to evaluate joint distribution of $g^{(2)}_{y_1,y_2}(y_1, y_2)$. Please note superscript $()^{(i)}$ signifies the variable and density function associated with i^{th} discipline. If $g^{(1)}_{y_2}(y_2)$ and $g^{(2)}_{y_1}(y_1)$ are marginal density functions of interdisciplinary compatible solutions then the joint distribution $g^{(1)}_{y_1,y_2}(y_1, y_2)$ and $g^{(2)}_{y_1,y_2}(y_1, y_2)$ will be same. Otherwise, one can iteratively modify $g^{(1)}_{y_2}(y_2)$ and $g^{(2)}_{y_1}(y_1)$ until $D\left(g^{(1)}_{y_1,y_2}(y_1, y_2), g^{(2)}_{y_1,y_2}(y_1, y_2)\right) = 0$, where $D()$ is the distance metric for a probability density function such as *K-L Divergence* [153]. This procedure is similar to the Moment-Matching method where instead of matching only

a few moments of probability density function, the entire joint density function of coupling variables from each discipline are matched. However, the iterative nature of this procedure may be computationally expensive and can easily become intractable for high dimensional problems.

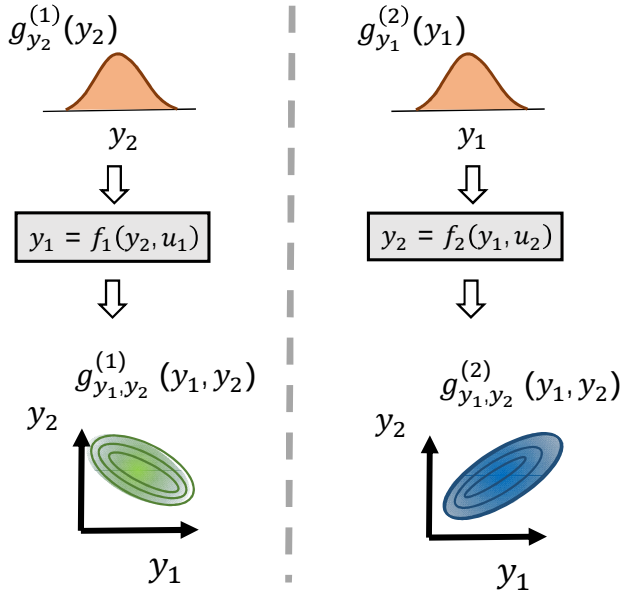

Figure 37: Propagation of uncertainty concurrently in each discipline with some assumed density functions over coupling variables

Instead of the iterative approach, in PADMA methodology the likelihood of Event of Interdisciplinary Compatibility (EIC) is calculated using the information from $g^{(1)}_{y_1,y_2}(y_1, y_2)$ and $g^{(2)}_{y_1,y_2}(y_1, y_2)$. Event of Interdisciplinary Compatibility or EIC for some setting of coupling variables (y_1^*, y_2^*) takes the value of 1 if it satisfies the deterministic interdisciplinary compatibility for some instance of uncertain variable, otherwise the value of EIC is 0. For example, for the notional example the EIC is given by Equation 44.

$$EIC(y_1^*, y_2^*) = \begin{cases} 1 & \text{if } y_1^* = f_1(y_2^*, u_1) \;\&\; y_2^* = f_2(y_1^*, u_2) \text{ for a instance of } (u_1, u_2) \\ 0 & \text{otherwise} \end{cases} \tag{44}$$

One can sample multiple instances of uncertain variables to evaluate the joint probability of $\mathrm{P}(EIC(y_1^*, y_2^*) = 1)$, which is equivalent to the probability of (y_1^*, y_2^*) satisfying interdisciplinary compatibility. The process can be repeated for different settings of y_1 and y_2 to estimate a joint probability density function $f^*_{y_1,y_2}(y_1, y_2)$ of interdisciplinary compatible solutions. However, for non-deterministic disciplines where sampling of disciplinary uncertain variables cannot be controlled, the likelihood of $EIC(y_1^*, y_2^*) = 1$ is estimated. The likelihood of $EIC(y_1^*, y_2^*) = 1$ is given as

$$\mathrm{L}\left(EIC(y_1^*, y_2^*) = 1\right) \propto f^{(1)}_{y_1|y_2}(y_1^*|y_2^*) \cdot f^{(2)}_{y_2|y_1}(y_2^*|y_1^*) \tag{45}$$

where $f^{(1)}_{y_1|y_2}(y_1|y_2)$ is the conditional probability density function of y_1 conditioned on y_2 evaluated by first discipline, and $f^{(2)}_{y_2|y_1}(y_2|y_1)$ is the conditional probability density function of y_2 conditioned on y_1 evaluated by the second discipline, as depicted in Figure 38. The conditional probability density function is evaluated using the general product rule as $f^{(1)}_{y_1|y_2}(y_1|y_2) = g^{(1)}_{y_1,y_2}(y_1, y_2)/g^{(1)}_{y_2}(y_2)$, where $g^{(1)}_{y_2}(y_2)$ is the guessed probability density of y_2 and $g^{(1)}_{y_1,y_2}(y_1, y_2)$ is the joint density of input y_2 and output y_1 evaluated after uncertainty propagation through the first discipline. Similarly, $f^{(2)}_{y_2|y_1}(y_2|y_1) = g^{(2)}_{y_1,y_2}(y_1, y_2)/g^{(2)}_{y_1}(y_1)$, where $g^{(2)}_{y_2 1}(y_1)$ is the guessed probability density of y_1 and $g^{(2)}_{y_1,y_2}(y_1, y_2)$ is the joint density of input y_1 and output y_2 evaluated after uncertainty propagation through the second discipline.

The joint probability density function for interdisciplinary compatibility is then given as

$$f^*_{y_1,y_2}(y_1, y_2) = \frac{1}{c} f^{(1)}_{y_1|y_2}(y_1|y_2) f^{(2)}_{y_2|y_1}(y_2|y_1) \tag{46}$$

where c is the constant such that probability axiom $\int f_{y_1,y_2}(y_1, y_2) dy_1 dy_2 = 1$ holds.The constant c is given as

$$c = \int_{y_1} \int_{y_2} f^{(1)}_{y_1|y_2}(y_1|y_2) f^{(2)}_{y_2|y_1}(y_2|y_1) dy_1 dy_2 \tag{47}$$

Extending the formulation of the probability of interdisciplinary compatibility for

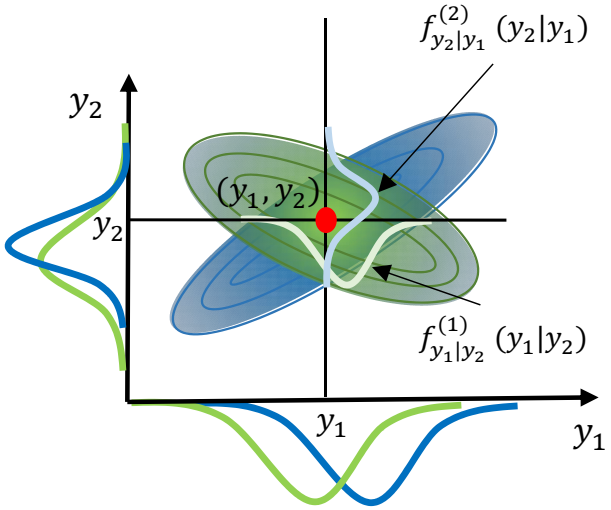

Figure 38: Notional representation of evaluation of probability of event of interdisciplinary compatibility

n disciplines, the joint probability density function of coupling variables is given as

$$f^{*}_{\mathbf{y_1},\ldots,\mathbf{y_n}}(\mathbf{y_1},\ldots,\mathbf{y_n}) = \frac{1}{c}\prod_{i=1}^{n} f^{(i)}_{\mathbf{y_i}|\mathbf{y_{.i}}}(\mathbf{y_i}|\mathbf{y_{.i}}) \tag{48}$$

where $\mathbf{y_i}$ represents output coupling variables of i^{th} discipline, $\mathbf{y_{.i}}$ represents input coupling variables to i^{th} discipline, and $f^{(i)}_{\mathbf{y_i}|\mathbf{y_{.i}}}$ is the conditional probability density of i^{th} discipline. Please note that the boldface is used to represent coupling variables to suggest that the disciplines can have more than one input and output. The constant c is given as

$$c = \int_{\mathbf{y_1}} \cdots \int_{\mathbf{y_n}} \prod_{i=1}^{n} f^{(i)}_{\mathbf{y_i}|\mathbf{y_{.i}}}(\mathbf{y_i}|\mathbf{y_{.i}})\, d\mathbf{y_1} \ldots d\mathbf{y_n} \tag{49}$$

To evaluate the conditional density function $f^{(i)}_{\mathbf{y_i}|\mathbf{y_{.i}}}(\mathbf{y_i}|\mathbf{y_{.i}})$ of i^{th} discipline, each discipline carries out uncertainty propagation with a guessed density function $g^{(i)}_{\mathbf{y_{.i}}}(\mathbf{y_{.i}})$ on input coupling variable and evaluates the joint distribution of input and output coupling variables $g^{(i)}_{\mathbf{y_i},\mathbf{y_{.i}}}(\mathbf{y_i},\mathbf{y_{.i}})$. The conditional density function is then given as

$$f^{(i)}_{\mathbf{y_i}|\mathbf{y_{.i}}}(\mathbf{y_i}|\mathbf{y_{.i}}) = \frac{g^{(i)}_{\mathbf{y_i},\mathbf{y_{.i}}}(\mathbf{y_i},\mathbf{y_{.i}})}{g^{(i)}_{\mathbf{y_{.i}}}(\mathbf{y_{.i}})} \tag{50}$$

It must be noted that the form of joint density function of coupling variables for feed-forward coupled UMDA given by Equation 39 and feedback coupled UMDA

given by Equation 48 are similar, except for the constant c in Equation 48. However, Equation 48 is a general form of joint density function of coupling variables which can be used for purely feed-forward coupled UMDA or UMDA with a mixture of feed-forward and feedback coupling.

4.2.3 Criteria for Guessed Probability Density Functions

The conditional density function given by Equation 50 is only valid within the domain or support of guessed probability density function $g^{(i)}_{\mathbf{y}_{.\mathbf{i}}}(\mathbf{y}_{.\mathbf{i}})$. For any value of $\mathbf{y}_{.\mathbf{i}}$ outside the domain of guessed probability density $g^{(i)}_{\mathbf{y}_{.\mathbf{i}}}(\mathbf{y}_{.\mathbf{i}})$, the conditional probability of $\mathbf{y}_{.\mathbf{i}}$ is zero and $f^{(i)}_{\mathbf{y_i}|\mathbf{y}_{.\mathbf{i}}}$ becomes indeterminate. Therefore, it is important that the domain of guessed probability density function $g^{(i)}_{\mathbf{y}_{.\mathbf{i}}}(\mathbf{y}_{.\mathbf{i}})$ is large enough such the interdisciplinary compatible solutions lie within this domain. For example, if $\Omega^*_{y_1,y_2}$ is the domain of interdisciplinary compatible solutions for notional examples given by Equation 41 and Ω'_{y_1,y_2} is the domain or support of guessed probability density function of y_1 and y_2, then $\Omega^*_{y_1,y_2} \subset \Omega'_{y_1,y_2}$ must satisfy, as shown in Figure 39.

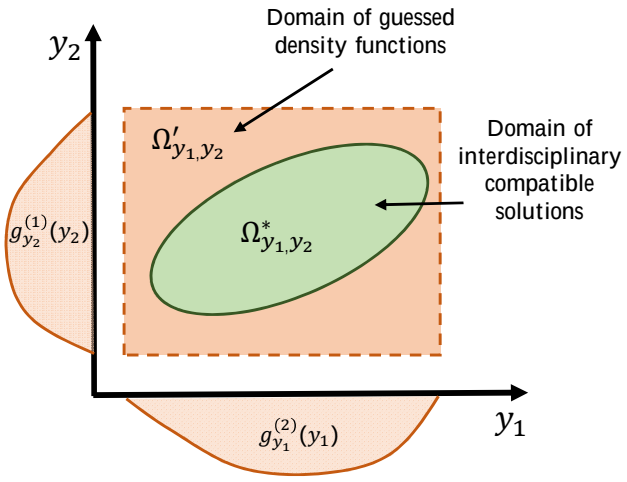

Figure 39: Criteria for domain of guessed density functions

Since, the probability distribution of compatible solution or its domain is not known apriori, engineering judgment can be used to start with conservatively wider

domain for guessed density functions. However, if the assumed domain of input coupling variables are excessively large then it might lead to an increase in computational expense for uncertainty propagation.

A semi-iterative alternative is to start with relatively smaller guessed domain of $g^{(i)}_{\mathbf{y_{.i}}}(\mathbf{y_{.i}})$ around the predefined deterministic baseline. Carry out the PADMA process to evaluate the likelihood of interdisciplinary compatibility of the coupling variables at the boundary of the guessed domain. If the likelihood is zero or smaller than some specified tolerance ϵ_{EIC}, at all the domain boundaries, then the guessed domain is appropriate. Otherwise, if the likelihood at any boundary is non-zero or greater than some specified tolerance ϵ_{EIC}, then domain boundaries are extended and $g^{(i)}_{\mathbf{y_{.i}}}(\mathbf{y_{.i}})$ is redefined for the extended domain and PADMA process is repeated.

If the disciplines are deterministic, then a quantitative approach to estimate a good approximation of the domain of compatible solutions can be done by carrying out a deterministic analysis at the mean of uncertain variables to evaluate the first order mean value of all coupling variables. First order variance of coupling variable y_{ij} which is the output of i^{th} discipline, and input to j^{th} discipline is estimated as

$$Var(y_{ij}) = \sum_{k=1}^{n} \left(\frac{dy_{ij}}{du_k} \right) Var(u_k) \tag{51}$$

where u_k are uncertain variables and the first order derivatives are calculated using Sobieski's Global Sensitivity Equations (GSE) [154] as

$$\frac{dy_{ij}}{du_k} = \frac{\partial y_{ij}}{\partial u_k} + \frac{\partial y_{ij}}{\partial y_{ji}} \frac{\partial y_{ji}}{\partial u_k} \tag{52}$$

where all the derivatives are evaluated at mean of uncertain variables. Using the first order values of mean and variance of compatible solutions, one can estimate the domain of coupling variable as $[\mu_{y_{ij}} - \kappa\sigma_{y_{ij}}, \mu_{y_{ij}} + \kappa\sigma_{y_{ij}}]$, where κ is a parameter to represent confidence interval. For example, if the coupling variable follows a Gaussian distribution, then the domain represented with $\kappa = 3.0$ will cover 99.7% of compatible solutions.

Functional form of guessed probability density functions No assumption is made for the functional form of guessed probability density functions $g^{(i)}_{\mathbf{y}_{\cdot\mathbf{i}}}(\mathbf{y}_{\cdot\mathbf{i}})$. Any parametric or non-parametric probability density function with appropriate domain can be used to carry out the PADMA method. However, using a functional form of *uniform distribution* for a guessed density function has an advantage. If uniform distribution is assumed, then $g^{(i)}_{\mathbf{y}_{\cdot\mathbf{i}}}(\mathbf{y}_{\cdot\mathbf{i}})$ is constant for any value of $\mathbf{y}_{\cdot\mathbf{i}}$. In such cases, the conditional density function of disciplinary output is given as

$$f^{(i)}_{\mathbf{y_i}|\mathbf{y}_{\cdot\mathbf{i}}}(\mathbf{y_i}|\mathbf{y}_{\cdot\mathbf{i}}) \propto g^{(i)}_{\mathbf{y_i},\mathbf{y}_{\cdot\mathbf{i}}}(\mathbf{y_i},\mathbf{y}_{\cdot\mathbf{i}}) \tag{53}$$

Therefore, the conditional density function $f^{(i)}_{\mathbf{y_i}|\mathbf{y}_{\cdot\mathbf{i}}}(\mathbf{y_i}|\mathbf{y}_{\cdot\mathbf{i}})$ can be directly estimated from the samples of coupling variables generated by disciplinary uncertainty propagation if uniform distribution is assumed for $g^{(i)}_{\mathbf{y}_{\cdot\mathbf{i}}}(\mathbf{y}_{\cdot\mathbf{i}})$.

4.2.4 Sampling of Interdisciplinary Compatible Solutions

In an UMDA with only feedback coupling, the dependency structure and the form of joint density function given by Equation 39 is exactly same as *directed acyclic graph*-based probabilistic model such as Bayesian Network. Any method used in Bayesian Network such as Markov Chain Monte Carlo (MCMC) method, Likelihood-weighting sampling [155], Importance sampling [156], Acceptance-Rejection sampling [157], etc. can be directly used for feed-forward UMDA problems. However, in feedback coupled UMDA, the dependency structure is not a directed acyclic graph due to feedback loops, and sampling methods used in Bayesian Network cannot be directly applied.

To sample interdisciplinary compatible solutions in feedback UMDA, the main challenge is to evaluate the integral c used in Equation 48 and given by Equation 49. The integral can be evaluated using numerical integration techniques such as *Gaussian quadrature*, *Simpson's quadrature*, etc [158]. Although most of the quadrature based algorithms are applicable only for a one-dimensional integral, one can decompose this multidimensional integral into multiple one-dimensional integrals and apply the

quadrature algorithm recursively.

$$\int_y \int_x f(x,y)dxdy = \int_y \left(\int_x f(x,y)dx \right) dy \tag{54}$$

Alternatively, Monte Carlo methods such as *Metropolis Hastings algorithm*, *Gibbs sampling*, etc [117] can be used to evaluate the integral. Some methods like *Slice sampling* [159] can bypass the evaluation of the integral c and directly sample the interdisciplinary compatible solutions by using the proportionality information

$$f^*_{\mathbf{y_1},\ldots,\mathbf{y_n}}(\mathbf{y_1},\ldots,\mathbf{y_n}) \propto \prod_{i=1}^{n} f^{(i)}_{\mathbf{y_i}|\mathbf{y}_{.\mathbf{i}}}(\mathbf{y_i}|\mathbf{y}_{.\mathbf{i}}). \tag{55}$$

In the current work a hybrid method for sampling has been used using Bayesian Network sampling and *weighted sampling* [160]. In the first step of the hybrid method, all the feedback coupling is ignored and samples of coupling variables are generated utilizing any approach used in Bayesian Network, such as Likelihood-weighting sampling, Importance sampling, Acceptance-Rejection sampling, etc. Next, each sample is given a weight based on conditional probability of feedback coupling variables. A weight associated with the k^{th} sample is given as

$$w_k = \prod_{i=1}^{n} f^{(i)}_{\mathbf{y^c_i}|\mathbf{y}_{.\mathbf{i}}}(\mathbf{y^c_i}_k|\mathbf{y}_{.\mathbf{i}k}) \tag{56}$$

$\mathbf{y^c_i}_k$ is the vector of values of feedback coupling variables of i^{th} discipline in k^{th} sample and $\mathbf{y}_{.\mathbf{i}k}$ is the vector of values of input to i^{th} discipline in k^{th} sample. A weighted re-sampling is carried out using the samples generated by Bayesian Network with feed-forward sampling and associated weight given by w_k.

For example, consider the dependency graph of coupling variables in Figure 40. Each arrow represents a conditional probability. The black arrow represents the feed-forward coupling and the red dashed arrow represents the feedback coupling. Since the graph is not a directed acyclic graph, a Bayesian Network sampler cannot be used to sample the coupling variables. However, if the feedback couplings are removed, then

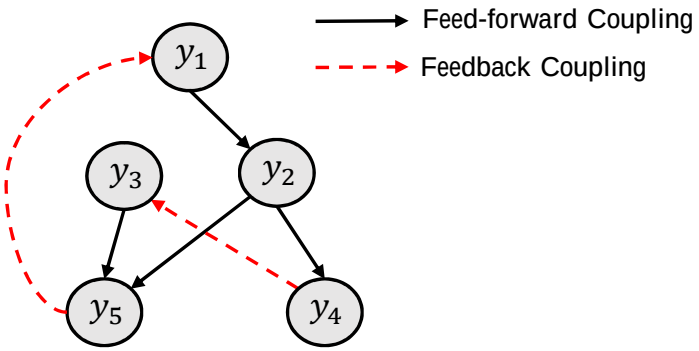

Figure 40: A notional dependency graph of coupling variables in UMDA

samples of coupling variables can be generated using any efficient Bayesian Network sampling method from the joint density function given as

$$f_{\mathbf{y}}(y_1, \ldots, y_5) = f_{y_5}(y_5|y_2, y_3) f_{y_4}(y_4|y_2) f_{y_2}(y_2|y_1) f_{y_1}(y_1) f_{y_3}(y_3) \tag{57}$$

Once the samples are generated from a feed-forward network, each of the samples is given a weight based on the conditional probability of feedback coupling as

$$w_k = f_{y_1}(y_{1_k}|y_{5_k}) f_{y_3}(y_{3_k}|y_{4_k}) \tag{58}$$

where $y_{1_k}, y_{3_k}, y_{4_k}$ and y_{5_k} is the value of y_1, y_3, y_4 and y_5 in k^{th} sample and $f_{y_1}(y_1|y_5)$ and $f_{y_3}(y_3|y_4)$ are the conditional probability function of y_1 and y_3. Finally a weighted re-sampling is carried with w_k as weight associated with k^{th} samples generated by Bayesian Network sampler. The new set of samples of $y_1, \ldots, y_5$ satisfies the dependency given by the dependency network Figure 40 and are interdisciplinary compatible solutions.

4.3 Numerical Procedure for PADMA

The flow chart of numerical procedure for PADMA is given in Figure 41. The details of each step are as follows:

1. **Start**

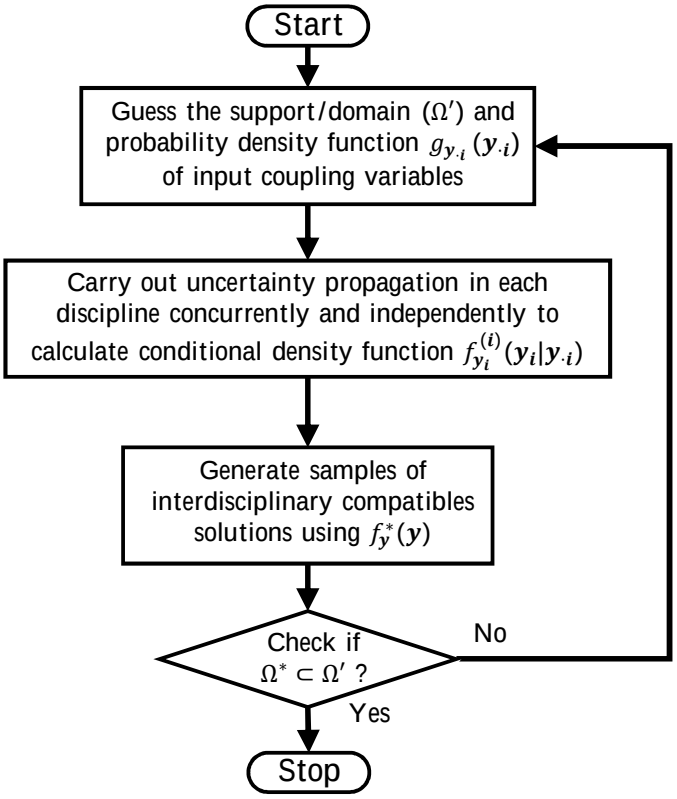

Figure 41: Flow chart of PADMA procedure

2. **Guess probability density function of input coupling variables:** Probability density functions of input coupling variables, $g_{\mathbf{y}_{\cdot \mathbf{i}}}^{(i)}(\mathbf{y}_{\cdot \mathbf{i}})$ are guessed. Although the functional form of probability density functions are not critical, but it is important that the assumed domain of input coupling variables should contain the compatible solutions, i.e. $\Omega_{\mathbf{y}_{\cdot i}}^{*} \subset \Omega_{\mathbf{y}_{\cdot i}}'$. Therefore, a best possible size of domain $\Omega_{\mathbf{y}_{\cdot i}}'$ is estimated to define the guessed probability density function.

3. **Concurrently carry out uncertainty propagation in each discipline:** Uncertainty propagation is carried out in each discipline concurrently and independently. Each discipline can use its preferred method of uncertainty propagation such as Monte Carlo Simulations, Markov Chain Monte Carlo, Polynomial Chaos Expansion, etc [161]. Next, the conditional probability density function

of output coupling conditioned on input coupling variable $f^{(i)}_{\mathbf{y_i}|\mathbf{y}_{.\mathbf{i}}}(\mathbf{y_i}|\mathbf{y}_{.\mathbf{i}})$ is evaluated and modeled. Conditional probability density functions can be modeled by using parametric methods like Bayesian regression, etc. or non-parametric approaches such as Gaussian Processes etc. In the current work quantile copula regression is used, details of which will be discussed in the following chapter.

4. **Generate samples of interdisciplinary compatible solutions:** After uncertainty propagation and modeling of conditional probability density functions of coupling variables in each discipline, samples of interdisciplinary compatibles solutions are generated using Equation 48 and joint density function coupling variables are evaluated.

5. **Check for convergence:** In the last step, the domain of interdisciplinary compatible solutions of all coupling variables are estimated. Domain ($\Omega^*_{\mathbf{y}_{.i}}$) of a coupling variable $\mathbf{y}_{.i}$ can be given as $[\mu_{\mathbf{y}_{.i}} - \kappa\sigma_{\mathbf{y}_{.i}}, \mu_{\mathbf{y}_{.i}} + \kappa\sigma_{\mathbf{y}_{.i}}]$, where $\mu_{\mathbf{y}_{.i}}$ and $\sigma_{\mathbf{y}_{.i}}$ is the statistical mean and standard deviation of interdisciplinary compatible samples of $\mathbf{y}_{.i}$ evaluated in step 4 and with a nominal value of $\kappa = 3.0$. If $\Omega^*_{\mathbf{y}_{.i}} \not\subset \Omega'_{\mathbf{y}_{.i}}$, then the process is repeated by updating the assumed domain $\Omega'_{y_{ij}}$ in step 2, such that $\Omega^*_{\mathbf{y}_{.i}} \subset \Omega'_{\mathbf{y}_{.i}}$. Otherwise, if $\Omega^*_{\mathbf{y}_{.i}} \subset \Omega'_{\mathbf{y}_{.i}}$, then process is terminated.

4.4 Numerical Experiments

Purpose of experiments: To prove that the PADMA method can accurately quantify the dependence among coupling variables and uncertainty on system metric, while allowing distributed and concurrent uncertainty analysis in a multidisciplinary problem under uncertainty

4.4.1 Benchmark and State of the Art methods

The benchmark method against which the results of the PADMA method is compared is Simulation Outside Fixed Point Iteration (SOFPI) which is a fully integrated UMDA method. The results are also compared with the Moment-Matching (MM) method, which is the current state of the art on decomposition and coordination-based UMDO strategy for non-deterministic disciplinary functions. Since most commonly used MM-based methods in literature (ex, CO-based, ATC-based, etc.) are developed for UMDO, MM method used in this chapter carries out UMDA by only minimizing the discrepancy between system target moments (mean and standard deviation) and disciplinary achievable moments of coupling variables to achieve interdisciplinary compatibility.

4.4.2 Experimental Metrics

To measure the accuracy of PADMA method to quantify the uncertainty on system metric, statistical mean (μ), standard deviation (σ), and skewness (γ) are compared with the SOFPI and MM methods. To compare the probability density functions of system metric, Kullback-Leibler (K-L) divergence is used, which is a commonly used divergence measure in probability theory and information theory.

Kullback–Leibler (K-L) divergence Kullback-Leibler (K–L) divergence is a divergence measure which measures the relative entropy between two probability distributions. K-L divergence is also used as a measure of mismatch between two probability density functions. For two distributions P and Q for continuous random variables K-L divergence is give as:

$$D_{\mathrm{KL}}(P\|Q) = \int_{-\infty}^{\infty} p(x)\, \log \frac{p(x)}{q(x)}\, \mathrm{d}x. \tag{59}$$

K-L divergence is not symmetric, i.e. $D_{\mathrm{KL}}(P\|Q) \neq D_{\mathrm{KL}}(Q\|P)$, and does not follow the triangle inequality. Therefore, it is not a true distance measure. KL divergence is

always non-negative and it is zero if and only if $p(x)$ and $q(x)$ are exactly the same.

To measure the accuracy of the PADMA method to capture the dependencies of coupling variables, two metrics are used: *Pearson's correlation coefficient (ρ)* and *Mutual Information (MI)*.

Pearson's correlation coefficient Pearson's correlation coefficient (ρ) is the measure of linear dependence between two random variables. The Pearson's correlation coefficient between two random variables X and Y is given as

$$\rho_{X,Y} = \frac{\mathrm{E}[(X - \mu_X)(Y - \mu_Y)]}{\sigma_X \sigma_Y} \tag{60}$$

where μ_X and μ_Y are the statistical mean and σ_X and σ_Y are the standard deviation of X and Y respectively and E is the expectation. The value of Pearson's correlation coefficient lies between -1 and 1, where -1 signifies total negative correlation, 0 signifies no correlation, and 1 signifies total positive correlation. Any non-zero value of correlation signifies there is some dependence between variables, however the reverse is not true.

Mutual Information Mutual Information (MI) is a measure of the mutual dependence between two random variables. For two discrete events A and B, the amount of information provided by the occurrence of an event B about the occurrence of an event A is known as the Mutual Information between A and B. For two continuous random variables X and Y Mutual Information is given as

$$MI(X;Y) = \int_Y \int_X p(x,y) \log \left(\frac{p(x,y)}{p(x)\, p(y)} \right) dx\, dy, \tag{61}$$

where $p(x,y)$ is the joint probability distribution function of X and Y, and $p(x)$ and $p(y)$ are the marginal probability distribution functions of X and Y respectively. High Mutual Information indicates a large dependency, low Mutual Information indicates a small dependency, and zero Mutual Information between two random variables means

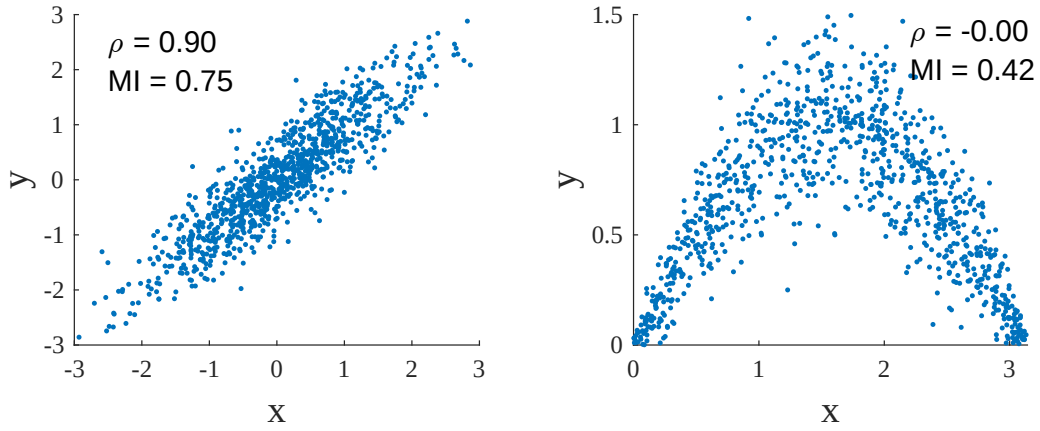

(a) Linearly dependent variables (b) Non-linearly dependent variables

Figure 42: Comparison of Pearson's correlation coefficient and Mutual Information between random variable with linear and non-linear dependence

the variables are independent. Mutual information is more general and determines how similar the joint distribution $p(X, Y)$ is to the products of factored marginal distribution $p(X)p(Y)$. As elaborated by Kraskov et al. [162]; '*In contrast to the linear correlation coefficient like Pearson's ρ, MI is sensitive also to dependencies which do not manifest themselves in the covariance. Indeed, MI is zero if and only if the two random variables are strictly independent*'. For example, consider the scatter plots of two random variables x and y in Figure 42. In Figure 42a, the variables are linearly dependent and they are well quantified by the Pearson correlation coefficient ($\rho = 0.90$) as well as Mutual Information ($MI = 0.75$). In Figure 42b the random variables are non-linearly dependent on each other with an underlying sinusoidal function. Mutual Information has been able to quantify the non-linear dependence with a value of $MI = 0.42$; however Pearson correlation coefficient being a linear dependence measure was unable to capture the non-linear dependence ($\rho = 0.00$).

4.4.3 Test Problem Characteristics

Test problems to carry out experiments are selected such that they have following characteristics:

- The UMDA problem can be hierarchically decomposed such that disciplinary analyses can carry out independent uncertainty analysis.
- The UMDA problem should have low to mid level of coupling between disciplines, both feed-forward and feedback.
- Disciplinary analyses have non-linear behavior, i.e. disciplinary state variables are a non-linear function of input coupling variables and uncertainty variables.
- The uncertainty variables can be embedded into disciplinary analyses such that disciplinary functions can be executed as non-deterministic functions.
- Characteristics of disciplinary uncertainty variables can be modified such that the method can be tested for non-Gaussian variables.
- Low to moderate number ($\sim$ 3 to 10) number of coupling variables.
- Problem can be evaluated using benchmark UMDA method, SOFPI.

Based on these characteristics two problems are selected. The first problem is a toll road bridge which is a feed-forward coupled UMDA problem. It has three disciplines, five coupling variables and five uncertainty variables. The second problem is an analytical problem with feedback coupling. It has two coupled disciplines, four coupling variables and five uncertainty variables. In both the problems two case studies have been carried out, one with all uncertainties defined by Gaussian distribution and the other one with uncertainties consisting a mixture of Gaussian and non-Gaussian distribution.

4.4.4 Toll Road Bridge Problem

The toll road bridge [163] is a low-fidelity beam loading analysis consisting of two subsystems, load analysis and beam analysis, and a system level economics discipline.

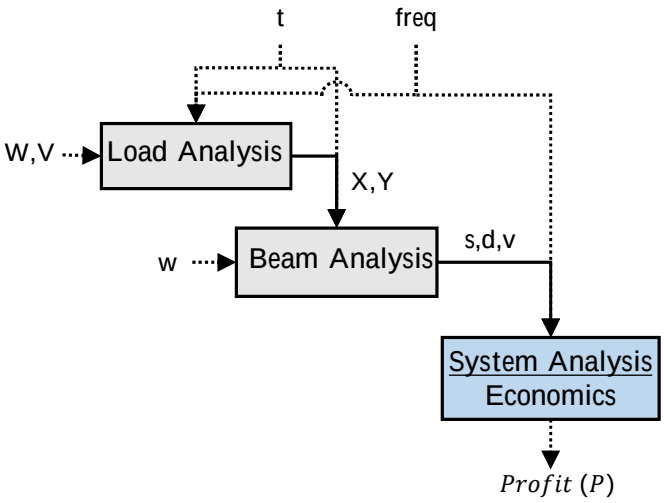

Figure 43: Information flow in toll road bridge problem

There is only feed-forward coupling in the subsystems. The flow of information is shown in Figure 43.

Load Discipline

$$X = \frac{1}{2} C_d \rho V^2 L t \tag{62a}$$

$$Y = W freq \tag{62b}$$

The load analysis evaluates the load on the bridge based on the traffic congestion and aerodynamic forces on the cross-section of the bridge as given by Equation 62. The input uncertainty variables to the load analysis are traffic frequency $freq$ $(1/vehicle)$, vehicle weight W $(lbf/vehicle)$, wind speed V (in/sec), and beam thickness t (in). Other deterministic parameters used in the discipline are coefficient of drag $C_d = 0.5$, air density $\rho = 4.14 \times 10^{-5} (lb/in^3)$, and beam length $L = 100(in)$. The output of the discipline are beam vertical load Y (lbf) and beam horizontal load X (lbf).

Beam Discipline

$$s = \frac{600}{wt^2}Y + \frac{600}{w^2t}X \tag{63a}$$

$$d = \frac{4L^3}{Ewt}\sqrt{\frac{Y}{t^2}^2 + \frac{X}{w^2}^2} \tag{63b}$$

$$v = Lwt \tag{63c}$$

The beam analysis carries out structural analysis on the bridge using a low fidelity beam model as given by Equation 63. The input uncertainty variables are beam width w (in), beam thickness t (in), vertical load Y (lbf), and beam horizontal load X (lbf). Deterministic parameters are beam length $L = 100(in)$ and Modulus of Elasticity $E = 2.9 \times 10^6(lbf/in^2)$. The output of the discipline are maximum stress s (lbf/in^2), maximum displacement d (in), and beam volume v (in^3).

Economics

$$p = freq - \frac{v - vol}{vol} - \frac{s - S}{S} - \frac{d - D}{D} \tag{64}$$

The economic discipline is the system level discipline which estimates system level metric, the non-dimensional profit p. The non-dimensional profit is calculated considering the over all earnings due to traffic and losses due to the maintenance of the bridge as given by Equation 64. The inputs to the system discipline are maximum stress s (lbf/in^2), beam volume v (in^3), and traffic frequency $freq$ $(1/vehicle)$. The deterministic parameters are maximum displacement $D = 7.0(in)$, maximum beam volume $vol = 1600(in^3)$, and yield stress $S = 2 \times 10^4(lbf/in^2)$.

Two case studies are carried for the toll bridge problem. In the first case, the uncertain variables $freq, W, V, t$ and w are assumed to have Gaussian distribution. The parameters of the distribution are given in Table 3. In the second case non-Gaussian distribution is assumed for uncertain variables as given in Table 4.

To carry out the PADMA method, the guessed distribution over horizontal load and vertical load has been assumed to be uniform. The domain of coupling variables has been estimated by propagating uncertainty through each discipline sequentially

Table 3: Description of characteristic of uncertainty variables for Toll Road Bridge problem case-1

Variable	Density Function	Parameters
$freq$	Gaussian	$\mu = 1.0$, $\sigma = 0.01$
W	Gaussian	$\mu = 1000$, $\sigma = 10$
V	Gaussian	$\mu = 160$, $\sigma = 4.47$
t	Gaussian	$\mu = 4$, $\sigma = 0.707$
w	Gaussian	$\mu = 4$, $\sigma = 0.707$

Note: μ is mean and σ is standard deviation for Gaussian distribution

Table 4: Description of characteristic of uncertainty variables for Toll Road Bridge problem case-2

Variable	Density Function	Parameters
$freq$	Triangular	$a = 0.0$, $b = 0.3$, $c = 2.0$
W	Uniform	$l = 960$, $u = 1030$
V	Uniform	$l = 145$, $u = 175$
t	Triangular	$a = 3.0$, $b = 4.3$, $c = 4.5$
w	Uniform	$l = 3.2$, $u = 4.8$

Note: For triangular distribution a is lower limit, b is peak location, and c is upper limit. For uniform distribution l the is lower bound, and u is the upper bound.

using 100 samples of uncertain variables. Based on the result of the uncertainty propagation, domain of horizontal load and vertical load were assumed to be $X \in [60, 150]$ and $Y \in [-500, 2500]$. Since, traffic frequency and beam thickness are common uncertainty variables, they are treated as coupling variables while modeling the conditional probability functions. Next, uncertainty propagation is carried out in load discipline and beam discipline independently and concurrently. For each discipline, 1000 samples of uncertain variables have been used to carry out uncertainty propagation. Based on the results of uncertainty propagation, conditional probability models $f_{\mathbf{y}_1}(X, Y|freq, t)$ and $f_{\mathbf{y}_2}(d, s, v|X, Y, t)$ are built in load and beam discipline. To model the conditional probability models, quantile copula regression has been used which is discussed in the next chapter. Joint probability density of coupling variables is then estimated as

$$f^*_{\mathbf{y}}(X, Y, s, d, v, freq, t) = f_{\mathbf{y}_1}(X, Y|freq, t) f_{\mathbf{y}_2}(d, s, v|X, Y, t) f_{freq}(freq) f_t(t) \quad (65)$$

To estimate the uncertainty on system metric p, samples of d, s, v and $freq$ are generated from joint density function given by Equation 65.and used as an input to the system level economics discipline. The scripts of the disciplinary functions have been written in MATLAB [164]. Also, to automate the PADMA process, scripts for PADMA method have been written and executed in MATLAB.

4.4.4.1 Results: Case-1

The probability density function (PDF) and cumulative distribution function (CDF) of system level metric p evaluated by PADMA method is plotted in Figure 44 and compared with benchmark result of SOFPI and MM methods. PDF and CDF estimated by PADMA method have been able to follow very closely to SOFPI method. However, the PDF estimated by the MM method has been found to be much wider. The inaccuracy in the MM method is mainly due to the assumption of independence of coupling variables. The true distribution has been found to be negatively skewed, which is well predicted by the PADMA method, whereas the MM method estimated a symmetrical distribution.

The statistics of system level metric, the non-dimensional profit p, is given in Table 5. Both MM and PADMA methods have been able to accurately estimate the mean; however the standard deviation estimate by the MM method has an error of 166% as compared to 27% by the PADMA method. Also, negative skewness has been estimated by the SOFPI method and the PADMA method, whereas the MM method estimates a very low value of skewness. In terms of closeness to the true distribution estimated by the SOFPI method, probability density function of p estimated by the PADMA method has been found to close with K–L div.= 0.13 as compared to the MM method with K–L div. = 0.86.

Scatter plot matrix of interdisciplinary compatible solutions of coupling variables is shown in Figure 45. In addition to scatter plot, each subplot also shows a single

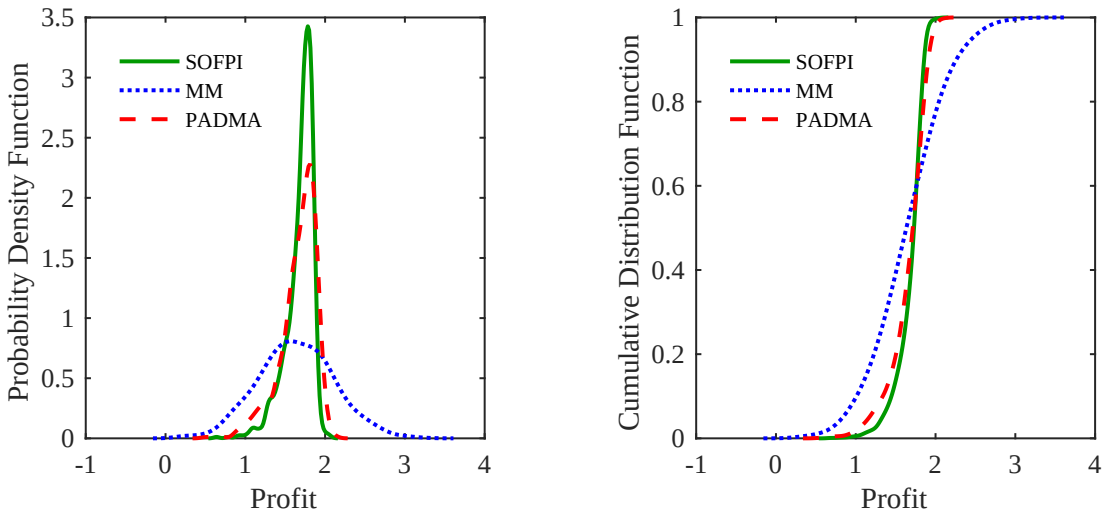

(a) Probability density function

(b) Cumulative distribution function

Figure 44: Comparison of probability density function and cumulative distribution function of non-dimensional profit p estimated using benchmark SOFPI method, Moment Matching method (MM) and PADMA method for toll road bridge problem case-1

Table 5: Comparison of statistical metrics of non-dimensional profit p for toll road bridge problem case-1

	SOFPI	**MM**	**PADMA**
Mean(μ_p)	1.68	1.65	1.66
Std. Dev.(σ_p)	0.18	0.48	0.23
Skewness (γ_f)	-1.79	-0.15	-1.43
K-L div.	-	0.86	0.13

iso-probability contour of value $0.02\mathrm{P}_{max}$, where P_{max} is the maximum probability density value attained by the true solution using the SOFPI method. As observed, vertical load Y, maximum stress s and maximum displacement d have been found to be strongly dependent on each other. Also, the dependency structure among these disciplines has been found to be non-Gaussian. Figure 46 compares the contour plot of joint probability density of optimum interdisciplinary compatible solution of Y and s estimated by all the SOFPI, MM and PAMDA methods. In addition to the strong dependency, the PADMA method has been able to capture the overall trend of joint probability density better than the MM method.

The linear dependency of coupling variables are compared between the SOFPI and PADMA methods in Table 6. The PADMA method has been able to capture all the linear dependency within 5% error. To compare the underlying non-linear dependency, Mutual Information is compared between the SOFPI and PADMA methods in Table 7. The difference of Mutual Information between SOFPI and PADMA has been found to be within tolerable limit, with maximum discrepancy of Δ MI = 0.21 between d and s.

4.4.4.2 Results: Case-2

In this case, the uncertain variables are assumed to have a non-Gaussian distribution. Comparison of probability density function (PDF) and cumulative distribution function (CDF) of system level metric p evaluated by the PADMA method is shown in Figure 47. PDF and CDF estimated by the PADMA method has been able to follow very closely to the SOFPI method, however similar to case-1, the MM method estimated a much wider distribution. The true distribution has been found to be negatively skewed, which is well predicted by the PADMA method, whereas the MM method estimates a almost symmetrical distribution.

The statistics of p is given in Table 8. The PADMA method has been able to

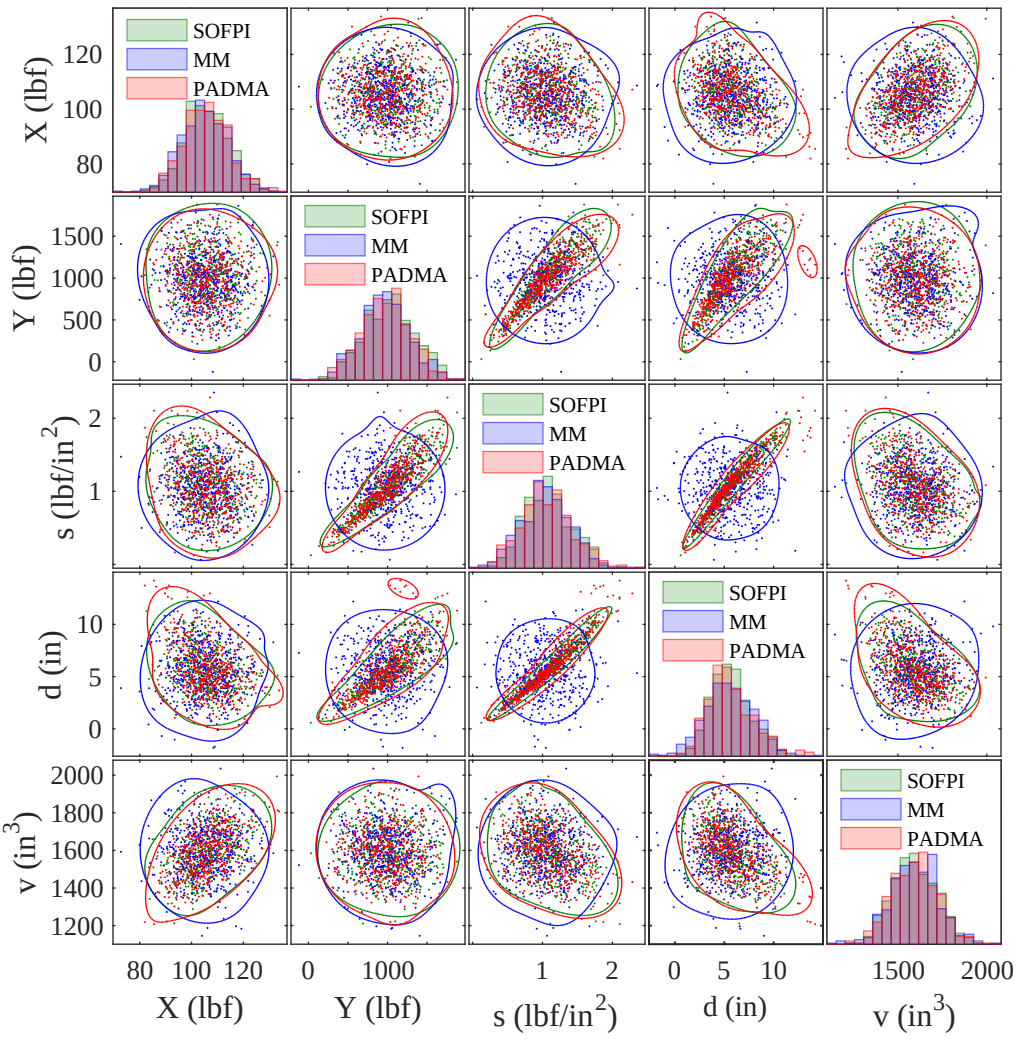

Figure 45: Scatter plot matrix of interdisciplinary compatible solution of coupling variables for toll road bridge problem case-1

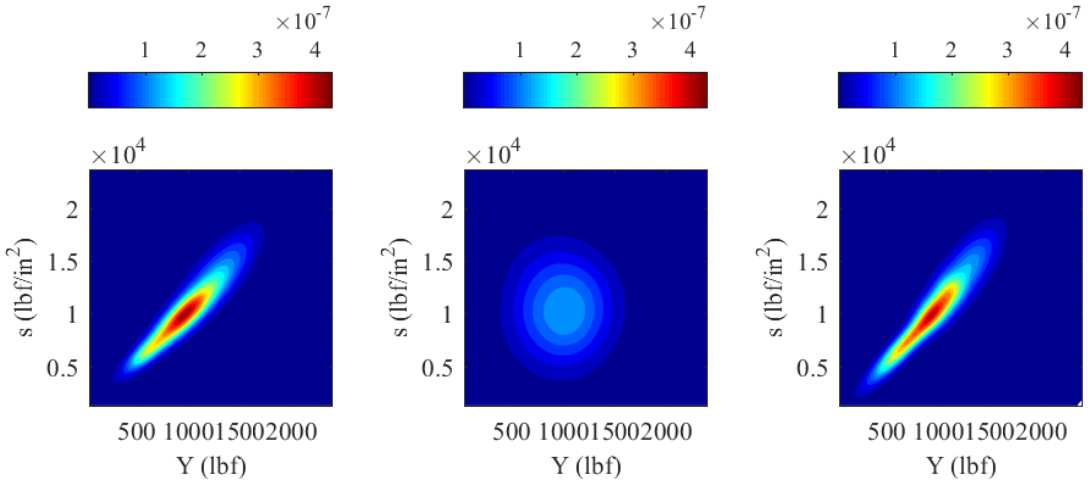

(a) SOFPI (b) MM (c) PADMA

Figure 46: Contour plot of joint probability density of interdisciplinary compatible solution of s and Y for toll road bridge problem case-1

Table 6: Comparison of Correlation Matrix of coupling variables for toll road bridge problem case-1

Correlation Matrix

		X	Y	s	d	v
SOFPI	X	1.00	-0.01	-0.24	-0.35	0.50
	Y	-0.01	1.00	0.91	0.85	-0.04
	s	-0.24	0.91	1.00	0.99	-0.41
	d	-0.35	0.85	0.99	1.00	-0.48
	v	0.50	-0.04	-0.41	-0.48	1.00
		X	Y	s	d	v
PADMA	X	1.00	-0.02	-0.24	-0.37	0.50
	Y	-0.02	1.00	0.92	0.80	-0.04
	s	-0.24	0.92	1.00	0.95	-0.36
	d	-0.37	0.80	0.95	1.00	-0.50
	v	0.50	-0.04	-0.36	-0.50	1.00
		X	Y	s	d	v
$\lvert\Delta\rho\rvert$	X	0.00	0.00	0.00	0.03	0.00
	Y	0.00	0.00	0.01	0.05	0.00
	s	0.00	0.01	0.00	0.04	0.05
	d	0.03	0.05	0.04	0.00	0.02
	v	0.00	0.00	0.05	0.02	0.00

Table 7: Comparison of Mutual Information Matrix of coupling variables for toll road bridge problem case-1

Mutual Information Matrix

		X	Y	s	d	v
SOFPI	X	1.30	0.02	0.05	0.09	0.17
	Y	0.02	1.29	0.83	0.67	0.02
	s	0.05	0.83	1.31	1.21	0.12
	d	0.09	0.67	1.21	1.35	0.15
	v	0.17	0.02	0.12	0.15	1.29
		X	Y	s	d	v
PADMA	X	1.33	0.02	0.05	0.09	0.16
	Y	0.02	1.31	0.87	0.55	0.03
	s	0.05	0.87	1.30	1.00	0.09
	d	0.09	0.55	1.00	1.33	0.16
	v	0.16	0.03	0.09	0.16	1.28
		X	Y	s	d	v
Δ MI	X	0.03	0.00	0.00	0.00	0.01
	Y	0.00	0.02	0.04	0.11	0.00
	s	0.00	0.04	0.00	0.21	0.03
	d	0.00	0.11	0.21	0.02	0.00
	v	0.01	0.00	0.03	0.00	0.01

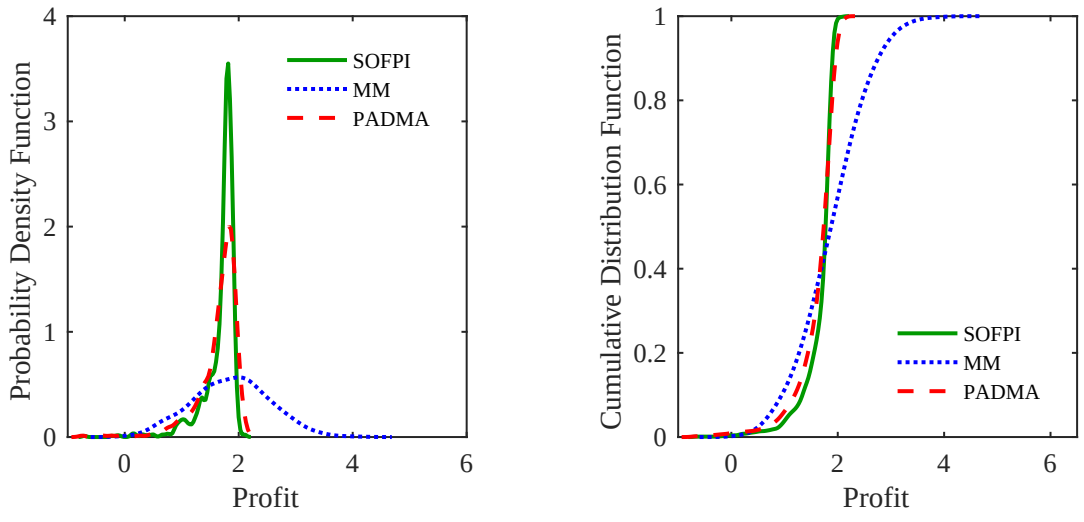

(a) Probability density function

(b) Cumulative distribution function

Figure 47: Comparison of probability density function and cumulative distribution function of non-dimensional profit p estimated using benchmark SOFPI method, Moment Matching method (MM) and PADMA method for toll road bridge problem case-2

Table 8: Comparison of statistical metrics of non-dimensional profit p for toll road bridge problem case-2

	SOFPI	**MM**	**PADMA**
Mean(μ_p)	1.66	1.89	1.64
Std. Dev.(σ_p)	0.31	0.64	0.36
Skewness (γ_p)	-2.65	-0.04	-2.04
K-L div.	-	1.03	0.22

Table 9: Comparison of Correlation Matrix of coupling variables for toll road bridge problem case-2

Correlation Matrix

		X	Y	s	d	v
SOFPI	X	1.00	-0.02	-0.16	-0.25	0.33
	Y	-0.02	1.00	0.91	0.86	0.04
	s	-0.16	0.91	1.00	0.98	-0.30
	d	-0.25	0.86	0.98	1.00	-0.34
	v	0.33	0.04	-0.30	-0.34	1.00
		X	Y	s	d	v
PADMA	X	1.00	-0.04	-0.21	-0.34	0.38
	Y	-0.04	1.00	0.92	0.79	0.01
	s	-0.21	0.92	1.00	0.95	-0.30
	d	-0.34	0.79	0.95	1.00	-0.39
	v	0.38	0.01	-0.30	-0.39	1.00
		X	Y	s	d	v
$\lvert\Delta\rho\rvert$	X	0.00	0.02	0.05	0.09	0.05
	Y	0.02	0.00	0.00	0.07	0.03
	s	0.05	0.00	0.00	0.04	0.00
	d	0.09	0.07	0.04	0.00	0.05
	v	0.05	0.03	0.00	0.05	0.00

accurately estimate the mean and the standard deviation, whereas, the MM method over predicted the mean by 13.8% and variance by 106%. Similar to case-1 PADMA has been able to capture the negative skewness whereas skewness evaluated by the MM method has been very close to zero. In terms of closeness to the true distribution estimated by the SOFPI method, probability density function of p estimated by the PADMA method has been found to be close with K–L div.= 0.23 as compared to the MM method with K–L div. = 1.03.

Scatter plot matrix of interdisciplinary compatible solutions of coupling variables

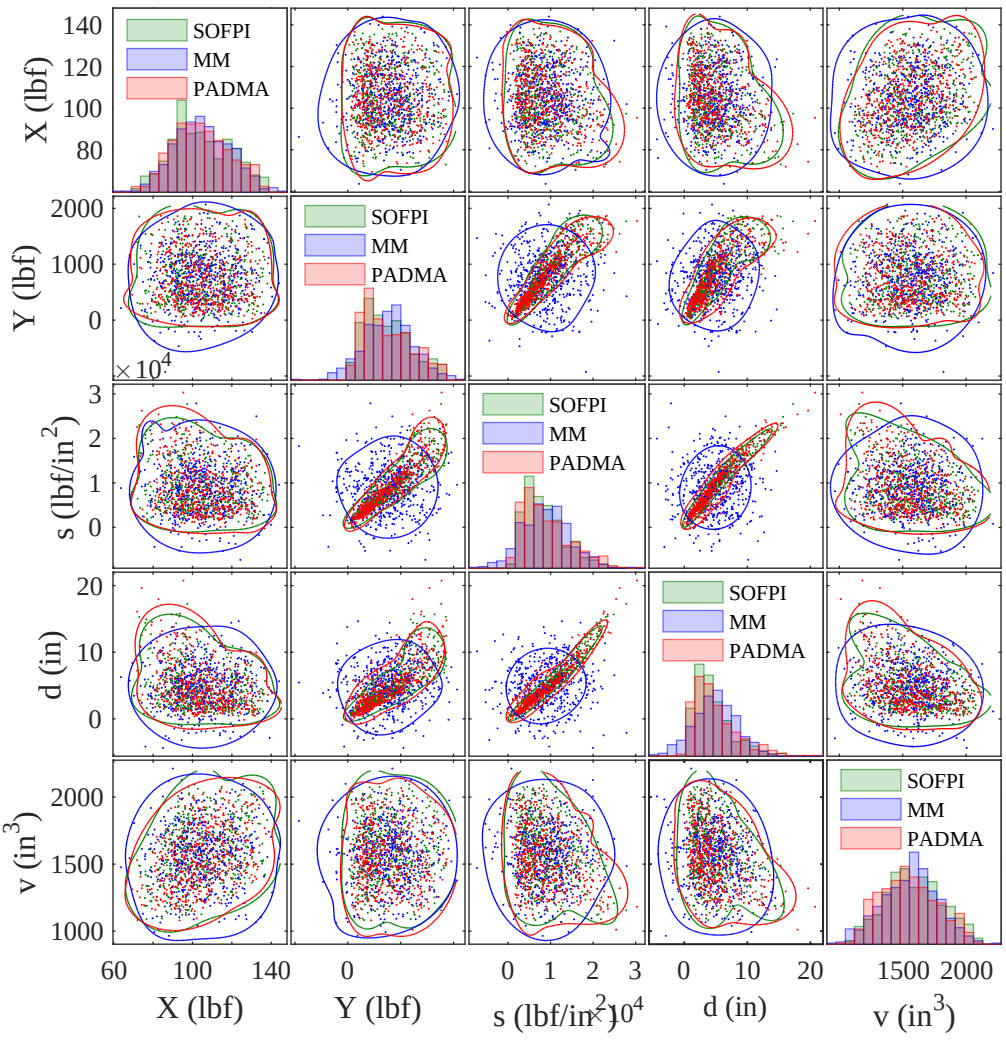

Figure 48: Scatter plot matrix of interdisciplinary compatible solution of coupling variables for toll road bridge problem case-2

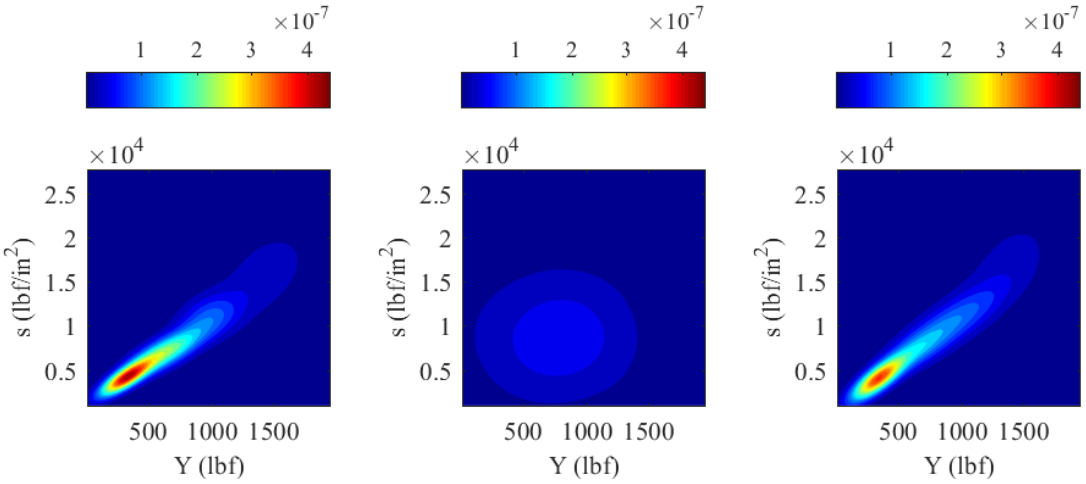

(a) SOFPI (b) MM (c) PADMA

Figure 49: Contour plot of joint probability density of interdisciplinary compatible solution of s and Y for toll road bridge problem case-2

Table 10: Comparison of Mutual Information Matrix of coupling variables for toll road bridge problem case-2

Mutual Information Matrix

		X	Y	s	d	v
SOFPI	X	1.17	-0.00	0.02	0.04	0.07
	Y	-0.00	1.17	0.80	0.70	0.00
	s	0.02	0.80	1.24	1.16	0.06
	d	0.04	0.70	1.16	1.31	0.07
	v	0.07	0.00	0.06	0.07	1.24
		X	Y	s	d	v
PADMA	X	1.20	-0.01	0.03	0.08	0.09
	Y	-0.01	1.12	0.77	0.51	0.00
	s	0.03	0.77	1.18	0.90	0.06
	d	0.08	0.51	0.90	1.33	0.10
	v	0.09	0.00	0.06	0.10	1.20
		X	Y	s	d	v
Δ MI	X	0.03	0.00	0.01	0.04	0.02
	Y	0.00	0.05	0.02	0.19	0.00
	s	0.01	0.02	0.06	0.25	0.00
	d	0.04	0.19	0.25	0.02	0.03
	v	0.02	0.00	0.00	0.03	0.04

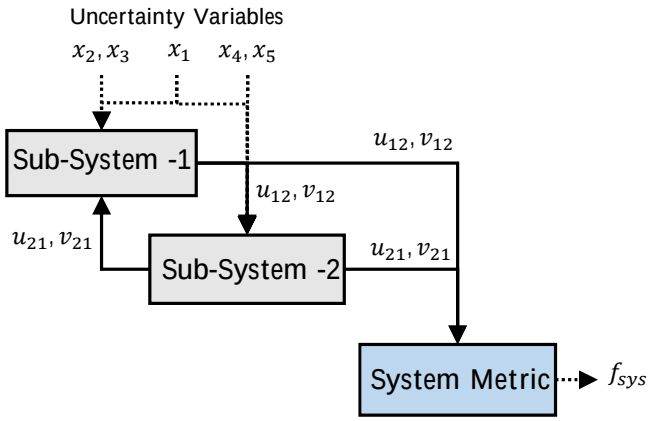

Figure 50: Information flow in analytical problem

is shown in Figure 48. Similar to case-1, vertical load Y, maximum stress s and maximum displacement d have been found be strongly dependent on each other. Due to non-Gaussian uncertain variables, almost all the dependencies have been found to be non-Gaussian. Also, the marginal distribution of Y, s, and d has been found to be non-Gaussian with positive skewness. The skewness is well predicted by the PADMA method, however MM estimates a symmetrical distribution. Figure 49 compares the contour plot of joint probability density of optimum interdisciplinary compatible solution of Y and s estimated by all the SOFPI, MM and PAMDA methods. The PADMA method has been able to capture the overall trend of joint probability density better than the MM method.

The linear dependency of coupling variables are compared between the SOFPI and PADMA methods in Table 9. The PADMA method has been able to capture all the linear dependency within a 9% error. To compare the underlying non-linear dependency, Mutual Information is compared in between the SOFPI and PADMA methods in Table 10. Similar to case-1, the difference of Mutual Information between SOFPI and PADMA has been found to be within tolerable limit with maximum Δ MI $= 0.25$ between d and s.

4.4.5 Analytical Problem

The analytical problem is a modified version of a problem discussed by Du and Chen [165] and used by [166] as shown in Figure 50. The problem consists of two coupled disciplines and a system level analysis. There are four coupling variables $\mathbf{y} = [u_{12}, v_{12}, u_{21}, v_{21}]$ and five uncertainty variables $[x_1, x_2, x_3, x_4, x_5]$. The analytical equations of each discipline is given as

$$\text{System} \qquad f_{sys} = u_{12}v_{12} - u_{21}v_{21} \tag{66}$$

$$\begin{aligned} \text{Subsystem-1} \qquad u_{12} &= x_1^2 + 2x_2 - x_3 + 2\sqrt{u_{21}} - 0.22v_{21} \qquad (67)\\ v_{12} &= 2x_1 + x_2x_3 - 0.31\sqrt{u_{21}} + 0.2v_{21} \\ \text{Subsystem-2} \qquad u_{21} &= x_1x_4 + x_4^2 + x_5 + u_{12} + 0.1\sqrt{v_{12}} \qquad (68)\\ v_{21} &= x_1x_5 + x_1x_4 + x_1 + 0.15u_{12} - 0.3v_{12} \end{aligned}$$

Two case studies have been carried out with the analytical problem by changing the characteristics of uncertain variables.

Case-1: In the first case, the uncertain variables are characterized with Gaussian distribution with mean $\mu_{x_i} = 1.0$ and standard deviation of $\sigma_{x_i} = 0.1$.

$$x_i \sim \mathcal{N}(1.0, 0.1^2) \qquad \forall i = 1, \ldots, 5 \tag{69}$$

Case-2: In the second case, shared uncertainty variable x_1 is characterized with Gaussian distribution with mean $\mu_1 = 1.0$ and standard deviation of $\sigma_1 = 0.1$, while x_2, x_3, x_4, x_5 are characterized with shifted Gamma distribution with shape parameter $K = 1.0$, scale parameter $\theta = 0.1$ and shift $\delta = 1.0$.

$$x_1 \sim \mathcal{N}(0, 0.1^2) \tag{70a}$$

$$x_i \sim 1.0 + \Gamma(1.0, 0.1) \qquad \forall i = 2, \ldots, 5 \tag{70b}$$

In the first step of the PADMA method, an approximate domain of coupling variables are estimated. To evaluate an approximate domain of coupling variables, deterministic analysis is carried out at mean value of uncertainty variables to evaluate the mean value of coupling variables. The mean value of coupling variables $\mathbf{y} = [u_{12}, v_{12}, u_{21}, v_{21}]$ are estimated to be $\mu_{\mathbf{y}} = [7.9, 2.6, 11.07, 3.39]$. Next, sensitivity analysis is carried out with respect to uncertainty variables and a rough estimate of variance of coupling variables using Global Sensitivity Equation is found to be $\sigma^2_{\mathbf{y}} = [0.17, 0.074, 0.39, 0.096]$. With the assumption that the compatible solutions lies within $\mu_{\mathbf{y}} \pm 6.0\sigma_{\mathbf{y}}$, lower bound of coupling variables is set at $\mathbf{y}^{LB} = [5.4, 0.96, 7.3, 1.5]$ and upper bound is set at $\mathbf{y}^{UB} = [10.4, 4.2, 14.8, 5.3]$. By assuming uniform distribution on all coupling variables with lower and upper bound specified by $\mathbf{y}^{LB}$ and $\mathbf{y}^{UB}$ respectively, uncertainty propagation is carried out in both the subsystems independently and concurrently.

To carry out uncertainty propagation in each discipline, 1000 samples of uncertainty variables and input coupling variables are used. After execution of uncertainty propagation, models of conditional probability functions $f_{u_{12},v_{12}}(u_{12}, v_{12}|u_{21}, v_{21}, x_1)$ and $f_{u_{21},v_{21}}(u_{21}, v_{21}|u_{12}, v_{12}, x_1)$ are built in subsystem-1 and subsystem-2, respectively. Since the uncertainty variable x_1 is shared between both disciplines it is also treated as a coupling variable and is used to build models of conditional probability functions. The conditional probability function is modeled using quantile copula regression which is discussed in the next chapter. Joint distribution of the interdisciplinary compatible coupling variable is given as

$$f^*_{\mathbf{y},x_1}(u_{12}, v_{12}, u_{21}, v_{21}, x_1) \propto f_{u_{12},v_{12}}(u_{12}, v_{12}|u_{21}, v_{21}, x_1) f_{u_{21},v_{21}}(u_{21}, v_{21}|u_{12}, v_{12}, x_1) f_{x_1}(x_1) \tag{71}$$

The joint density function is then used to generate samples of interdisciplinary compatible solutions of coupling variables which is then used to estimate the system metric f_{sys}. The scripts of the disciplinary functions have been written in MATLAB. Also,

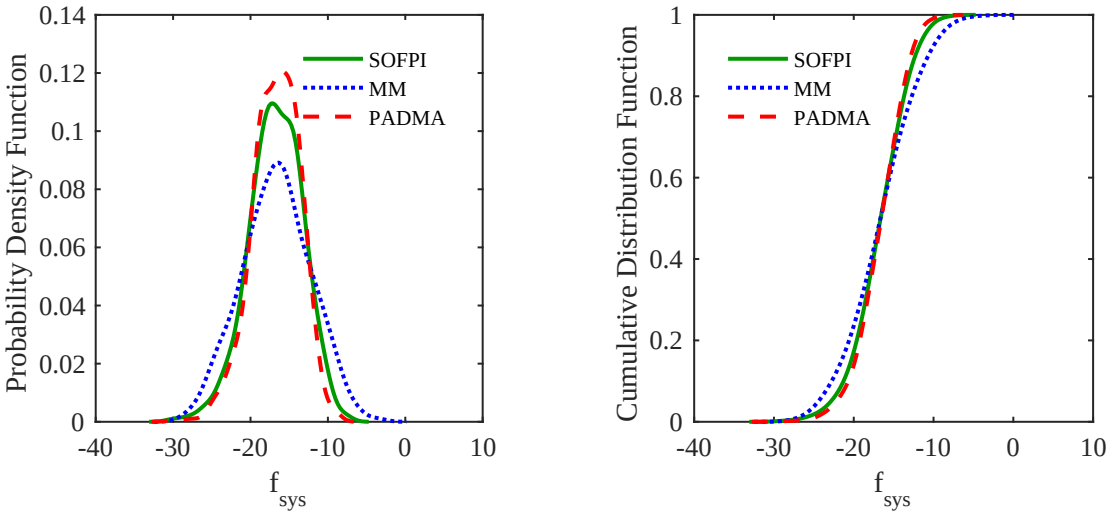

(a) Probability density function

(b) Cumulative distribution function

Figure 51: Comparison of probability density function and cumulative distribution function of system metric f_{sys} estimated using benchmark SOFPI method, Moment Matching method (MM) and PADMA method for analytical problem case-1

to automate the PADMA process, scripts for PADMA method have been written and executed in MATLAB.

4.4.5.1 Result: Case-1

In the first case, all the uncertain variables are assumed to have Gaussian distribution. The probability density function and cumulative distribution function of system metric estimated by the PADMA methods is plotted in Figure 51 and compared with the SOFPI and MM method. The general trend of the distribution has been found to be very similar to Gaussian distribution. Both the PADMA and MM methods have been found to be close to the SOFPI solution however; probability density function estimated by the MM method has been found to be slightly wider. The statistics of system metric is compared in Table 11. The mean estimated by the PADMA and MM methods has been found to be very close to the SOFPI solution. However, the MM method over predicted the standard deviation and the PAMDA method slightly under predicted the standard deviation. The skewness estimate by PADMA methods

Table 11: Comparison of statistical metrics of system metric f_{sys} for analytical problem case-1

	SOFPI	**MM**	**PADMA**
Mean(μ_f)	-16.75	-16.68	-16.70
Std. Dev.(σ_f)	3.47	4.45	3.05
Skewness (γ_f)	-0.36	-0.02	-0.44
K-L div.	-	0.09	0.01

has been found to be close to the SOFPI solution, whereas skewness estimated by MM method has been found to be very close to zero. In terms of over all closeness of probability density function, the PADMA method with K-L div. $= 0.01$ has been found to be closer to the SOFPI solution when compared to the MM method, for which K-L div. $= 0.09$.

Scatter plot matrix of interdisciplinary compatible solutions of coupling variables is shown in Figure 52. In addition to scatter plot of interdisciplinary compatible samples from each method, each subplot also shows a single iso-probability contour of value $0.02\mathrm{P}_{max}$, where P_{max} is the maximum probability value attained by the true solution using the SOFPI method. All the coupling variables are found to be statistically dependent on each other. The dependency structure among all the coupling variables has been found be very close to Gaussian form. The PADMA method has been found to closely match the dependency structure with the SOFPI solution. Although the MM method has been able to match the marginal distribution of all the coupling variables, it has assumed that the coupling variables are all independent. Figure 53 compares the contour plot of joint probability density of optimum interdisciplinary compatible solution of u_{12} and u_{21} estimated by all the SOFPI, MM and PAMDA methods. In addition to the strong dependency, the PADMA method has been able to capture the overall trend of joint probability density better than the MM method.

The linear dependency of coupling variables are compared between the SOFPI

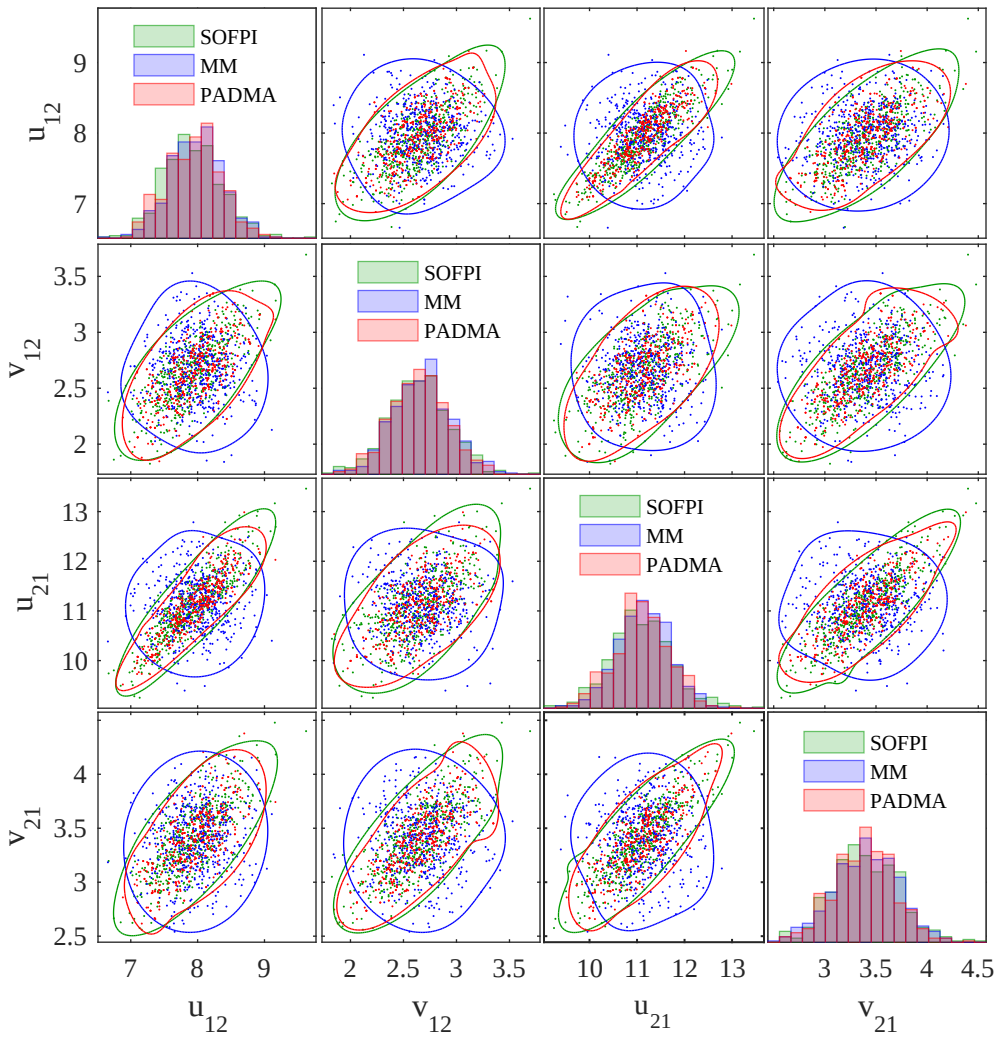

Figure 52: Scatter plot matrix of interdisciplinary compatible solution of coupling variables for analytical problem case-1

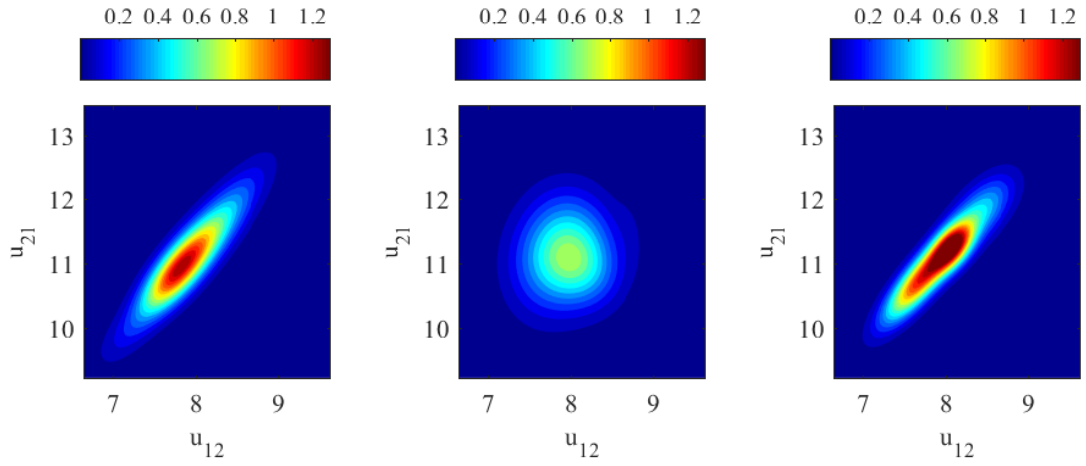

(a) SOFPI (b) MM (c) PADMA

Figure 53: Contour plot of joint probability density of interdisciplinary compatible solution of u_{12} and u_{21} for analytical problem case-1

and PADMA methods in Table 12. The PADMA method has been able to capture all the linear dependency within a 7% error. To compare the underlying non-linear dependency, Mutual Information is compared in between SOFPI and PADMA methods in Table 13. The difference of Mutual Information (Δ MI) between SOFPI and PADMA has been found to be within tolerable limit with maximum value of Δ MI = 0.12.

4.4.5.2 Results: Case-2

In the second case, all the uncertain variables are assumed to have gamma distribution except for x_1. The probability density function and cumulative distribution function of system metric estimated by PADMA method is plotted in Figure 54 and compared with the SOFPI and MM methods. Unlike case-1, the distribution of system metric has been found to be non-Gaussian and with negative skewness. The distribution estimated by the PADMA method has been found to be close to the SOFPI solution; however the MM method has been found to have a wider distribution. The statistics of system metric is compared in Table 14. Both the PADMA and MM methods have

Table 12: Comparison of Correlation Matrix of coupling variables for analytical problem case-1

Correlation Matrix

		u_{12}	v_{12}	u_{21}	v_{21}
SOFPI	u_{12}	1.00	0.71	0.89	0.73
	v_{12}	0.71	1.00	0.65	0.76
	u_{21}	0.89	0.65	1.00	0.85
	v_{21}	0.73	0.76	0.85	1.00
		u_{12}	v_{12}	u_{21}	v_{21}
PADMA	u_{12}	1.00	0.64	0.89	0.69
	v_{12}	0.64	1.00	0.61	0.75
	u_{21}	0.89	0.61	1.00	0.79
	v_{21}	0.69	0.75	0.79	1.00
		u_{12}	v_{12}	u_{21}	v_{21}
$\lvert\Delta\rho\rvert$	u_{12}	0.00	0.07	0.00	0.05
	v_{12}	0.07	0.00	0.04	0.01
	u_{21}	0.00	0.04	0.00	0.06
	v_{21}	0.05	0.01	0.06	0.00

Table 13: Comparison of Mutual Information Matrix of coupling variables for analytical problem case-1

Mutual Information Matrix

		u_{12}	v_{12}	u_{21}	v_{21}
SOFPI	u_{12}	1.33	0.34	0.71	0.38
	v_{12}	0.34	1.34	0.29	0.42
	u_{21}	0.71	0.29	1.37	0.59
	v_{21}	0.38	0.42	0.59	1.32
		u_{12}	v_{12}	u_{21}	v_{21}
PADMA	u_{12}	1.31	0.29	0.73	0.33
	v_{12}	0.29	1.32	0.27	0.42
	u_{21}	0.73	0.27	1.37	0.47
	v_{21}	0.33	0.42	0.47	1.25
		u_{12}	v_{12}	u_{21}	v_{21}
Δ MI	u_{12}	0.02	0.05	0.03	0.05
	v_{12}	0.05	0.02	0.01	0.00
	u_{21}	0.03	0.01	0.00	0.12
	v_{21}	0.05	0.00	0.12	0.07

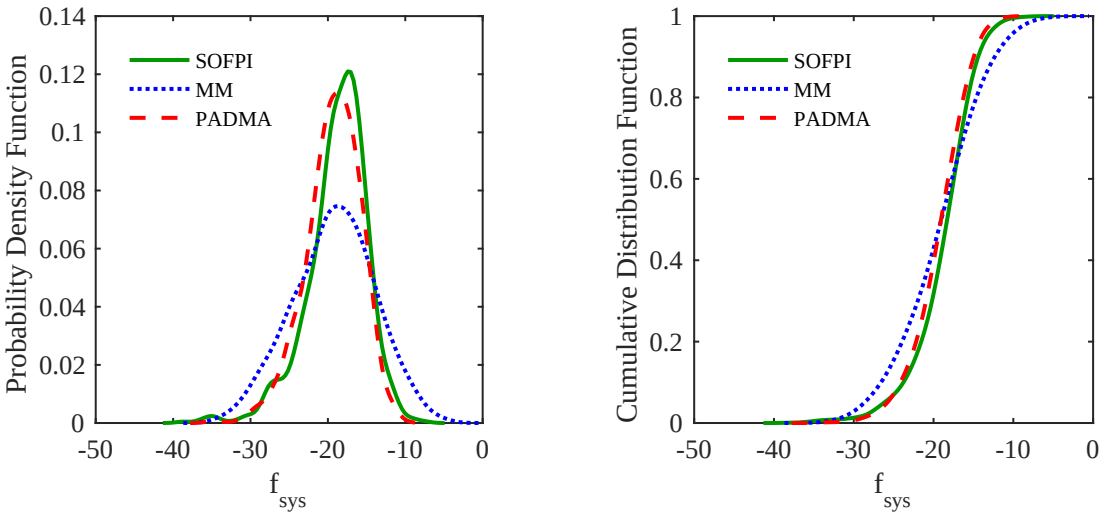

(a) Probability density function

(b) Cumulative distribution function

Figure 54: Comparison of probability density function and cumulative distribution function of system metric f_{sys} estimated using benchmark SOFPI method, Moment Matching method (MM) and PADMA method for analytical problem case-2

Table 14: Comparison of statistical metrics of system metric f_{sys} for analytical problem case-2

	SOFPI	**MM**	**PADMA**
Mean(μ_f)	-18.79	-19.25	-19.34
Std. Dev.(σ_f)	3.90	5.27	3.54
Skewness (γ_f)	-1.03	-0.15	-0.58
K-L div.	-	0.17	0.04

been found to slightly over predict the mean. However, similar to case-1, the MM method over predicted the standard deviation and PAMDA method slightly under predicted the standard deviation. Although, the PADMA method has not be able to estimate the skewness very accurately, it has performed better than the MM method. In terms of over all closeness of probability density function, the PADMA method with K-L div. = 0.04 has been found to be closer to the SOFPI solution when compared to the MM method, for which K-L div. = 0.17.

Scatter plot matrix of interdisciplinary compatible solutions of coupling variables is shown in Figure 55. All the coupling variables are found to be statistically dependent on each other. Unlike case-1, the dependency structure has been found to be non-Gaussian, which has been well captured by the PADMA method. Similar to case-1, the MM method has been able to match the marginal distribution of all the coupling variables, but it has assumed that the coupling variables are all independent. Figure 56 compares the contour plot of joint probability density of optimum interdisciplinary compatible solution of u_{12} and u_{21} estimated by all the SOFPI, MM and PAMDA methods. Similar to case-1, the PADMA method has been able to capture the overall trend of joint probability density better than the MM method.

The linear dependency of coupling variables are compared between SOFPI and PADMA methods in Table 15. The PADMA method has been able to capture all the linear dependency within an 8% error. To compare the underlying non-linear dependency, Mutual Information is compared between SOFPI and PADMA methods in Table 16. The difference of Mutual Information (Δ MI) between SOFPI and PADMA has been found to be within tolerable limit with maximum value of Δ MI = 0.12.

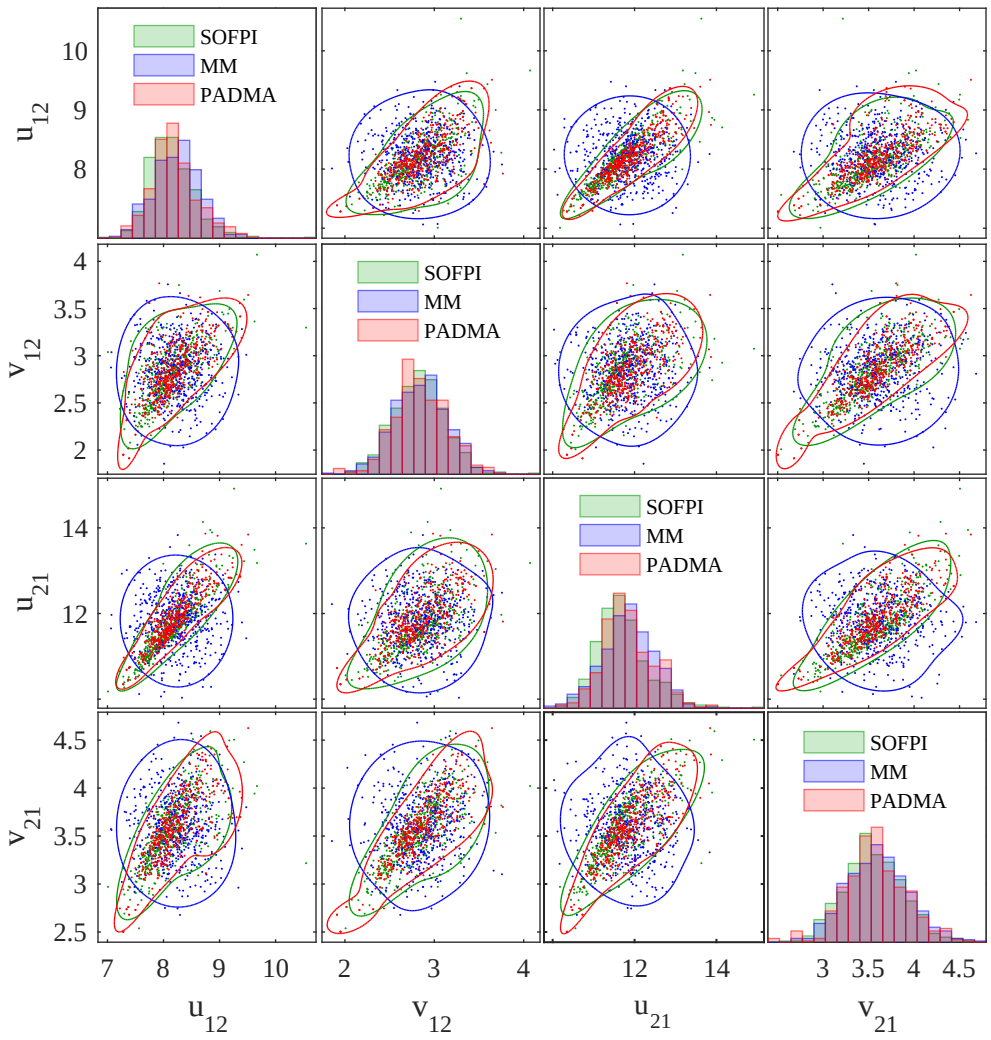

Figure 55: Scatter plot matrix of interdisciplinary compatible solution of coupling variables for analytical problem case-2

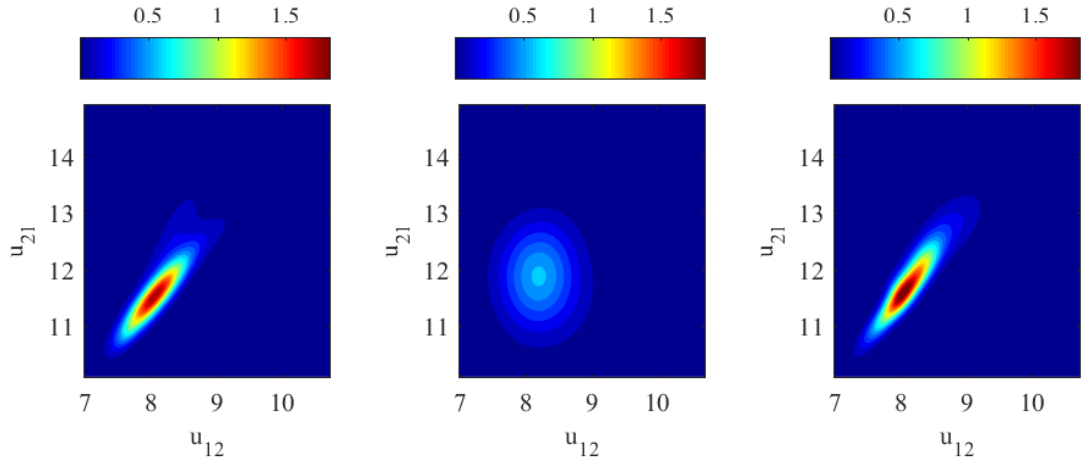

(a) SOFPI (b) MM (c) PADMA

Figure 56: Contour plot of joint probability density of interdisciplinary compatible solution of u_{12} and u_{21} for analytical problem case-2

Table 15: Comparison of Correlation Matrix of coupling variables for analytical problem case-2

Correlation Matrix

		u_{12}	v_{12}	u_{21}	v_{21}
SOFPI	u_{12}	1.00	0.67	0.85	0.67
	v_{12}	0.67	1.00	0.57	0.73
	u_{21}	0.85	0.57	1.00	0.79
	v_{21}	0.67	0.73	0.79	1.00
		u_{12}	v_{12}	u_{21}	v_{21}
PADMA	u_{12}	1.00	0.73	0.90	0.75
	v_{12}	0.73	1.00	0.69	0.81
	u_{21}	0.90	0.69	1.00	0.83
	v_{21}	0.75	0.81	0.83	1.00
		u_{12}	v_{12}	u_{21}	v_{21}
$\lvert\Delta\rho\rvert$	u_{12}	0.00	0.06	0.04	0.07
	v_{12}	0.06	0.00	0.12	0.08
	u_{21}	0.04	0.12	0.00	0.04
	v_{21}	0.07	0.08	0.04	0.00

Table 16: Comparison of Mutual Information Matrix of coupling variables for analytical problem case-2

	Mutual Information Matrix				
		u_{12}	v_{12}	u_{21}	v_{21}
SOFPI	u_{12}	1.29	0.36	0.73	0.44
	v_{12}	0.36	1.30	0.29	0.45
	u_{21}	0.73	0.29	1.37	0.58
	v_{21}	0.44	0.45	0.58	1.30
		u_{12}	v_{12}	u_{21}	v_{21}
PADMA	u_{12}	1.38	0.46	0.80	0.53
	v_{12}	0.46	1.33	0.40	0.57
	u_{21}	0.80	0.40	1.35	0.61
	v_{21}	0.53	0.57	0.61	1.34
		u_{12}	v_{12}	u_{21}	v_{21}
Δ MI	u_{12}	0.08	0.10	0.07	0.09
	v_{12}	0.10	0.03	0.11	0.12
	u_{21}	0.07	0.11	0.03	0.03
	v_{21}	0.09	0.12	0.03	0.04

4.5 Chapter Summary

In this chapter, a Probabilistic Analysis of Distributed Multidisciplinary Architectures (PADMA) has been developed to accurately quantify the uncertainty on system metrics and joint distribution of coupling variables by evaluation of probability of Event of Interdisciplinary Compatibility (EIC), in a distributed multidisciplinary analysis under uncertainty. The methodology allows each discipline to carry out uncertainty quantification and propagation independently and concurrently and build the models of conditional probability functions of disciplinary metrics. The conditional probability functions of disciplinary metrics are then used by a system level analyzer to evaluate the joint distribution of interdisciplinary compatible solutions.

The formulation of joint distribution of coupling variables is derived from general product rule of probability. For an UMDA, with only feed-forward coupling, the formulation is very similar to Bayesian Network, which is a probabilistic graphical model for a directed acyclic graph. However, for an UMDA with feedback coupling,

joint distribution is evaluated by estimating the probability of event of interdisciplinary compatible solutions. One of the critical aspects of PADMA is guessing the probability distribution of input coupling variables to each discipline. Although the functional form of the probability distribution does not matter, the domain of the guessed probability should be large enough to encompass the interdisciplinary compatible solutions. If the domain of guessed probability density functions is too large, then it leads to computation expense as well as inaccuracy in building conditional probability models. On the other hand, if the domain of guessed probability density functions is smaller than the domain of interdisciplinary compatible solutions, then evaluation of joint distribution of interdisciplinary compatible solutions will be inaccurate and another iteration of the PADMA process will be required.

To validate the hypothesis to the first research question, two numerical problems have been selected. For each problem, two case studies have been carried out, one with all uncertainty variables with Gaussian distribution and another one with mixture of Gaussian and non-Gaussian distribution. In both problems, strong dependencies have been observed among some of the coupling variables. In the cases with non-Gaussian uncertainty, the dependency structure have been found to be non-Gaussian. In all cases the PADMA method has been able to capture the dependency structure as well as accurately estimate correlation coefficient and Mutual Information among coupling variables. The PADMA method has also been able to accurately quantify the uncertainty on system metric as compared to state of art Moment-Matching method for distributed UMDO.

The only assumption in the PADMA method is that accurate models of conditional probability functions are available from each discipline. In this work, quantile copula regression is used to model the conditional probability functions which is discussed in next chapter. The accuracy of the PADMA method to quantify the uncertainties is directly related to the accuracy of the probabilistic models. Figure 57 shows accuracy

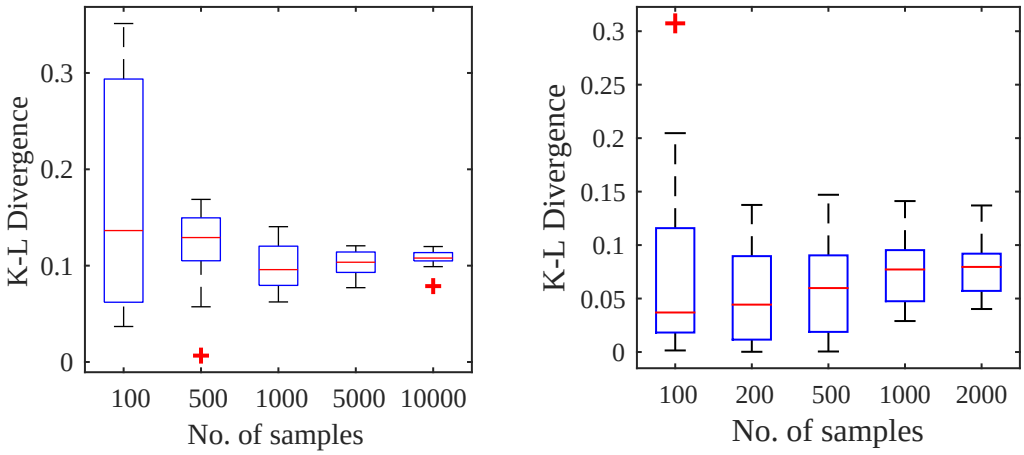

(a) Toll road problem case-1

(b) Analytical problem case-1

Figure 57: Accuracy of PADMA method measured by K–L divergence of system metric when compared to SOFPI method as a function of number of disciplinary samples

of the PADMA method as a function of number of samples used to build the models of conditional probability functions. Accuracy is evaluated as K-L divergence of system metrics estimated by the PADMA method when compared with the SOFPI solution. The results are shown for case-1 of both the toll road problem and the analytical problem. As observed, lower samples leads to higher error in the models of conditional probability functions, which leads to possible higher inaccuracy in the PADMA method.

CHAPTER V

PROBABILISTIC MODELING USING QUANTILE COPULA REGRESSION

Building surrogate models or emulators of disciplinary metrics is one of the computational efficient ways to carry out design space exploration and optimization. This is one of the common approaches in UMDO, where each discipline builds disciplinary surrogates of disciplinary metric as a function of input variables and uncertainty variables. If the disciplinary analyses are explicit functions of local uncertain variables i.e , $\mathbf{y}_i = f_i(\mathbf{x}_i, \mathbf{u}_i)$, where $\mathbf{x}_i$ are input variables and $\mathbf{u}_i$ are local uncertain variables, then it is appropriate to build a surrogate model with local uncertain variables $\mathbf{u}_i$ as one of the input variables, i.e. $\tilde{\mathbf{y}}_i = \tilde{f}_i(\mathbf{x}_i, \mathbf{u}_i)$. Please note that $\tilde{()}$ used on any function in this chapter signifies approximate models for both deterministic and non-deterministic functions unless stated otherwise. Nevertheless, in many scenarios the disciplines may have inherent uncertainties or noises such as numerical error, structural uncertainty, experimental uncertainty, interpolation uncertainty, expert judgment, etc. Processes like multi-fidelity analysis and intrusive error propagation can also create inherent uncertainties in the disciplinary metrics. In these scenarios, a statistical surrogate model or a probabilistic model, i.e. $\mathrm{P}(\mathbf{y}_i|\mathbf{x}_i) = \tilde{f}_{y_i}(\mathbf{y}_i|\mathbf{x}_i)$, is appropriate, where the surrogate model does not have local uncertainties as input but the effect of the local uncertainties on outputs are captured probability distribution.

In this chapter, quantile copula regression is developed to build models of conditional probability density function. The hypothesis to research question 2 is given as

Research Question 2.0: *What is an appropriate probabilistic modeling technique to comprehensively model conditional probability of multivariate disciplinary responses with heteroskedasticity and statistical dependence ?*

Hypothesis 2.0: *If the disciplinary responses are continuous variables and if the dependencies among responses are monotonic, then quantile copula regression is an appropriate method to comprehensively model the conditional probability density functions of disciplinary metrics using quantile regressions and model dependencies among them using copula.*

In the next section, a general overview of probabilistic modeling is discussed. After that, the theory of quantile regression will be presented, which is used to model the conditional probability density of each response. Next, *Copula* theory is presented which is used to model the statistical dependencies among the responses. Following that, quantile copula regression is developed which merges the theory of quantile regression and copula theory to build a probabilistic model for multiple responses with dependencies. Next, a numerical demonstration is presented on an application of quantile copula regression. Finally, the chapter is summarized in the last section.

5.1 Overview: Probabilistic Modeling

In machine learning literature, probabilistic models can be categorized into two broad categories; **generative models** and **discriminative models**. Let's say input variables (also called *explanatory, predictor, covariates, independent variables* etc.) are defined as x and output variables (also called *response, predicted , measured, outcome, dependent, target variables*, etc.) are defined by y. Generative models specify joint probability distribution of input and output variables, i.e. $\mathrm{P}(x, y)$. Examples of generative models are *Gaussian distribution, kernel density estimation, Gaussian mixture model, Naive Bayes, Hidden Markov Models, Bayesian Networks, Markov random fields*, and so on [108]. Discriminative models on the other hand specify

dependencies of output variables on input variables through conditional probability distribution $\mathrm{P}(y|x)$. Examples of discriminative models are *Bayesian linear regression, generalized linear regression, neural networks, support vector machines,* etc. [108]. As discussed in the last chapter, conditional probabilities are used to evaluate the dependency and compatibility of the coupling variables; discriminative models are preferred to model disciplinary functions. Although it should be noted that any joint distribution from generative models can be converted to a discriminative conditional model by Bayes' rule as

$$\mathrm{P}(y|x) = \frac{\mathrm{P}(x,y)}{\mathrm{P}(x)} \tag{72}$$

The main goal of a discriminative probabilistic model is to predict the uncertainty of output variables y at a new value of input variable x on the basis of available set of N training data $\mathbf{X} = (\mathbf{x}_1, \mathbf{x}_2, \ldots, \mathbf{x}_N)^T$ and their corresponding outputs $\mathbf{y} = (y_1, y_2, \ldots, y_N)^T$, where each input training data consists of D predictor variables $\mathbf{x} = (x_1, x_2, \ldots, x_D)$. The uncertainty over the output variables are expressed using probability distribution. Generally, it is assumed that for a given value of $\mathbf{x}$, y follows a fixed parametric probability distribution family like Gaussian distribution as

$$\mathrm{P}(y|\mathbf{x}, \mathbf{w}) = \mathcal{N}(y|\mu(\mathbf{x}, \mathbf{w}), \beta^{-1}) \tag{73}$$

where $\mu(\mathbf{x}, \mathbf{w})$ is the function determining the mean for a given value of $\mathbf{x}$, $\mathbf{w}$ are the unknown parameters of mean function, β is the unknown precision or inverse of variance. Typically homoscedasticity, is assumed, i.e. dependent variables have constant variance across the range of input variables, therefore β is independent of $\mathbf{x}$. Details of parameter estimation in a discriminative probabilistic model is given in Appendix II.

5.1.1 Types of Discriminative Probabilistic Models

Depending upon the functional form of $\mu(\mathbf{x}, \mathbf{w})$, the discriminative models can be categorized into three classes; linear models, nonlinear models, and non-parametric

models.

5.1.1.1 Linear Models

These are the models $\mu(\mathbf{x}, \mathbf{w})$ which are a linear function of $\mathbf{w}$. The simplest linear model can be given as

$$\mu(\mathbf{x}, \mathbf{w}) = w_0 + w_1 x_1 + \ldots_+ w_D x_D \tag{74}$$

Although the model represented by Equation 74 is linear with respect to input variables $\mathbf{x}$, it can be extended to handle a nonlinear relationship with $\mathbf{x}$ by considering a linear combination of fixed nonlinear functions $\boldsymbol{\phi}(\mathbf{x})$ as

$$\mu(\mathbf{x}, \mathbf{w}) = \sum_{j=0}^{M-1} w_j \phi_j(\mathbf{x}) = \mathbf{w}^T \boldsymbol{\phi}(\mathbf{x}) \tag{75}$$

where $\phi_j(\mathbf{x})$ are known as basis functions. Please note that the model given by Equation 75 is nonlinear with respect to $\mathbf{x}$ but still linear with respect to $\mathbf{w}$, therefore this still falls under the linear model category. One of the commonly used models in statistics literature is called Response Surface Methodology (RSM) and is given as

$$\mu(\mathbf{x}, \mathbf{w}) = w_0 + \sum_{i=1}^{N} w_i x_i + \sum_{i=1}^{n} \sum_{j=i}^{n} w_{ij} x_i x_j \tag{76}$$

RSM can be further extended by including higher order polynomial terms to introduce more nonlinearity in the model.

5.1.1.2 Nonlinear Models

These are the models $\mu(\mathbf{x}, \mathbf{w})$ which are nonlinear functions of parameters $\mathbf{w}$. As discussed in the last section, to capture nonlinear behavior with respect to input space $\mathbf{x}$, a linear model can use fixed basis functions with higher order terms. An alternate approach is to use adaptive basis functions, i.e. to use a parametric basis function, while fixing the number of basis functions in advance. In this approach

both $\mathbf{w}$ and the parameters of the basis function are evaluated during the training. A general form of this kind of model is given as

$$\mu(\mathbf{x}, \mathbf{w}) = f\left(\sum_{j=1}^{M} w_j \phi_j(\mathbf{x})\right) \tag{77}$$

where $f(.)$ is a nonlinear activation function and the basis function $\phi_j(\mathbf{x})$ depends on some parameters, which get adjusted along with w_j during the training.

One of the commonly used nonlinear models is *Feed-Forward Neural Network*. A general function form of a Feed-Forward Neural Network with two-layer is given as

$$\mu(\mathbf{x}, \mathbf{w}) = \sum_{j=0}^{M} w_{kj}^{(2)} h\left(\sum_{i=0}^{D} w_{ji}^{(1)} x_i\right) \tag{78}$$

where $h(.)$ is a nonlinear activation function such as hyperbolic tangent function, radial basis function, etc.

5.1.1.3 Non-parametric Models

Both linear and non-linear models assume a fixed functional form to model the entire input space. In non-parametric models, the functional form of the model is not predetermined but is constructed according to the information derived from the data. One of the simplest approaches is to divide the input space into regions and use different basis function in each region, for example a Gaussian basis function

$$\phi_j(\mathbf{x}) = \exp\left\{-\frac{(\mathbf{x} - \gamma_j)^2}{2s^2}\right\} \tag{79}$$

where γ_j is the location parameter in input space and s governs the spatial scale. In machine learning literature *Kernel methods* [167] are commonly used to build non-parametric models. These are *memory-based* methods in which the training data set or subset of them are stored and used during prediction for new data points. The prediction at a new value of $\mathbf{x}$ is carried out using *kernel function* evaluated at training point and by recasting the linear parametric model into an equivalent "dual representation" as

$$\mu(\mathbf{x}) = \mathbf{w}^T \boldsymbol{\phi}(\mathbf{x}) = \mathbf{k}(\mathbf{x})^T (\mathbf{K} + \lambda \mathbf{I}_N)^{-1} \mathbf{y} \tag{80}$$

where $\mathbf{k}(\mathbf{x})$ is a vector with elements in kernel function $k_n(\mathbf{x}) = k(\mathbf{x}_n, \mathbf{x})$ evaluated at point $\mathbf{x}_n$, $\mathbf{K}$ is *Gram* matrix $\mathbf{K} = \mathbf{\Phi}\mathbf{\Phi}^T$, $\mathbf{\Phi}$ is the design matrix whose n^{th} row is given as $\boldsymbol{\phi}(\mathbf{x}_n)^T$, and λ is regularization parameter with $\lambda \geq 0$. For a fixed nonlinear feature space mapping $\boldsymbol{\phi}(\mathbf{x})$, the kernel function is given by the relation

$$k(\mathbf{x}, \mathbf{x}') = \boldsymbol{\phi}(\mathbf{x})^T \boldsymbol{\phi}(\mathbf{x}'). \tag{81}$$

Two commonly used kernel method-based models are *Radial Basis Function Network* and *Gaussian Processes* which uses radial basis kernel function $k(\mathbf{x}, \mathbf{x}') = h(||\mathbf{x} - \mathbf{x}'||)$ and Gaussian kernel $k(\mathbf{x}, \mathbf{x}') = \exp(||\mathbf{x} - \mathbf{x}'||^2/2\sigma^2)$ respectively.

5.1.2 Applicability and Limitation

The discriminative probabilistic models discussed in the previous section have a wide range of application in building surrogate models for engineering analysis. Depending on the functional behavior of the analysis, linear or nonlinear models can be selected and applied. These models can be built using a relatively lower number of data from analysis or experiments and are an order of magnitude faster to execute compared to actual analysis. Applying these models instead of actual analysis during the design process reduces the computational cost and allows the designer to carry out quick trade studies such as optimization. These probabilistic models not only allow the designer to quantify the random uncertainty or the noises, but also help in quantifying the model form uncertainty which arises due to limited number of experimental or analysis data.

Although there are a few limitations of these models like the *curse of dimensionality*, under fitting, over fitting, etc., there are three limitations that are of relevance to the current work, namely *non-Gaussian noises*, *heteroskedasticity*, and *multivariate response*. Generally, most of the models discussed in the previous sections assume that the uncertainty on output variables has Gaussian distribution as given in Equation 73. Although, these assumptions are valid for most of the scenarios where these

uncertainties arise due to random noise. But, these may not be valid if some local disciplinary uncertainty causes non-Gaussian behavior in the disciplinary outputs. To overcome this problem, some other distribution form in Equation 73 can be used or *Generalized linear model (GLM)* [168] can be used which allows an uncertainty distribution model other than Gaussian distribution. But, this approach assumes that uncertainty will follow the same distribution form in the entire space of $\mathbf{x}$. Another challenge is to model *heteroskedasticity*, which refers to the situation where variance of output variables varies in the range of input variables. As stated in Equation 73, typically these models assume that the variance or precision of output variable is constant in the design space. One way to overcome this issue is to model the precision as a function of input variables similar to the mean function as $\beta(\mathbf{x}, \mathbf{v})$, where $\mathbf{v}$ is the parameter of the precision model.

Probabilistic models can be tweaked to overcome some of the limitations of non-Gaussian noises and heteroskedasticity, but their applicability will be limited to a fixed distribution form of uncertainty of output variables. Also it is necessary to have some prior information regarding the behavior of output so that the proper form of the noise or uncertainty can be selected. It also becomes challenging when the noise or the uncertainty does not have a fixed parametric form. For example, consider an empirical equation of aircraft wing weight [169] given by

$$\frac{W_{Wing}}{W_{OEW}} = p_1 n_{ult}^{p_2} t_{r,max}^{p_3} \left(\frac{b}{\cos\Lambda_{c/2}}\right)^{p_4} \left(1 + \sqrt{\frac{p_5 \cos\Lambda_{c/2}}{b}}\right) \left(\frac{W_{OEW}}{S}\right)^{p_6} \tag{82}$$

The nominal values of parameters p_i are $p_1 = 0.0017,\ p_2 = 0.55,\ p_3 = -0.3,\ p_4 = 1.05,\ p_5 = 6.25$ and $p_6 = -0.3$. These are parameters are generally estimated by fitting historical data and therefore they have some uncertainty associated with it. Let's consider uncertainty on parameter p_4 is given by a Gaussian distribution as $p_4 \sim \mathcal{N}(1.05, 0.002)$. With uncertainty on p_4, the samples of normalized wing weight W_{Wing}/W_{OEW} as a function of span b for a notional aircraft is plotted in Figure 58a.

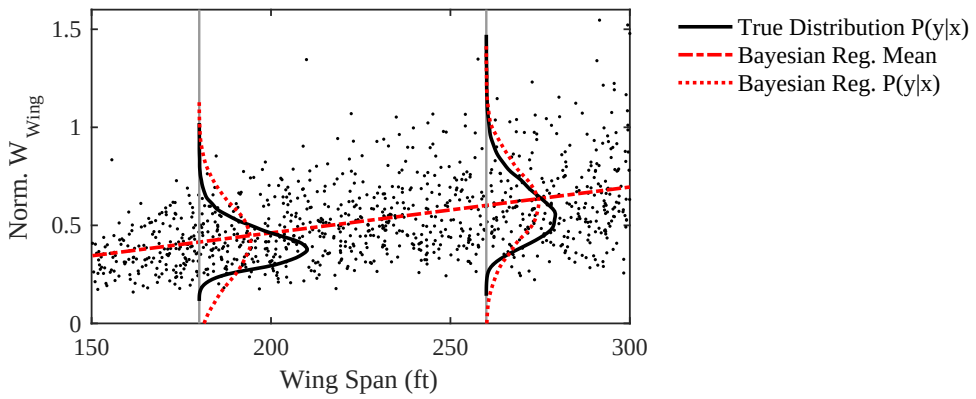

(a) Bayesian Regression

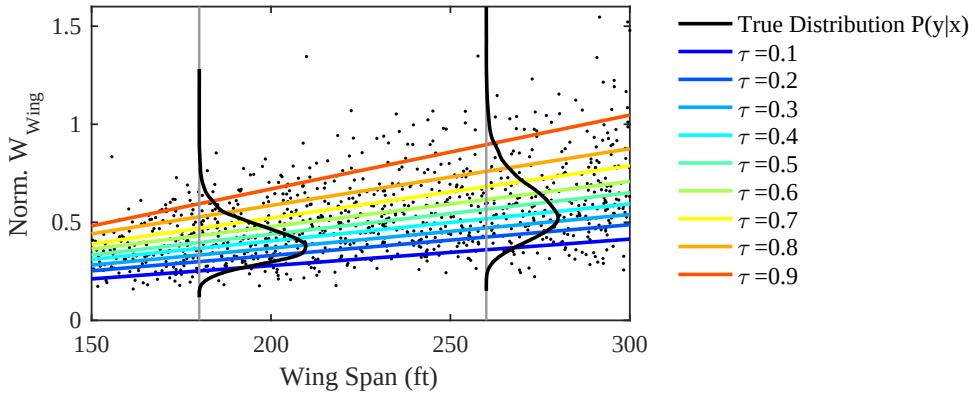

(b) Quantile Regression

Figure 58: Comparison of Bayesian regression and quantile regression on predictive capability of conditional statistics of normalized wing weight data

As observed, the samples have heteroskedasticity and the noises are not of Gaussian form, even for a simple empirical equation with only one Gaussian uncertainty. If Bayesian regression is used as probabilistic model, then the conditional density functions are not accurate (also shown in Figure 58a). To handle these challenges, an alternate approach is to build models for the quantiles of the output variables, and use the quantile information to generate the distribution of the uncertainty. For example, Figure 58b shows regression curve of different conditional quantiles of normalized wing weight as a function wing span. The conditional quantiles provides a overall and a comprehensive view of conditional probability density without assuming any functional form of conditional distribution.

5.2 Quantile Regression

The main focus of the probabilistic model discussed in the previous section is to evaluate the conditional mean and the uncertainty with some parametric assumption of probability densities. Instead of mean, modeling of quantiles allows a broader approach to predict the conditional distribution without any assumptions of the uncertainty distribution. For example, for uncertain variables with skewed distribution, the 50^{th} quantile or median, when used as a measure of center, is more robust than mean [170]. This can be seen in Figure 59 where two distributions may differ by mean or by specific quantiles. Also, quantile provides a straightforward and a better approach to estimate tail probabilities which are required for reliability analysis. Therefore, in a scenario where output variable may not strictly follow a fixed parametric probability density function and is heteroscedastic with respect to input space, regression on conditional quantiles or Quantile regression provides a more complete statistical model than the mean regression.

Koenker and Bassett (1978) [171] pioneered the development of quantile regression and discussed its various properties. Since then, these methods have been further developed and improved by many researchers, and have been comprehensively reviewed by Koenker [172]. Quantile regression has found its application in various fields of research including medicine, finance and economics, environmental modeling, etc, some of which are discussed by Keming et al. [173].

For a random variable Y with distribution function $F(Y) = \mathrm{P}(Y \leq y)$, τ^{th} quantile is defined as

$$Q(\tau) = F_Y^{-1}(\tau) = \inf\{y : F(y) \geq \tau\} \tag{83}$$

where $0 \leq \tau \leq 1$. $Q(0.25)$, $Q(0.5)$ and $Q(0.75)$ are generally known as *lower quartile, median,* and *upper quartile.* Similar to distribution function $F(Y)$ and density function $f(Y)$, a quantile function $Q(\tau)$ provides a better characterization of the random variable Y. To evaluate the sample quantile $Q(\tau)$ based on a random sample

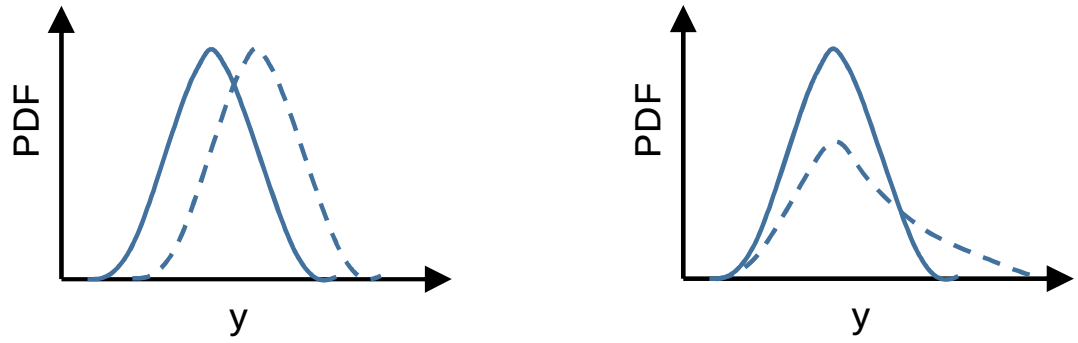

(a) Distribution differ by mean (b) Distribution differ by quantiles

Figure 59: Two distributions may differ with respect to (a) their mean only or (b) specific quantiles

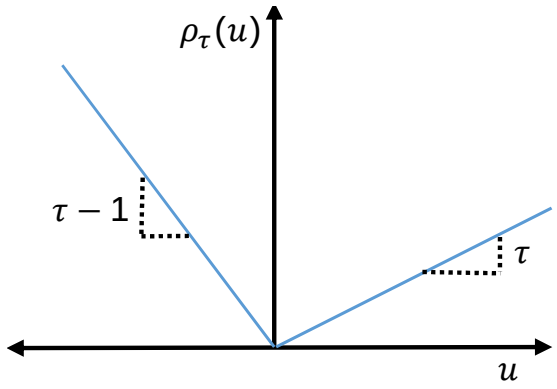

Figure 60: Check function $\rho_\tau(u)$ for quantile regression

$\{y_1, y_2, \ldots, y_n\}$, one common approach is to define the sample quantile in terms of order statistics $y_{(1)} \leq y_{(2)} \leq \ldots y_{(n)}$, by rearranging and sorting the original sample. Rather, a more generalized approach is given in terms of an optimization problem, where τ^{th} sample quantile can be found by solving

$$\min_{\xi \in \mathbb{R}} \sum_{i=1}^{n} \rho_\tau(y_i - \xi) \tag{84}$$

where $\rho_\tau(.)$ is a "check function" as shown in Figure 60 and is given as $\rho_\tau(u) = |u(\tau - \mathbb{I}_{(u<0)})|$ and $\mathbb{I}$ is the indicator variable.

Similar to conditional mean in regression, τ^{th} conditional quantile is defined as

$$Q_{Y|\mathbf{x}}(\tau|\mathbf{x}) = F^{-1}_{Y|\mathbf{x}}(\tau|\mathbf{x}) \tag{85}$$

where $\mathbf{x}$ is a vector of input variables and $F_{Y|\mathbf{x}}$ is the conditional distribution function

of Y given $\mathbf{x}$. In quantile regression, τ^{th} conditional quantile is modeled by a parametric function of input variable $\mathbf{x}$ as $Q_{Y|\mathbf{x}}(\tau|\mathbf{x}) = y_\tau(\mathbf{x}, \boldsymbol{\beta}_\tau)$, where $\boldsymbol{\beta}_\tau$ is the vector of quantile regression coefficients of parametric function $y_\tau(\mathbf{x}, \boldsymbol{\beta}_\tau)$. The parameter $\boldsymbol{\beta}_\tau$ is evaluated by modifying the optimization problem Equation 84 as

$$\hat{\boldsymbol{\beta}}_\tau = \arg\min_{\boldsymbol{\beta} \in R^k} \sum_{i=1}^{n} \rho_\tau \left(y_i - y_\tau(\mathbf{x}_i, \boldsymbol{\beta}_\tau) \right). \tag{86}$$

This optimization problem is analogous to estimating the conditional mean by minimizing the sum of squared error $\sum_{i=1}^{n} (y_i - \mu\left(\mathbf{x}_i, \boldsymbol{\beta}_\tau\right))^2$.

5.2.1 Modeling and Estimation

One of the common approaches to model quantile regression function for τ^{th} conditional quantile $y_\tau(\mathbf{x}, \boldsymbol{\beta})$ is linear models which is given as

$$\mathbf{y}_\tau = \mathbf{X}\boldsymbol{\beta}_\tau + \boldsymbol{\epsilon} \tag{87}$$

where $\mathbf{y}_\tau \in \mathbb{R}^{n \times 1}$ the vector of τ^{th} quantiles, $\boldsymbol{\beta}_\tau \in \mathbb{R}^{q \times 1}$ is the vector of quantile regression coefficient for τ^{th} quantile and $\boldsymbol{\epsilon} \in \mathbb{R}^{n \times 1}$ is the vector of errors. $\mathbf{X} \in \mathbb{R}^{n \times q}$ is the *design matrix* given as

$$\mathbf{X} = \begin{pmatrix} \mathbf{x}_1^{\mathrm{T}} \\ \mathbf{x}_2^{\mathrm{T}} \\ \vdots \\ \mathbf{x}_n^{\mathrm{T}} \end{pmatrix} = \begin{pmatrix} x_{11} & \cdots & x_{1q} \\ x_{21} & \cdots & x_{2q} \\ \vdots & \ddots & \vdots \\ x_{n1} & \cdots & x_{nq} \end{pmatrix}, \tag{88}$$

$\mathbf{x}_i = [x_{i1}, \ldots, x_{iq}]^T$ is the vector of q predictors for i^{th} sample.

To set this up as a standard linear programming minimization problem, quantile regression is rewritten as

$$\mathbf{y}_\tau = \mathbf{X}\boldsymbol{\beta}_\tau + (\mathbf{u} - \mathbf{v}) \tag{89}$$

where $\mathbf{u} = \boldsymbol{\epsilon}\mathbb{I}(\boldsymbol{\epsilon} > 0)$ and $\mathbf{v} = |\boldsymbol{\epsilon}|\mathbb{I}(\boldsymbol{\epsilon} < 0)$. Then the optimization problem given by

Equation 86 can be remodeled into standard linear programming as

$$\begin{aligned} \text{minimize} \quad & \tau \mathbf{1}_n^T \mathbf{u} + (1-\tau)\mathbf{1}_n^T \mathbf{v} && \text{(90a)} \\ \text{with respect to} \quad & \boldsymbol{\beta}_\tau, \mathbf{u}, \mathbf{v} \\ \text{subject to} \quad & \mathbf{y}_\tau - \mathbf{X}\boldsymbol{\beta}_\tau = \mathbf{u} - \mathbf{v} && \text{(90b)} \\ & \boldsymbol{\beta}_\tau \in \mathbb{R}^{q\times 1}, \mathbf{u} \geq 0, \mathbf{v} \geq 0. \end{aligned}$$

The optimization problem in Equation 90 can be solved by *Simplex methods* or *interior point methods* [172, 174, 175].

Two other common approaches to estimate the parameters of quantile regression are *likelihood-based approach* [176] and *full Bayesian treatment* [177, 178]. For examples, in a full Bayesian treatment, a prior distribution is assumed on the parameters $\pi(\boldsymbol{\beta}_\tau)$ and posterior distribution is estimated by employing the asymmetric Laplace likelihood function as

$$\pi(\boldsymbol{\beta}_\tau|\mathbf{y}) \propto L(\mathbf{y}|\boldsymbol{\beta}_\tau)\pi(\boldsymbol{\beta}_\tau) \tag{91}$$

Yu et al. [179] has demonstrated the full Bayesian treatment by taking improper uniform prior distribution for $\boldsymbol{\beta}_\tau$. Kottas et al. [180] proposed an approach of using mixture model for the errors to estimate the median regression model.

In current work, each quantiles are modeled with linear models. Approaches for non-linear models-based quantile regression includes Neural Network [181], Gaussian Process [182], non-parametric models [183], etc.

5.2.2 Modeling Multiple Quantile Regressions

Previous section provides the approaches to model quantile regression for τ^{th} conditional quantile. However to estimate the entire conditional quantile distribution comprehensively, quantile regressions are required for multiple settings of $\tau_1, \ldots, \tau_k$, where $\tau_i \in (0, 1)$. For the ease of implementation, it is assumed the the setting of τ_i are monotonically increasing, i.e. $\tau_i > \tau_{i-1}$.

A straightforward approach is to model separate quantile regressions for each τ_i^{th} quantile, $Q_{Y|\mathbf{x}}(\tau_i|\mathbf{x}) = y_{\tau_i}(\mathbf{x}, \boldsymbol{\beta}_{\tau_i})$, where $\boldsymbol{\beta}_{\tau_i}$ is the vector of quantile regression coefficients of τ_i^{th} quantile. For the linear modeling approach given by Equation 87, it can be assumed that each quantile regression are built using the same design matrix $\mathbf{X}$, such the length of each vector $\boldsymbol{\beta}_{\tau_i}$ is same. Let $\boldsymbol{\beta} = [\boldsymbol{\beta}_{\tau_1}, \ldots, \boldsymbol{\beta}_{\tau_k}]$ be a matrix of size $q \times k$, containing the coefficients of the quantile regressions for all the settings of τ. Then, for a given value of predictor $\mathbf{x}$, quantiles are estimated as $\hat{\mathbf{y}} = \mathbf{x}^T\boldsymbol{\beta}$, where $\hat{\mathbf{y}} = [\hat{y}_{\tau_1}, \ldots, \hat{y}_{\tau_k}]$ is the vector containing all the estimated quantiles corresponding to $\boldsymbol{\tau} = [\tau_1, \ldots, \tau_k]$. In the current work, multiple quantile regression models of a variable y is represented as $Q_{Y|\mathbf{x}}(\boldsymbol{\tau}|\mathbf{x}) = y_{\boldsymbol{\tau}}(\mathbf{x}, \boldsymbol{\beta})$, unless otherwise specified.

For a monotonically increasing setting of $\tau_1, \ldots, \tau_k$, the conditional quantiles $y_{\tau_1}, \ldots, y_{\tau_k}$ should also be monotonically increasing for any given value of $\mathbf{x}$. However, in some scenarios the estimated quantiles $\hat{y}_{\tau_1}, \ldots, \hat{y}_{\tau_k}$ at some values of $\mathbf{x}$ using quantile regression may not be monotonically increasing, i.e. $\hat{y}_{\tau_i} \not> \hat{y}_{\tau_{i-1}}$, for some values of i. This occurs when the quantile curves cross each other, also known as *quantile crossing problem*, which can occurs when inaccuracy is introduced in quantile regression modeling due to sparse data, non-linearity, etc. An approach to overcome the issue of quantile crossing problem is to build the quantile regression models for all the levels of τ simultaneously and impose the non-crossing quantile constraints [184]. In the current work an approach known as *quantile bootstrap* or *quantile rearrangement* [185] is used, which allows natural monotonization of quantiles by using estimated non-monotonic conditional quantiles from quantile regression and applying a monotone rearrangement procedure, which results in conditional quantiles which by construction are monotonic.

In quantile bootstrap or quantile rearrangement approach, a non-monotone quantile function $\widehat{Q}(\tau|\mathbf{x})$ is transformed into a monotone function $\widehat{Q}^*(\tau|\mathbf{x})$, which is used to generate monotonic quantiles. $\widehat{Q}^*(\tau|\mathbf{x})$ is the quantile function of a random variable

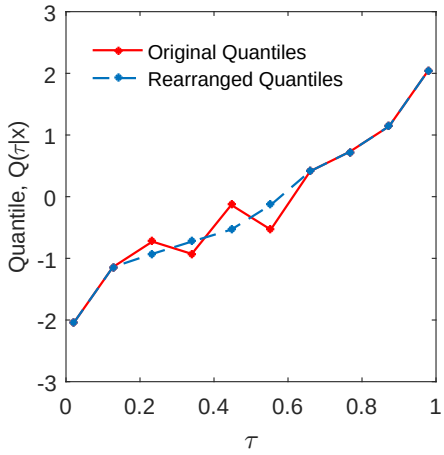

Figure 61: Quantile rearrangement of non-monotonic quantiles

Y, which is related to the original quantile as $Y := \widehat{Q}(U|\mathbf{x})$ where $U \sim Uniform(0,1)$. The quantile function of Y is given as

$$\widehat{Q}^*(\tau|\mathbf{x}) = \widehat{F}^{-1}(\tau|\mathbf{x}) = \inf\{y : \widehat{F}(y|\mathbf{x}) \geq \tau\} \tag{92}$$

which is naturally monotonic with respect to τ. If the original quantile function $\widehat{Q}(\tau|\mathbf{x})$ is monotonically increasing then $\widehat{Q}^*(\tau|\mathbf{x})$ coincide with $\widehat{Q}(\tau|\mathbf{x})$. An example of quantile rearrangement approach is shown in Figure 61.

5.2.3 Probability Density Estimation Using Conditional Quantile

If $Q_{Y|\mathbf{x}}(\tau|\mathbf{x})$ is the conditional quantile function and $F_{Y|\mathbf{x}}(y|\mathbf{x})$ is the distribution function of a random variable Y for given $\mathbf{x}$, then $F_{Y|\mathbf{x}}\left(Q_{Y|\mathbf{x}}(\tau|\mathbf{x})\right) = \tau$. Taking the derivative, one gets $f_{Y|\mathbf{x}}\left(Q_{Y|\mathbf{x}}(\tau|\mathbf{x})\right) Q'_{Y|\mathbf{x}}(\tau|\mathbf{x}) = 1$, which is used to estimate the conditional probability density function as

$$f_{Y|\mathbf{x}}(y|\mathbf{x}) = \frac{1}{Q'_{Y|\mathbf{x}}\left(Q^{-1}_{Y|\mathbf{x}}(y|\mathbf{x})\right)} \tag{93}$$

where $Q'_{Y|\mathbf{x}}(.)$ is also called quantile density function.

In terms of implementation, quantile regressions $Q_{Y|\mathbf{x}}(\boldsymbol{\tau}|\mathbf{x},\boldsymbol{\beta}) = \mathbf{y}_{\boldsymbol{\tau}}(\mathbf{x},\boldsymbol{\beta})$ are only modeled for a finite number of levels of $\boldsymbol{\tau} = [\tau_1,\ldots,\tau_k]$. If $\hat{y}_{\tau_1},\ldots,\hat{y}_{\tau_k}$ are non-decreasing conditional quantiles estimated by quantile regression at $\tau_1,\ldots,\tau_k$, the

predictive density $\hat{p}(y)$ is estimated by interpolating between the estimated quantiles. For the lower and upper tails, probability density is assumed to decay exponentially ensuring that the probability density function integrates to one [186]. Probability density $\hat{p}(y)$ at any value y is estimated as

1. If $\hat{y}_{\tau_1} < y < \hat{y}_{\tau_k}$ and τ_i and τ_{i+1} are such that $\hat{y}_{\tau_i} < y < \hat{y}_{\tau_{i+1}}$ then

$$\hat{p}(y) = \frac{\tau_{i+1} - \tau_i}{\hat{y}_{\tau_{i+1}} - \hat{y}_{\tau_i}} \tag{94}$$

2. else if, $y < \hat{y}_{\tau_1}$, then

$$\hat{p}(y) = \alpha_1 \exp\left(-\frac{|y - \hat{y}_{\tau_1}|}{\beta_1}\right) \tag{95}$$

   where $\alpha_1 = (\tau_2 - \tau_1)/(\hat{y}_{\tau_2} - \hat{y}_{\tau_1})$ and $\beta_1 = \tau_1/\alpha_1$

3. else if, $y > \hat{y}_{\tau_k}$, then

$$\hat{p}(y) = \alpha_k \exp\left(-\frac{|y - \hat{y}_{\tau_k}|}{\beta_k}\right) \tag{96}$$

   where $\alpha_k = (\tau_k - \tau_{k-1})/(\hat{y}_{\tau_k} - \hat{y}_{\tau_{k-1}})$ and $\beta_k = \tau_k/\alpha_k$

An example of interpolated predictive density estimation using quantile information at $\boldsymbol{\tau} = [0.10, 0.15, 0.3, 0.5, 0.7, 0.84, 0.9]$ for a Gaussian distribution is given in Figure 62a.

Similarly, the cumulative distribution function $\hat{F}(y)$ at any value y is estimated by taking the derivative of probability density and is given as

1. If $\hat{y}_{\tau_1} < y < \hat{y}_{\tau_k}$ and τ_i and τ_{i+1} are such that $\hat{y}_{\tau_i} < y < \hat{y}_{\tau_{i+1}}$ then

$$\hat{F}(y) = \tau_i + \frac{\tau_{i+1} - \tau_k}{\hat{y}_{i+1} - \hat{y}_i}(\hat{y}_i - y) \tag{97}$$

2. else if, $y < \hat{y}_{\tau_1}$, then

$$\hat{F}(y) = \alpha_1\beta_1 \exp\left(-\frac{y - \hat{y}_{\tau_1}}{\beta_1}\right) \tag{98}$$

   where $\alpha_1 = (\tau_2 - \tau_1)/(\hat{y}_{\tau_2} - \hat{y}_{\tau_1})$ and $\beta_1 = \tau_1/\alpha_1$

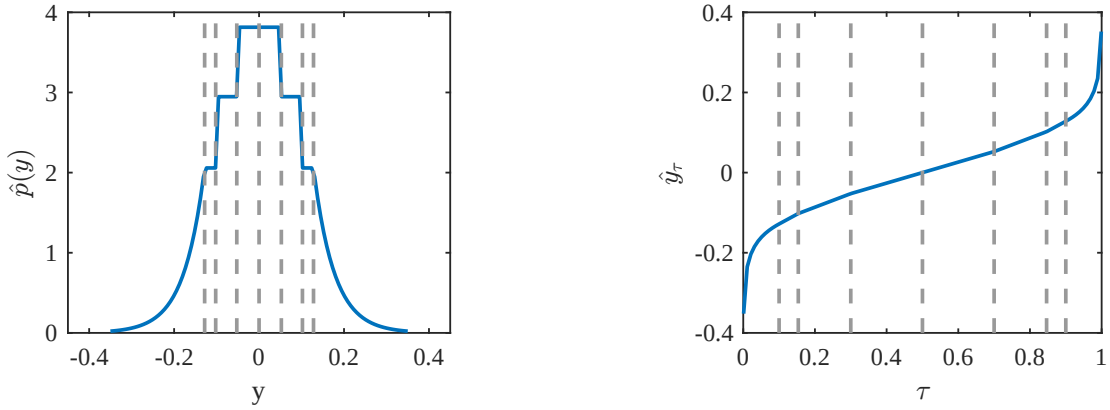

(a) Interpolated probability density

(b) Interpolated quantiles

Figure 62: Interpolated predictive probability density and quantiles using quantiles estimated from Gaussian distribution at $\boldsymbol{\tau} = [0.10, 0.15, 0.30, 0.50, 0.70, 0.84, 0.90]$ given by dashed lines

3. else if, $y > \hat{y}_{\tau_k}$, then

$$\hat{F}(y) = 1 - \alpha_k \beta_k \exp\left(-\frac{y - \hat{y}_{\tau_k}}{\beta_k}\right) \tag{99}$$

where $\alpha_k = (\tau_k - \tau_{k-1})/(\hat{y}_{\tau_k} - \hat{y}_{\tau_{k-1}})$ and $\beta_k = \tau_k/\alpha_k$

5.2.4 Quantile Formula for Mean and Variance

If $Q_{Y|\mathbf{x}}(\tau|\mathbf{x})$ is the conditional quantile function of a random variable Y for given $\mathbf{x}$, then the mean and variance is given as

$$E_{Y|\mathbf{x}}(Y|\mathbf{x}) = \int_{-\infty}^{\infty} y dF_{Y|\mathbf{x}}(y|\mathbf{x}) = \int_0^1 Q_{Y|\mathbf{x}}(\tau|\mathbf{x}) d\tau \tag{100a}$$

$$Var_{Y|\mathbf{x}}(Y|\mathbf{x}) = \int_0^1 (Q_{Y|\mathbf{x}}(\tau|\mathbf{x}) - E_{Y|\mathbf{x}}(Y|\mathbf{x}))^2 d\tau \tag{100b}$$

Similarly, higher order moments can be estimated.

5.2.5 Distribution Parameters from Quantiles

If Y is assumed to follow some parametric distribution family, then quantile informations at fewer values of τ can be used to evaluate the parameters of the distribution. For example, if Y is assumed to follow any of the two parameter families like normal,

log normal, Cauchy, Weibull, gamma, and inverse gamma, then the quantile at two different values of τ is sufficient to determine the parameters. For example, y_1 and y_2 are two quantiles with respect to τ_1 and τ_2. For consistency, it is required that $(y_1 - y_2)(\tau_1 - \tau_2) > 0$. Then, for normal distribution, mean μ and standard deviation σ are given as

$$\mu = \frac{y_1 \Phi^{-1}(\tau_2) - y_2 \Phi^{-1}(\tau_1)}{\Phi^{-1}(\tau_2) - \Phi^{-1}(\tau_1)} \tag{101a}$$

$$\sigma = \frac{y_2 - y_1}{\Phi^{-1}(\tau_2) - \Phi^{-1}(\tau_1)} \tag{101b}$$

where Φ is the cumulative distribution function (CDF) of the standard normal distribution Z with mean 0 and standard deviation 1. For derivation and parameters of other distribution families please refer to Cook [187].

5.2.6 Sampling Using Conditional Quantile

If U is a random variable with uniform distribution $U \sim Uniform(0, 1)$, then for any quantile function $Q_Y(\tau)$

$$\mathrm{P}[Q_Y(U) \leq y] = \mathrm{P}[U \leq F(y)] = F(y) = \mathrm{P}(Y \leq y) \tag{102}$$

Therefore, samples of Y can be generated by sampling a standard uniform distribution $U \sim Uniform(0, 1)$ and evaluating the quantiles for each samples using $Q_Y(u)$. Similarly, conditional sample of Y can be generated using conditional quantiles by using $Y \underset{d}{=} Q_{Y|\mathbf{x}}(U|\mathbf{x})$, where conditional quantiles can be estimated using quantile regression $Q_{Y|\mathbf{x}}(\tau|\mathbf{x})$.

As discussed earlier, quantile regressions $Q_{Y|\mathbf{x}}(\boldsymbol{\tau}|\mathbf{x}, \boldsymbol{\beta}) = \mathbf{y}_{\boldsymbol{\tau}}(\mathbf{x}, \boldsymbol{\beta})$ are only modeled for a finite number of levels of $\boldsymbol{\tau} = [\tau_1, \ldots, \tau_k]$. If $\hat{y}_{\tau_1}, \ldots, \hat{y}_{\tau_k}$ are non-decreasing conditional quantiles estimated by quantile regression at $\tau_1, \ldots, \tau_k$, the predictive quantiles $\hat{y}_\tau$ at a new value of $\tau = u$ is estimated as

1. If $\tau_1 < \tau < \tau_k$ and $\hat{y}_{\tau_{i+1}}$ and $\hat{y}_{\tau_i}$ are such that $\tau_i < \tau < \tau_{i+1}$ then

$$\hat{y}_\tau = \hat{y}_i + \frac{\hat{y}_{i+1} - \hat{y}_i}{\tau_{i+1} - \tau_i}(\tau - \tau_i) \tag{103}$$

2. else if $\tau < \tau_1$ then

$$\hat{y}_\tau = \hat{y}_{\tau_1} + \beta_1 \log\left(\frac{\tau_1}{\alpha_1 \beta_1}\right) \tag{104}$$

where $\alpha_1 = (\tau_2 - \tau_1)/(\hat{y}_{\tau_2} - \hat{y}_{\tau_1})$ and $\beta_1 = \tau_1/\alpha_1$

3. else if $\tau > \tau_k$ then

$$\hat{y}_\tau = \hat{y}_{\tau_k} - \beta_k \log\left(\frac{1 - \tau_k}{\alpha_k \beta_k}\right) \tag{105}$$

where $\alpha_k = (\tau_k - \tau_{k-1})/(\hat{y}_{\tau_k} - \hat{y}_{\tau_{k-1}})$ and $\beta_k = \tau_k/\alpha_k$

An example of interpolated quantile estimation using quantile information at $\boldsymbol{\tau} = [0.10, 0.15, 0.3, 0.5, 0.7, 0.84, 0.9]$ for a Gaussian distribution is given in Figure 62b. The interpolated quantile can then be used to generate samples of conditional Y.

5.3 Modeling Dependence Between Multiple Responses

In the last section, modeling conditional probability density of responses of a subsystem or disciplinary analysis has been discussed. In general, due to underlying functional dependency and uncertainty, these responses are statistically dependent. For example, in an aircraft sizing, discipline empennage area and wing area are two possible outcomes, which are functionally dependent based on a stability factor. Further, in the presence of uncertainties, these multiple responses are also statistically dependent on each other. Therefore, it is important to model their dependencies to carry out uncertainty propagation and quantification accurately.

One approach is to extend the probabilistic modeling described in section 5.1 for multivariate responses by using a parametric multivariate distribution function such as multivariate Gaussian distribution in place of univariate Gaussian distribution in Equation 73 for multiple responses. A multivariate Gaussian distribution is given as

$$\mathrm{P}(\mathbf{y}|\mathbf{x}, \mathbf{w}) = \mathcal{N}(\mathbf{y}|\boldsymbol{\mu}(\mathbf{x}, \mathbf{w}), \boldsymbol{\Sigma}) \tag{106}$$

where $\mathbf{y} \in \mathbb{R}^{1\times n}$ is the vector of n outputs and $\boldsymbol{\mu}(\mathbf{x}, \mathbf{w})$ is the multivariate regression of conditional mean and $\boldsymbol{\Sigma} \in \mathbb{R}^{n\times n}$ is a covariance matrix. The issue with using

multivariate Gaussian distribution is that it assumes that marginal distribution for each response is a Gaussian distribution. Limited options are available to model non-Gaussian marginal distributions using a parametric multivariate distribution function such as *Matrix gamma distribution*, *Multivariate t-distribution*, *Wishart distribution*, *Hotelling's T-squared distribution*, etc. Models using any of these parametric multivariate distribution function have the following limitations:

1. The marginal distributions and dependency structures are fixed.

2. The dependence information is coupled with the marginal distributions.

For example, consider the scatter plot of two random variables given in Figure 63a. In this example, both the marginals have Gaussian distribution; however the dependency structure is non-Gaussian. Therefore, these random variables cannot be modeled with multivariate Gaussian distribution as it assumes an elliptical dependency structure. Also, consider the scatter plot of two random variables given in Figure 63b. In this case one of the marginals is a Gaussian distribution whereas the other one is a gamma distribution. This cannot be modeled with any parametric multivariate distribution function as there does not exist any such parametric function which can model a Gaussian distribution and a gamma distribution as marginals.

To overcome these challenges *Copula* theory is used in the current work to model multivariate dependencies of the responses. Copulas are multivariate distribution functions defined over n unit space, whose marginals are uniform distribution over unit interval, i.e. $U \sim Uniform(0, 1)$. Since, by using probability integral transformation, any continuous random variable can be transformed into a unit random variable, copula can be used to couple different marginal distributions to construct multivariate distributions. The main benefit of copula is that it decouples the marginal distribution from the dependency structure, therefore allows multiple options for dependency structures.

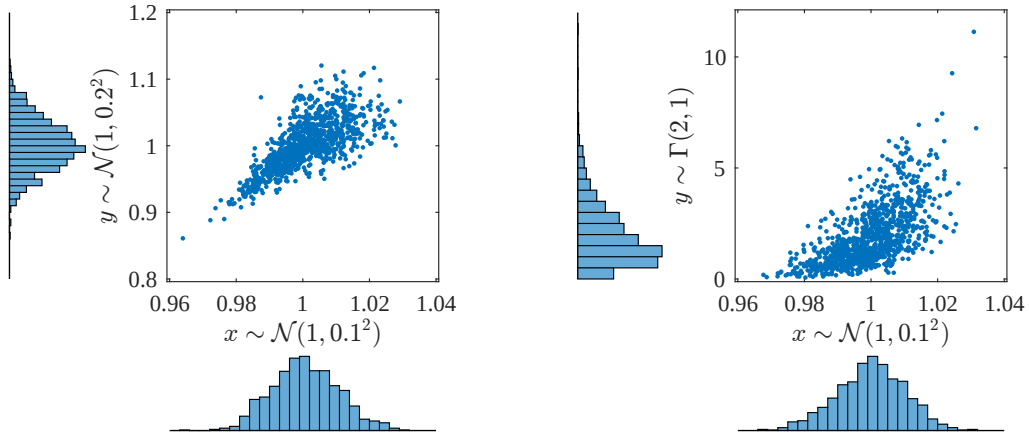

(a) Joint distribution with Gaussian distributions as marginals

(b) Joint distribution with Gaussian and Gamma distribution as marginals

Figure 63: Example of joint distribution of random variables with different marginals and dependency structure

Copula-based models have been used in various fields including but not limited to modeling of financial risk [188, 189, 190], modeling credibility and losses [191, 192], modeling correlated event times and competing risks [193, 194], reliability analysis in engineering [195, 196, 197], and so on. A brief introduction is given in the next section.

5.3.1 Introduction to Copula Theory

In Latin, the word *coupla* means " a link, tie, bond". The word copula was employed in the field of statistics by Abe Sklar (1959) [198] which was defined as the function that "*join together one-dimensional distribution functions to form multivariate distribution functions*". One of the comprehensive books in this topic by Nelson [199] describe it as "*Copulas are functions that join or couple multivariate distribution functions to their one dimensional marginal distribution functions. Alternatively, copulas are multivariate distribution functions whose one-dimensional margins are uniform on the interval* $[0, 1]$".

The main idea behind copula theory is to decompose an n-dimensional distribution

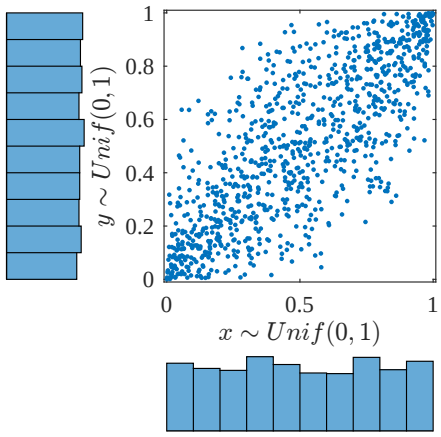

(a) Gaussian Copula

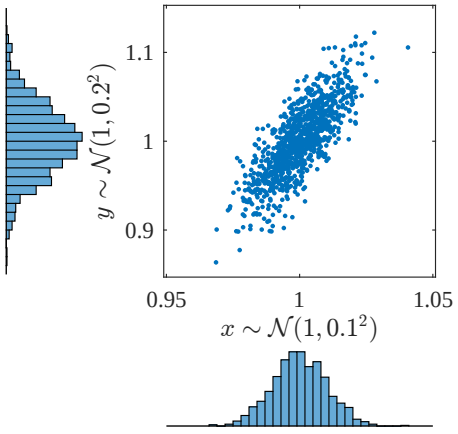

(b) Joint distribution with Gaussian and Gamma distribution as marginals

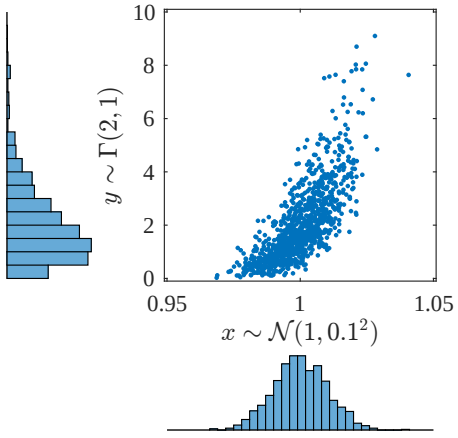

(c) Joint distribution with Gaussian and Gamma distribution as marginals

Figure 64: Example of joint distribution of random variables with different marginals and dependency structure using Gaussian Copula

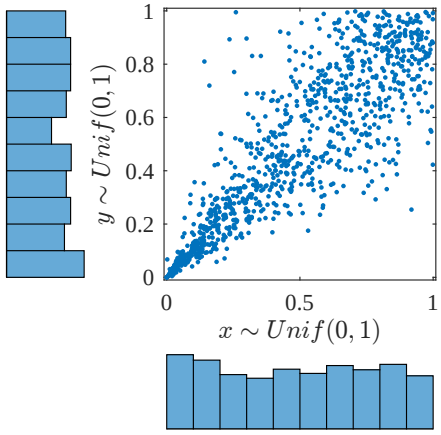

(a) Clayton Copula

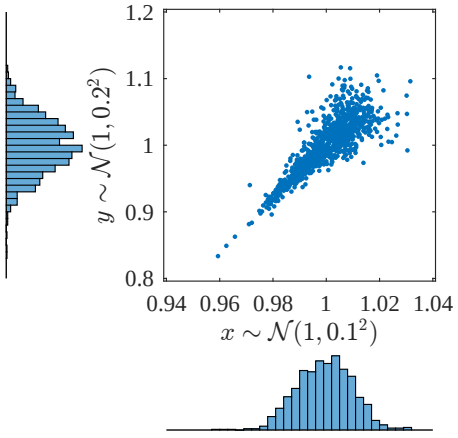

(b) Joint distribution with Gaussian and Gamma distribution as marginals

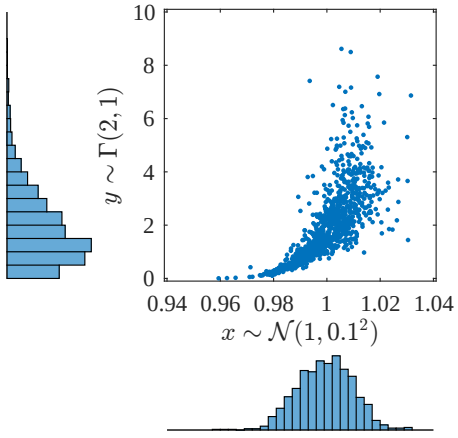

(c) Joint distribution with Gaussian and Gamma distribution as marginals

Figure 65: Example of joint distribution of random variables with different marginals and dependency structure using Clayton Copula

function F into marginal distribution functions F_i and the copula C which defines the structure of the dependence of the distribution.

Definition: Copula Let $U = (U_1, \ldots, U_n)^T$ be an n dimensional random vector with U_i be a uniform random variable over the unit interval, then the copula C is defined as

$$C(u_1, \ldots, u_n) = \mathrm{P}(U_1 \leq u_1, \ldots, U_n \leq u_n) \tag{107}$$

which is a joint cumulative distribution function of $(U_1, \ldots, U_n)$ and function C is called an n-dimensional copula.

Using probability integral transformation, any multivariate distribution function can be defined with copula. Consider a random vector $(x_1, \ldots, x_n)^T$ with joint distribution function $F(x_1, \ldots, x_n)$. If F_i, $i = 1, \ldots, n$ are the marginal cumulative distribution function of X_i, then $U_i = F_i(X_i)$ is a uniform random variable over a unit area. Therefore, a copula can be defined as

$$C(u_1, \ldots, u_n) = F\left(F_1^{-1}(u_1), \ldots, F_n^{-1}(u_n)\right) \tag{108}$$

Similarly, copula can be used to construct a multivariate distribution with any arbitrary marginal distributions. Suppose if i^{th} component of random vector X is desired to have marginal distribution of G_i, then a multivariate distribution function of G is defined as

$$G(x_1, \ldots, x_n) = C\left(G_1(x_1), \ldots, G_n(x_n)\right) \tag{109}$$

Equation 108 and Equation 109 demonstrate a close relationship between copula and multivariate distribution which is generalized by Sklar's thoerem.

Sklar's Theorem. Let $F \in \mathcal{F}(F_1, \ldots, F_n)$ be an n dimensional distribution function with marginal distribution $F_1, \ldots, F_n$. Then there exists an n dimensional copula C such that, for a x in the domain of F,

$$F(x_1, \ldots, x_n) = C(F_1(x_1), \ldots, F_n(x_n)) \tag{110}$$

C is unique if $F_1, \ldots F_n$ are continuous, other wise C is uniquely determined on $RanF_1 \times \cdots \times RanF_n$ where $RanH$ is the range of H. Similarly, if C is an n dimensional copula and $F_1, \ldots F_n$ are marginal distributions, then F defines the n dimensional distribution function of $x_1, \ldots, x_n$.

The details of the proof of Sklar's theorem can be found in Sklar [200]. Sklar's theorem decouples the marginal distribution from the dependence structure, thereby allowing analysis of the marginal and dependence separately. The relationship between copula and multivariate density function f is derived by differentiating Equation 110 and is given as

$$f(x_1, \ldots, x_n) = c(F_1(x_1), \ldots, F_n(x_n)) \prod_{i=1}^{n} f_i(x_i) \tag{111}$$

where f_i are marginal density functions and c is the density function of copula given as

$$c(u_1, \ldots, u_n) = \frac{\partial^n C(u_1, \ldots, u_n)}{\partial u_1 \ldots \partial u_n} \tag{112}$$

5.3.2 Concordance Measure for Copula

Copula of two random variables can be used to evaluate dependence measure between the random variables. Conversely, dependence measures, also called copula parameters, can be used to construct different families of copulas. Since, copula are invariant under monotonically increasing transformations [199], it is desirable to

have a dependence measure which are scale invariant under monotonically increasing transformation of the marginal distribution. For example, the most commonly used dependence parameter, Pearson's rho correlation, which measures linear correlation between random variables, does not always satisfy this property.

Commonly used dependence measures in copula modeling are called *concordance measures*. Two random variables are said to be concordant if large values of one variable can be associated with large values of the other and correspondingly small values of one variable with small values of the other. Concordance is defined by concordance function Q which is the difference between the probability of concordance and the probability of discordance between a pair of random variables. Concordance function between two continuous random vectors (X_1, X_2) and (X_1', X_2') with different joint distributions G and H but common marginal distribution F_1 and F_2 is given as

$$Q = \mathrm{P}((X_1 - X_1')(X_2 - X_2') > 0) - \mathrm{P}((X_1 - X_1')(X_2 - X_2') < 0) \tag{113}$$

which can be shown to be

$$Q = Q(C_G, C_H) = 4 \int_0^1 \int_0^1 C_G(u, v) dC_H(u, v) - 1 \tag{114}$$

where C_G and C_H are the copulas of G and H, respectively.

Two most widely used concordance measures are *Kendall's tau* and *Spearman's rho*. Kendall's tau is defined as $Q(C, C)$ of two independent and identically distributed observations and is given as

$$\tau = 4 \int_0^1 \int_0^1 C(u_1, u_2) dC(u_1, u_2) - 1 \tag{115}$$

where $\tau \in [-1, 1]$. Kendall's tau can also be evaluated from samples of data. Let $[(x_1, y_1), \ldots, (x_{ns}, y_{ns})]^T$ be ns paired samples of data. Two paired samples (x_i, y_i) and (x_j, y_j) are concordant if $x_i < x_j$ and $y_i < y_j$ or $x_i > x_j$ and $y_i > y_j$, else they are discordant. Then Kendall's tau is defined as

$$\tau = \frac{c - d}{c + d} = \frac{c - d}{\binom{ns}{2}} \tag{116}$$

where c and d are the number of concordant and discordant pairs among $\binom{ns}{2}$ pairs, respectively.

Spearman's rho is defined as $3Q(C, \Pi)$, where Π is the product copula obtained under independence. Spearman's rho is given as

$$\rho = 12 \int_0^1 \int_0^1 u_1 u_2 dC(u_1, u_2) - 3 \tag{117}$$

where $\rho \in [-1, 1]$. Let $[(x_1, y_1), \ldots, (x_{ns}, y_{ns})]^T$ be ns paired samples, Spearman's rho can be evaluated as

$$\rho = 1 - \frac{6 \sum_{i=1}^{ns} d_i^2}{ns(ns^2 - 1)} \tag{118}$$

where d_i is the difference of two rankings.

5.3.3 Types of Copulas

Two commonly used copulas are *Elliptical copulas* and *Archimedean copulas*.

5.3.3.1 Elliptical Copulas

Copulas of elliptical distribution are called elliptical copulas. A multivariate elliptical distribution is defined by the characteristic function of form $e^{it^T \mu} \Psi(t^T \Sigma t)$ [201], where $t \in \mathbb{R}^n$, specific or mean vector $\mu \in \mathbb{R}^n$ and positive definite dispersion matrix $\Sigma \in \mathbb{R}^{n \times n}$. Typically, for copula modeling the distribution is centered around zero, i.e. $\mu = 0$ and the dispersion matrix Σ is parameterized such that $\Sigma_{ij} = Cov(X_i, X_j)$ [202], where $Cov(.,.)$ is the covariance measure. If r_{ij} is the Pearson's linear correlation coefficient and τ_{ij} is the Kendall's tau between two random variables X_i and X_j, they are related as

$$\tau_{ij} = \frac{2}{\pi} \arcsin(r_{ij}). \tag{119}$$

This relationship between Pearson's correlation matrix and Kendall's tau matrix allows a wide range of dependence structures.

Elliptical copulas provide a wide range of multivariate distributions with array of dependence structures which enable modeling of multivariate extremes and non-normal dependencies. Another advantage of elliptical copulas is that they share similar tractable properties of multivariate distribution. Two most commonly used elliptical copulas are Gaussian copulas and t copulas which are derived from multivariate Gaussian and multivariate t distributions.

Let Φ_Σ be the joint cumulative distribution function of a multivariate Gaussian distribution with correlation matrix Σ. Let Φ be the cumulative distribution function of standard Gaussian distribution with zero mean and unit standard deviation. A Gaussian copula with dispersion matrix Σ is given as

$$C(u_1, \ldots, u_n; \Sigma) = \Phi_\Sigma \left[\Phi^{-1}(u_1), \ldots, \Phi^{-1}(u_n)\right] \tag{120}$$

Similarly, for t copula consider joint cumulative distribution function of a multivariate Student's t distribution is given by $T_{\Sigma,\nu}$ where Σ is the correlation matrix and ν specifies the degree of freedom. Let F_{t_ν} be the cumulative distribution function of univariate t distribution with ν degrees of freedom. Then t copula with dispersion matrix Σ and ν degrees of freedom is given as

$$C(u_1, \ldots, u_n; \Sigma, \nu) = T_{\Sigma,\nu} \left[F_{t_\nu}^{-1}(u_1), \ldots, F_{t_\nu}^{-1}(u_n)\right] \tag{121}$$

Gaussian and t copulas given by Equation 120 and Equation 121, respectively, can be used with Equation 110 to construct multivariate distribution with range of dependence structure by modifying the parameters Σ and ν. Gaussian copula and t copula at different settings of parameters are plotted in Figure 66. Due to tractable calculus of Gaussian copula it is widely used in various fields of research.

5.3.3.2 Archimedean Copula

Archimedean copulas are another class of popular copula which are different from elliptical copula in the way it is generated. To construct an Archimedean copula a

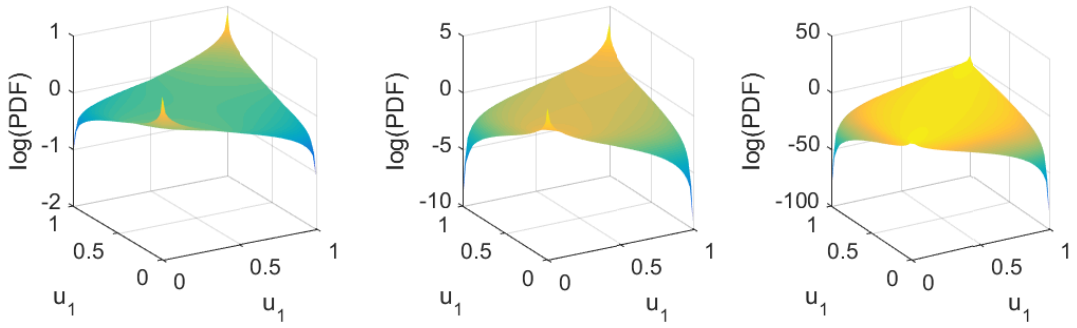

(a) Gaussian Copula, $\rho = 0.1$ (b) Gaussian Copula, $\rho = 0.5$ (c) Gaussian Copula, $\rho = 0.9$

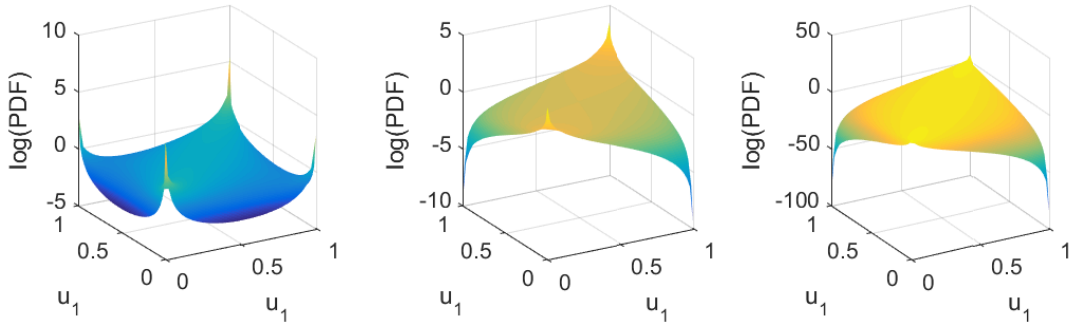

(d) t Copula, $\rho = 0.1, \nu = 2$ (e) t Copula, $\rho = 0.5, \nu = 2$ (f) t Copula, $\rho = 0.9, \nu = 2$

Figure 66: Commonly used Elliptical copulas at different setting of parameters

generator function is required and it has to be a completely monotonic decreasing function. Let $\varphi(t)$ be a continuous strictly decreasing function such that $\varphi : [0,1] \times \Theta \to [0,\infty)$, where θ is a parameter within some parameter space Θ. If $\varphi(1;\theta) = 0$ and $\varphi(0;\theta) = \infty$ and the inverse φ^{-1} is monotonic on $[0,\infty)$, then an n dimensional Archimedean copula is given as

$$C(u_1,\ldots,u_d;\theta) = \varphi^{-1}\left(\varphi(u_1;\theta) + \cdots + \varphi(u_d;\theta);\theta\right) \tag{122}$$

for $n \geq 2$ and the function φ is called the *generator* of copula. Each Archimedean copula has a unique generator function which can be used to generate the copula function. For Archimedean copula, the concordance measure Kendal's tau can be evaluated using generator function as

$$\tau = 1 + 4\int_0^1 \frac{\varphi(t;\theta)}{\varphi'(t;\theta)}dt \tag{123}$$

Table 17: Copula Functions, Generator Functions, and Domains of Correlation Parameters

Copula	$C(u,v\|\theta)$	$\varphi_\theta(t)$	$\theta \in \Sigma^\theta$
Clayton	$\left[\max\left\{u^{-\theta}+v^{-\theta}-1;0\right\}\right]^{-1/\theta}$	$\frac{1}{\theta}\left(t^{-\theta}-1\right)$	$\theta \in [-1,\infty)\backslash\{0\}$
Frank	$-\frac{1}{\theta}\log\left[1+\frac{(\exp(-\theta u)-1)(\exp(-\theta v)-1)}{\exp(-\theta)-1}\right]$	$-\log\left(\frac{\exp(-\theta t)-1}{\exp(-\theta)-1}\right)$	$\theta \in \mathbb{R}\backslash\{0\}$
Gumbel	$\exp\left[-\left((-\log(u))^\theta+(-\log(v))^\theta\right)^{1/\theta}\right]$	$(-\log(t))^\theta$	$\theta \in [1,\infty)$
AMH [1]	$\frac{uv}{1-\theta(1-u)(1-v)}$	$\log\left[\frac{1-\theta(1-t)}{t}\right]$	$\theta \in [-1,1)$

This equation can be used with Equation 116 to estimate the theoretical value of parameter of assumed parametric copula family so that it equates the sample Kendall's tau measure.

Archimedean copulas have been used in a wide range of applications because of the ease with which they can be constructed, the great variety of families of copulas belonging to this class, and the many useful properties possessed by the members of this class. Table 17 summarizes a few commonly used Archimedean copulas with one parameter and Figure 67 shows various elliptical copulas at different settings of parameters.

5.3.4 Statistical Inference

One of the methods used to infer the parameters of copula from a given set of samples is maximum likelihood (ML) approach. Let $(X_{i1},\ldots,X_{ip})^T,\ i=1,\ldots,n$ be the observed n random samples of p dimensional data. Let the parameter be $\boldsymbol{\gamma}=[\boldsymbol{\phi},\boldsymbol{\theta}]$, where $\boldsymbol{\phi}=[\boldsymbol{\phi}_1,\ldots,\boldsymbol{\phi}_p]$ and $\boldsymbol{\phi}_i$ is the vector of parameters associated with i^{th} marginal distribution and $\boldsymbol{\theta}$ is the vector of parameters associated with copula function C. Then, the log-likelihood of the parameter vector $\boldsymbol{\gamma}$ is given as

$$L(\boldsymbol{\gamma})=\sum_{i=1}^{n}\log\ c\left[F_1(X_{i1}|\boldsymbol{\phi}_1),\ldots,F_p(X_{ip}|\boldsymbol{\phi}_p)|\boldsymbol{\theta}\right]+\sum_{i=1}^{n}\sum_{j=1}^{p}\log\ f_j(X_{ij}|\boldsymbol{\phi}_j) \qquad (124)$$

[1] Acronym for Ali-Mikhail-Haq copula

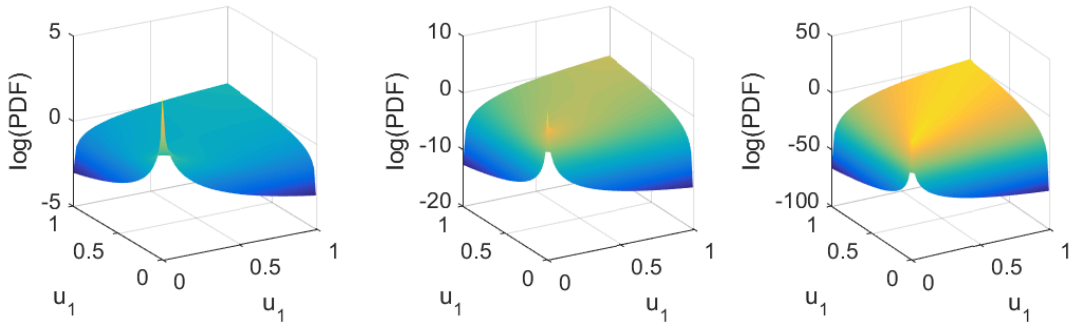

(a) Clayton Copula, $\theta = 0.5$ (b) Clayton Copula, $\theta = 2.0$ (c) Clayton Copula, $\theta = 10.0$

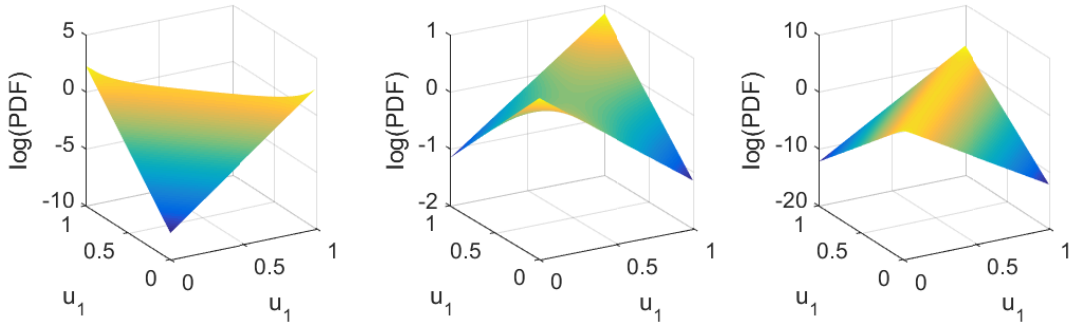

(d) Frank Copula, $\theta = -10.0$ (e) Frank Copula, $\theta = 2.0$ (f) Frank Copula, $\theta = 15.0$

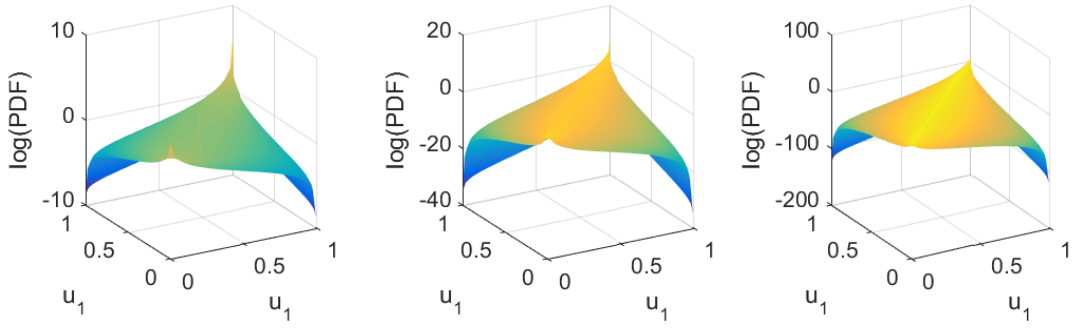

(g) Gumbel Copula,$\theta = 2.0$ (h) Gumbel Copula, $\theta = 5.0$ (i) Gumbel Copula, $\theta = 15.0$

Figure 67: Commonly used Archimedean copulas at different values of θ

where $c()$ is the copula density function, $F_j()$ and $f_j()$ are the cumulative distribution functions and probability density function of i^{th} marginal. Then, ML estimator of $\boldsymbol{\gamma}$ can be evaluated by optimizing

$$\hat{\boldsymbol{\gamma}}_{ML} = \arg\max_{\boldsymbol{\gamma}\in\Gamma} L(\boldsymbol{\gamma}) \tag{125}$$

where Γ is the parameter space.

Instead of optimizing the entire set of parameters of copula and marginal distribution to estimate $\hat{\boldsymbol{\phi}}_{ML} = [\hat{\boldsymbol{\phi}}_{ML}, \hat{\boldsymbol{\theta}}_{ML}]$, another approach known as *Inference Functions for Margins* (IFM) as proposed by Joe and Xu [203] can be used, which is based on the following decomposition:

$$L = L_C(\boldsymbol{\theta}, \boldsymbol{\phi}) + \sum_{j=1}^{p} L_j(\boldsymbol{\phi}_j) \tag{126}$$

where $L_C(\boldsymbol{\theta}, \boldsymbol{\phi}) = \sum_{i=1}^{n} \log\, c\left[F_1(X_{i1}|\boldsymbol{\phi}_1), \ldots, F_p(X_{ip}|\boldsymbol{\phi}_p)|\boldsymbol{\theta}\right]$ is the log-likelihood contribution from the dependence structure in the data represented by copula C and $L_j(\beta_j) = \sum_{i=1}^{n} \log\, f_i(X_{ij}|\boldsymbol{\phi}_j),\ j = 1, \ldots, p$ are the log-likelihood contribution from each marginals. Since, $\sum_{j=1}^{p} L_j(\boldsymbol{\phi}_j)$ is exactly similar to the log-likelihood under independence assumption, the first stage of IFM method estimates the maximum likelihood of marginal parameters as

$$\hat{\boldsymbol{\phi}}_j^{\,IFM} = \arg\max_{\boldsymbol{\phi}_j} L_j(\boldsymbol{\phi}_j) = \arg\max_{\boldsymbol{\phi}_j} \sum_{i=1}^{n} \log\, f_i(X_{ij}|\boldsymbol{\phi}_j) \tag{127}$$

In the next stage of IFM method, maximum log-likelihood of copula parameters $\boldsymbol{\theta}$ is computed by maximizing L_C, while replacing marginals parameter $\boldsymbol{\phi}_j$ with $\hat{\boldsymbol{\phi}}_j^{\,IFM}$ as

$$\hat{\boldsymbol{\theta}}^{IFM} = \arg\max_{\boldsymbol{\theta}} L_C(\boldsymbol{\theta}, \hat{\boldsymbol{\phi}}^{IFM}) = \sum_{i=1}^{n} \log\, c\left[F_1(X_{i1}|\hat{\boldsymbol{\phi}}_1^{IFM}), \ldots, F_p(X_{ip}|\hat{\boldsymbol{\phi}}_p^{IFM})|\boldsymbol{\theta}\right] \tag{128}$$

IFM method estimator has been found to be consistent and asymptotically normal under the usual regularity condition and a highly efficient alternative to MLE estimation of multivariate models parameters [204].

5.4 Quantile-Copula Regression for Dependent Responses

As discussed in the section 5.2, quantile regression provides an approach to modeling conditional quantile function $Q_{Y|\mathbf{x}}(\boldsymbol{\tau}|\mathbf{x}, \boldsymbol{\beta})$, which can be used to evaluate the conditional distribution function $F_{Y|\mathbf{x}}(y|\mathbf{x}, \boldsymbol{\beta})$. If there are multiple responses, quantile

regression models can be built for each response separately as $Q_{Y_i|\mathbf{x}}(\boldsymbol{\tau}|\mathbf{x}, \boldsymbol{\beta}_i)$ which can be used to evaluate conditional the marginal distribution function for each response, $F_{Y_i|\mathbf{x}}(y_i|\mathbf{x}, \boldsymbol{\beta}_i)$. To model the complete joint distribution for multiple responses, one also has to model a dependence structure in addition to the marginal distribution. Copula theory discussed in section 5.3.1 provides the mechanism to decouple the marginal distributions from the dependence structure so that each of them can be modeled separately. Quantile regressions can be combined with copula functions to build a *Quantile-Copula regression model*, which can be used to model a wide range of marginal distributions with arrays of dependence structures.

Let $\boldsymbol{\beta}_1, \ldots, \boldsymbol{\beta}_p$ be the matrices of parameters associated with quantile regressions of p responses and $\boldsymbol{\theta}$ be the parameter associated with the copula function. Then the quantile copula regression model is given as

$$F(\mathbf{y}|\mathbf{x}, \boldsymbol{\beta}_1, \ldots, \boldsymbol{\beta}_p, \boldsymbol{\theta}) = C(F_1(y_1|\mathbf{x}, \boldsymbol{\beta}_1), \ldots, F_p(y_p|\mathbf{x}, \boldsymbol{\beta}_p)|\boldsymbol{\theta}) \tag{129}$$

where $F_i(y|\mathbf{x}) = Q^{-1}_{Y_i|\mathbf{x}}(y_i|\mathbf{x}, \boldsymbol{\beta}_i)$ and $Q_{Y_i|\mathbf{x}}(\boldsymbol{\tau}|\mathbf{x}, \boldsymbol{\beta}_i)$ is the quantile regression model for i^{th} response. Equation 129 assumes that the copula parameter $\boldsymbol{\theta}$ is fixed for all values of $\mathbf{x}$, i.e. the dependence structure does not vary with $\mathbf{x}$. If the dependence parameter varies with $\mathbf{x}$, a regression model can be used for copula parameters as $\boldsymbol{\theta} = f_\theta(\mathbf{x}, \boldsymbol{\alpha})$, for example $\boldsymbol{\theta} = \mathbf{X}\boldsymbol{\alpha}$. Then, Equation 129 can be modified as

$$F(\mathbf{y}|\mathbf{x}, \boldsymbol{\beta}_1, \ldots, \boldsymbol{\beta}_p, \alpha) = C(F_1(y_1|\mathbf{x}, \boldsymbol{\beta}_1), \ldots, F_p(y_p|\mathbf{x}, \boldsymbol{\beta}_p)|\mathbf{x}, \boldsymbol{\alpha}) \tag{130}$$

Parameter inference for Quantile-Copula regression for dependent responses can be built in two stages in a manner which is similar to the Inference Function for Margins (IFM) method discussed in Section 5.3.4 and is referred in the current work as modified IFM method. In the first stage, models for quantile regressions are built for each response separately as discussed in Section 5.2.1, to estimate the parameters associated with quantile regression, i.e. $\hat{\boldsymbol{\beta}}_1, \ldots, \hat{\boldsymbol{\beta}}_p$. In the second stage copula

parameters $\boldsymbol{\alpha}$ are estimated by maximizing the log likelihood function as

$$\hat{\boldsymbol{\alpha}} = \arg\max_{\boldsymbol{\alpha}} \sum_{i=1}^{n} \log\, c\left[F_1(y_1|\mathbf{x}, \hat{\boldsymbol{\beta}}_1), \ldots, F_p(y_p|\mathbf{x}, \hat{\boldsymbol{\beta}}_p)|\mathbf{x}, \boldsymbol{\alpha}\right] \tag{131}$$

Details of implementation and a tutorial on parameter estimation of quantile copula regression is given in Appendix III. In the current work, quantile copula regression models of multivariate variable $\mathbf{y}$ is represented as $\tilde{f}_{qcr_{\mathbf{y}}}(\mathbf{y}|\mathbf{x}, \hat{\boldsymbol{\beta}}_1, \ldots, \hat{\boldsymbol{\beta}}_p, \hat{\boldsymbol{\alpha}})$, unless otherwise specified.

5.4.1 Copula Selection for Quantile Copula Regression

Many copula functions exist in literature [199] and some of the commonly used copula functions are given in Section 5.3.3. However, in the quantile copula regression discussed in the previous section it is assumed that copula function is fixed for the entire input space $\mathbf{x}$. An appropriate copula function can be selected based on the information available from the data. Some of the quantitative methods to select copula functions are the Akaike Information Criterion (AIC) [205], the Bayesian Information Criterion (BIC) [206], the Deviance Information Criterion (DIC) [207], etc. For more details please refer to [208, 209]. Other graphical techniques to determine the copula type are QQ plot [210], Kendall's tau plot[211], etc.

In the current work the Gaussian copula function is used to model quantile copula regression. The reason are as follows

- Most of the engineering disciplinary analysis contains multiple responses. Gaussian copula is one of the few copulas that have a practical n-dimensional generalization.

- In a Gaussian copula, the joint probability density function or cumulative density function can be uniquely determined based on marginals of the variables and the correlation coefficient matrix [212].

- Both positive and negative correlations can be handily represented by a Gaussian copula [212].
- In a typical engineering problem, the number of data samples are limited due to the expense associated with engineering analyses. For a limited amount of data, only marginals and correlation information can be determined, which are the only input to a Gaussian copula [213].
- There is a large statistical uncertainty associated with identifying the best fit copula for limited data [213].
- In some scenarios, complete multivariate data are not available. A Gaussian copula is the only copula that can be constructed using bivariate data information [213].

However, careful consideration should be made about using elliptical copulas like the Gaussian copula when extreme values are critical, as an elliptical copula does not capture the tail dependence appropriately [42].

5.4.2 Conditional Probability Density Function Using Quantile Copula Regression

With the assumption that the Gaussian copula is used in the current work, the copula density function c used in Equation 131 for a p-dimensional distribution is given as

$$c(u|\Sigma) = \frac{1}{\sqrt{|\Sigma|}} \exp\left(-\frac{1}{2}u^T(\Sigma^{-1} - I)u\right) \tag{132}$$

where $u_i = \Phi^{-1}(F_i(y_i))$, Φ^{-1} is the inverse cumulative distribution function of standard normal, $F_i(y_i)$ is the marginal cumulative distribution function of y_i, $i = 1, \ldots, p$, and Σ is the correlation matrix with the entries ρ_{ij} being the pairwise correlation between y_i and y_j.

If $\hat{\boldsymbol{\beta}}_1, \ldots, \hat{\boldsymbol{\beta}}_p$ are the matrices of parameters associated with quantile regression models of $y_1, \ldots, y_p$ and $\hat{\boldsymbol{\alpha}}$ is the vector of parameters associated with copula parameter regression, then the conditional probability function $f_{\mathbf{y}|\mathbf{x}}(\mathbf{y}|\mathbf{x}, \hat{\boldsymbol{\beta}}_1, \ldots, \hat{\boldsymbol{\beta}}_p, \hat{\boldsymbol{\alpha}})$ conditioned at $\mathbf{x}$ is given as

$$f_{\mathbf{y}|\mathbf{x}}(\mathbf{y}|\mathbf{x}, \hat{\boldsymbol{\beta}}_1, \ldots, \hat{\boldsymbol{\beta}}_p, \hat{\boldsymbol{\alpha}}) = \frac{1}{\sqrt{|\Sigma|}} \exp\left(-\frac{1}{2} u^T (\Sigma^{-1} - I) u\right) \prod_{j=1}^{p} f_{y_j|\mathbf{x}}(y_j|\mathbf{x}, \hat{\boldsymbol{\beta}}_i) \quad (133)$$

where each element $\Sigma_{ij} = \hat{\theta}_{ij}$ is estimated using the model $\hat{\boldsymbol{\theta}} = f_\theta(\mathbf{x}, \hat{\boldsymbol{\alpha}})$ which is used for copula parameter regression. $u_i = \Phi^{-1}(F_i(y_i|\mathbf{x}, \hat{\boldsymbol{\beta}}_i))$ where Φ^{-1} is the inverse cumulative distribution function of standard normal and $F_i(y_i|\mathbf{x}, \hat{\boldsymbol{\beta}}_i)$ is the conditional cumulative distribution function and $f_{y_j|\mathbf{x}}(y_j|\mathbf{x}, \hat{\boldsymbol{\beta}}_i)$ is the conditional probability density function estimated using quantile regression of y_i at $\mathbf{x}$ for given quantile regression parameter matrix $\hat{\boldsymbol{\beta}}_i$.

5.4.3 Conditional Sampling Using Quantile Copula Regression

With the assumption that the Gaussian copula is used in the current work, sampling from a quantile copula regression conditioned at $\mathbf{x}$ for given quantile copula regression parameters $[\hat{\boldsymbol{\beta}}_1, \ldots, \hat{\boldsymbol{\beta}}_p, \hat{\boldsymbol{\alpha}}]$, the following steps are carried out

1. Estimate correlation matrix Σ, where each element $\Sigma_{ij} = \hat{\theta}_{ij}$ using the model $\hat{\boldsymbol{\theta}} = f_\theta(\mathbf{x}, \hat{\boldsymbol{\alpha}})$ for given $\mathbf{x}$.

2. Generate samples of p-dimensional random variables $\mathbf{z} = [z_1, \ldots, z_p]$ from a p-dimensional joint standard Gaussian distribution with correlation matrix Σ.

3. Evaluate $u_i = \Phi(z_i)$, where Φ is the cumulative standard Gaussian distribution function, for $i = 1, \ldots, p$.

4. Determine $y_i = Q_{Y_i|\mathbf{x}}(u_i|\mathbf{x}, \hat{\boldsymbol{\beta}}_i)$ for given $\mathbf{x}$ using quantile regression with parameter matrix $\hat{\boldsymbol{\beta}}_i$, for $i = 1, \ldots, p$.

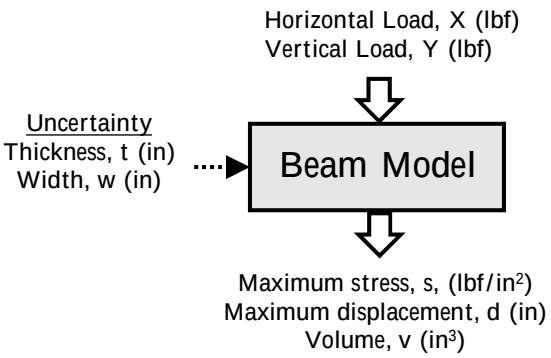

Figure 68: Variables associated with beam model

5.5 Numerical Demonstration

For the numerical demonstration of quantile copula regression a low fidelity beam model is used as given by Equation 63. As shown in Figure 68, the input space is defined by vertical load Y (lbf) and horizontal load X (lbf). The uncertainty variables are beam width w (in) with distribution $Unif(3.2, 4.8)$ and beam thickness t (in) with distribution $Triangular(3.0, 4.3, 4.5)$, which are assumed to be embedded in the discipline such that the discipline acts like a non-deterministic function. Deterministic parameters are beam length $L = 100(in)$ and Modulus of Elasticity $E = 2.9 \times 10^6(lbf/in^2)$. The outputs of the discipline are maximum stress s (lbf/in^2), maximum displacement d (in), and beam volume v (in^3).

To demonstrate modeling of quantile copula regression, the uncertain variable t is assumed to have a triangular distribution and w is assumed to have a uniform distribution. The ranges of input variables are assumed to be $X \in [500, 1500]$ and $Y \in [1500, 2500]$. $10,000$ samples are uniformly generated within the range of X and Y. For each sample, a beam model is executed to generate a random sample of s, d and v.

To build quantile copula regression, quantile regression models have been built for 20 levels of τ uniformly spaced between 0.02 and 0.98. For each quantile regression model, a quadratic response surface model has been used as a function of X and

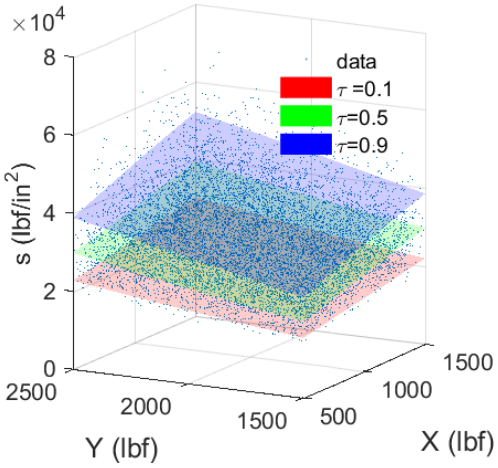

(a) Quantile surface of max stress s (lbf/in^2)

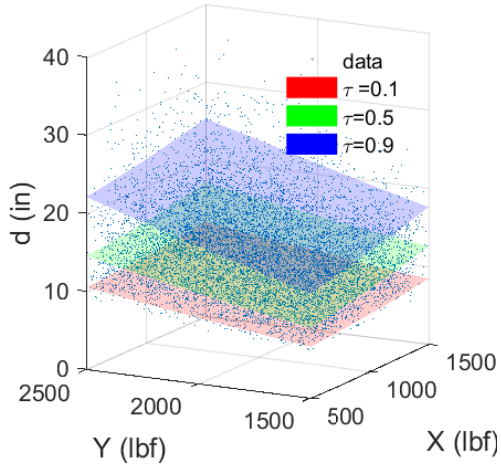

(b) Quantile surface of maximum displacement d (in)

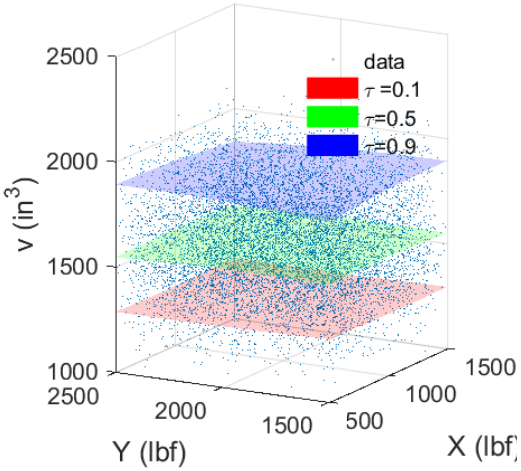

(c) Quantile surface of beam volume v (in^3)

Figure 69: Quantile surfaces of responses at level $\tau = [0.1, 0.5, 0.9]$ as function of input variables, horizontal load X (lbf) and vertical load Y (lbf)

Y. The quantile surface with τ level of $0.1, 0.5$ and 0.9 is shown in Figure 69. It is observed that for both s and d the gap between the quantile surfaces are not constant in the input space. This signifies heteroskedasticity in these variables. However, the gap between the quantiles surfaces of v are nearly constant, which signifies that v has homeostatic behavior. Also, the quantiles surfaces of v are very flat. This is due to the fact that v is not a function of X and Y.

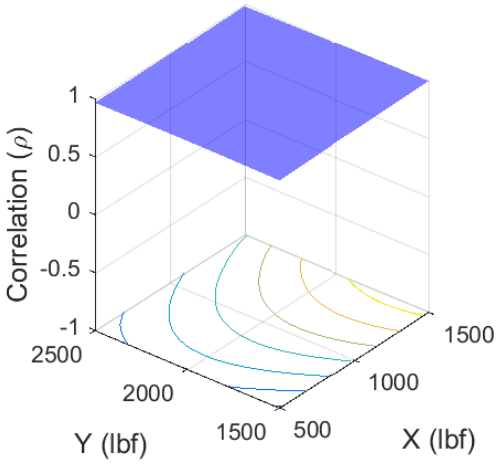

(a) Correlation between maximum displacement d and max stress s

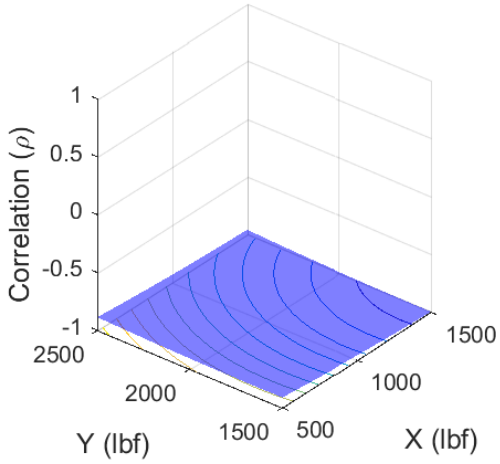

(b) Correlation between maximum displacement d and beam volume v

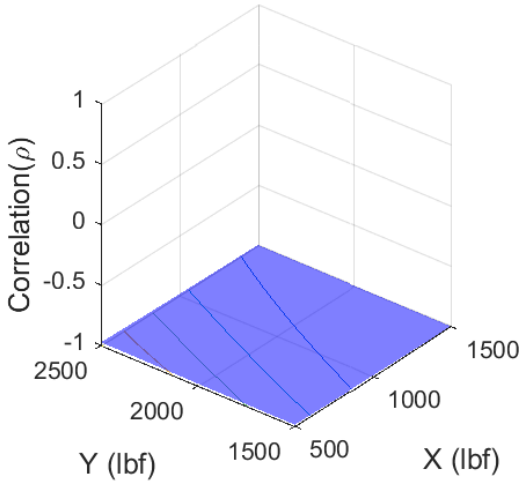

(c) Correlation between max stress s and beam volume v

Figure 70: Correlation regression surfaces as function of input variables, horizontal load X (lbf) and vertical load Y (lbf)

Similar to quantile regression, correlation parameters are regressed with quadratic response surfaces as a function X and Y. A pairwise correlation regression surface between s, d and v is shown in Figure 70. As observed, the correlations between any pair of variables are not constant in the input design space. The correlation between d and s has been found to be positive and very close to 1.0 in the entire design space, which also validates the fact that with increase in displacement, stress

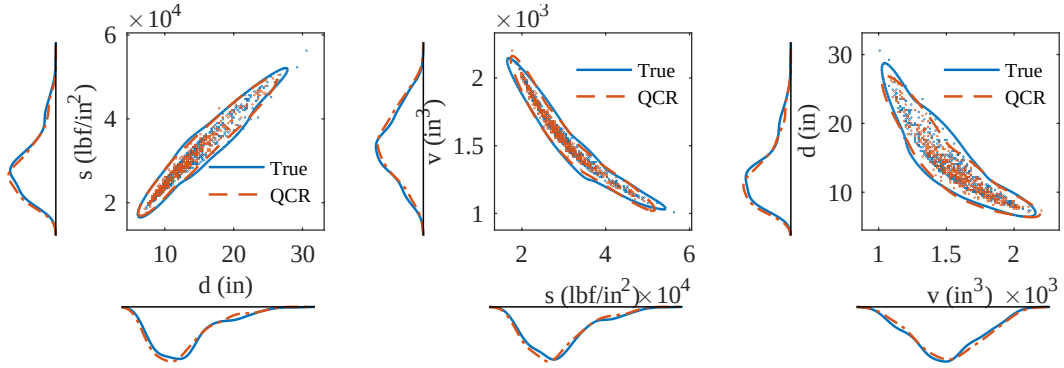

(a) Joint distribution between s and d (b) Joint distribution between v and s (c) Joint distribution between d and v

Figure 71: Scatter plot from joint distribution between variables at $X = 1000$ and $Y = 2000$ generated by true disciplinary analysis and quantile copula regression (QCR)

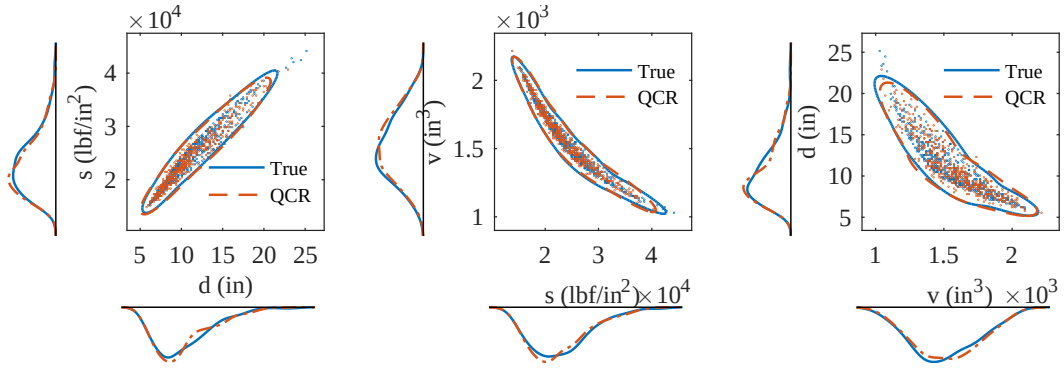

(a) Joint distribution between s and d (b) Joint distribution between v and s (c) Joint distribution between d and v

Figure 72: Scatter plot from joint distribution between variables at $X = 700$ and $Y = 1700$ generated by true disciplinary analysis and quantile copula regression (QCR)

increases. Correlation of d and s with v is negative in entire design space. This is because reduction in beam volume leads to increase in displacement and stress.

To study the accuracy of quantile copula regression, conditional samples are generated at five different locations in input space (X, Y) at $(1000, 2000)$, $(700, 1700)$, $(1300, 2300)$, $(700, 2300)$, $(1300, 1700)$. The bivariate scatter plots between the response variables generated by quantile copula regression at the aforementioned locations are compared with samples from true disciplinary analysis in Figure 71, 72, 73,

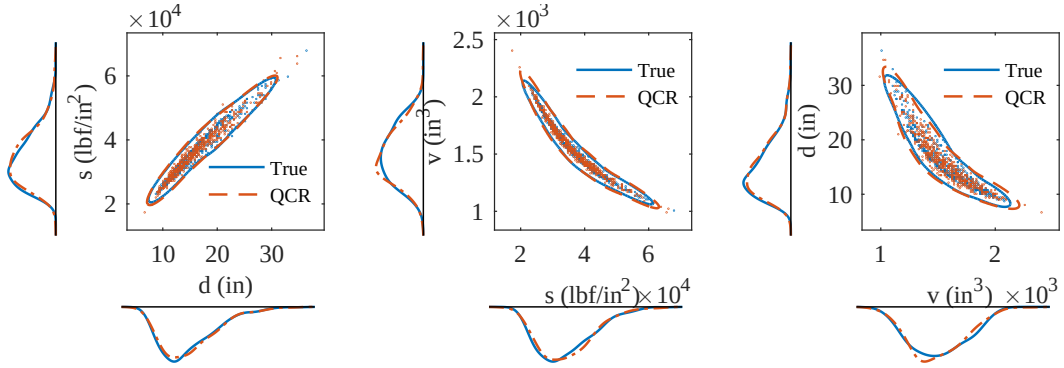

(a) Joint distribution between s and d (b) Joint distribution between v and s (c) Joint distribution between d and v

Figure 73: Scatter plot from joint distribution between variables at $X = 1300$ and $Y = 2300$ generated by true disciplinary analysis and quantile copula regression (QCR)

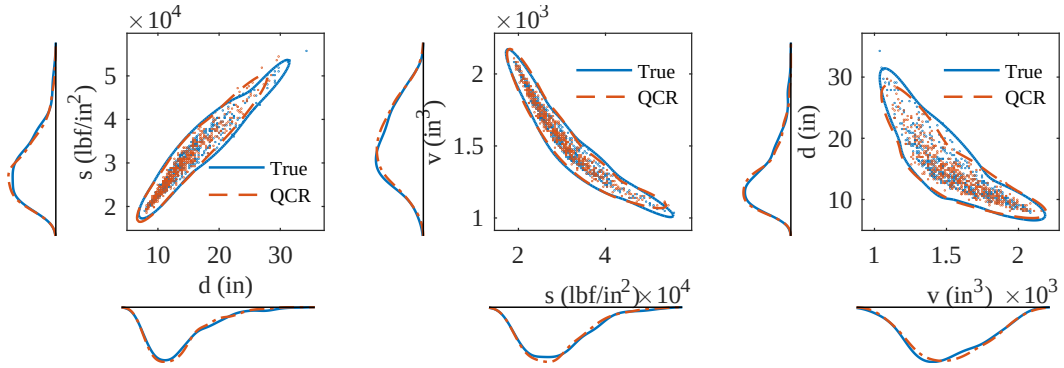

(a) Joint distribution between s and d (b) Joint distribution between v and s (c) Joint distribution between d and v

Figure 74: Scatter plot from joint distribution between variables at $X = 700$ and $Y = 2300$ generated by true disciplinary analysis and quantile copula regression (QCR)

74 and 75. As observed, the trend of the scatter plot generated by quantile copula regression has been found to be very similar to true disciplinary analysis. To compare the dependency structure, a single iso-probability contour of value $0.02\mathrm{P}_{max}$, where P_{max} is the maximum probability value attained by the true solution, is plotted in each figure. The dependency between s and d has been found to be very close to elliptical. The dependency of s and d with respect to v has been found to have a non-linear trend. The dependency structure generated by quantile copula regression

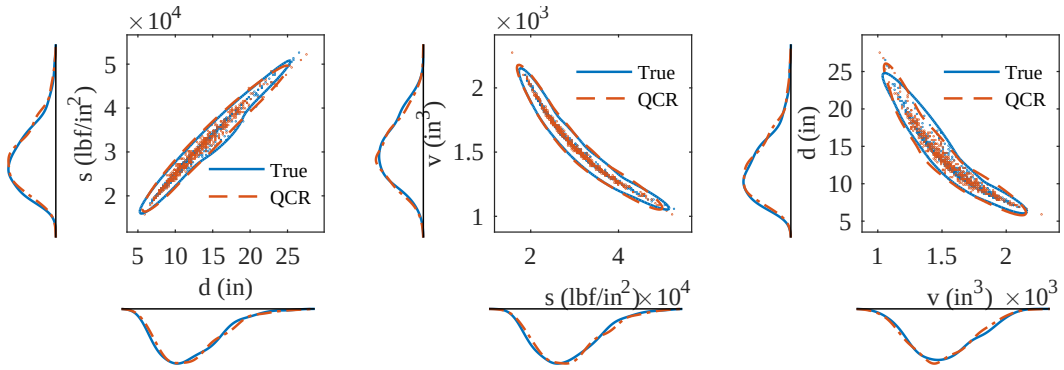

(a) Joint distribution between s and d (b) Joint distribution between v and s (c) Joint distribution between d and v

Figure 75: Scatter plot from joint distribution between variables at $X = 1300$ and $Y = 1700$ generated by true disciplinary analysis and quantile copula regression (QCR)

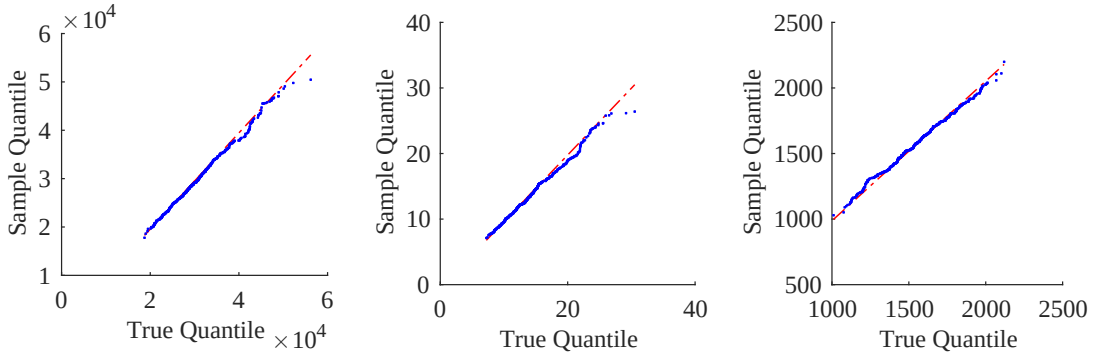

(a) QQ plot of s (b) QQ plot of d (c) QQ plot of v

Figure 76: Quantile-Quantile (Q–Q) plot of variables at $X = 1000$ and $Y = 2000$

has been found to match very closely that of true dependency. Each figure also shows the marginal probability density function of each response. Although almost all the marginal distribution variables are non-Gaussian, quantile copula regression has been found to capture these accurately.

The accuracy of the marginal distributions generated by quantile copula regression at aforementioned location is also validated with the Quantile-Quantile (Q–Q) plot in Figure 76, 77, 78, 79 and 80. Almost all the sample quantiles have matched very closely with true quantiles. Some discrepancy has been found near the upper tail of both s and d. This is due to the fact that both these variables are positively skewed

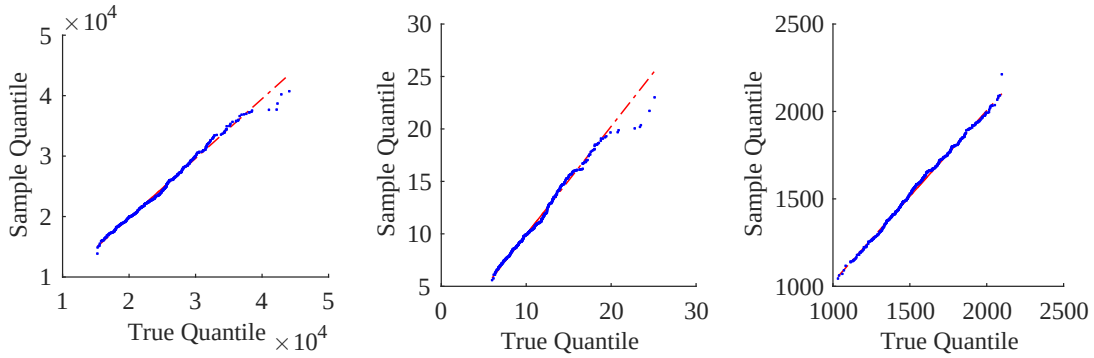

(a) QQ plot of s (b) QQ plot of d (c) QQ plot of v

Figure 77: Quantile-Quantile (Q–Q) plot of variables at $X = 700$ and $Y = 1700$

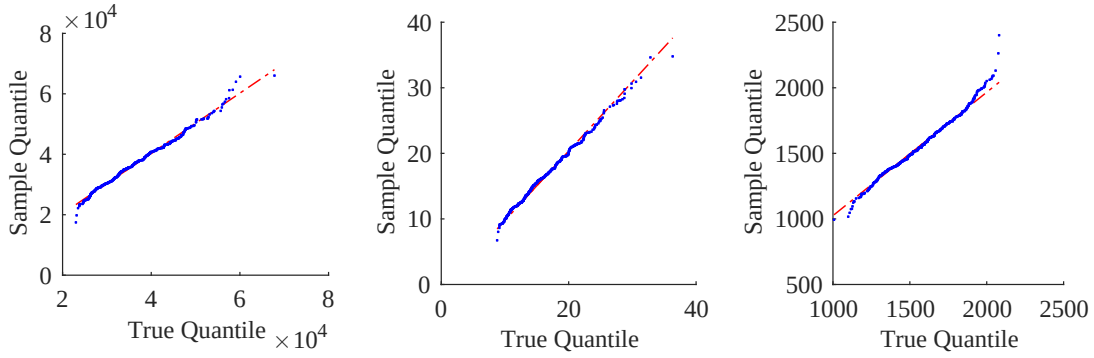

(a) QQ plot of s (b) QQ plot of d (c) QQ plot of v

Figure 78: Quantile-Quantile (Q–Q) plot of variables at $X = 1300$ and $Y = 2300$

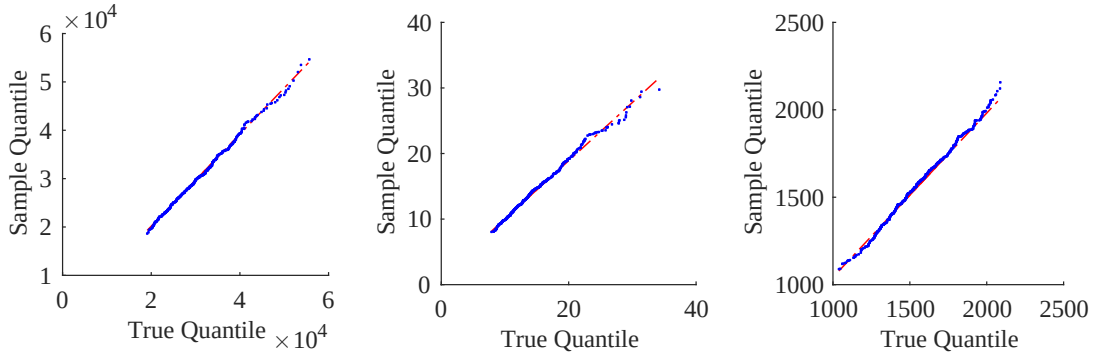

(a) QQ plot of s (b) QQ plot of d (c) QQ plot of v

Figure 79: Quantile-Quantile (Q–Q) plot of variables at $X = 700$ and $Y = 2300$

and have a longer upper tail. The accuracy near the tail can be improved by adding more samples and modeling additional quantile regression near the tails.

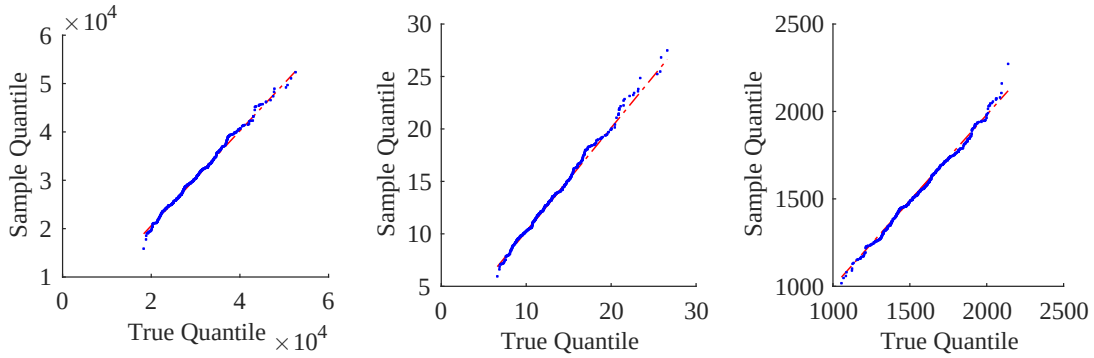

(a) QQ plot of s (b) QQ plot of d (c) QQ plot of v

Figure 80: Quantile-Quantile (Q–Q) plot of variables at $X = 1300$ and $Y = 1700$

Table 18: Comparison of difference in K-L divergence of variables between true marginal distribution and marginal distribution estimated by quantile copula regression

	d	s	v
$(X, Y) = (1000, 2000)$	0.04	0.02	0.01
$(X, Y) = (700, 1700)$	0.02	0.01	0.01
$(X, Y) = (1300, 2300)$	0.01	0.02	0.02
$(X, Y) = (700, 2300)$	0.02	0.01	0.00
$(X, Y) = (1300, 1700)$	0.01	0.01	0.01

To quantify the accuracy of quantile copula regression to model the marginal distributions, K-L divergence is used for each test case and presented in Table 18. As observed, quantile copula regression has been able to accurately estimate the probability density functions of each response. To quantify the accuracy of quantile copula regression to capture the dependence, the difference between mutual information of

Table 19: Comparison of difference in mutual information (ΔMI) among variables between true joint distribution and joint distribution estimated by quantile copula regression

	s **vs** d	d **vs** v	v **vs** s
$(X, Y) = (1000, 2000)$	-0.01	0.03	-0.03
$(X, Y) = (700, 1700)$	0.01	0.00	0.03
$(X, Y) = (1300, 2300)$	0.03	-0.04	0.00
$(X, Y) = (700, 2300)$	-0.02	-0.02	-0.02
$(X, Y) = (1300, 1700)$	-0.02	-0.02	-0.02

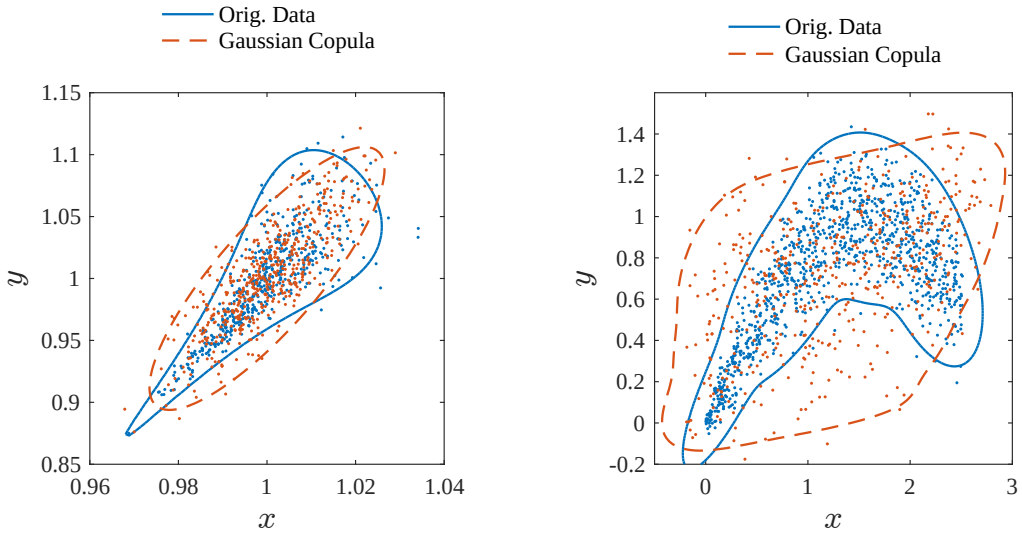

(a) Data with tail dependence

(b) Data with non-linear and non-monotonic dependence

Figure 81: Limitation of Gaussian copula to model data with tail dependence and non-linear with non-monotonic dependence

true solution and quantile copula regressions for each test case is presented in Table 19. It has been found that quantile copula regression has been able to closely match with true mutual information with the worst case of $\Delta MI = -0.04$.

5.6 Chapter Summary

In this chapter, quantile copula regression is presented to model conditional probability density of multivariate responses of a discipline, model, subsystem or even a multidisciplinary system, as a function of predictor or input variables. The quantile copula regression uses quantile regression technique to model the conditional probabilities of each response independently. Since the quantile regression does not assume any functional form of probability densities and instead models different levels of quantiles, it provides a comprehensive information regarding the true probability densities. To handle the dependence between multiple responses, copulas are used to couple the the conditional probabilities with the statistical dependencies. One of

the main advantages of a copula is that it can couple any arbitrary marginal distribution with various ranges of dependency structures. Since copula decouples the marginal distributions from the dependence structure, it allows independent modeling of marginal distributions which are carried out by quantile regression.

To test the hypothesis, a simple beam problem with three responses and two input variables has been used. The uncertainty variables in the beam models are assumed to have non-Gaussian distribution. Due to non-Gaussian uncertainties, the true probability distribution of responses are non-Gaussian. It has been observed that quantile copula regression has been able to accurately and comprehensively estimate the marginal distributions as well as dependencies.

Since multiple quantile regressions are used to estimate the conditional probability densities, the accuracy of the method increases with an increase in number of quantile levels. Also, accuracy of the quantile regression depends upon the number of samples available. This is particularly important to capture the tail probabilities, where the inaccuracy of the quantile regression increases due to relatively smaller samples around that region. In the current work, a quadratic response surface has been used to model the quantile surfaces. For non-linear problems, higher order models or non-linear methods like spline, Artificial Neural Network can be used.

One of the main assumptions in this work is the use of a Gaussian copula to model the dependencies. Although a Gaussian copula is very robust and easily applicable to a large variety of problems, one should be careful while using it. For example, the Gaussian copula is an elliptical copula and cannot model the tail dependence accurately. This is shown in an example given in Figure 81a. Although a Gaussian copula can handle certain non-linear dependencies, it cannot capture the non-monotonic dependencies. This is shown in Figure 81b, where the true data has both non-linear and non-monotonic dependency.

CHAPTER VI

CONCURRENT OPTIMIZATION USING PROBABILISTIC ANALYSIS OF DISTRIBUTED MULTIDISCIPLINARY ARCHITECTURES (CO-PADMA)

In the previous chapters, a method to carry out uncertainty-based multidisciplinary analysis (UMDA) in a distributed procedure while capturing the functional dependencies and interdisciplinary compatibility using PADMA, and modeling of conditional probability densities using quantile copula regression has been discussed. A straightforward way to carry out design optimization is to run an optimization algorithm by treating the UMDA process using the PADMA method as an analysis block. But, as discussed in Chapter 3 and problem set-up research question 3.0, it is desirable to allow each discipline to carry out a local optimization process so that the computational load on system optimization is reduced, in addition to allowing the disciplinary experts to make the best decision in their area of expertise.

In the current chapter, Concurrent Optimization using Probabilistic Analysis of Distributed Multidisciplinary Architectures (CO-PADMA), is developed to carry out distributed multidisciplinary design optimization for non-deterministic disciplines. CO-PADMA is a bi-level optimization procedure where the top level or the system level is mainly responsible for system level optimization and interdisciplinary compatibility using PADMA method. At a lower level, subsystem or disciplines are responsible for carrying out uncertainty propagation and optimization using their respective high fidelity disciplinary analyses and using quantile copula regression of non-local variables. The proposed method is derived by taking features from deterministic MDO methods like the surrogate-based CSSO method. The hypothesis to

the third research question is given as:

Research Question 3.0: *What is an appropriate procedure to carry out distributed optimization of a multidisciplinary system under uncertainty to accurately quantify the dependency and uncertainty on coupling variables and system metric for non-deterministic disciplinary analyses ?*

Hypothesis 3.0: *If accurate models of conditional probability densities of disciplinary metrics can be built, then Concurrent Optimization using Probabilistic Analysis of Distributed Multidisciplinary Architectures (CO-PADMA) can find the optimum design and estimate the uncertainty and dependence of system metrics and state variables accurately, while allowing distributed optimization and uncertainty analysis for a multidisciplinary system.*

In the next section, an overview of the approach is discussed. Next, the CO-PADMA method is presented in detail which is followed by the numerical procedure. After that, numerical experiments are carried out on two problems to test the hypothesis. Finally the chapter is summarized in the last section.

6.1 Approach Overview

A probabilistic formulation for the uncertainty-based multidisciplinary design optimization (UMDO) problem can be stated as

$$\begin{aligned} \text{minimize} \quad & F = F(\mu_{y_{sys}}(\mathbf{x},\mathbf{y}), \sigma_{y_{sys}}(\mathbf{x},\mathbf{y})) && \text{(134a)} \\ \text{with respect to} \quad & \mathbf{x} \\ \text{such that} \quad & \mathrm{P}[g_j(\mathbf{x},\mathbf{y}) \leq 0] > R_{ieq_j} \qquad \text{for } j = 1,\ldots,n_g && \text{(134b)} \\ & \mathbf{x}^L \leq \mathbf{x} \leq \mathbf{x}^U && \text{(134c)} \end{aligned}$$

where $F()$ is the cost or objective function. For example, to carry out robust design optimization one can use $F = \kappa\mu_{y_{sys}}(\mathbf{x},\mathbf{y}) + (1-\kappa)\sigma_{y_{sys}}(\mathbf{x},\mathbf{y})$, where $\mu_{y_{sys}}$ is the statistical mean and $\sigma_{y_{sys}}$ is the standard deviation of system level metric y_{sys} and

$0 \leq \kappa \leq 1$ is a numerical factor specified by the designer. $\mathbf{x}$ is the vector of design variables consisting of shared design variables $\mathbf{x}_{sh}$ and disciplinary design variables $\mathbf{x}_1, \ldots, \mathbf{x}_n$, where $\mathbf{x}_i$ is the design variable vector associated with i^{th} discipline and n is the total number of disciplines. $\mathbf{y}$ is the vector of disciplinary state variables and is uncertain due to uncertainties associated with disciplinary analyses. The system level response y_{sys} is assumed to be an element of state variable vector $\mathbf{y}$. Also, the uncertain coupling variables $\mathbf{y}_{ij} :: \forall i, j$ i.e. the variables which are the output of i^{th} discipline and input to j^{th} discipline, are assumed to be a subset of state variable vector $\mathbf{y}$. The state variables for a given setting of design variable are evaluated by carrying out an UMDA such that the coupling variables satisfy the interdisciplinary compatibility constraints.

A straightforward approach to carry out uncertainty-based multidisciplinary design optimization (UMDO), while allowing concurrent and independent disciplinary uncertainty analysis, is to execute the PADMA procedure for UMDA at each step of the optimization step. As shown in Figure 82, system level optimization is carried out with respect to design variable $\mathbf{x}$ and during each step of the optimization process the PADMA procedure is executed to evaluate the interdisciplinary compatible state variable $\mathbf{y}$. The state variable $\mathbf{y}$ evaluated by the PADMA procedure is used to evaluate the system level cost function and all the design reliability constraints. During each step of the optimization process the PADMA procedure allows all disciplines or subsystems to carry out uncertainty analysis independently and concurrently. Although this approach allows decomposition and concurrent execution of uncertainty analysis among disciplines, the entire burden of optimization lies on the system level optimizer. This approach does not decompose the optimization process among disciplines and exploit the advantages of high fidelity disciplinary subspace exploration.

Decomposition and coordination-based UMDO are categories of methods which

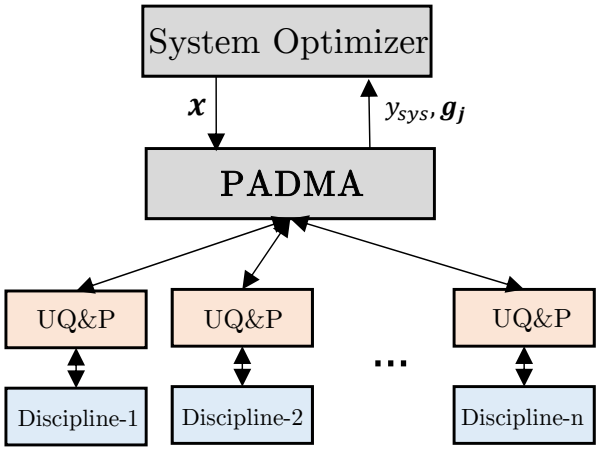

Figure 82: An UMDO approach using PADMA enabling concurrent and independent disciplinary uncertainty analysis

allow decomposition of large scale computationally prohibitive problems into manageable disciplinary sub-optimization problems which are coordinated through a certain strategy to achieve a interdisciplinary compatible optimum solution. The core difference between these methods lies in their coordination strategies through which information between disciplinary optimizer and system optimizer are coordinated so that a compatible and optimum solution is achieved. There are two commonly used coordination strategies; first one is *target matching strategy* and the second one is *approximate model sharing strategy.*

6.1.1 Target Matching Strategy

This strategy is used by UMDO methods based on Collaborative Optimization (CO), Analytical Target Cascading (ATC), etc. In the first strategy, the system optimizer sets the target for the disciplinary optimizers and applies interdisciplinary compatibility constraints such that the optimum solution is a consistent design. The main goal of a subsystem or disciplinary optimizer is to achieve the targets set by the system level optimizer. In a typical bi-level UMDO procedure based on target matching strategy, the optimization process is decomposed into system level optimization at the

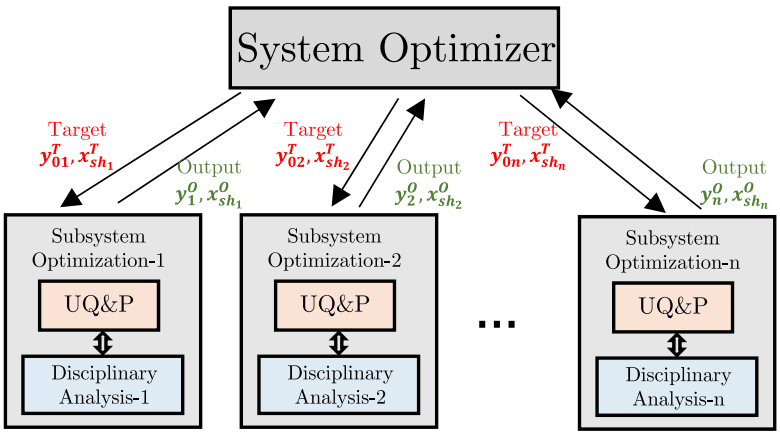

Figure 83: A general target matching strategy for decomposition and coordination-based UMDO

top level and disciplinary level optimization at the lower level as shown in Figure 83. A general system level optimization statement is given by Equation 135.

System Optimization

$$\begin{aligned}
\text{minimize} \quad & F = f(\Xi_1(y_{sys}), \ldots, \Xi_k(y_{sys})) && \text{(135a)}\\
\text{with respect to} \quad & \mathbf{x}_{sh_0}, \Xi_1(\mathbf{y}_0), \ldots, \Xi_k(\mathbf{y}_0) && \\
\text{such that} \quad & \mathrm{P}[g_{j_0}(\mathbf{x}_{sys}, \mathbf{x}_{sh_0}, \mathbf{y}_0) \leq 0] > R_{ieq_j} \qquad \text{for } j = 1, \ldots, n_{g_0} && \text{(135b)}\\
& C_{c_i}(\boldsymbol{\Xi}(\mathbf{y}_{0_i}), \boldsymbol{\Xi}(\mathbf{y}_i), \mathbf{x}_{sh_{0_i}}, \mathbf{x}_{sh_i}) = 0 \quad \forall i && \text{(135c)}
\end{aligned}$$

The cost function of system optimization is a function of uncertainty measure (Ξ_i) of system level metric y_{sys}. Some of the commonly used measures (Ξ_i) in probability theory are expected value, standard deviation, higher order moments, percentile, correlation, etc. The design variables consist of copies of shared design variables ($\mathbf{x}_{sh_0}$) and copies of statistical measures of disciplinary state variables $\mathbf{y}_0$. Please note that the subscript $()_0$ signifies copies of variables associated with system level optimization. $g_j^0(\mathbf{x}_{sys}, \mathbf{x}_{sh_0}, \mathbf{y}_0)$ are the system level constraints and R_{ieq_j} is the reliability factor set up by the designer. Similarly, $\mathbf{x}_{sh_{0_i}}$ is the subset of $\mathbf{x}_{sh_0}$ consisting of copies of shared design variables associated with i^{th} discipline. $\mathbf{x}_{sh_i}$ and $\boldsymbol{\Xi}(\mathbf{y}_i)$ are the shared design variables and statistical measures of state variables evaluated and received from the

i^{th} discipline. $C_{c_i}(\mathbf{\Xi}(\mathbf{y}_{0_i}), \mathbf{\Xi}(\mathbf{y}_i), \mathbf{x}_{sh_{0_i}}, \mathbf{x}_{sh_i}) = 0$ are the interdisciplinary compatibility constraints required to achieve a consistent solution at the optimum. For example, in MM-RCO [141] method interdisciplinary compatibility constraints are given as

$$C_{c_i} = ||\mathbf{x}_{sh_{0_i}} - \mathbf{x}_{sh_i}|| + ||\mu_{\mathbf{y}_{0_i}} - \mu_{\mathbf{y}_i}|| + ||\sigma_{\mathbf{y}_{0_i}} - \sigma_{\mathbf{y}_i}|| \tag{136}$$

where $\mu()$ and $\sigma()$ are mean and standard deviation of respective variables. [144]

At subsystem level, the optimization procedure is given by Equation 137.

i^{th} Subsystem Optimization

$$\begin{aligned}
\text{Given} \quad & \Xi_1(\mathbf{y}_{0_i}), \ldots, \Xi_k(\mathbf{y}_{0_i}), \mathbf{x}_{sh_{0_i}} && \text{(137a)}\\
& \mathbf{y}_i = f_i(\mathbf{x}_{loc_i}, \mathbf{x}_{sh_i}, \mathbf{y}_{.i}, \mathbf{u_i}) \text{ or } \mathbf{y}_i = f_i(\mathbf{x}_{loc_i}, \mathbf{x}_{sh_i}, \mathbf{y}_{.i}) + \epsilon_i && \text{(137b)}\\
\text{minimize} \quad & f_{c_i} && \text{(137c)}\\
\text{with respect to} \quad & \mathbf{x}_{loc_i}, \mathbf{x}_{sh_i}, \Xi_1(\mathbf{y}_i), \ldots, \Xi_k(\mathbf{y}_i) &&\\
\text{such that} \quad & \mathrm{P}[g_{i_j}(\mathbf{x}_{loc_i}, \mathbf{x}_{sh_i}, \mathbf{y}_i) \leq 0] > R_{ieq_j} \qquad \text{for } j = 1, \ldots, n_{i_g} && \text{(137d)}
\end{aligned}$$

where target value of $\Xi_1(\mathbf{y}_{0_i}), \ldots, \Xi_k(\mathbf{y}_{0_i})$, and $\mathbf{x}_{sh_{0i}}$ are set and given by the system optimizer. Disciplinary analyses are available either as an explicit function of uncertain variables $\mathbf{y}_i = f_i(\mathbf{x}_{loc_i}, \mathbf{x}_{sh_i}, \mathbf{y}_{.i}, \mathbf{u_i})$ or non-explicit and non-deterministic function $\mathbf{y}_i = f_i(\mathbf{x}_{loc_i}, \mathbf{x}_{sh_i}, \mathbf{y}_{.i}) + \epsilon_i$, where ϵ_i is the random noise function due to inherent uncertainty in the subsystem. Design variables at subsystem level are local design variables x_{loc_i}, local copies of shared design variables x_{sh_i} and statistical measure of state variables $\Xi_1(\mathbf{y}_i), \ldots, \Xi_k(\mathbf{y}_i)$. The objective of the disciplinary optimization is to reduce the discrepancy from the target specified by the system level.

$$f_{c_i} = ||\mathbf{x}_{sh_{0_i}} - \mathbf{x}_{sh_i}|| + \sum_{i=1}^{k} ||\Xi_i(\mathbf{y}_{0_i}) - \Xi_i(\mathbf{y}_i)|| \tag{138}$$

The objective may also include optimizing the disciplinary metrics which are not dealt with at system level.

Comments Uncertainty quantification and propagation (UQP) takes place during each step of subsystem optimization to evaluate the uncertainty on local state variables and constraint. It is inconsequential if disciplinary analyses are deterministic ($\mathbf{y}_i = f_i(\mathbf{x}_{loc_i}, \mathbf{x}_{sh_i}, \mathbf{y}_{.i}, \mathbf{u}_i)$) or non-deterministic ($\mathbf{y}_i = f_i(\mathbf{x}_{loc_i}, \mathbf{x}_{sh_i}, \mathbf{y}_{.i}) + \epsilon_i$) or can or cannot be represented explicitly as a function of uncertain variables. The optimization formulation only requires statistical information of disciplinary state variables from the disciplinary uncertainty analysis process.

Another point to be noted here is that this strategy does not guarantee interdisciplinary compatibility at each step of the optimization process. Therefore, if the optimization process is terminated before the optimum solution is reached, the design may be inconsistent.

6.1.2 Approximate Model Sharing Strategy

This strategy is used by UMDO methods based on Concurrent SubSpace Optimization (CSSO), etc. In this strategy, approximate models of state variables are built and used in both system optimization as well as subsystem optimization as shown in Figure 84. The first step in this strategy is to build approximate models of disciplinary state variables $\tilde{\mathbf{y}}_i = \tilde{f}_i(\mathbf{x}_i, \mathbf{x}_{sh}, \mathbf{u}_i)$ by executing individual disciplinary analysis separately using appropriate design of experiment techniques or global sensitivity methods. Some methods directly build the approximate model of interdisciplinary compatible solution of all the state variables $\tilde{\mathbf{y}} = \tilde{f}(\mathbf{x}, \mathbf{u})$, where $\mathbf{x} = [\mathbf{x}_{sys}, \mathbf{x}_{sh}, \mathbf{x}_1, \ldots, \mathbf{x}_n]$ and $\mathbf{u} = [\mathbf{u}_1, \ldots, \mathbf{u}_n]$ by executing an integrated UMDA. The approximate models of state variables are then used to carry out system level optimization given by Equation 139. Please note that $\tilde{()}$ used on any function in this chapter signifies approximate models for both deterministic and non-deterministic functions unless stated otherwise.

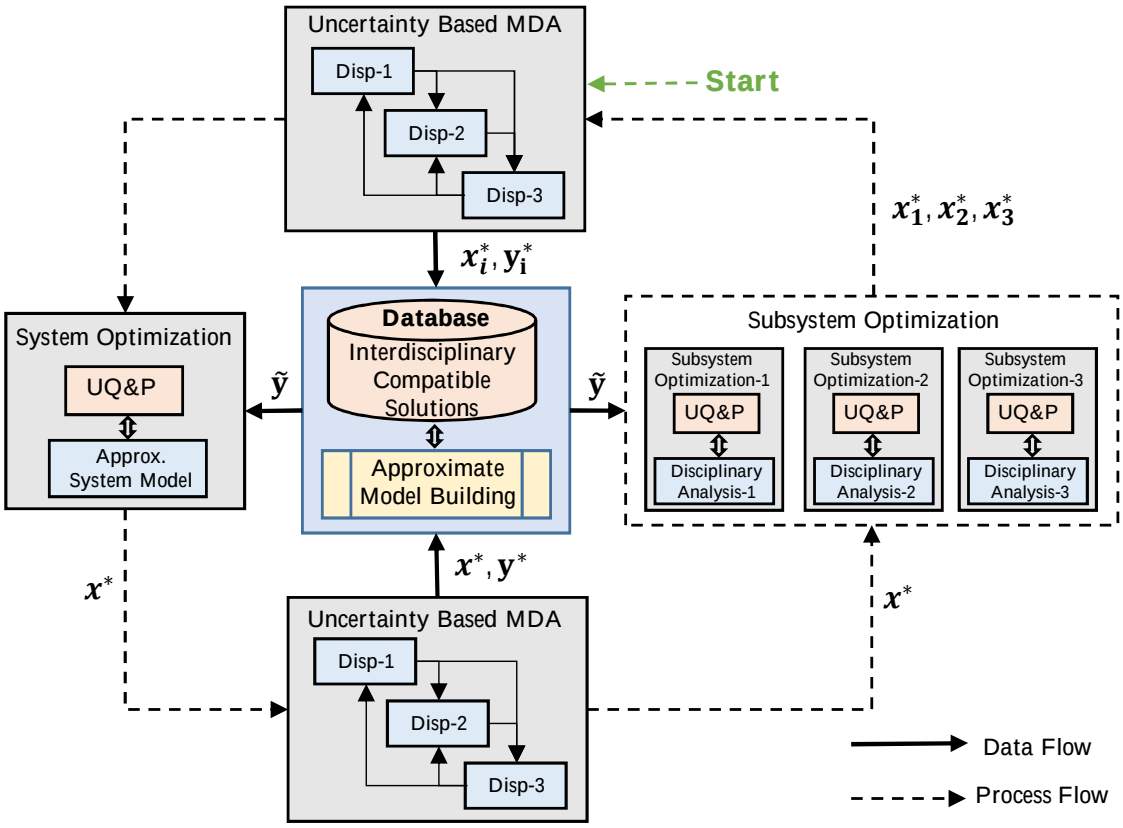

Figure 84: An approximate model sharing strategy for decomposition and coordination based UMDO

System Optimization

$$\begin{aligned}
\text{Given} \quad & \tilde{\mathbf{y}}_i = \tilde{f}_i(\mathbf{x}_i, \mathbf{x}_{sh}, \mathbf{u}_i) \text{ or } \tilde{\mathbf{y}} = \tilde{f}(\mathbf{x}, \mathbf{u}) && \text{(139a)} \\
\text{minimize} \quad & F = f(\tilde{y}_{sys}) && \text{(139b)} \\
\text{with respect to} \quad & \mathbf{x} \\
\text{such that} \quad & \mathrm{P}[g_j(\mathbf{x}, \tilde{\mathbf{y}}) \leq 0] > R_{ieq_j} \qquad \text{for } j = 1, \ldots, n_g && \text{(139c)}
\end{aligned}$$

where design variable $\mathbf{x}$ consists of shared design variables $\mathbf{x}_{sh}$ and disciplinary level design variables $\mathbf{x}_i$. A system level objective function is similar to a target matching strategy. If an approximate model of interdisciplinary compatible solution of state variables $\tilde{\mathbf{y}} = \tilde{f}(\mathbf{x}, \mathbf{u})$ is available, then the system cost function can be directly evaluated from the model. If approximate models of disciplinary state variables $\tilde{\mathbf{y}}_i = \tilde{f}_i(\mathbf{x}_i, \mathbf{x}_{sh}, \mathbf{u}_i)$ are available, then UMDA needs to be carried out using approximate models to evaluate interdisciplinary compatible state variables and system level cost function. Once the optimum design variable at k^{th} cycle, $\mathbf{x}_k^*$ is evaluated, UMDA using the actual disciplinary analyses is carried out to evaluate the true solution and error associated with the approximate model. The true solution is also added to the database which is used to update the approximate models in the following cycle.

At subsystem level, subspace optimization is carried out using local design variables. The coupling variables which the are output of other disciplines and input to the subspace analysis are evaluated using approximate models. The subspace optimization formulation is given in Equation 140.

i^{th} Subsystem Optimization

$$\text{Given} \qquad \mathbf{x}_k^*, \tilde{\mathbf{y}}_{\cdot i} = \tilde{f}_{\cdot i}(\mathbf{x}, \mathbf{u}) \tag{140a}$$

$$\mathbf{y}_i = f_i(\mathbf{x}_i, \mathbf{x}_{sh}, \tilde{\mathbf{y}}_{\cdot i}, \mathbf{u}_i) \tag{140b}$$

$$\text{minimize} \qquad f(\tilde{\mathbf{y}}_{\cdot i}, \mathbf{y}_i) \tag{140c}$$

$$\text{with respect to} \qquad \mathbf{x}_{loc}^i, \mathbf{x}_{sh}^i$$

$$\text{such that} \qquad \mathrm{P}[g_j(\mathbf{x}, \tilde{\mathbf{y}}_{\cdot i}, \mathbf{y}_i) \leq 0] > R_{ieq_j} \qquad \text{for } j = 1, \ldots, n_g \tag{140d}$$

where system level optimum solution of k^{th} cycle $\mathbf{x}_k^*$ is used for non-local design variables. The approximate model $\tilde{\mathbf{y}}_{\cdot i} = \tilde{f}_{\cdot i}(\mathbf{x}, \mathbf{u})$ is used to estimate input coupling variables $\tilde{\mathbf{y}}_{\cdot i}$. Local state variable is evaluated by true or high-fidelity disciplinary analysis $\mathbf{y}_i = f_i(\mathbf{x}_i, \mathbf{x}_{sh}, \tilde{\mathbf{y}}_{\cdot i}, \mathbf{u}_i)$. The cost function is similar to system level optimization. Similarly, in the constraint function $g_j(\mathbf{x}, \tilde{\mathbf{y}}_{\cdot i}, \mathbf{y}_i)$ local state variables are estimated using true disciplinary analysis and non-local state variables are estimated using approximate models. Once the optimum is evaluated from each subsystem, an UMDA is carried out to evaluate the true solution and is added to the database which is used to update the approximate models in the following cycle. The cycle is repeated until convergence criteria set by designer are met.

Comments Since interdisciplinary compatible solutions of state variables $\mathbf{y}$ are evaluated using approximate models of disciplinary state variables $\tilde{\mathbf{y}}_i = \tilde{f}_i(\mathbf{x}_i, \mathbf{x}_{sh}, \mathbf{u}_i)$, interdisciplinary consistency constraint is not required in the optimization process. Also, at the end of the each cycle, an UMDA is carried out at optimum solution to ensure a consistent solution is achieved. Therefore, if the optimization process is terminated at any intermediate cycle, interdisciplinary compatibility is guaranteed. However, the approximate models built in this strategy are deterministic models and are a function of uncertainty variables $\mathbf{u}$ as well. Generally, it is assumed that the disciplinary analyses can be determined as a explicit function of uncertain variables

$\mathbf{y}_i = f_i(\mathbf{x}_{loc_i}, \mathbf{x}_{sh_i}, \mathbf{y}_{.i}, \mathbf{u}_i)$. Therefore most UMDO methods based on this strategy may not be directly applicable for problems which have non-deterministic disciplinary analyses or the disciplinary analyses which have inherent uncertainty and cannot be explicitly determined as functions of uncertain variables.

The CO-PADMA methodology is based on the approximate model sharing approach. To overcome some of the shortcomings of existing methods based on the approximate model sharing approach, PADMA procedure and quantile copula regression is used. PADMA procedure enables distributed and concurrent disciplinary analysis to estimate an interdisciplinary compatible solution, therefore reducing the computational burden associated with an integrated UMDA procedure required in each cycle of the approximate model sharing approach. Quantile copula regression allows modeling of non-deterministic disciplinary analysis, where disciplinary state variables cannot be explicitly determined as a function of uncertain variables. Quantile copula regression also enables the handling of the dependencies and allows modeling of non-Gaussian marginal distributions of the state variables.

6.2 CO-PADMA Methodology

Concurrent Optimization using Probabilistic Analysis of Distributed Multidisciplinary Architectures (CO-PADMA) is a bi-level UMDO procedure which uses an approximate model sharing approach as coordination strategy. The CO-PADMA method starts by executing UMDA to evaluate samples of interdisciplinary compatible solutions of state variables at multiple design points and store them in a database. Instead of solving an integrated UMDA, CO-PADMA uses the PADMA procedure to evaluate the interdisciplinary compatible solutions of state variables. Next, approximate probabilistic models are built using quantile copula regression incorporating the samples of state variables in the database. Instead of building a separate quantile copula regression model of each state variable, a single probabilistic model using

quantile copula regression $\tilde{f}_{qcr_{\mathbf{y}}}(\mathbf{y}|\mathbf{x})$ is built, which models the joint probability density function of interdisciplinary compatible solutions of all the state variables as a function of design variables $\mathbf{x}$, where $\mathbf{y} = [\mathbf{y}_1, \ldots, \mathbf{y}_{n_D}]$ is the vector of all the state variables, $\mathbf{y}_i$ is the vector of state variables which are output of i^{th} discipline and n_D is the number of disciplines. Please note that the quantile copula regression are also function of model parameters $\hat{\boldsymbol{\beta}}_1, \ldots, \hat{\boldsymbol{\beta}}_p$, and $\hat{\boldsymbol{\alpha}}$ as $\tilde{f}_{qcr_{\mathbf{y}}}(\mathbf{y}|\mathbf{x}, \hat{\boldsymbol{\beta}}_1, \ldots, \hat{\boldsymbol{\beta}}_p, \hat{\boldsymbol{\alpha}})$. However for clarity, these parameters are omitted in this chapter and the quantile copula regression models are represented as $\tilde{f}_{qcr_{\mathbf{y}}}(\mathbf{y}|\mathbf{x})$. The design variable vector $\mathbf{x}$ consists of vector of shared design variable $\mathbf{x}_{sh}$ and vector of disciplinary design variables $\mathbf{x}_i$, i.e. $\mathbf{x} = [\mathbf{x}_{sh}, \mathbf{x}_1, \ldots, \mathbf{x}_\mathbf{n}]$. Building a single quantile copula regression model is the necessary criteria to capture the dependence between the state variables. If reliability constraints $\mathbf{g}_j$ are present, then a quantile copula regression model of constraints is also built as $\tilde{f}_{qcr_{\mathbf{g}_j}}(\mathbf{g}_j|\mathbf{x})$, for $j = 1, \ldots, n_D$, where j signifies j^{th} discipline and n_D is the total number of disciplines. If dependence between state variables and constraints is required during the optimization or disciplinary analyses process, then a single quantile copula regression model of combined variable $\mathbf{y}_{combined} = [\mathbf{y}, \mathbf{g}]$, can be built.

6.2.1 System Optimization

The next step is to carry out system optimization using a quantile copula regression model of state variables instead of true disciplinary analyses. The formal optimization

statement of system optimization at r^{th} cycle is given by Equation 141.

$$\text{Given} \qquad \tilde{f}_{qcr_{\mathbf{y}}}(\mathbf{y}|\mathbf{x}), \tilde{f}_{qcr_{\mathbf{g}_j}}(\mathbf{g}_j|\mathbf{x}) \tag{141a}$$

$$\tilde{y}_{sys} = f_{sys}(\mathbf{x}, \tilde{\mathbf{y}}_1, \ldots, \tilde{\mathbf{y}}_{n_D}) \tag{141b}$$

$$\text{minimize} \qquad \tilde{F} = f_{obj}(\Xi_1(\tilde{y}_{sys}), \ldots, \Xi_k(\tilde{y}_{sys})) \tag{141c}$$

$$\text{with respect to} \qquad \mathbf{x}$$

$$\text{such that} \qquad \mathrm{P}[\tilde{\mathbf{g}}_j(\mathbf{x}) \leq 0] > R_{ieq_j} \qquad \text{for } j = 1, \ldots, n_D \tag{141d}$$

$$\mathbf{x}^{L(r)} \leq \mathbf{x} \leq \mathbf{x}^{U(r)} \tag{141e}$$

$$\text{Output} \qquad \mathbf{x}^{*(r)}, \tilde{f}^{*(r)}_{y_{sys}}(y_{sys}), F^{*(r)} \tag{141f}$$

where $\tilde{f}_{qcr_{\mathbf{y}}}(\mathbf{y}|\mathbf{x})$ and $\tilde{f}_{qcr_{\mathbf{g}_j}}(\mathbf{g}_j|\mathbf{x})$ are quantile copula regression models which are used to quantify the uncertainty or probability density function on state variables $\tilde{\mathbf{y}}$ and constraint $\tilde{\mathbf{g}}_j$, respectively. Please note that the $\tilde{()}$ over any variable represents that uncertainty or probability density function on that particular variable is estimated directly or indirectly using quantile copula regression model. The uncertainty of system metric $\tilde{y}_{sys}$ is evaluated by system level function $f_{sys}(\mathbf{x}, \tilde{\mathbf{y}}_1, \ldots, \tilde{\mathbf{y}}_{n_D})$, where $\tilde{\mathbf{y}}_i \subseteq \tilde{\mathbf{y}}$ is the state variable vector of i^{th} discipline. The cost function of system optimization $f_{obj}()$ is a function of uncertainty measure (Ξ_i) of approximate system level metric $\tilde{y}_{sys}$. $\mathbf{x}^{L(r)}$ and $\mathbf{x}^{U(r)}$ are lower and upper limits of design variable at r^{th} cycle. $\mathbf{x}^{*(r)}$ is the optimum design variable, $\tilde{f}^{*(r)}_{y_{sys}}(y_{sys})$ approximate probability density function of system metric, and $\tilde{F}^{*(r)}$ is the optimum cost function at the end of r^{th} cycle. At the end of the optimization process, the PADMA procedure is carried out using high-fidelity disciplinary analyses at the optimum design of r^{th} cycle, $\mathbf{x}^{*(r)}$, to evaluate the accurate probability density of system metric $f^{*(r)}_{y_{sys}}(y_{sys})$, accurate cost function $F^{*(r)}$, and samples of interdisciplinary compatible solutions of all the state variables. The samples of accurate interdisciplinary compatible solutions of state variables at $\mathbf{x}^{*(r)}$ are added to the database, which are used to update the quantile copula regression for the $(r+1)^{th}$ cycle.

If the convergence is not achieved, the system level optimum design point $\mathbf{x}^{*(r)}$ is passed on to all the disciplines, where it is used as the initial point for subsystem optimization.

6.2.2 Subsystem Optimization

Subsystem optimization is carried out independently and concurrently by each discipline or subsystem. In the subsystem optimization, the high fidelity or the true disciplinary analysis is used to evaluate the local state variables $\mathbf{y}_i$ and local constraints $\mathbf{g}_i$. The non-local state variables $\mathbf{y}_{j\neq i}$ and non-local constraints $\mathbf{g}_{j\neq i}$ are estimated using quantile copula regression used by the system level optimization. The formal optimization statement of system optimization at r^{th} cycle is given by Equation 142.

$$\begin{aligned}
\text{Given} \quad & \tilde{f}_{qcr_{\mathbf{y}}}(\mathbf{y}|\mathbf{x}), \tilde{f}_{qcr_{\mathbf{g}_j}}(\mathbf{g}_j|\mathbf{x}), \mathbf{x}^{*(r)} && \text{(142a)}\\
& \mathbf{y}_i = f_i(\mathbf{x}_i, \tilde{\mathbf{y}}_{\cdot i}, \mathbf{u}_i) + \epsilon_{y_i} && \text{(142b)}\\
& \mathbf{g}_i = g_i(\mathbf{x}_i, \tilde{\mathbf{y}}_{\cdot i}, \mathbf{u}_i) + \epsilon_{g_i} && \text{(142c)}\\
& \tilde{y}_{SS_i} = f_{sys}(\mathbf{x}, \tilde{\mathbf{y}}_1, \ldots, \tilde{\mathbf{y}}_{i-1}, \mathbf{y}_i, \tilde{\mathbf{y}}_{i+1}, \ldots, \tilde{\mathbf{y}}_{n_D}) && \text{(142d)}\\
\text{minimize} \quad & \tilde{F}_i = f_{obj}(\Xi_1(\tilde{y}_{SS_i}), \ldots, \Xi_k(\tilde{y}_{SS_i})) && \text{(142e)}\\
\text{with respect to} \quad & \mathbf{x} &&\\
\text{such that} \quad & \mathrm{P}[\mathbf{g}_i(\mathbf{x}, \tilde{\mathbf{y}}_{\cdot i}) \leq 0] > R_{ieq_i} && \text{(142f)}\\
& \mathrm{P}[\tilde{\mathbf{g}}_j(\mathbf{x}) \leq 0] > R_{ieq_j} \qquad \text{for } j \neq i && \text{(142g)}\\
& \mathbf{x}^{L(r)} \leq \mathbf{x} \leq \mathbf{x}^{U(r)} && \text{(142h)}\\
\text{Output} \quad & \mathbf{x}_i^{*(r)}, \tilde{f}^{*(r)}_{y_{SS_i}}(y_{SS_i}), F_i^{*(r)} && \text{(142i)}
\end{aligned}$$

where $\mathbf{y}_i = f_i(\mathbf{x}_i, \tilde{\mathbf{y}}_{\cdot i}, \mathbf{u}_i) + \epsilon_{y_i}$ is the true high-fidelity disciplinary analysis function and $\mathbf{g}_i = g_i(\mathbf{x}_i, \tilde{\mathbf{y}}_{\cdot i}, \mathbf{u}_i) + \epsilon_{g_i}$ is the true high-fidelity disciplinary constraint function, which are function of parametric or epistemic uncertainties $\mathbf{u}_i$ and aleatory uncertainties or random noise ϵ_{y_i} and ϵ_{g_i}. $\mathbf{x}_i \subseteq \mathbf{x}$ are the local design variables and $\tilde{\mathbf{y}}_{\cdot i} \subseteq \tilde{\mathbf{y}}$

is the vector of non-local state variables. Uncertainty on $\tilde{\mathbf{y}}_{\cdot i}$ are estimated through quantile copula regression $\tilde{f}_{qcr_{\mathbf{y}}}(\mathbf{y}|\mathbf{x})$. The system metric function f_{sys} and the cost function f_{obj} on the system metric is same as in system optimization. To estimate the uncertainty on system metric, uncertainty of local state variables $\mathbf{y}_i$ are estimated with true high-fidelity local disciplinary analysis while uncertainty on non-local state variables $\tilde{\mathbf{y}}_j$ for $j \neq i$ are estimated using quantile copula regression. The local reliability constraints are evaluated using local disciplinary analysis whereas reliability on non-local constraints are estimated through quantile copula regression $\tilde{f}_{qcr_{\mathbf{g}_j}}(\mathbf{g}_j|\mathbf{x})$ for $j \neq i$. Instead of optimizing with respect to local design variables $\mathbf{x}_i$ only, subsystem optimization uses the entire set of system level design variable $\mathbf{x}$. This allows the subsystem to explore non-local design space as well, by evaluating the non-local state variables with quantile copula regression. The final output of subsystem optimization after r^{th} cycle are optimum design variable $\mathbf{x}_i^{*(r)}$, probability density function of system metric $\tilde{f}_{y_{SS_i}}^{*(r)}(y_{SS_i})$, and optimum cost function $\tilde{F}_i^{*(r)}$.

At the end of all subsystem optimizations, PADMA analysis is carried out using all the high-fidelity disciplinary analyses at each subsystem optimum designs, $\mathbf{x}_i^{*(r)}, \forall i = 1 \ldots n_D$, to evaluate the accurate probability density function $f_{y_{SS_i}}^{*(r)}(y_{SS_i})$ and true cost function $F_i^{*(r)}$. Also, samples of accurate interdisciplinary compatible solutions are generated at the subsystem optimum design and are added to the database which are in turn used to update and improve the quantile copula regression for the $(r+1)^{th}$ cycle.

6.2.3 Design Space Reduction

The main reason to add accurate samples of interdisciplinary compatible solutions of system and subsystem optimum designs to the database is to improve the accuracy of quantile copula regression near the optimum region in the design space. This allows both system and subsystem optimizer to exploit the region of probable optimum

with better accuracy. However, to improve the exploratory behavior of the optimizer, accuracy of quantile copula regression models needs to be improved in overall design space. To achieve this, design space of $\mathbf{x}$ is reduced at the end of each cycle. As the design space is reduced with every passing cycle, the nonlinear trend of the response variables tend to reduce. This allows the quantile copulate regression model, which assumes some fixed order of polynomial functions, to improve the accuracy of estimating uncertainty on state variables. An example of design space reduction and effect on quantile regression is shown in Figure 85 with notional data. As seen in the figure, the original data is generated from a nonlinear noisy function and quantile regression is built using quadratic model for quantile level of $\tau = 0.1, 0.5$ and 0.9. With reduction of design space in each cycle, the accuracy of the quantile regression tends to improve.

In CO-PADMA, design space reduction is carried out after the completion of all the subsystem optimizations. Also, the domain size is reduced gradually with iterations so that premature convergence to unreliable optimum can be avoided. The methods used here are modified from the method used by Altus [214]. First an arbitrary reduction factor R_f is selected, typically between 5% to 20%, which defines the maximum percentage of design space reduction after each cycle. The lower and upper bound of design variables for $(r+1)^{th}$ cycle is given by Equation 143.

$$\mathbf{x}(i)^{L(r+1)} = \mathbf{x}^*(i)_{min} - \left(1 - \frac{R_f}{100}\right)\left(\mathbf{x}^*(i)_{min} - \mathbf{x}(i)^{L(r)}\right) \tag{143a}$$

$$\mathbf{x}(i)^{U(r+1)} = \mathbf{x}^*(i)_{max} + \left(1 - \frac{R_f}{100}\right)\left(\mathbf{x}(i)^{U(r)} - \mathbf{x}^*(i)_{min}\right) \tag{143b}$$

where $\mathbf{x}(i)^{L(r+1)}$ and $\mathbf{x}(i)^{U(r+1)}$ is the lower and upper bound of i^{th} variable in design variable vector $\mathbf{x}$ for the $(r+1)^{th}$ cycle. $\mathbf{x}^*(i)_{min}$ is the minimum of i^{th} design variable among the optimum solutions of all the previous cycles. Similarly, $\mathbf{x}^*(i)_{max}$ is the maximum of i^{th} design variable among the optimum solutions of all the previous

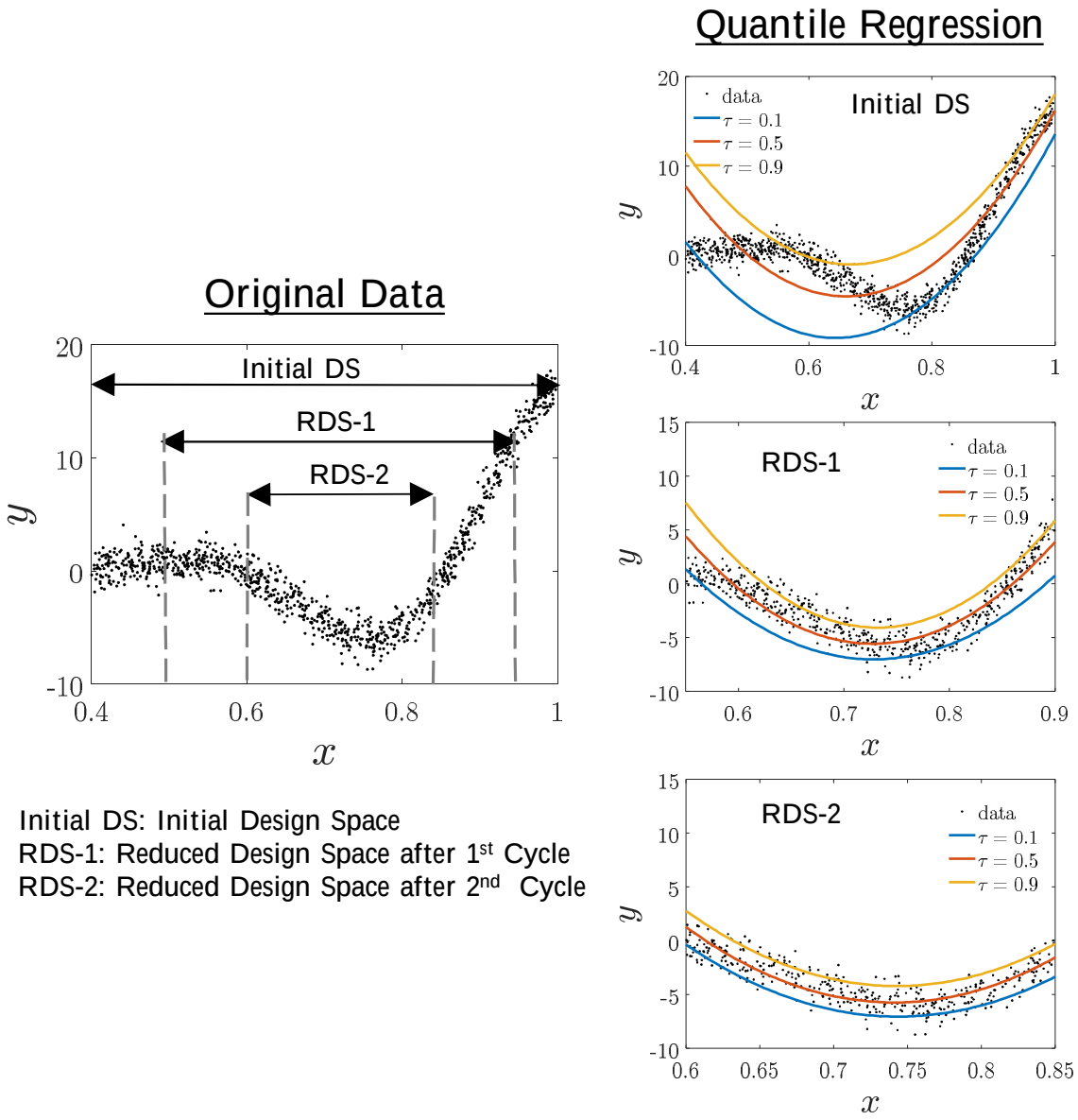

Figure 85: Improvement of accuracy of quantile regression based on quadratic polynomial with reduction of design space

cycles. $\mathbf{x}(i)^{L(r)}$ and $\mathbf{x}(i)^{U(r)}$ is the lower and upper bound of i^{th} variable in the r^{th} cycle. This formulation guarantees that design space in $(r+1)^{th}$ cycle will encompass all the optimum design estimated in all the previous cycles. Once the design space reduction is complete, samples of interdisciplinary compatible solutions are selected from the database which are within the reduced design space. These selected samples are then used to rebuild quantile copula regression for the $(r+1)^{th}$ cycle.

With every cycle, the domain of design variables converges towards the region around the optimum solution with the design space reduction technique. Therefore, the designer can start the CO-PADMA process with design of experiment consisting of a relatively smaller number of experiments in the first cycle. With each cycle, the designer can carry out additional experiments in the reduced design space and add the samples of interdisciplinary compatible solutions to the database. These additional samples allow further improvement of the accuracy of quantile copula regression. Also, this approach can prevent wastage of experimental resources by generating experiments adaptively after each cycle around the region of optimum solution.

6.2.4 Convergence Criteria

At the end of each cycle, convergence criteria of the CO-PADMA process is checked to decide if another cycle is necessary. The convergence criteria are:

Convergence of design variable This is similar to deterministic optimization techniques where current optimum design is compared with optimum design from last cycle.

$$\|\mathbf{x}_{sys}^{*(r)} - \mathbf{x}_{sys}^{*(r-1)}\| \leq \epsilon_{DV} \text{ or } \|\left(\mathbf{x}_{sys}^{*(r)} - \mathbf{x}_{sys}^{*(r-1)}\right)/\mathbf{x}_{sys}^{*(r-1)}\| \leq \epsilon_{DV_{norm}} \tag{144}$$

where $\mathbf{x}_{sys}^{*(r)}$ and $\mathbf{x}_{sys}^{*(r-1)}$ are the optimum design variables estimated by system optimizations from current and previous cycle respectively, ϵ_{DV} and $\epsilon_{DV_{norm}}$ are the tolerance limit set by designer

Convergence of cost function Like the design variable, convergence of cost function is checked by

$$\|F_{sys}^{*(r)} - F_{sys}^{*(r-1)}\| \leq \epsilon_F \text{ or } \|\left(F_{sys}^{*(r)} - F_{sys}^{*(r-1)}\right)/F_{sys}^{*(r-1)}\| \leq \epsilon_{F_{norm}} \tag{145}$$

$F_{sys}^{*(r)}$ and $F_{sys}^{*(r-1)}$ are the optimum cost functions estimated by system optimizations from current and last cycle respectively, ϵ_F and $\epsilon_{F_{norm}}$ are the tolerance limits set by designer

Convergence of distribution of system metric Although this convergence criteria is not important, it is necessary when probability distribution of system metric is a critical factor. Convergence of the distribution of system level metric can be verified by checking

$$D_{\mathrm{KL}}(f_{y_{sys}}^{*(r)} \| f_{y_{sys}}^{*(r-1)}) < \epsilon_f \tag{146}$$

where $D_{\mathrm{KL}}()$ is the K-L divergence.

Maximum number of cycles r_{max} This criteria is important when the cost function is noisy or when the optimizer starts oscillating around the optimum.

.

6.3 Numerical Procedure for CO-PADMA

The flow chart of the CO-PADMA method is given in Figure 86. The step by step numerical procedure to carry out CO-PADMA is given as

1. Start
2. Initialize the variables
   (a) Initialize the ranges of design variables, $\mathbf{x}^{L(1)}$ and $\mathbf{x}^{U(1)}$
   (b) Define baseline design $\mathbf{x}_{baseline}$ which is used as a starting point for optimization

(c) Characterize uncertainty variables $\mathbf{u}_i, \forall i = 1, \ldots, n_D$ if required

(d) Start cycle count: $r = 1$

3. Experimental design and quantile copula regression modeling

(a) If this is the first cycle ($r = 1$)

i. Generate samples of design points within the domain $\mathbf{x}^{L(1)}$ and $\mathbf{x}^{U(1)}$. The samples of design points are generated using methods like Latin hypercube designs, Response Surface Designs, D-Optimal designs, etc. [127]. The number of design point samples can be kept relatively low; however the limit on the minimum number of design points depends on the order of polynomial used in quantile copula regression. For example, for a quantile copula regression with linear models for n dimensional design variables, at least $n+1$ design points are required.

ii. For each design point, carry out UMDA using the PADMA procedure to evaluate samples of interdisciplinary compatible solutions of all the state variables $\mathbf{y}$ and the constraints $\mathbf{g}_j$ for $j = 1, \ldots, n_D$.

iii. Add the design point and respective samples of the interdisciplinary compatible state variables and the constraints to the database.

iv. Build quantile copula regression of all the state variables $\tilde{f}_{qcr_{\mathbf{y}}}(\mathbf{y}|\mathbf{x})$ and the constraints $\tilde{f}_{qcr_{\mathbf{g}_j}}(\mathbf{g}_j|\mathbf{x})$ using the samples from database.

(b) If this is not the first cycle ($r > 1$)

i. Filter and select the samples from the database which are within the reduced domain defined by $\mathbf{x}^{L(r)}$ and $\mathbf{x}^{U(r)}$

ii. Generate a new set of samples of design points within the reduced domain $\mathbf{x}^{L(r)}$ and $\mathbf{x}^{U(r)}$.

iii. For each new design point, carry out UMDA using the PADMA procedure to evaluate samples of interdisciplinary compatible solutions of

the state variables $\mathbf{y}$ and the constraints $\mathbf{g}_j$ for $j = 1, \ldots, n_D$.

iv. Add design point and respective samples of the state variables and the constraints to the database.

v. Re-build or update quantile copula regression of all the state variables $\tilde{f}_{qcr_{\mathbf{y}}}(\mathbf{y}|\mathbf{x})$ and the constraints $\tilde{f}_{qcr_{\mathbf{g}_j}}(\mathbf{g}_j|\mathbf{x})$ using the new samples and filtered samples from database.

4. System Optimization:

   (a) Using the quantile copula regression of the state variables $\tilde{f}_{qcr_{\mathbf{y}}}(\mathbf{y}|\mathbf{x})$ and the constraints $\tilde{f}_{qcr_{\mathbf{g}_j}}(\mathbf{g}_j|\mathbf{x})$, carry out system optimization as given by Equation 141.

   (b) Carry out the PADMA procedure using the high-fidelity disciplinary analyses at the optimum design of r^{th} cycle, $\mathbf{x}^{*(r)}$, to evaluate the accurate probability density of system metric $f^{*(r)}_{y_{sys}}(y_{sys})$, accurate cost function $F^{*(r)}$, and samples of interdisciplinary compatible solutions of all the state variables and the constraints.

   (c) Add the samples of accurate interdisciplinary compatible solutions of all the state variables and the constraints to the database and pass on the optimum design variables $\mathbf{x}^{*(r)}$ to subsystem optimizers.

5. Subsystem Optimization:

   (a) Using the quantile copula regression of state variables $\tilde{f}_{qcr_{\mathbf{y}}}(\mathbf{y}|\mathbf{x})$ and constraints $\tilde{f}_{qcr_{\mathbf{g}_j}}(\mathbf{g}_j|\mathbf{x})$, and $\mathbf{x}^{*(r)}$ as starting point, carry out optimization using high-fidelity disciplinary analysis as given by Equation 142 in each subsystem, concurrently and independently.

   (b) Carry out the PADMA procedure using high-fidelity disciplinary analyses at all the subsystem's optimum design of r^{th} cycle, $\mathbf{x}_i^{*(r)}, \forall i = 1, \ldots, n_D$,

to evaluate the accurate probability density of system metric $f_{y_{SS_i}}^{*(r)}(y_{SS_i})$, accurate cost function $F_i^{*(r)}$, and samples of interdisciplinary compatibles solutions of all the state variables and the constraints.

(c) Add the samples of accurate interdisciplinary compatible solutions of all the state variables and the constraints to the database

6. Check Convergence: Check the convergence criteria given in Section 6.2.4.

(a) If converged, STOP

(b) Otherwise:

i. Increment the cycle count ($r = r + 1$)

ii. Design Space Reduction: Reduce the domain of design variables using Equation 143.

iii. Repeat from Step 3.

6.4 Numerical Experiments

Purpose of experiments: To prove that the CO-PADMA method can find the optimum design and estimate the uncertainty and dependence of system metrics and state variables accurately, while allowing distributed optimization and uncertainty analysis for a multidisciplinary system for non-deterministic disciplinary analyses.

6.4.1 Benchmark and State of the Art methods

The benchmark method against which the results of CO-PADMA method is compared is a fully integrated UMDO method. In the fully integrated UMDO method, uncertainty propagation and analysis of an integrated multidisciplinary system is carried out using Simulation Outside Fixed Point Iteration (SOFPI). Treating the uncertainty analysis using SOFPI as a black box function, an optimizer is wrapped around it to carry out the UMDO process.

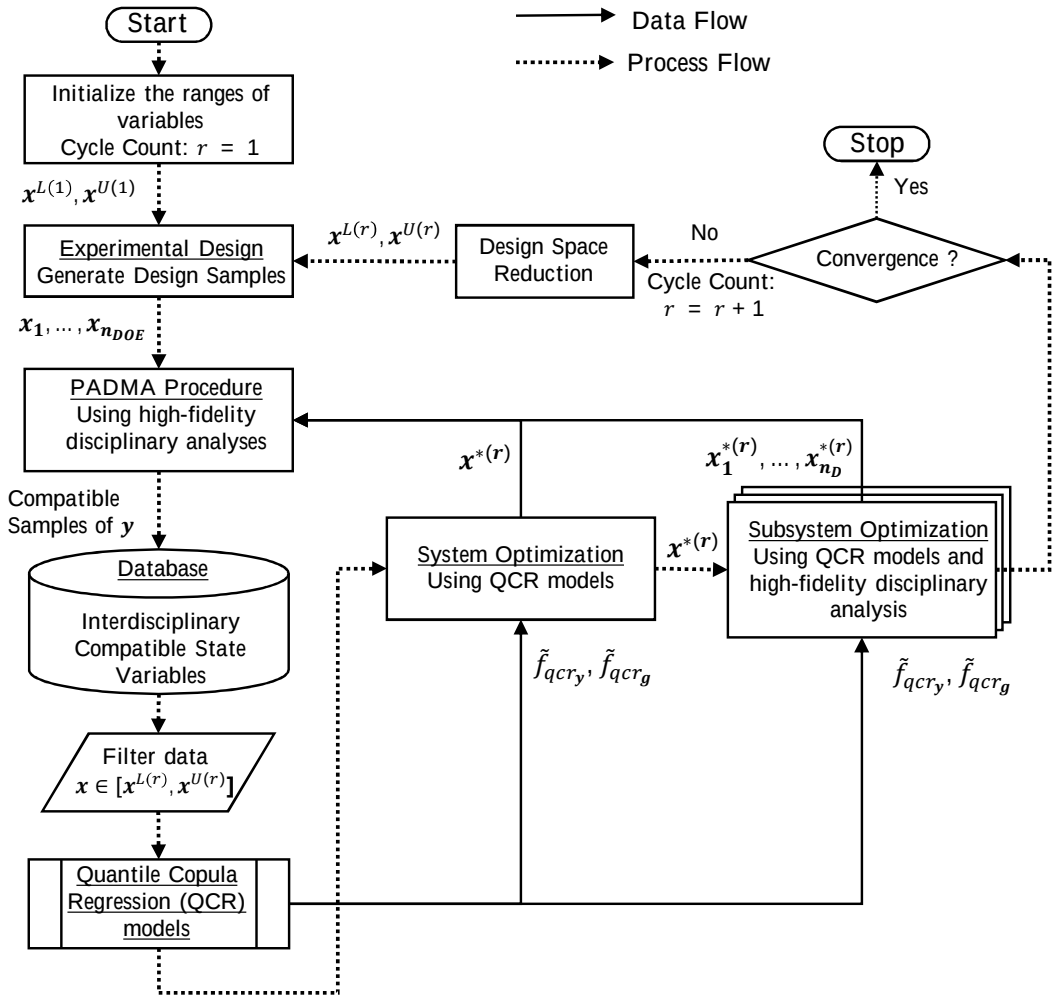

Figure 86: Process and data flow of CO-PADMA process

The results are also compared with Moment-Matching (MM), mean and standard deviation matching method. Moment-Matching methods are the current state of the art on a decomposition and coordination-based UMDO method for non-deterministic disciplinary functions, which is based on target matching strategy. There are multiple Moment-Matching-based UMDO methods in literature (ex, CO based, ATC based, etc.). The efficiency and accuracy of these methods to find the optimum design depends on the coordination strategies, the optimization algorithm and the UMDO problem itself. Therefore, it is not fair to compare these methods to problems which favor one method over another. Moreover, the motivation behind the CO-PADMA method is to overcome deficiencies with respect to accurate quantification of uncertainty and dependencies of state variables and system metric as compared to existing decomposition and coordination-based methods. The claim of the hypothesis is not that the CO-PAMDA method is more efficient than the current state of the art. Therefore, it is assumed that the current state of the art methods based on the Moment-Matching method can accurately estimate the true optimum design. Only the accuracy of uncertainty quantification of optimum system metrics and other state variables are compared between the CO-PADMA method and the Moment-Matching method, by executing Moment-Matching analysis at true optimum.

6.4.2 Experimental Metrics

To measure the accuracy of the CO-PADMA method to find the true optimum design, optimum design variable evaluated by the CO-PADMA method ($\mathbf{x}^*_{CO-PADMA}$) is compared to true optimum evaluated by the UMDO-SOFPI method ($\mathbf{x}^*_{True}$) using metric $\Delta\mathbf{x}^*_{norm} = \|\mathbf{x}^*_{CO-PADMA} - \mathbf{x}^*_{True}\|$. To measure the accuracy of the CO-PADMA method to estimate the uncertainty characteristics, the statistical mean ($\mu_{y_{sys}}$), standard deviation ($\sigma_{y_{sys}}$), and skewness ($\gamma_{y_s ys}$) of optimum system metric is compared with the UMDO-SOFPI and MM methods. To compare the overall uncertainty, KL

divergence of probability density function of system metric estimated by the CO-PADMA and MM methods are compared with UMDO-SOFPI.

To evaluate the strength of the CO-PADMA method to capture the dependence among state variables, error in Pearson's correlation (ρ) and Mutual Information (MI) among state variables are estimated as

$$\Delta\rho \textbf{ error} = \|\rho_{CO-PADMA} - \rho_{True}\| \tag{147a}$$

$$\Delta MI \textbf{ error} = \|MI_{CO-PADMA} - MI_{True}\| \tag{147b}$$

6.4.3 Test Problem Characteristics

The test problems to carry out experiments are selected such that they have following characteristics:

- The UMDO problem can be hierarchically decomposed such that disciplinary analyses can carry out independent uncertainty analysis and optimization.
- The UMDO problem should have low to mid level of coupling between disciplines, both feed-forward and feedback.
- Disciplinary analyses are of low to mid fidelity. This ensures that the optimization and uncertainty analyses are tractable to study the behavior of the method.
- Disciplinary analyses have non-linear behavior, i.e. disciplinary state variables are non-linear function of local design variables, input coupling variables and uncertainty variables.
- The uncertainty variables can be embedded into disciplinary analyses such that disciplinary functions can be executed as non-deterministic functions.
- Characteristics of disciplinary uncertainty variables can be modified such that the method can be tested for non-Gaussian variables.

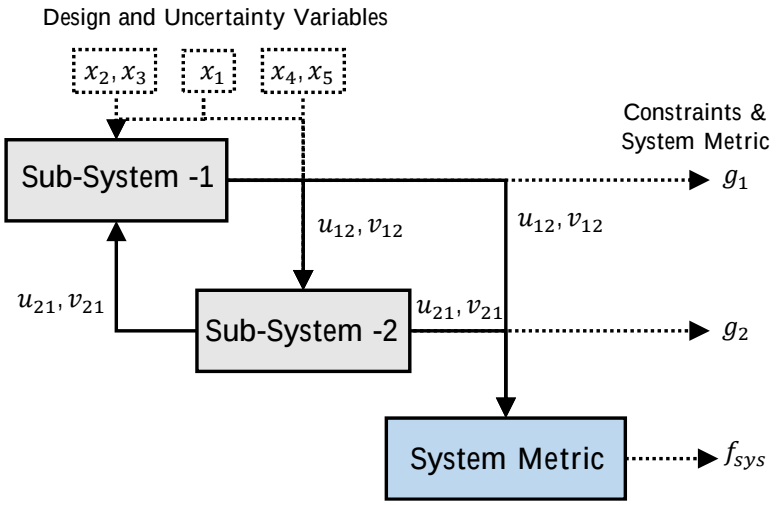

Figure 87: Notional multidisciplinary analysis example with feedback coupling

- Low to moderate number ($\sim$ 3 to 10) number of design and coupling variables, with design constraints.

Based on these characteristics two problems are selected. The first problem is an analytical problem with two coupled disciplines and a system level discipline. The second problem is a mid-fidelity Supersonic Transport (SST) aircraft design problem with three coupled disciplines and a system level discipline.

6.4.4 Analytical Problem

The analytical problem is given by Figure 87 and is similar to the analytical problem in Chapter 4. The problem consists of two coupled disciplines with four coupling variables. There are five input variables $[x_1, x_2, x_3, x_4, x_5]$. Uncertainty is associated with the input variables, while the mean of input variables are design variables. Analytical equations of each discipline are given as

$$\text{System} \quad f = u_{12}v_{12} - u_{21}v_{21} \tag{148}$$

$$\begin{aligned} \text{Subsystem-1} \quad u_{12} &= x_1^2 + 2x_2 - x_3 + 2\sqrt{u_{21}} - 0.22v_{21} \\ v_{12} &= 2x_1 + x_2x_3 - 0.31\sqrt{u_{21}} + 0.2v_{21} \\ g_1 &= u_{12}v_{12} \end{aligned} \tag{149}$$

$$\begin{aligned} \text{Subsystem-2} \quad u_{21} &= x_1x_4 + x_4^2 + x_5 + u_{12} + 0.1\sqrt{v_{12}} \\ v_{21} &= x_1x_5 + x_1x_4 + x_1 + 0.15u_{12} - 0.3v_{12} \\ g_2 &= u_{21}v_{21} \end{aligned} \tag{150}$$

The optimization problem is given as

$$\begin{aligned} \text{minimize} \quad & \mu_f && \text{(151a)} \\ \text{with respect to} \quad & \mu_{\mathbf{x}} = [\mu_{x_1}, \mu_{x_2}, \mu_{x_3}, \mu_{x_4}, \mu_{x_5}] \\ \text{such that} \quad & \mathrm{P}[g_1 \leq 24.6] \geq 0.9 && \text{(151b)} \\ & \mathrm{P}[g_2 \leq 48.2] \geq 0.9 && \text{(151c)} \\ & 0.8 \leq \mu_{x_i} \leq 1.2 \qquad \forall i = 1, \ldots, 5 && \text{(151d)} \end{aligned}$$

where μ_f is the mean of system metric f and μ_{x_i} is the mean of system metric x_i. To decouple design variables from uncertain variables, input variables are modeled as $x_i = \mu_{x_i} + \epsilon_i$, where μ_{x_i} are the design variables and ϵ_i are the uncertain variables.

For the CO-PADMA process, the disciplinary analyses are modeled such that the uncertainties associated with the variables x_2, x_3, x_4 and x_5 (except shared variable

x_1) are embedded in discipline. Subsystem-1 is re-modeled as

$$u_{12} = \mu_{x_1}^2 + 2(\mu_{x_2} + \epsilon_2) - (\mu_{x_3} + \epsilon_3) + 2\sqrt{u_{21}} - 0.22v_{21} \tag{152a}$$

$$v_{12} = 2\mu_{x_1} + (\mu_{x_2} + \epsilon_2)(\mu_{x_3} + \epsilon_3) - 0.31\sqrt{u_{21}} + 0.2v_{21} \tag{152b}$$

$$g_1 = u_{12}v_{12} \tag{152c}$$

where ϵ_2 and ϵ_3 are the uncertainties associated with x_2 and x_3 respectively. This makes the subsystem-1 a non-deterministic function of design variables, i.e. for a given value of $[\mu_{x_1}, \mu_{x_2}, \mu_{x_3}, u_{21}, v_{21}]$ subsystem will generate a random value of u_{12}, v_{12} and g_1. Similarly, subsystem-2 is re-modeled as

$$u_{21} = \mu_{x_1}(\mu_{x_4} + \epsilon_4) + (\mu_{x_4} + \epsilon_4)^2 + (\mu_{x_5} + \epsilon_5) + u_{12} + 0.1\sqrt{v_{12}} \tag{153a}$$

$$v_{21} = \mu_{x_1}(\mu_{x_5} + \epsilon_5) + \mu_{x_1}(\mu_{x_4} + \epsilon_4) + \mu_{x_1} + 0.15u_{12} - 0.3v_{12} \tag{153b}$$

$$g_2 = u_{21}v_{21} \tag{153c}$$

where ϵ_4 and ϵ_5 are the uncertainties associated with x_4 and x_5, respectively. The uncertainty of the design variable x_1 is not embedded in the subsystems because it is a shared uncertain variable and will influence the dependence of the coupling variables from both disciplines.

Two case studies are carried out with the analytical problem by changing the characteristics of uncertain variables.

Case-1: In the first case, the uncertain variables are characterized with a Gaussian distribution with zero mean $\mu_i = 0.0$ and standard deviation of $\sigma_i = 0.1$.

$$\epsilon_i \sim \mathcal{N}(0.0, 0.1^2) \qquad \forall i = 1, \ldots, 5 \tag{154}$$

Case-2: In the second case, ϵ_1 is characterized with a Gaussian distribution with zero mean $\mu_1 = 0.0$ and standard deviation of $\sigma_1 = 0.1$, while x_2, x_3, x_4, x_5 are characterized with a Gamma distribution with shape parameter $k = 1$ and scale

parameter $\theta = 0.1$.

$$\epsilon_1 \sim \mathcal{N}(0.0, 0.1^2) \tag{155a}$$

$$\epsilon_i \sim \Gamma(1.0, 0.1) \qquad \forall i = 2, \ldots, 5 \tag{155b}$$

6.4.4.1 CO-PADMA Procedure

The step by step numerical procedure of the CO-PADMA method for solving analytical problem is given as follows.

1. Start
2. Initialize the variables
   (a) Ranges of design variables are initialized: $\mu_{x_i}^{L(1)} = 0.8$ and $\mu_{x_i}^{U(1)} = 1.2$ $\forall i = 1, \ldots, 5$.
   (b) Baseline design is defined as $\mu_{x_{ibaseline}} = 0,\ \forall i = 1, \ldots, 5$, which is used as starting point for optimization.
   (c) Uncertainty variables $\epsilon_i, \forall i = 1, \ldots, 5$ are characterized as mentioned in the previous section.
   (d) Cycle counter is set to $r = 1$.
3. Experimental design and quantile copula regression modeling
   (a) For the first cycle ($r = 1$)
      i. 50 samples of design points $[\mu_{x_1}, \mu_{x_2}, \mu_{x_3}, \mu_{x_4}, \mu_{x_5}]$ are generated within the domain defined in Step 2(a) using Latin hypercube design.
      ii. For each design point, UMDA using the PADMA procedure is carried out to evaluate 300 samples of interdisciplinary compatible solutions of $\mathbf{y} = [u_{12}, v_{12}, u_{21}, v_{21}]$.
      iii. Design points and respective samples of state variables are added to the database.

iv. Using the samples from the database, quantile copula regression of all the state variables, $\tilde{f}_{qcr_{\mathbf{y}}}(\mathbf{y}|\mu_{x_1}, \mu_{x_2}, \mu_{x_3}, \mu_{x_4}, \mu_{x_5})$, is built.

(b) For cycle ($r > 1$)

i. Samples are filtered and selected from the database which are within the reduced domain defined by Step 6(b).

ii. n_{new} set of new samples of design points are generated within the reduced domain, where $n_{new} = n_{filter} - 50$ and n_{filter} is the number of unique design points in the database which are within the reduced domain. This allows the maintaining of at least 50 unique design points to model quantile copula regression.

iii. For each new design point, UMDA using the PADMA procedure is carried out to evaluate samples of interdisciplinary compatible solutions of disciplinary state variables $\mathbf{y} = [u_{12}, v_{12}, u_{21}, v_{21}]$.

iv. Design points and their respective samples of state variables are added to the database.

v. Using new and filtered samples from the database, quantile copula regression of all the state variables, $\tilde{f}_{qcr_{\mathbf{y}}}(\mathbf{y}|\mu_{x_1}, \mu_{x_2}, \mu_{x_3}, \mu_{x_4}, \mu_{x_5})$, is built.

4. System Optimization:

(a) Using the quantile copula regression of state variables system optimization

is carried out as:

$$\begin{aligned}
\text{Given} \quad & \tilde{f}_{qcr_{\mathbf{y}}}(\mathbf{y}|\mu_{x_1}, \mu_{x_2}, \mu_{x_3}, \mu_{x_4}, \mu_{x_5}) && \text{(156a)}\\
& \text{where } \tilde{\mathbf{y}} \equiv [\tilde{u}_{12}, \tilde{v}_{12}, \tilde{u}_{21}, \tilde{v}_{21}] \\
& \tilde{f} = f_{sys}(\tilde{u}_{12}, \tilde{v}_{12}, \tilde{u}_{21}, \tilde{v}_{21}) && \text{(156b)}\\
& \tilde{g}_1 = g_1(\tilde{u}_{12}, \tilde{v}_{12}) && \text{(156c)}\\
& \tilde{g}_2 = g_2(\tilde{u}_{21}, \tilde{v}_{21}) && \text{(156d)}\\
\text{minimize} \quad & \tilde{F} = \mu_{\tilde{f}} && \text{(156e)}\\
\text{with respect to} \quad & \mu_{x_1}, \mu_{x_2}, \mu_{x_3}, \mu_{x_4}, \mu_{x_5} \\
\text{such that} \quad & \mathrm{P}[\tilde{g}_1 \leq 24.6] \geq 0.9 && \text{(156f)}\\
& \mathrm{P}[\tilde{g}_2 \leq 48.2] \geq 0.9 && \text{(156g)}\\
& \mu_{x_i}^{L(r)} \leq \mu_{x_i} \leq \mu_{x_i}^{U(r)} \qquad \forall i = 1, \ldots, 5 && \text{(156h)}\\
\text{Output} \quad & \mu_{\mathbf{x}}^{*(r)}, \tilde{f}_f^{*(r)}(f), \tilde{F}^{*(r)}
\end{aligned}$$

where uncertainty on state variables $\tilde{\mathbf{y}}$ are estimated through quantile copula regression $\tilde{f}_{qcr_{\mathbf{y}}}(\mathbf{y}|\mu_{x_1}, \mu_{x_2}, \mu_{x_3}, \mu_{x_4}, \mu_{x_5})$ and are used to evaluate the uncertainty on system metric f.

(b) The PADMA procedure is carried out using high-fidelity disciplinary analyses at the optimum design of r^{th} cycle, $\mu_{\mathbf{x}}^{*(r)}$, to evaluate the accurate probability density of system metric $f_f^{*(r)}(f)$, accurate cost function $F^{*(r)}$. Also 300 samples of interdisciplinary compatible solutions of all the state variables are generated at the system optimum design and added to the database.

5. Subsystem Optimization:

(a) Subsystem optimization is carried out using high-fidelity disciplinary analysis, while uncertainty on non-local state variables are approximated using

quantile copula regression. The subsystem-1 optimization problem is given as:

Subsystem-1 Optimization

$$\begin{aligned}
\text{Given} \quad & \tilde{f}_{qcr_{\mathbf{y}}}(\mathbf{y}|\mu_{x_1}, \mu_{x_2}, \mu_{x_3}, \mu_{x_4}, \mu_{x_5}) && \text{(157a)}\\
& \text{where } \tilde{\mathbf{y}}_{21} \equiv [\tilde{u}_{21}, \tilde{v}_{21}] \\
& \mathbf{y}_1 = SS_1(\mu_{x_1}, \mu_{x_2}, \mu_{x_3}, \tilde{u}_{21}, \tilde{v}_{21}) && \text{(157b)}\\
& \text{where } \mathbf{y}_1 \equiv [u_{12}, v_{12}, g_1] \\
& \tilde{g}_2 = g_2(\tilde{u}_{21}, \tilde{v}_{21}) && \text{(157c)}\\
& \tilde{f} = f_{sys}(u_{12}, v_{12}, \tilde{u}_{21}, \tilde{v}_{21}) && \text{(157d)}\\
\text{minimize} \quad & \tilde{F} = \mu_{\tilde{f}} && \text{(157e)}\\
\text{with respect to} \quad & \mu_{x_1}, \mu_{x_2}, \mu_{x_3}, \mu_{x_4}, \mu_{x_5} \\
\text{such that} \quad & \mathrm{P}[g_1 \leq 24.6] \geq 0.9 && \text{(157f)}\\
& \mathrm{P}[\tilde{g}_2 \leq 48.2] \geq 0.9 && \text{(157g)}\\
& \mu_{x_i}^{L(r)} \leq \mu_{x_i} \leq \mu_{x_i}^{U(r)} \qquad \forall i = 1, \ldots, 5 && \text{(157h)}\\
\text{Output} \quad & \mu_{\mathbf{x}}^{*(r)}|_{SS1}, \tilde{f}_f^{*(r)}(f)|_{SS1}, \tilde{F}^{*(r)}|_{SS1}
\end{aligned}$$

where the uncertainty of non-local state variables $\tilde{u}_{21}$ and $\tilde{v}_{21}$ is approximately estimated through quantile copula regression. The uncertainty on local state variables is estimated using high-fidelity subsystem function $\mathbf{y}_1 = SS_1(\mu_{x_1}, \mu_{x_2}, \mu_{x_3}, \tilde{u}_{21}, \tilde{v}_{21})$. Also, the local constraint g_1 is evaluated using high-fidelity data while the non-local constraint $\tilde{g}_2$ is evaluated quantile copula regression. Once the optimization is over, the PADMA procedure using the high-fidelity analyses of all subsystems is carried out for $\mu_{\mathbf{x}}^{*(r)}|_{SS1}$, to evaluate the accurate probability density of system metric $f_f^{*(r)}(f)|_{SS1}$, and accurate cost function $F^{*(r)}|_{SS1}$. Also, 300 samples of interdisciplinary compatible solutions of all state variables are generated

at the subsystem optimum design and added to the database.

Similarly, subsystem-2 optimization problem is given as:

Subsystem-2 Optimization

$$\text{Given} \quad \tilde{f}_{qcr_{\mathbf{y}}}(\mathbf{y}|\mu_{x_1}, \mu_{x_2}, \mu_{x_3}, \mu_{x_4}, \mu_{x_5}) \tag{158a}$$

$$\text{where } \tilde{\mathbf{y}}_{12} \equiv [\tilde{u}_{12}, \tilde{v}_{12}]$$

$$\mathbf{y}_2 = SS_2(\mu_{x_1}, \mu_{x_4}, \mu_{x_5}, \tilde{u}_{12}, \tilde{v}_{12}) \tag{158b}$$

$$\text{where } \mathbf{y}_2 \equiv [u_{21}, v_{21}, g_2]$$

$$\tilde{g}_1 = g_1(\tilde{u}_{12}, \tilde{v}_{12}) \tag{158c}$$

$$\tilde{f} = f_{sys}(\tilde{u}_{12}, \tilde{v}_{12}, u_{21}, v_{21}) \tag{158d}$$

$$\text{minimize} \quad \tilde{F} = \mu_{\tilde{f}} \tag{158e}$$

$$\text{with respect to} \quad \mu_{x_1}, \mu_{x_2}, \mu_{x_3}, \mu_{x_4}, \mu_{x_5}$$

$$\text{such that} \quad \mathrm{P}[\tilde{g}_1 \leq 24.6] \geq 0.9 \tag{158f}$$

$$\mathrm{P}[g_2 \leq 48.2] \geq 0.9 \tag{158g}$$

$$\mu_{x_i}^{L(r)} \leq \mu_{x_i} \leq \mu_{x_i}^{U(r)} \qquad \forall i = 1, \ldots, 5 \tag{158h}$$

$$\text{Output} \quad \mu_{\mathbf{x}}^{*(r)}|_{SS2}, \tilde{f}_f^{*(r)}(f)|_{SS2}, \tilde{F}^{*(r)}|_{SS2}$$

where the uncertainty of non-local state variables $\tilde{u}_{12}$ and $\tilde{v}_{12}$ is approximately estimated through quantile copula regression. The uncertainty on local state variables is estimated using high-fidelity subsystem function $\mathbf{y}_2 = SS_2(\mu_{x_1}, \mu_{x_4}, \mu_{x_5}, \tilde{u}_{12}, \tilde{v}_{12})$. Once the optimization is over, the PADMA procedure using the high-fidelity analyses of all subsystems is carried out at $\mu_{\mathbf{x}}^{*(r)}|_{SS2}$, to evaluate the accurate probability density of system metric $f_f^{*(r)}(f)|_{SS2}$, and accurate cost function $F^{*(r)}|_{SS2}$. Also, 300 samples of interdisciplinary compatible solutions of all state variables are generated at the subsystem optimum design and added to the database.

6. Check Convergence: Check the convergence criteria given in Section 6.2.4.

(a) If converged, STOP

(b) Otherwise:

i. Increment the cycle count ($r = r + 1$)

ii. Design Space Reduction: The domain of design variables is reduced by factor of $R_f = 20\%$ using approach given in Equation 143.

iii. Repeat from Step 3.

For all the optimization processes, Covariance Matrix Adaptation Evolution Strategy (CMAES) [215] has been used for optimization, which is an Evolution Strategy (ES)-based stochastic, derivative-free method for non-linear, non-convex and noisy problem. The scripts of the disciplinary functions have been written in MATLAB. Also, to automate the CO-PADMA process, scripts for CO-PADMA method have been written and executed in MATLAB.

6.4.4.2 Results: Analytical Problem Case-1

In case-1 of the analytical problem, all the uncertain variables are assumed to have Gaussian distribution. The problem is solved using the CO-PADMA method and compared with true optimum which is evaluated using the benchmark UMDO-SOFPI method. Moment matching (MM) method is also used to carry out analysis at true optimum to study the improvement in accuracy with current state of the art for the distributed UMDO method.

The CO-PADMA procedure is carried out using the methodology discussed in the previous section and the optimum has been achieved within 12 cycles. The optimum design variables estimated by the CO-PADMA procedure are compared with the UMDO-SOFPI method in Table 20. The CO-PADMA procedure has been able to find the optimum design with reasonable accuracy, with the worst case being that of $\Delta x*_{error} = 5\%$ for μ_{x_5}.

Table 20: Comparison of optimum design for analytical problem case-1

	$\mu^*_{x_1}$	$\mu^*_{x_2}$	$\mu^*_{x_3}$	$\mu^*_{x_4}$	$\mu^*_{x_5}$
UMDO-SOFPI	0.89	0.79	0.79	1.20	1.20
CO-PADMA	0.91	0.82	0.80	1.16	1.14
$\Delta \mathbf{x}^*_{norm}$	0.03	0.03	0.01	0.03	0.05

Table 21: Comparison of statistical metrics of objective function for analytical problem case-1

	UMDO-SOFPI	**MM**	**CO-PADMA**
Mean(μ_f)	-24.70	-24.84	-24.82
Std. Dev.(σ_f)	3.83	4.68	3.44
Skewness (γ_f)	-0.35	-0.19	-0.29
K-L div.	-	0.06	0.03

The probability density function and cumulative distribution function of system metric at optimum design evaluated by the CO-PADMA method is compared with the integrated UMDO-SOFPI method and MM method estimated at true optimum in Figure 88. It is observed that the system metric has similar characteristics as a Gaussian distribution. As seen from the cumulative distribution plot, both MM and CO-PADMA methods were able to estimate the similar trend as compared to the UMDO-SOFPI solution. The statistical metric of f is compared in Table 21. The statistical mean of f evaluated by the MM and CO-PADMA methods is very close to the benchmark method. However, the MM method over predicted the standard deviation by 22% while the CO-PADMA method under-predicted by 10%. The true skewness of the distribution has been found to be $\gamma = -0.35$. The CO-PADMA method has been able to find a better estimate of skewness ($\gamma = -0.29$) when compared to the MM method ($\gamma = -0.19$). In terms of closeness to the true distribution, measured using K-L divergence, the CO-PADMA method has been found to be closer (K-L div. = 0.03) when compared to MM method (K-L div. = 0.06).

Figure 89 shows the optimum design estimated by the system and subsystem optimizer at the end of each cycle. As observed, all the optimizers converged to

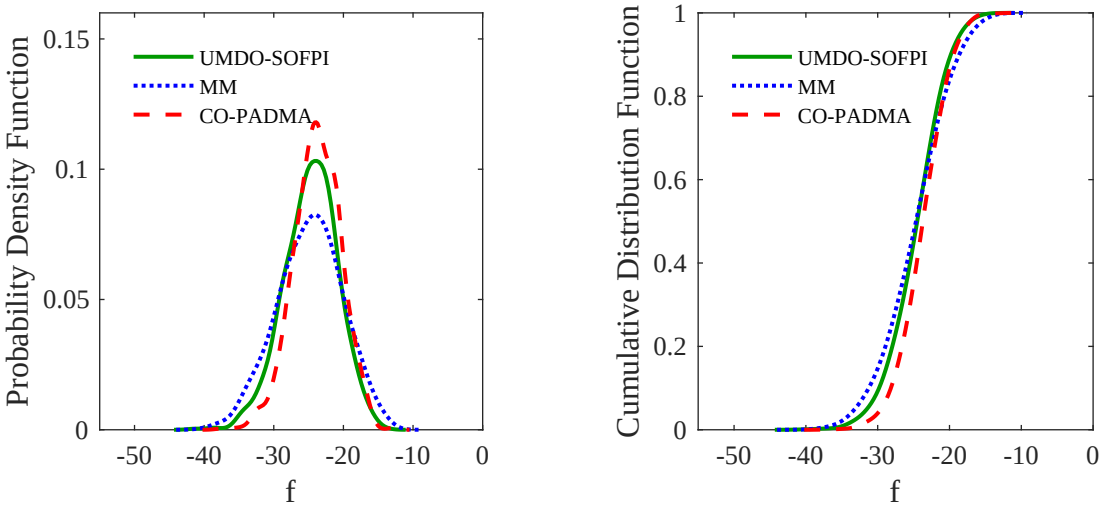

(a) Probability density function

(b) Cumulative distribution function

Figure 88: Comparison of probability density function and cumulative distribution function of system metric f at optimum design estimated using benchmark UMDO-SOFPI method, Moment Matching method (MM) and CO-PADMA method for analytical problem case-1

the same optimum solution for all the design variables at the end of the 12^{th} cycle. Figure 89 also shows design space used to carry out optimization in each cycle. The rate of reduction of design space has been found to be different for each design variable. The design space reduction strategy ensures that the design space at any given cycle will encompass all the optimum solutions achieved by the system optimizer in all the previous cycles. Therefore, the rate and the limit of design space reduction depends upon inconsistencies and variation of the optimum solution achieved by the system optimizer in the initial cycles. For example, system and subsystem optimizers have been found to be inconsistent in finding the optimum value of design variable μ_{x_2} in the first four cycles. The inconsistency is due to the inaccuracy of initial quantile copula regression with respect to μ_{x_2}. The inconsistency of the optimizers forced the design space reduction strategy to not reduce the design space beyond a certain limit and keep the design space open so that the optimizers can find a consistent solution with the improvement of quantile copula regression in the later cycle. On the other

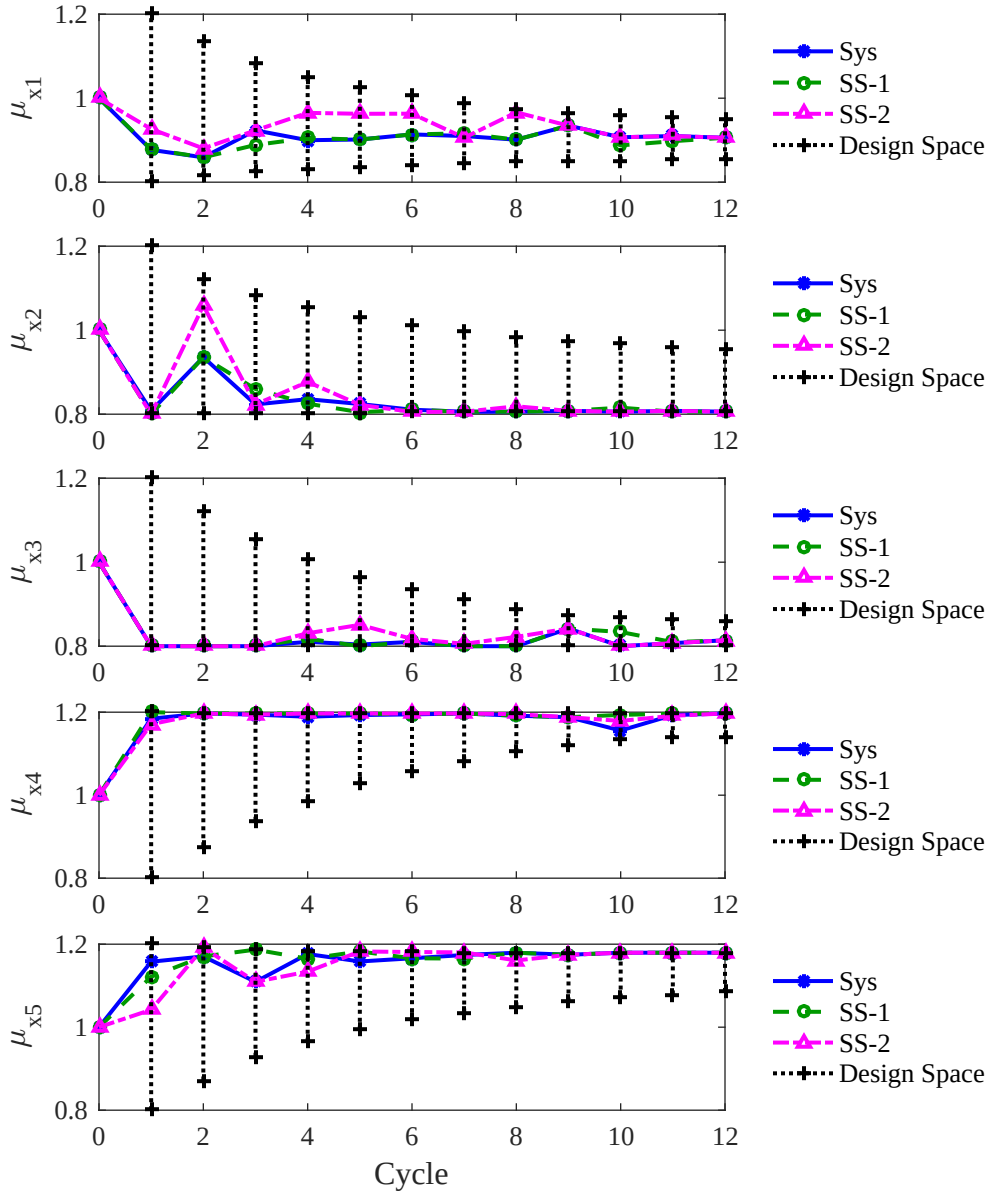

Figure 89: Optimum design estimated by system and subsystem optimizers and design space reduction at the end of each cycle analytical problem case-1

hand, the consistency of the optimizer to find the optimum design for μ_{x_3} and μ_{x_4} allows the design space reduction techniques to reduce the design space to less than 20% of initial range after 12 cycles.

In addition to the design space reduction technique, additional design points in the reduced design space and samples of interdisciplinary compatible solutions are added to the database at the end of each cycle. The histogram of design points at the end of the $1^{st}, 6^{th}$ and 12^{th} cycle is shown in Figure 90. It is observed that with each cycle, the new design point gets concentrated near the expected minimum which further allows improvement in the accuracy of quantile copula regression. The improvement in accuracy of a quantile copula regression is shown in Figure 91. The figure shows the uncertainty quantification, represented by probability density function (PDF), of optimum system metric f using quantile copula regression at the end of $1^{st}, 6^{th}$ and 12^{th} cycle and is compared with true uncertainty evaluated using integrated SOFPI analysis. As observed and expected, the accuracy of uncertainty quantification using quantile regression improves with each cycle.

To compare the dependency of the coupling variables, scatter plot matrix of coupling variables at the optimum design is compared between UMDO-SOFPI, MM and CO-PADMA in Figure 92. In addition to scatter plot of interdisciplinary compatible samples from each method, each subplot also shows a single iso-probability contour of value $0.02\mathrm{P}_{max}$, where P_{max} is the maximum probability value attained by the true solution using the UMDO-SOFPI method. As observed, all the coupling variables are positively dependent with respect to each other, which is well predicted by the CO-PADMA method. On the other hand, the MM method assumed the coupling variables are independent and does not capture the dependencies. Figure 93 compares the contour plot of joint probability density of optimum interdisciplinary compatible solution of u_{12} and u_{21} estimated by all the UMDO-SOFPI, MM and CO-PAMDA methods. In addition to the strong dependency, the CO-PADMA method has been

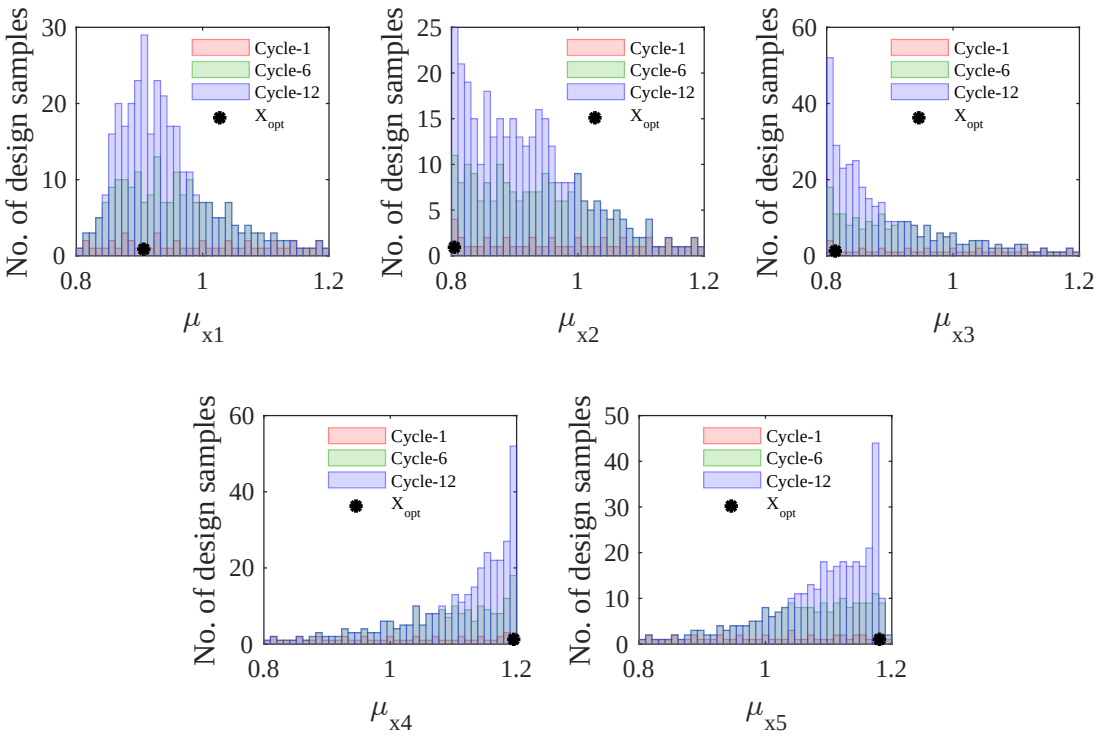

Figure 90: Histogram of design points at end of $1^{st}, 6^{th}$ and 12^{th} cycle for analytical problem case-1

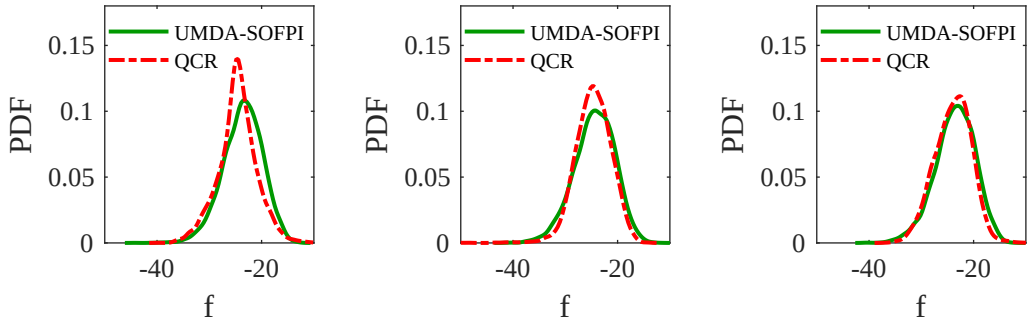

(a) Cycle-1 (b) Cycle-6 (c) Cycle-12

Figure 91: Improvement in accuracy of quantile copula regression (QCR) with each cycle for analytical problem case-1

Table 22: Comparison of Correlation Matrix of coupling variables of analytical problem case-1

	Correlation Matrix				
		u_{12}	v_{12}	u_{21}	v_{21}
UMDO-SOFPI	u_{12}	1.00	0.61	0.85	0.68
	v_{12}	0.61	1.00	0.56	0.81
	u_{21}	0.85	0.56	1.00	0.79
	v_{21}	0.68	0.81	0.79	1.00
		u_{12}	v_{12}	u_{21}	v_{21}
CO-PADMA	u_{12}	1.00	0.60	0.88	0.66
	v_{12}	0.60	1.00	0.57	0.82
	u_{21}	0.88	0.57	1.00	0.77
	v_{21}	0.66	0.82	0.77	1.00
		u_{12}	v_{12}	u_{21}	v_{21}
$\Delta\rho$ **error**	u_{12}	0.00	0.02	0.02	0.02
	v_{12}	0.02	0.00	0.01	0.02
	u_{21}	0.02	0.01	0.00	0.03
	v_{21}	0.02	0.02	0.03	0.00

able to capture the overall trend of joint probability density better than the MM method.

The dependencies of coupling variables are quantified using Pearson's correlation matrix and compared between the UMDO-SOFPI and CO-PADMA methods in Table 22. All correlations estimated by the CO-PADMA process have been found to be within 3% of true correlation estimated by the UMDO-SOFPI method. To quantify the non-linear dependency, Mutual Information (MI) among coupling variables are estimated and compared between the UMDO-SOFPI and CO-PADMA methods in Table 23. The CO-PADMA method has also been able to accurately estimate any underlying non-linear dependencies with maximum ΔMI of 0.04.

To study the convergence characteristics of the CO-PADMA method, convergence of the optimum objective function with respect to disciplinary uncertainty quantification and propagation (UQP) function calls are plotted and compared in Figure 94. It must be noted that the number for actual disciplinary function calls for each UQP function call can vary depending upon method used for uncertainty propagation and

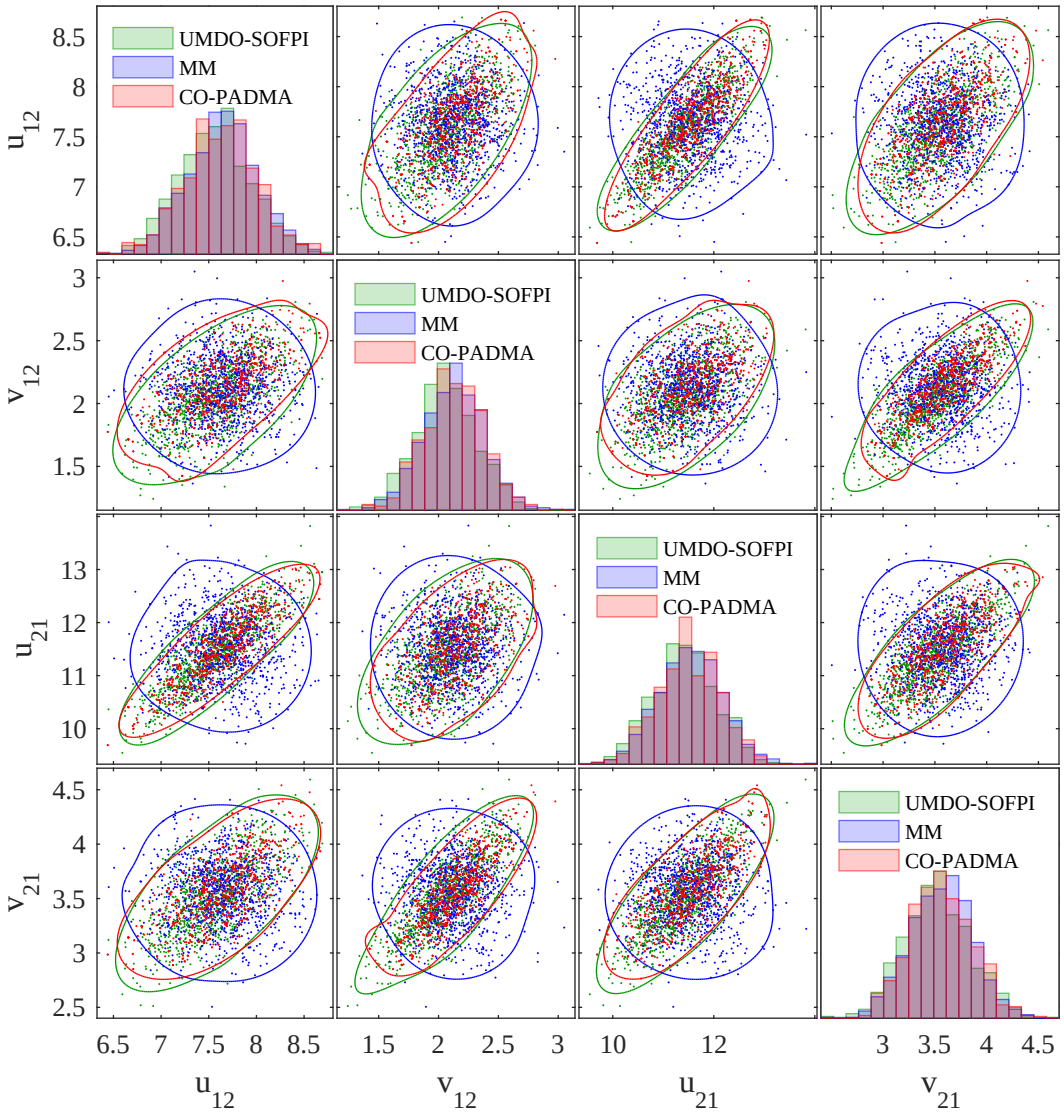

Figure 92: Scatter plot matrix of coupling variables at optimum design of analytical problem case-1

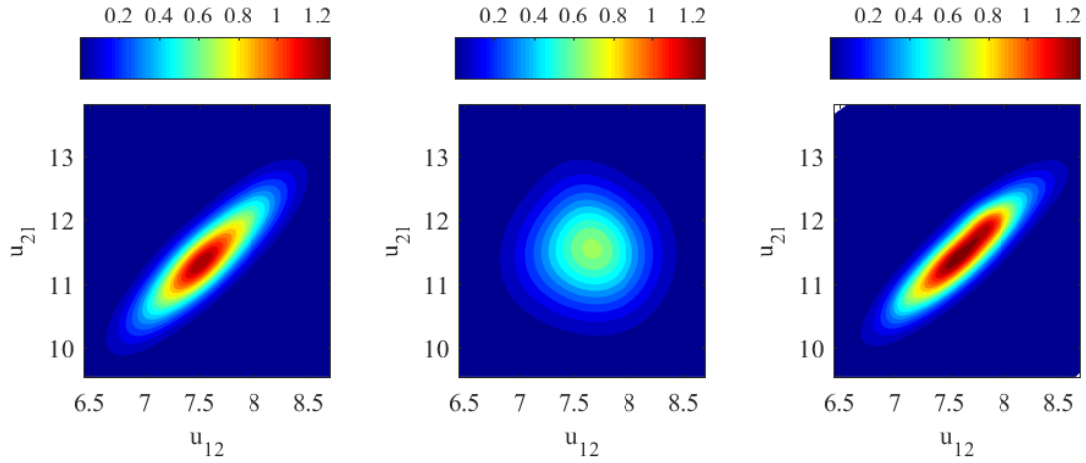

(a) UMDO-SOFPI (b) MM (c) CO-PADMA

Figure 93: Contour plot of joint probability density of optimum interdisciplinary compatible solution of u_{12} and u_{21} for analytical problem case-1

Table 23: Comparison of Mutual Information (MI) matrix of coupling variables of analytical problem case-1

Mutual Information Matrix

		u_{12}	v_{12}	u_{21}	v_{21}
UMDO-SOFPI	u_{12}	1.28	0.25	0.61	0.31
	v_{12}	0.25	1.37	0.19	0.51
	u_{21}	0.61	0.19	1.29	0.47
	v_{21}	0.31	0.51	0.47	1.29
		u_{12}	v_{12}	u_{21}	v_{21}
CO-PADMA	u_{12}	1.35	0.27	0.68	0.32
	v_{12}	0.27	1.30	0.23	0.55
	u_{21}	0.68	0.23	1.29	0.43
	v_{21}	0.32	0.55	0.43	1.27
		u_{12}	v_{12}	u_{21}	v_{21}
ΔMI error	u_{12}	0.07	0.02	0.07	0.01
	v_{12}	0.02	0.06	0.03	0.04
	u_{21}	0.07	0.03	0.00	0.04
	v_{21}	0.01	0.04	0.04	0.02

accuracy required. In the current case, Monte Carlo simulations with $10,000$ disciplinary function calls has been used for each UQP call for both the UMDO-SOFPI and CO-PADMA methods. One can use any other efficient methods to carry out uncertainty propagation in each discipline which requires far less disciplinary function calls. Therefore, to separate out the effect of disciplinary UQP method used, the convergence history is plotted against UQP function calls rather than disciplinary function calls.

As observed in Figure 94, both the UMDO-SOFPI and CO-PADMA methods have the similar trend of convergence history. Both methods have been able to reach the optimum solution with around $2,000$ UQP function calls (end of cycle 5 for CO-PADMA method). However, the convergence history with respect to UQP calls does not depict the actual benefit of the CO-PADMA process. The main advantage of the CO-PADMA process is the concurrent uncertainty quantification and design optimization of each disciplines. This allows the CO-PADMA process to carry out parallel UQP in each discipline. Assuming that each disciplinary UQP call takes an average time of t_{avg}, the convergence history of the optimum objective function is plotted against time in Figure 95. As depicted in the figure, CO-PADMA process reaches the optimum solution in around half the time (Cycle 5, with $2,000$ UQP calls) as compared to the UMDO-SOFPI method. This is due to the fact that there are two disciplines in the problem which can be run in parallel for UQP analysis in the CO-PADMA process.

6.4.4.3 Results: Analytical Problem Case-2

In case-2 of the analytical problem, all the uncertain variables, except x_1, are assumed to have a gamma distribution. As in case-1, a study has been carried out with the CO-PADMA method and compared it with the UMDO-SOFPI and MM methods. Due to non-Gaussian uncertain variables, case-2 took longer to converge both with

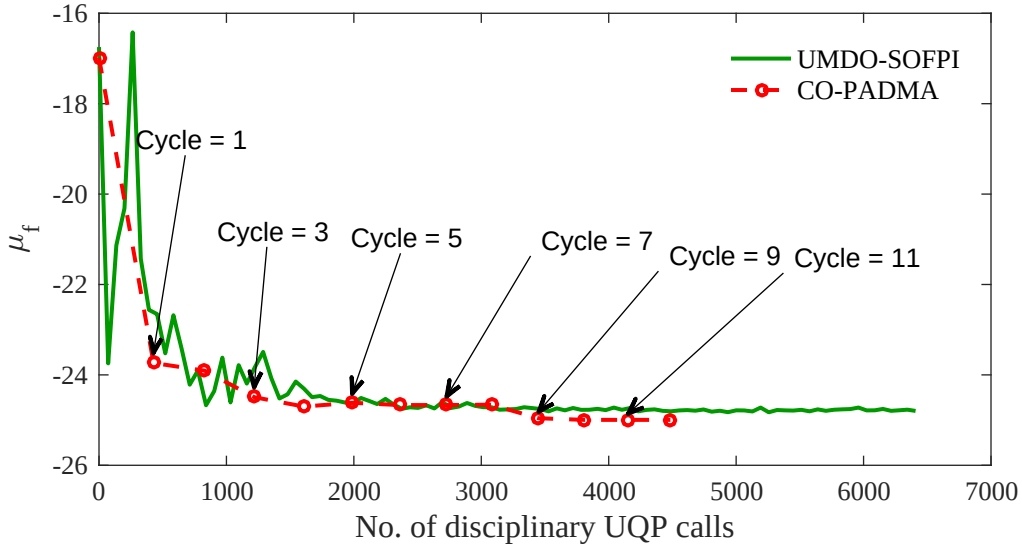

Figure 94: Comparison of convergence characteristics of optimum objective function with respect to disciplinary uncertainty quantification and propagation function calls for analytical problem case-1

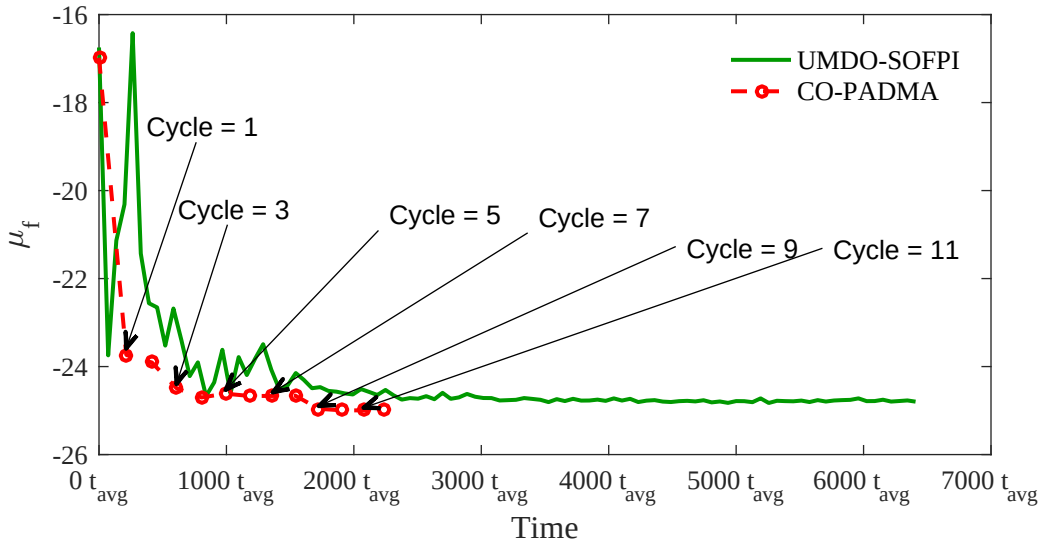

Figure 95: Comparison of convergence characteristics of optimum objective function with respect to time for analytical problem case-1, where t_{avg} is the average time for each disciplinary UQP call

Table 24: Comparison of optimum design for analytical problem case-1

	$\mu^*_{x_1}$	$\mu^*_{x_2}$	$\mu^*_{x_3}$	$\mu^*_{x_4}$	$\mu^*_{x_5}$
UMDO-SOFPI	0.84	0.82	0.80	1.20	1.02
CO-PADMA	0.84	0.84	0.88	1.18	1.03
$\Delta\mathbf{x}^*_{norm}$	0.01	0.02	0.10	0.02	0.01

the CO-PADMA and UMDO-SOFPI methods. The CO-PADMA procedure took 15 cycles ($5,000$ UQP calls) while UMDO-SOFPI took $7,000$ UQP calls to converge. The optimum design variables estimated by the CO-PADMA procedure is compared with the benchmark UMDO-SOFPI method in Table 24. Other than μ_{x_3} (with $\Delta x*_{error} = 10\%$) the CO-PADMA procedure has been able to find the optimum design with reasonable accuracy (within $\Delta x*_{error} = 2\%$) for all the design variables.

The probability density function and cumulative distribution function of system metric f at optimum design evaluated by the CO-PADMA method is compared with the integrated UMDO-SOFPI and MM methods in Figure 96. Unlike case-1, the probability density function of f has been found to be non-symmetrical and skewed towards the lower end. The skewness has been found to be well captured by the CO-PADMA process; however the MM method assuming Gaussian distribution has not been able to capture it. The statistical metric of f is compared in Table 25. The statistical mean of f evaluated by the MM and CO-PADMA methods has been found to be reasonably accurate with the true solution. However, similar to case-1 the MM method over predicted the standard deviation by 29%. The CO-PADMA method has been found to be accurate (less than 5% error), while considering the numerical noises associated with the statistical estimation of standard deviation. The CO-PADMA method has also been able to accurately estimate the skewness ($\gamma = -0.75$) when compared to true skewness estimated by the UMOD-SOFPI method ($\gamma = -0.71$). In terms of closeness to the true distribution measured using K-L divergence, the CO-PADMA method has been found to be very close (K-L div. $= 0.03$) to the true solution when compared to the MM method (K-L div. $= 0.13$).

Table 25: Comparison of statistical metrics of objective function for analytical problem case-1

	UMDO-SOFPI	**MM**	**CO-PADMA**
Mean(μ_f)	-23.78	-23.01	-23.31
Std. Dev.(σ_f)	3.77	4.87	3.94
Skewness (γ_f)	-0.71	-0.03	-0.75
K-L div.	-	0.13	0.03

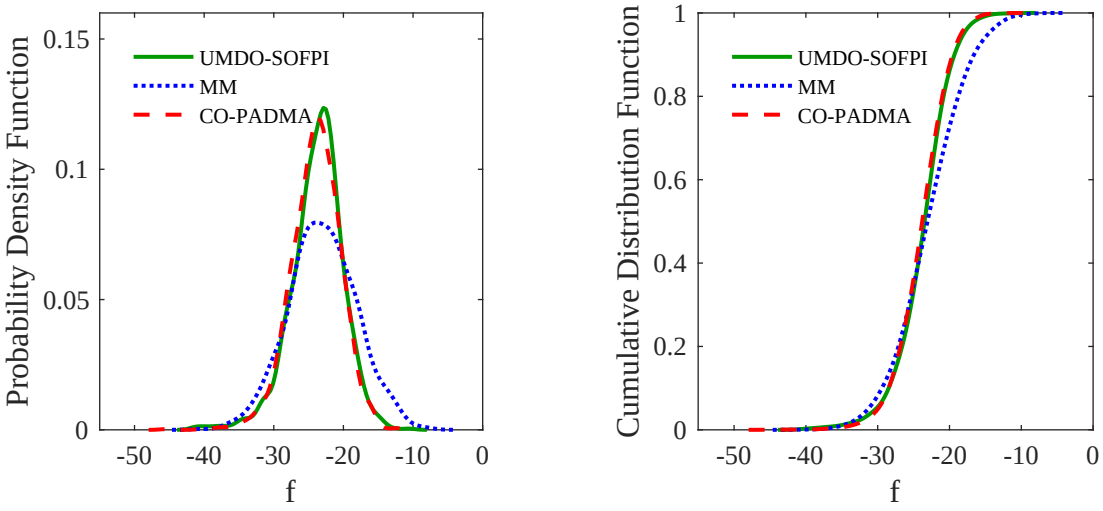

(a) Probability density function

(b) Cumulative distribution function

Figure 96: Comparison of probability density function and cumulative distribution function of system metric f at optimum design estimated using benchmark UMDO-SOFPI method, Moment Matching method (MM) and CO-PADMA method for analytical problem case-2

Figure 97 shows the optimum design evaluated by system and subsystem optimizers at the end of each cycle. Although all the subsystem optimizers did not converge to the same optimum design by 15^{th} cycle, they were close to a system level optimum solution. Figure 97 also shows the design space used to carry out optimization in each cycle. Compared to case-1, more inconsistencies have been found among the optimizers in the intial cycles.

In addition to the design space reduction technique, additional design points and samples of interdisciplinary compatible solutions in the reduced design space are added to the database at the end of each cycle. The histogram of design points at the end of $1^{st}, 6^{th}$ and 12^{th} cycle is shown in Figure 98. It is observed that with each cycle, the new design points get concentrated near the expected optimum solution which further allows improvement in accuracy of quantile copula regression. However, due to the inconsistencies among the optimizers, the peak of the histogram has not been found near the optimum solution for μ_{x_3} and μ_{x_5}.

The improvement in accuracy of the quantile copula regression is shown in Figure 99. The figure shows the uncertainty quantification, represented by the probability density function (PDF), of the optimum system metric f using quantile copula regression at the end of the $1^{st}, 6^{th}$ and 12^{th} cycle and is compared with true uncertainty evaluated using integrated SOFPI analysis. Similar to case-1, the accuracy of uncertainty quantification using quantile regression improved with each cycle.

The dependency structure of the coupling variables at the optimum design is compared between UMDO-SOFPI, MM and CO-PADMA and shown in the scatter plot matrix in Figure 100. Similar to case-1, each subplot in scatter plot matrix also shows a single iso-probability contour of value $0.02\mathrm{P}_{max}$, where P_{max} is the maximum probability value attained by the true solution using the UMDO-SOFPI method. As in case-1, all the coupling variables are positively dependent with respect to each other, however all the dependency structures are non-elliptical. The dependecny structure

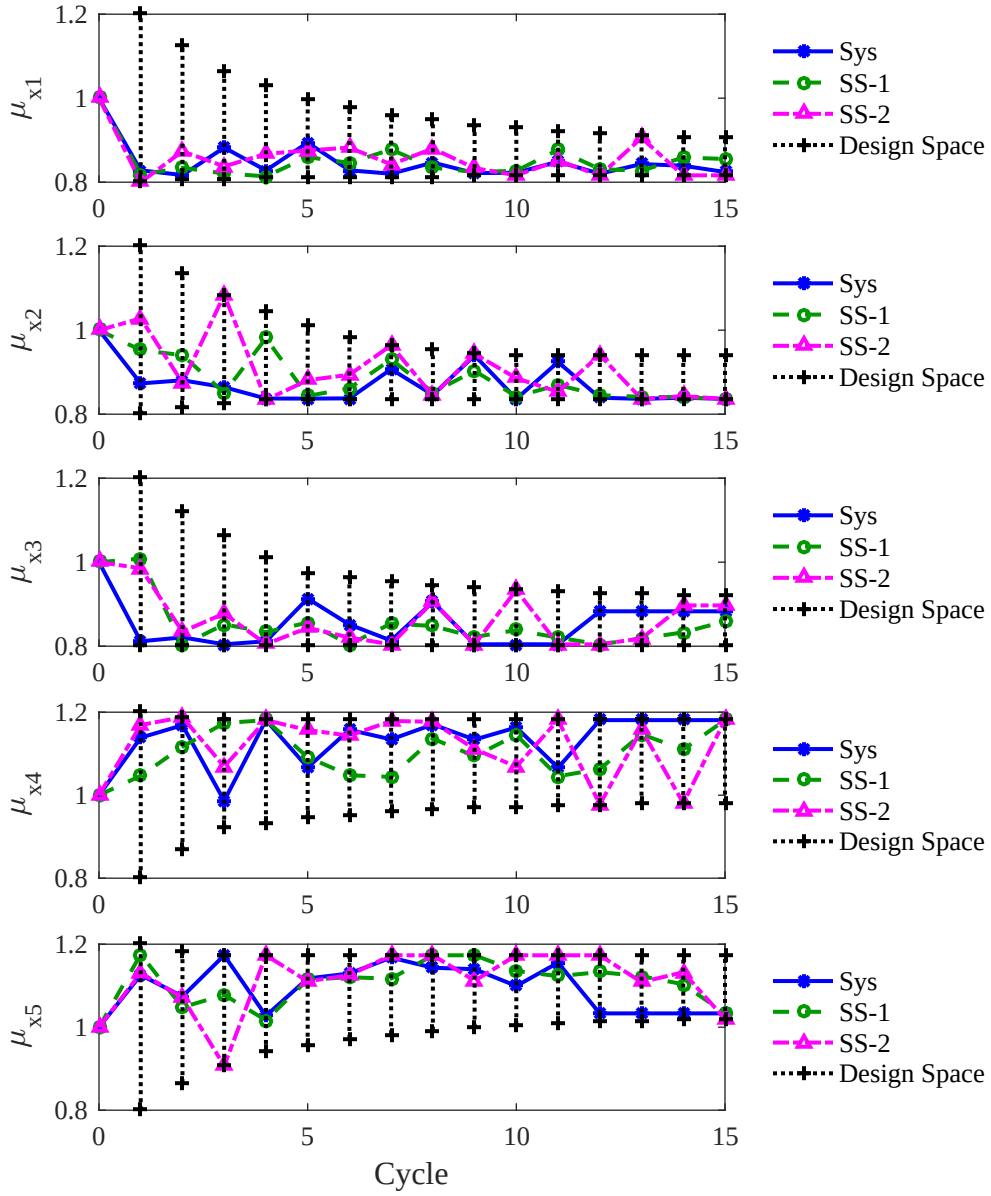

Figure 97: Optimum design estimated by system and subsystem optimizers and design space reduction at the end of each cycle analytical problem case-2

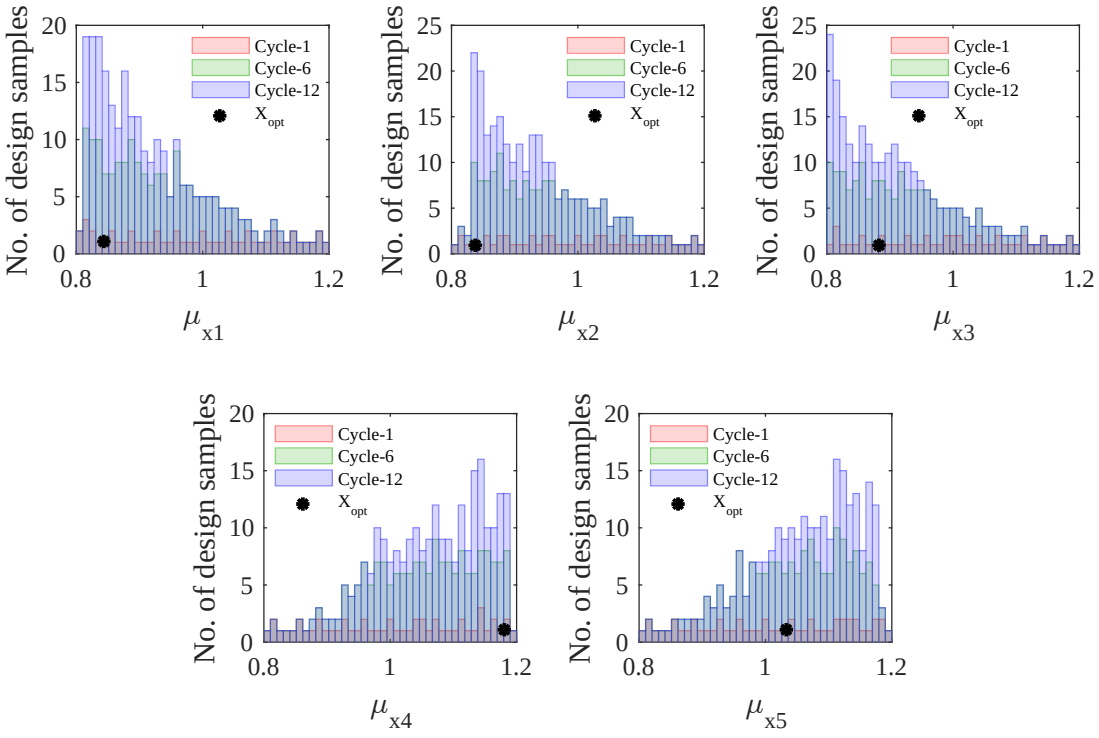

Figure 98: Histogram of design points at end of $1^{st}, 6^{th}$ and 12^{th} cycle for analytical problem case-2

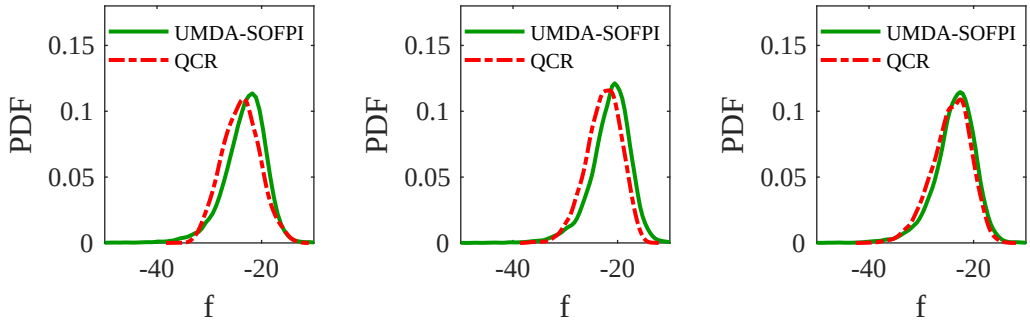

(a) Cycle-1 (b) Cycle-6 (c) Cycle-12

Figure 99: Improvement in accuracy of quantile copula regression (QCR) with each cycle for analytical problem case-2

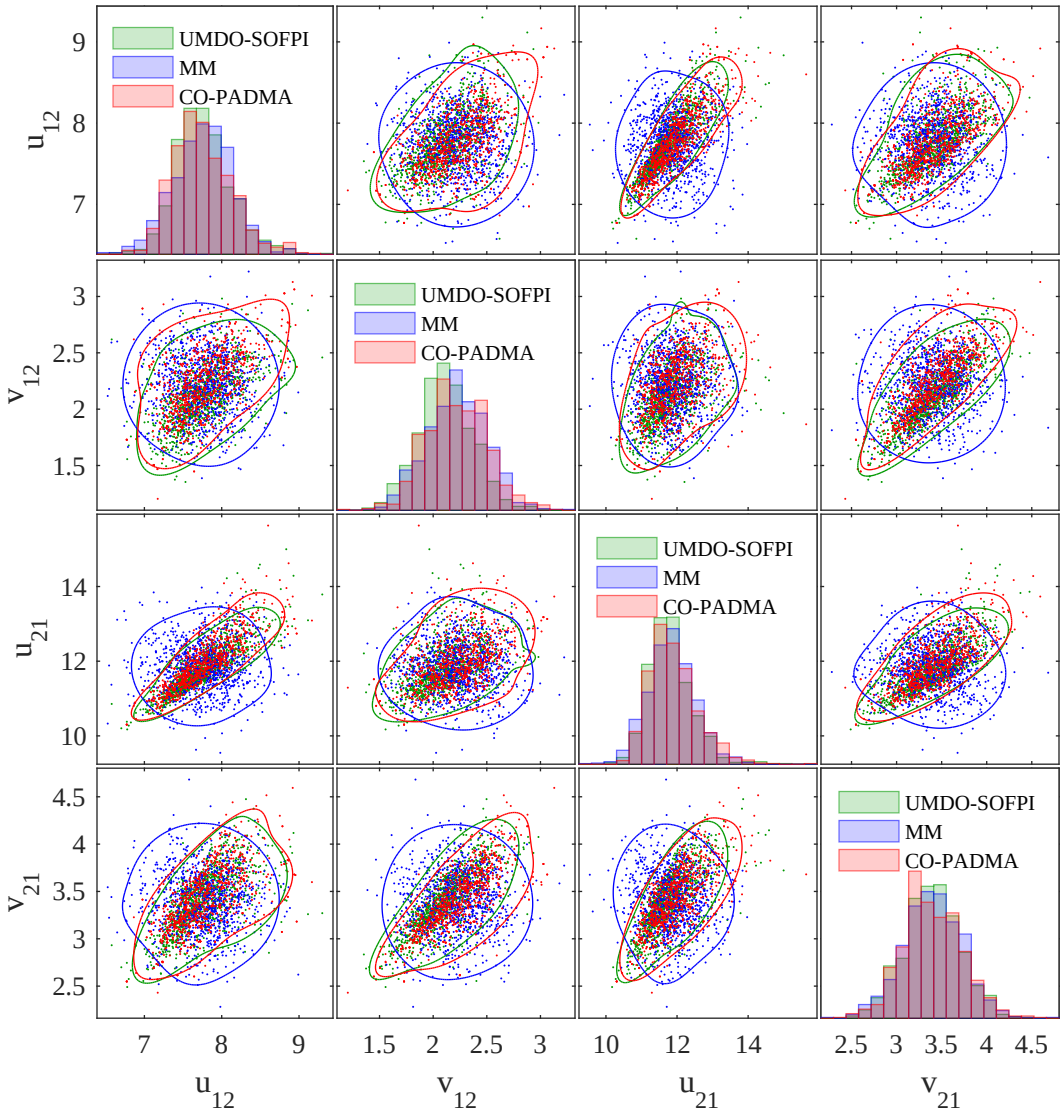

Figure 100: Scatter plot matrix of coupling variables at optimum design of analytical problem case-2

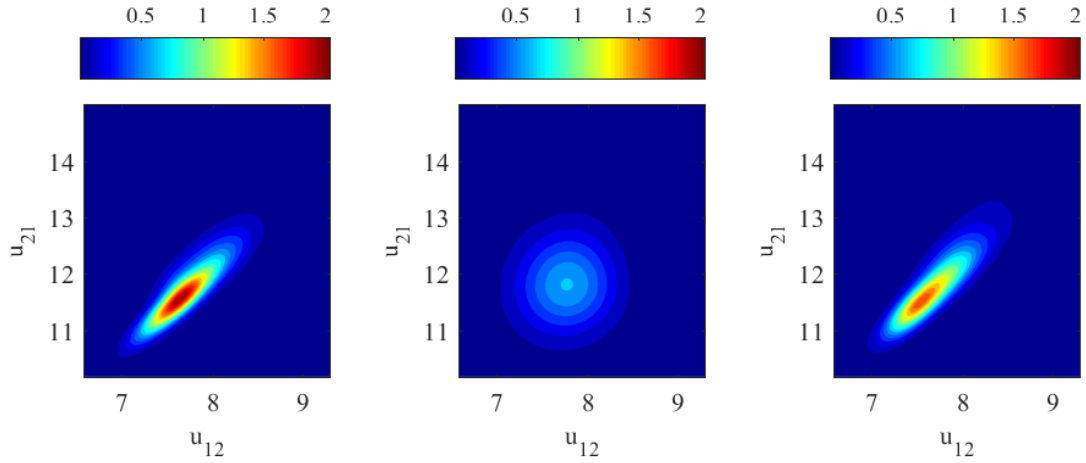

(a) UMDO-SOFPI (b) MM (c) CO-PADMA

Figure 101: Contour plot of joint probability density of optimum interdisciplinary compatible solution of u_{12} and u_{21} for analytical problem case-2

Table 26: Comparison of Correlation Matrix of coupling variables of analytical problem case-2

		Correlation Matrix			
		u_{12}	v_{12}	u_{21}	v_{21}
UMDO-SOFPI	u_{12}	1.00	0.55	0.85	0.65
	v_{12}	0.55	1.00	0.48	0.77
	u_{21}	0.85	0.48	1.00	0.74
	v_{21}	0.65	0.77	0.74	1.00
		u_{12}	v_{12}	u_{21}	v_{21}
CO-PADMA	u_{12}	1.00	0.56	0.85	0.66
	v_{12}	0.56	1.00	0.49	0.78
	u_{21}	0.85	0.49	1.00	0.73
	v_{21}	0.66	0.78	0.73	1.00
		u_{12}	v_{12}	u_{21}	v_{21}
$\Delta\rho$ error	u_{12}	0.00	0.02	0.00	0.01
	v_{12}	0.02	0.00	0.01	0.01
	u_{21}	0.00	0.01	0.00	0.01
	v_{21}	0.01	0.01	0.01	0.00

Table 27: Comparison of Mutual Information (MI) matrix of coupling variables of analytical problem case-2

Mutual Information Matrix

		u_{12}	v_{12}	u_{21}	v_{21}
UMDO-SOFPI	u_{12}	1.34	0.24	0.70	0.37
	v_{12}	0.24	1.35	0.20	0.51
	u_{21}	0.70	0.20	1.37	0.48
	v_{21}	0.37	0.51	0.48	1.31
		u_{12}	v_{12}	u_{21}	v_{21}
CO-PADMA	u_{12}	1.29	0.25	0.67	0.34
	v_{12}	0.25	1.27	0.20	0.53
	u_{21}	0.67	0.20	1.32	0.42
	v_{21}	0.34	0.53	0.42	1.29
		u_{12}	v_{12}	u_{21}	v_{21}
ΔMI **error**	u_{12}	0.05	0.01	0.03	0.04
	v_{12}	0.01	0.07	0.01	0.02
	u_{21}	0.03	0.01	0.05	0.06
	v_{21}	0.04	0.02	0.06	0.02

has been well captured by the CO-PADMA process, while the MM method assumed the coupling variables are independent and does not capture the dependencies. Figure 101 compares the contour plot of joint probability density of optimum interdisciplinary compatible solution of u_{12} and u_{21} estimated by all the UMDO-SOFPI, MM and CO-PAMDA methods. Similar to case-1, the CO-PADMA method has been able to capture the overall trend of joint probability density better than the MM method.

The dependencies of coupling variables are quantified using Pearson's correlation matrix and compared between the UMDO-SOFPI and CO-PADMA methods in Table 26. All correlation estimated by the CO-PADMA process has been found to be within 2% of true correlation estimated by the UMDO-SOFPI method. To quantify the non-linear dependency, Mutual Informations (MI) among coupling variables are estimated and compared between the UMDO-SOFPI and CO-PADMA methods in Table 27. The CO-PADMA method has also accurately estimated any underlying non-linear dependencies with maximum ΔMI of 0.07.

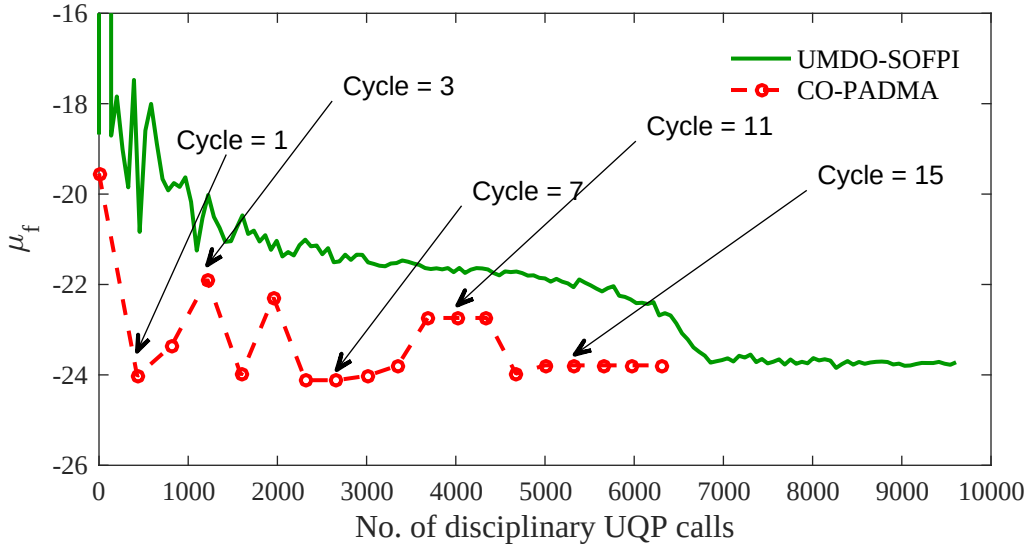

Figure 102: Comparison of convergence characteristics of optimum objective function with respect to disciplinary uncertainty quantification and propagation function calls for analytical problem case-2

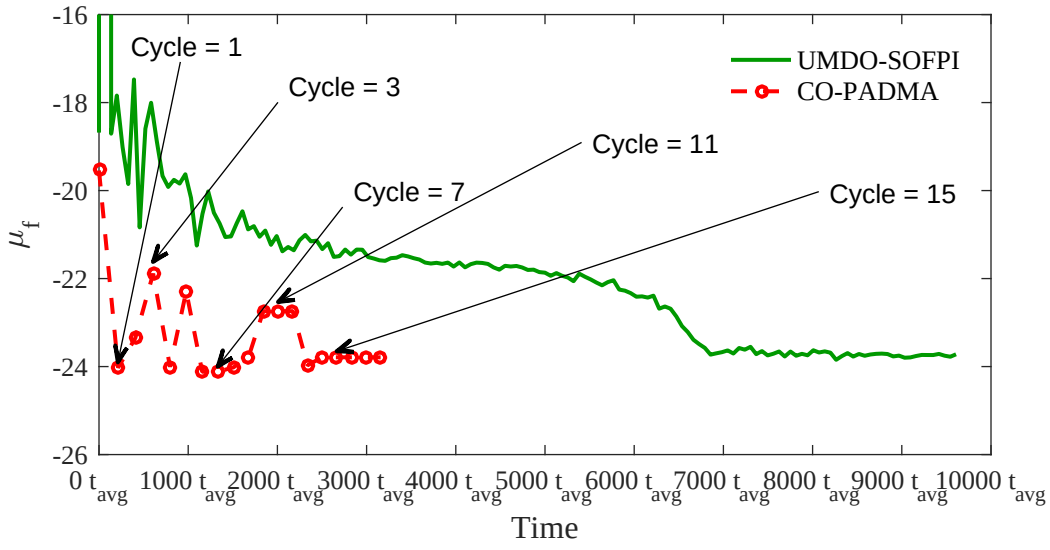

Figure 103: Comparison of convergence characteristics of optimum objective function with respect to time for analytical problem case-2, where t_{avg} is the average time for each disciplinary UQP call

The convergence history of the optimum objective function with respect to disciplinary uncertainty quantification and propagation (UQP) function calls are plotted and compared in Figure 102. Unlike the case-1, UMDO-SOFPI required around $7,000$ UQP calls to converge to an optimum solution. This also shows the increase in complexity of the problem due to non-Gaussian uncertain variables. Similarly, the CO-PADMA method also took around $5,000$ UQP calls when compared to $2,000$ UQP calls in case-1. The convergence history of the optimum objective function is plotted against time in Figure 103, where t_{avg} is the average time for each disciplinary UQP call. As in case-1 and depicted in figure, the CO-PADMA process took around half the time to reach the optimum solution as compared to the UMDO-SOFPI method.

6.4.5 Supersonic Transport (SST) Design Problem

This problem was designed for Supersonic Transport (SST) by Sobieszczanski [216] and has been used as a test bench for the deterministic BLISS process. The disciplinary analysis are mid-fidelity models which allow users to examine the effects of interdisciplinary interactions in an aircraft design problem while minimizing the computational requirements. The multidisciplinary analysis consists of four disciplinary modules: structures, aerodynamics, propulsion and range. The overall flow of information is given in Figure 104.

The problem consist of ten design variables $\mathbf{x} = [\lambda, x, C_f, t/c, h, M, AR, \Lambda, S_{ref}]$. Among ten design variables, six are shared design variables $\mathbf{x}_{sh} = [h, M, AR, \Lambda, S_{ref}]$, while four are disciplinary design variables, $\mathbf{x}_s = [\lambda, x]$ for structures, $\mathbf{x}_a = C_f$ for aerodynamics, and $\mathbf{x}_p = T$ for propulsion. The details of design variables are given in Table 28. There are nine state variables $\mathbf{y} = [W_T, W_f, \theta, L, D, L/D, SFC, ESF, W_E]$, with $\mathbf{y}_s = [W_T, W_f, \theta]$ as the output of structures, $\mathbf{y}_a = [L, D, L/D]$ as output of aerodynamics and $\mathbf{y}_p = [SFC, ESF, W_E]$ as output of propulsion. The description and deterministic baseline value of state variables are given in Table 29.

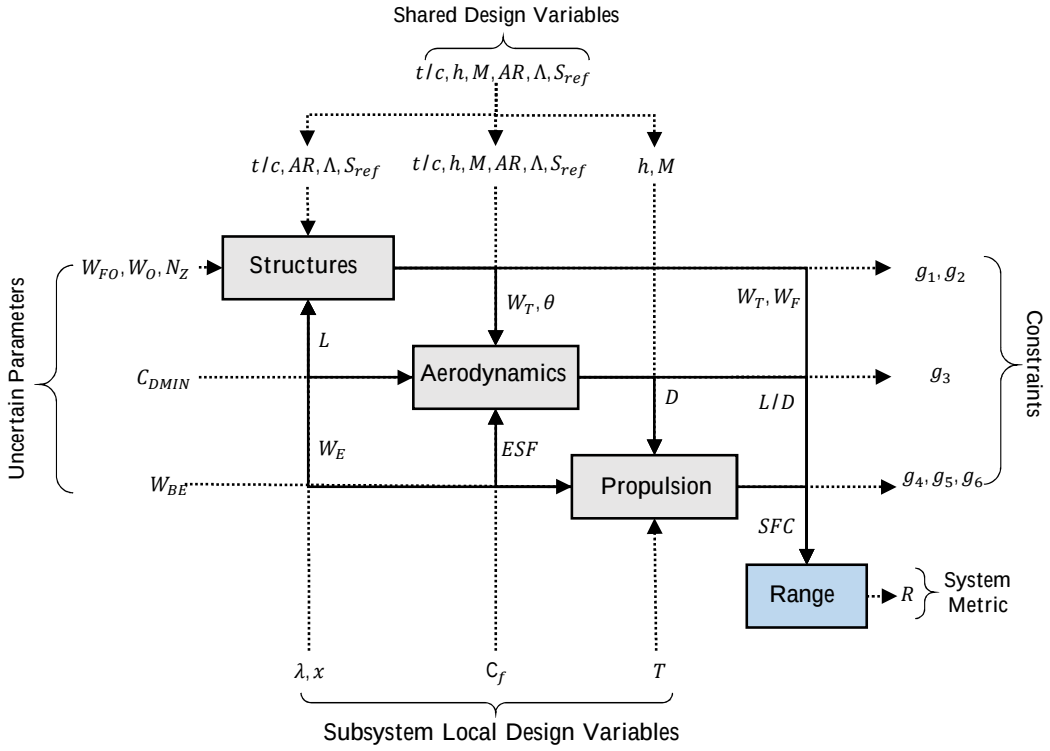

Figure 104: Supersonic Transport (SST) reliability-based robust design optimization problem

There are five disciplinary parameters $\mathbf{p} = [W_{FO}, W_O, N_Z, W_{BE}, C_{DMIN}]$ as given in Table 30, which are assumed to be uncertain. The uncertain variables are embedded in the disciplinary analyses such that each discipline acts like a non-deterministic function with aleatory uncertainty. For the UMDO problem, there are six disciplinary inequality constraints given in Table 31. The disciplinary constraint consist of both deterministic ($\mathbf{g}_d = [\sigma_{avg}, \theta, ESF]$) and non-deterministic ($\mathbf{g}_r = [\partial p/\partial x, E_{Temp}, T]$) variables. For non-deterministic variables reliability constraints are applied, for examples $\mathrm{P}(\mathbf{g}_r < \mathbf{g}_r^{max}) > 0.9$. The system level metric is range ($y_{sys} = R$), which is evaluated by range discipline using Equation 159.

$$R = \frac{661\sqrt{0.7519}(L/D)M}{SFC} \log\left(\frac{W_T}{W_T - W_F}\right) \tag{159}$$

The objective of the problem is to find the robust solution with respect to the range while maintaining the disciplinary reliability constraints. The optimization

Table 28: Description of shared and subsystem's design variables for SST problem

Variable (unit)	**Symbol (x)**	**Discipline**	**Lower Bound ($\mathbf{x}^L$)**	**Upper Bound ($\mathbf{x}^U$)**	**Baseline**
Taper Ratio	λ	Structures	0.25	0.35	0.3
Wingbox x-sect thickness ratio	x	Structures	0.75	0.85	0.8
Skin friction coeff.	C_f	Aerodynamics	0.75	0.85	0.8
Throttle Setting	T	Propulsion	0.1	0.4	0.25
Thickness/Chord	t/c	shared	0.05	0.09	0.07
Altitude (ft)	h	shared	$50,000$	$60,000$	$55,000$
Mach No.	M	shared	1.4	1.6	1.5
Aspect Ratio	AR	shared	2.5	5.5	3.5
Sweep (^{o})	Λ	shared	55	70	60
Wing Area (ft^2)	S_{ref}	shared	1200	1500	1350

statement is given by Equation 160

$$\begin{aligned}
\text{minimize} \quad & F = -\mu_R + 3.0\sigma_R && \text{(160a)}\\
\text{with respect to} \quad & \mathbf{x} \\
\text{such that} \quad & \mathrm{P}(g_1 < 1.09) > 0.9 && \text{(160b)}\\
& \mathrm{P}(0.96 < g_2 < 1.04) > 0.9 && \text{(160c)}\\
& g_3 < 1.04 && \text{(160d)}\\
& \mathrm{P}(0.5 < g_4 < 1.5) > 0.9 && \text{(160e)}\\
& g_5 < 1.02 && \text{(160f)}\\
& g_6 < 0.0 && \text{(160g)}\\
& \mathbf{x}^L \leq \mathbf{x} \leq \mathbf{x}^U && \text{(160h)}
\end{aligned}$$

where μ_R is the mean and σ_R is the standard deviation of system metric range (R).

Two case studies are carried out with the SST design problem by changing the characteristics of uncertain parameter variables.

Case-1: In the first case, all the uncertain variables are characterized with Gaussian

Table 29: Description of state variables for SST problem

Variable (unit)	**Symbol** (**y**)	**Discipline** (Output)	**Baseline** (Deterministic)
Total Weight (lb)	W_T	Structures	6.76×10^4
Fuel Weight (lb)	W_f	Structures	1.66×10^4
Twist (n/a)	θ	Structures	0.95
Lift (lb)	L	Aerodynamics	6.76×10^4
Drag (lb)	D	Aerodynamics	1.107×10^4
Lift to Drag ratio	L/D	Aerodynamics	6.1
Specific Fuel Consumption ($1/hr$)	SFC	Propulsion	1.048
Engine Scale Factor	ESF	Propulsion	0.91
Engine Weight (lb)	W_E	Propulsion	1.19×10^4

Note: Variables with unit n/a are unit-less and normalized with reference value

Table 30: Description of uncertain disciplinary parameters for SST problem

Variable	**Symbol**	**Discipline**
Misc. Fuel Weight (lb)	W_{FO}	Structures
Misc. Weight (lb)	W_O	Structures
Max. Load Factor	N_Z	Structures
Min. Drag Coeff.	C_{DMIN}	Aerodynamics
Baseline Engine Weight (lb)	W_{BE}	Propulsion

Table 31: Description of disciplinary constraints for SST problem

Variable	**Symbol**	**Discipline**	**Constraint**
Avg. Stress [a](n/a)	$g_1 = \sigma_{avg}$	Structures	$\mathrm{P}(\sigma_{avg} < 1.09) > 0.9$
Twist (n/a)	$g_2 = \theta$	Structures	$\mathrm{P}(0.96 < \theta < 1.04) > 0.9$
Pres. Grad. (n/a)	$g_3 = \partial p/\partial x$	Aerodynamics	$\partial p/\partial x < 1.04$
Engine Scale Factor	$g_4 = ESF$	Propulsion	$\mathrm{P}(0.5 < ESF < 1.5) > 0.9$
Engine Temp. (n/a)	$g_5 = E_{Temp}$	Propulsion	$E_{Temp} < 1.02$
Throt. Setting (n/a)	$g_6 = T$	Propulsion	$T < 0$

Note: Variables with unit n/a are unit-less and normalized with reference value

[a] non-dimensional stress averaged over five different locations on wing

Table 32: Description of characteristic of uncertainty variables for case-1 of SST problem

Variable	**Density Function**	**Parameters**
W_{FO}	Gaussian	$\mu = 2000$, $\sigma = 20$
W_O	Gaussian	$\mu = 25000$, $\sigma = 250$
N_Z	Gaussian	$\mu = 6$, $\sigma = 0.06$
C_{DMIN}	Gaussian	$\mu = 4360$, $\sigma = 43.6$
W_{BE}	Gaussian	$\mu = 1.375 \times 10^{-2}$, $\sigma = 1.375 \times 10^{-4}$

Note: μ is mean and σ is standard deviation for Gaussian distribution

Table 33: Description of characteristic of uncertainty variables for case-2 of SST problem

Variable	**Density Function**	**Parameters**
W_{FO}	Gaussian	$\mu = 2000$, $\sigma = 20$
W_O	Triangular	$a = 24200$, $b = 24500$, $c = 25600$
N_Z	Gaussian	$\mu = 6$, $\sigma = 0.06$
C_{DMIN}	Triangular	$a = 4250$, $b = 4300$, $c = 4500$
W_{BE}	Shifted Gamma	$\delta = 1.34 \times 10^{-2}$, $k = 3.0$, $\theta = 1.375 \times 10^{-}4$

Note: For triangular distribution a is lower limit, b is peak location, and c is upper limit. For shifted gamma distribution δ is shift, k is shape parameter, and θ is scale parameter.

distribution with mean and standard deviation given in Table 32.

Case-2: In the second case, mixture of Gaussian and non-Gaussian distribution is used. The density functions and parameters are given in Table 33.

The uncertain variables are embedded in their respective disciplines so that each of the disciplinary functions are non-deterministic and cannot be explicitly determined as a function of uncertain variables.

6.4.5.1 CO-PADMA Procedure

The step by step numerical procedure of the CO-PADMA method for the analytical problem is given as follows.

1. Start

2. Initialize the variables.

(a) Ranges of design variables are initialized: $\mathbf{x} \in [\mathbf{x}^L, \mathbf{x}^U]$.

(b) Baseline design is defined as $\mathbf{x}_{baseline}$, which is used as the starting point for optimization.

(c) Uncertainty variables are characterized, as defined in the previous section.

(d) Cycle counter is set to $r = 1$.

3. Experimental design and quantile copula regression modeling

(a) For the first cycle ($r = 1$)

i. 100 samples of design points $\mathbf{x}$ are generated using Latin hypercube design within the domain defined in Step 2(a).

ii. For each sample of design, UMDA using the PADMA procedure is carried out to evaluate 300 samples of interdisciplinary compatible solutions of $\mathbf{y}$ and constraints $\mathbf{g}$.

iii. Design points and respective samples of state variables and constraints are added to the database.

iv. Using the samples from the database, quantile copula regression $\tilde{f}_{qcr_{\mathbf{y}}}(\mathbf{y}|\mathbf{x})$ of all the state variables are built. Also quantile copula regression of all the reliability constraints $\tilde{f}_{qcr_{\mathbf{g}_r}}(\mathbf{g}_r|\mathbf{x})$ are built. For the deterministic constraints, quadratic response surface models are built similar to deterministic CSSO method $\mathbf{g}_d = \tilde{f}_{rsm_{\mathbf{g}_d}}(\mathbf{x})$.

(b) For cycle ($r > 1$)

i. Samples are filtered and selected from the database which are within the reduced domain defined by Step 6(b).

ii. n_{new} set of new samples of design points are generated within the reduced domain, where $n_{new} = n_{filter} - 100 + 5r$ and n_{filter} is the number of unique design points in the database which are within the

reduced domain. This allows the maintaining of at least 100 unique design points to model quantile copula regression.

iii. For each new sample of design, UMDA using the PADMA procedure is carried out to evaluate samples of interdisciplinary compatible solutions of disciplinary state variables $\mathbf{y}$ and constraints $\mathbf{g}$.

iv. Design points and their respective samples of state variables are added to the database.

v. Using new and filtered samples from the database, quantile copula regression of all the state variables $\tilde{f}_{qcr_{\mathbf{y}}}(\mathbf{y}|\mathbf{x})$ are built. Similarly quantile copula regression of all the reliability constraints $\tilde{f}_{qcr_{\mathbf{g}_r}}(\mathbf{g}_r|\mathbf{x})$ are built. For the deterministic constraints, quadratic response surface models are built similar to the deterministic CSSO method $\mathbf{g}_d = \tilde{f}_{rsm_{\mathbf{g}_d}}(\mathbf{x})$.

4. System Optimization:

   (a) Using the quantile copula regression, system optimization is carried out as

given by:

$$\begin{aligned}
&\text{Given} && \tilde{f}_{qcr_{\mathbf{y}}}(\mathbf{y}|\mathbf{x}), \tilde{f}_{qcr_{\mathbf{g}_r}}(\mathbf{g}_r|\mathbf{x}), \tilde{f}_{rsm_{\mathbf{g}_d}}(\mathbf{x}) && \text{(161a)}\\
&&& \tilde{R} = f_{sys}(\mathbf{x}, \tilde{\mathbf{y}}) && \text{(161b)}\\
&\text{minimize} && \tilde{F} = -\mu_{\tilde{R}} + 3.0\sigma_{\tilde{R}} && \text{(161c)}\\
&\text{with respect to} && \mathbf{x} &&\\
&\text{such that} && \mathrm{P}(\tilde{g}_1 < 1.09) > 0.9 && \text{(161d)}\\
&&& \mathrm{P}(0.96 < \tilde{g}_2 < 1.04) > 0.9 && \text{(161e)}\\
&&& \tilde{g}_3 < 1.04 && \text{(161f)}\\
&&& \mathrm{P}(0.5 < \tilde{g}_4 < 1.5) > 0.9 && \text{(161g)}\\
&&& \tilde{g}_5 < 1.02 && \text{(161h)}\\
&&& \tilde{g}_6 < 0.0 && \text{(161i)}\\
&&& \mathbf{x}^{L(r)} \leq \mathbf{x} \leq \mathbf{x}^{U(r)} && \text{(161j)}\\
&\text{Output} && \mathbf{x}^{*(r)}, \tilde{f}_R^{*(r)}(R), \tilde{F}^{*(r)} &&
\end{aligned}$$

where uncertainty on state variables $\tilde{\mathbf{y}}$ is estimated through quantile copula regression which is used to approximate the uncertainty on system metric $\tilde{f}_R^{*(r)}(R)$.

(b) The PADMA procedure is carried out using high-fidelity disciplinary analyses at the optimum design of r^{th} cycle, $\mathbf{x}^{*(r)}$, to evaluate the accurate probability density of system metric $f_R^{*(r)}(R)$, accurate cost function $F^{*(r)}$. Also 300 samples of interdisciplinary compatible solutions of all the state variables are generated and added to the database.

5. Subsystem Optimization:

(a) Subsystem optimization is carried out using high-fidelity disciplinary analysis, while non-local state variables are approximated using quantile copula regression. The structure discipline subsystem optimization problem is given as:

Structure Discipline Optimization

$$
\begin{aligned}
\text{Given} \quad & \tilde{f}_{qcr_{\mathbf{y}_{\cdot s}}}(\mathbf{y}_{\cdot s}|\mathbf{x}), \tilde{f}_{qcr_{\mathbf{g}_r}}(\mathbf{g}_r|\mathbf{x}), \tilde{f}_{rsm_{\mathbf{g}_d}}(\mathbf{x}) && \text{(162a)}\\
& [\mathbf{y}_s, \mathbf{g}_s] = f_{Structure}(\mathbf{x}_{sh}, \mathbf{x}_s, \tilde{\mathbf{y}}_{\cdot s}) && \text{(162b)}\\
& \tilde{R} = f_{sys}(\mathbf{x}, \mathbf{y}_s, \tilde{\mathbf{y}}_{\sim s}) && \text{(162c)}\\
\text{minimize} \quad & \tilde{F} = -\mu_{\tilde{R}} + 3.0\sigma_{\tilde{R}} && \text{(162d)}\\
\text{with respect to} \quad & \mathbf{x} &&\\
\text{such that} \quad & \mathrm{P}(g_1 < 1.09) > 0.9 && \text{(162e)}\\
& \mathrm{P}(0.96 < g_2 < 1.04) > 0.9 && \text{(162f)}\\
& \tilde{g}_3 < 1.04 && \text{(162g)}\\
& \mathrm{P}(0.5 < \tilde{g}_4 < 1.5) > 0.9 && \text{(162h)}\\
& \tilde{g}_5 < 1.02 && \text{(162i)}\\
& \tilde{g}_6 < 0.0 && \text{(162j)}\\
& \mathbf{x}^{L(r)} \leq \mathbf{x} \leq \mathbf{x}^{U(r)} && \text{(162k)}\\
\text{Output} \quad & \mathbf{x}_s^{*(r)}, \tilde{f}_{R_s}^{*(r)}(R_s), \tilde{F}_s^{*(r)} &&
\end{aligned}
$$

where uncertainty on input coupling variables to structure disciplines $\tilde{\mathbf{y}}_{\cdot s}$ is evaluated using the quantile copula regression while output coupling variables ($\mathbf{y}_s$) and constraints ($\mathbf{g}_s = [g_1, g_2]$) of structures disciplines are evaluated using high-fidelity disciplinary analysis $f_{Structure}(\mathbf{x}_{sh}, \mathbf{x}_s, \tilde{\mathbf{y}}_{\cdot s})$. System response R is evaluated as a function of design variables $\mathbf{x}$, high-fidelity state variables of structures discipline $\tilde{\mathbf{y}}_{\cdot s}$, and approximate state variables of other disciplines $\tilde{\mathbf{y}}_{\sim s}$. Uncertainty on non-local reliability constraints are

estimated using $\tilde{f}_{qcr_{\mathbf{g}_r}}(\mathbf{g}_r|\mathbf{x})$. Similarly, non-local deterministic constraints are estimated using $\tilde{f}_{rsm_{\mathbf{g}_d}}(\mathbf{x})$.

The aerodynamics discipline subsystem optimization problem is given as:

Aerodynamics Discipline Optimization

$$
\begin{aligned}
\text{Given} \quad & \tilde{f}_{qcr_{\mathbf{y}_{\cdot a}}}(\mathbf{y}_{\cdot a}|\mathbf{x}), \tilde{f}_{qcr_{\mathbf{g}_r}}(\mathbf{g}_r|\mathbf{x}), \tilde{f}_{rsm_{\mathbf{g}_d}}(\mathbf{x}) && \text{(163a)}\\
& [\mathbf{y}_a, \mathbf{g}_a] = f_{Aerodynamics}(\mathbf{x}_{sh}, \mathbf{x}_a, \tilde{\mathbf{y}}_{\cdot a}) && \text{(163b)}\\
& \tilde{R} = f_{sys}(\mathbf{x}, \mathbf{y}_a, \tilde{\mathbf{y}}_{\sim a}) && \text{(163c)}\\
\text{minimize} \quad & \tilde{F} = -\mu_{\tilde{R}} + 3.0\sigma_{\tilde{R}} && \text{(163d)}\\
\text{with respect to} \quad & \mathbf{x} &&\\
\text{such that} \quad & \mathrm{P}(\tilde{g}_1 < 1.09) > 0.9 && \text{(163e)}\\
& \mathrm{P}(0.96 < \tilde{g}_2 < 1.04) > 0.9 && \text{(163f)}\\
& g_3 < 1.04 && \text{(163g)}\\
& \mathrm{P}(0.5 < \tilde{g}_4 < 1.5) > 0.9 && \text{(163h)}\\
& \tilde{g}_5 < 1.02 && \text{(163i)}\\
& \tilde{g}_6 < 0.0 && \text{(163j)}\\
& \mathbf{x}^{L(r)} \leq \mathbf{x} \leq \mathbf{x}^{U(r)} && \text{(163k)}\\
\text{Output} \quad & \mathbf{x}_a^{*(r)}, \tilde{f}_{R_a}^{*(r)}(R_a), \tilde{F}_a^{*(r)} &&
\end{aligned}
$$

where uncertainty on input coupling variables to aerodynamic disciplines $\tilde{\mathbf{y}}_{\cdot a}$ is estimated using the quantile copula regression while output coupling variables ($\mathbf{y}_a$) and constraints ($\mathbf{g}_a = [g_3]$) of aerodynamics disciplines are evaluated using high-fidelity disciplinary analysis $f_{Aerodynamics}(\mathbf{x}_{sh}, \mathbf{x}_a, \tilde{\mathbf{y}}_{\cdot a})$. System response R is evaluated as a function of design variables $\mathbf{x}$, high fidelity state variables of aerodynamics discipline $\tilde{\mathbf{y}}_{\cdot a}$, and approximate state variables of other disciplines $\tilde{\mathbf{y}}_{\sim a}$. Uncertainty on non-local reliability constraints are estimated using $\tilde{f}_{qcr_{\mathbf{g}_r}}(\mathbf{g}_r|\mathbf{x})$. Similarly, non-local deterministic

constraints are estimated using $\tilde{f}_{rsm_{\mathbf{g}_d}}(\mathbf{x})$.

The propulsion discipline subsystem optimization problem is given as:

Propulsion Discipline Optimization

$$
\begin{aligned}
\text{Given} \quad & \tilde{f}_{qcr_{\mathbf{y}_{\cdot p}}}(\mathbf{y}_{\cdot p}|\mathbf{x}), \tilde{f}_{qcr_{\mathbf{g}_r}}(\mathbf{g}_r|\mathbf{x}), \tilde{f}_{rsm_{\mathbf{g}_d}}(\mathbf{x}) && \text{(164a)}\\
& [\mathbf{y}_p, \mathbf{g}_p] = f_{Propulsion}(\mathbf{x}_{sh}, \mathbf{x}_p, \tilde{\mathbf{y}}_{\cdot p}) && \text{(164b)}\\
& \tilde{R} = f_{sys}(\mathbf{x}, \mathbf{y}_p, \tilde{\mathbf{y}}_{\sim p}) && \text{(164c)}\\
\text{minimize} \quad & \tilde{F} = -\mu_{\tilde{R}} + 3.0\sigma_{\tilde{R}} && \text{(164d)}\\
\text{with respect to} \quad & \mathbf{x} &&\\
\text{such that} \quad & \mathrm{P}(\tilde{g}_1 < 1.09) > 0.9 && \text{(164e)}\\
& \mathrm{P}(0.96 < \tilde{g}_2 < 1.04) > 0.9 && \text{(164f)}\\
& \tilde{g}_3 < 1.04 && \text{(164g)}\\
& \mathrm{P}(0.5 < g_4 < 1.5) > 0.9 && \text{(164h)}\\
& g_5 < 1.02 && \text{(164i)}\\
& g_6 < 0.0 && \text{(164j)}\\
& \mathbf{x}^{L(r)} \leq \mathbf{x} \leq \mathbf{x}^{U(r)} && \text{(164k)}\\
\text{Output} \quad & \mathbf{x}_p^{*(r)}, \tilde{f}_{R_p}^{*(r)}(R_p), \tilde{F}_p^{*(r)} &&
\end{aligned}
$$

where uncertainty on input coupling variables to propulsion disciplines $\tilde{\mathbf{y}}_{\cdot p}$ is estimated using the quantile copula regression while output coupling variables ($\mathbf{y}_p$) and constraints ($\mathbf{g}_p = [g_4, g_5, g_6]$) of propulsion disciplines are evaluated using high-fidelity disciplinary analysis $f_{Propulsion}(\mathbf{x}_{sh}, \mathbf{x}_p, \tilde{\mathbf{y}}_{\cdot p})$. System response R is evaluated as a function of design variables $\mathbf{x}$, high fidelity state variables of propulsion discipline $\tilde{\mathbf{y}}_{\cdot p}$, and approximate state variables of other disciplines $\tilde{\mathbf{y}}_{\sim p}$. Uncertainty on non-local reliability constraints are estimated using $\tilde{f}_{qcr_{\mathbf{g}_r}}(\mathbf{g}_r|\mathbf{x})$. Similarly, non-local deterministic constraints are estimated using $\tilde{f}_{rsm_{\mathbf{g}_d}}(\mathbf{x})$.

Once the subsystem optimizations are over, the PADMA procedure using the high-fidelity analyses of all the subsystems are carried out for $\mathbf{x}_s^{*(r)}, \mathbf{x}_a^{*(r)}$ and $\mathbf{x}_p^{*(r)}$, to evaluate the accurate probability density of system metric $f_{R_s}^{*(r)}(R_s), f_{R_a}^{*(r)}(R_a)$ and $f_{R_p}^{*(r)}(R_p)$, and accurate cost function $F_s^{*(r)}, F_a^{*(r)}$ and $F_p^{*(r)}$. Also, 300 samples of interdisciplinary compatible solutions of all the state variables are generated at each subsystem optimum design and added to the database.

6. Check Convergence: Check the convergence criteria given in Section 6.2.4.

   (a) If converged, STOP

   (b) Otherwise:

      i. Increment the cycle count ($r = r + 1$)

      ii. Design Space Reduction: Reduce the domain of design variables using Equation 143.

      iii. Repeat from Step 3.

Similar to analytical problem, the CMAES optimization algorithm has been used to carry out all the optimization processes. The scripts of the disciplinary functions have been written in MATLAB. Also, to automate the CO-PADMA process, scripts for CO-PADMA method have been written and executed in MATLAB.

6.4.5.2 Results: SST design problem Case-1

In the first case of the SST design problem all the uncertain variables are assumed to have a Gaussian distribution. Similar to the analytical problem, a study has been carried out with the CO-PADMA method and compared it with the UMDO-SOFPI and MM methods.

For the SST design problem case-1 the CO-PADMA method took 15 cycles to converge to optimum solution. The system level optimum design variables are listed

in Table 34 and subsystem level optimum design variables are listed in Table 35. The table also compares the results of the CO-PADMA process with true optimum results evaluated using the UMDO-SOFPI method. All the system level design variables have been found to converge with a 1% error. Except for t/c and S_{ref}, all the other system design variables have converged at the boundary of design space. The subsystem design variables also converged to the value very close to a true solution with the worst cases of λ (2.5% error) and C_f (3.6% error).

The probability density function and cumulative distribution function of optimum system metric range (R) evaluated by the CO-PADMA process is plotted in Figure 105. Results are compared with the probability density function and cumulative distribution function estimated by the UMDO-SOFPI and MM methods estimated at true optimum obtained by the UMDO-SOFPI method. The uncertainty of the range has been found to follow the Gaussian distribution very closely. The CO-PADMA process has been able to estimate the uncertainty very close to the UMDO-SOFPI method; however the MM method seems to predict a wider variance. The statistical metrics of range is listed and compared in Table 36. Both the CO-PADMA and MM methods have been able to predict the statistical mean accurately. However, as predicted by probability density plot, the standard deviation of the MM method is off by 31% when compared to the CO-PADMA method which is off by only 2%. Due to the symmetric nature of the probability density function, the skewness is very close to zero, which is well predicted by both the MM and CO-PADMA methods. In terms of closeness of overall distribution measured by K-L divergence, the CO-PAMDA method with K-L div. = 0.02 has been able to find a better solution when compared to the MM method with K-L div. = 0.09.

Figure 106 shows the optimum system level design variables evaluated by system and all the subsystem optimizers at the end of each cycle. All the optimizers have been found to be very consistent for all the system design variables which allow a design

Table 34: Comparison of optimum system level design variables for SST design problem case-1

	t/c	$h(ft)$	M	AR	$\Lambda(^o)$	$S_{ref}(ft^2)$
UMDO-SOFPI	0.0839	60000.00	1.40	2.50	70.00	1460.00
CO-PADMA	0.0841	59985.28	1.40	2.50	70.00	1462.94
$\Delta \mathbf{x}^*_{norm}$	0.0024	0.00	0.00	0.00	0.00	0.002

Table 35: Comparison of optimum subsystem level design variables for SST design problem case-1

	λ	x	C_f	T
UMDO-SOFPI	0.281	0.751	0.760	0.156
CO-PADMA	0.274	0.750	0.787	0.156
$\Delta \mathbf{x}^*_{norm}$	0.025	0.001	0.036	0.001

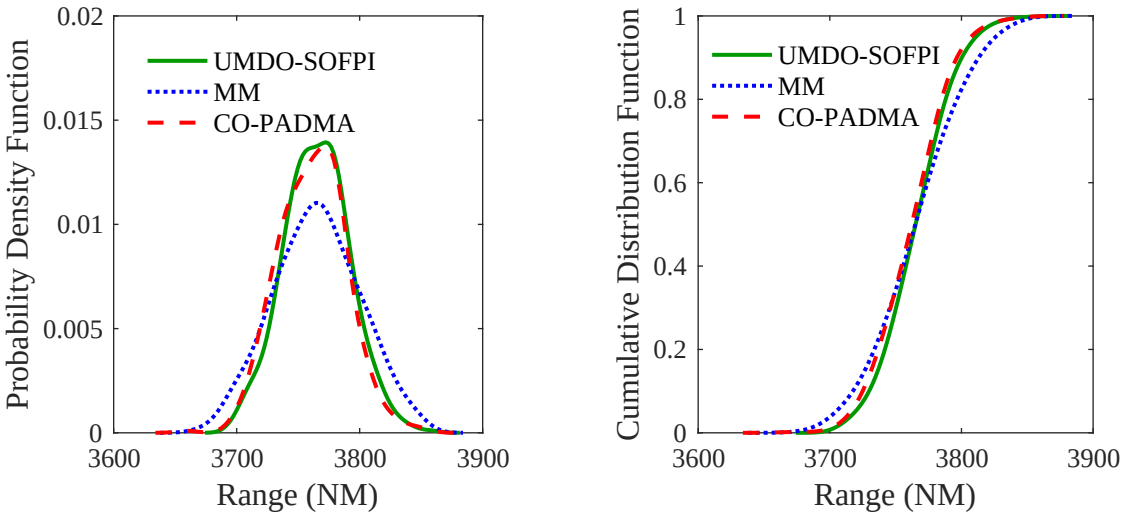

(a) Probability density function

(b) Cumulative distribution function

Figure 105: Comparison of probability density function and cumulative distribution function of system metric range (R) at optimum design estimated using benchmark UMDO-SOFPI method, Moment Matching method (MM) and CO-PADMA method for analytical problem case-1

Table 36: Comparison of statistical metrics of system metric range (R) for SST design problem case-1

	UMDO-SOFPI	**MM**	**CO-PADMA**
Mean(μ_R)	3765.15	3765.09	3761.58
Std. Dev.(σ_R)	26.61	34.81	27.15
Skewness (γ_R)	0.10	0.01	0.06
K-L div.	-	0.09	0.02

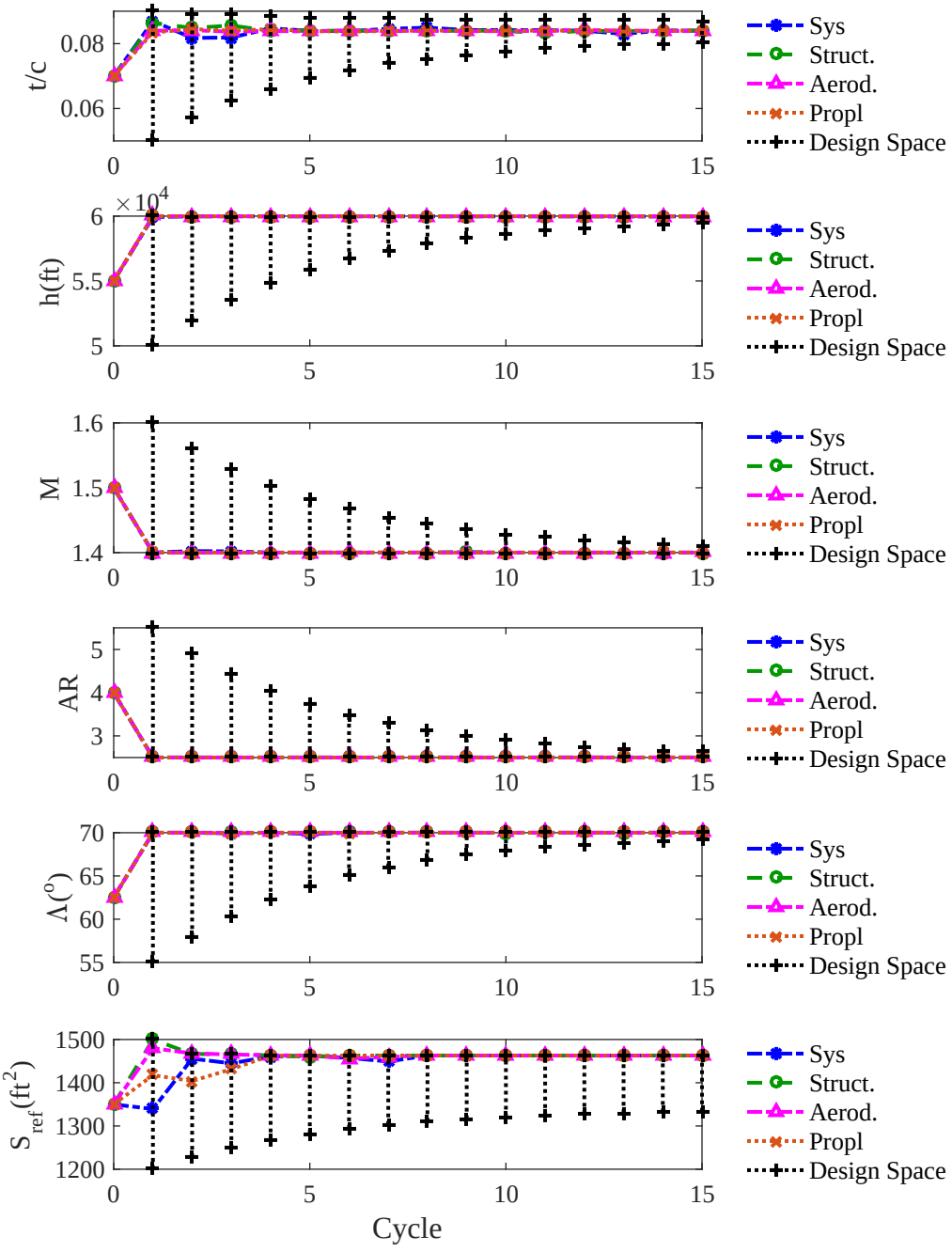

Figure 106: Optimum system design variables estimated by system and subsystem optimizers and design space reduction at the end of each cycle for SST design problem case-1

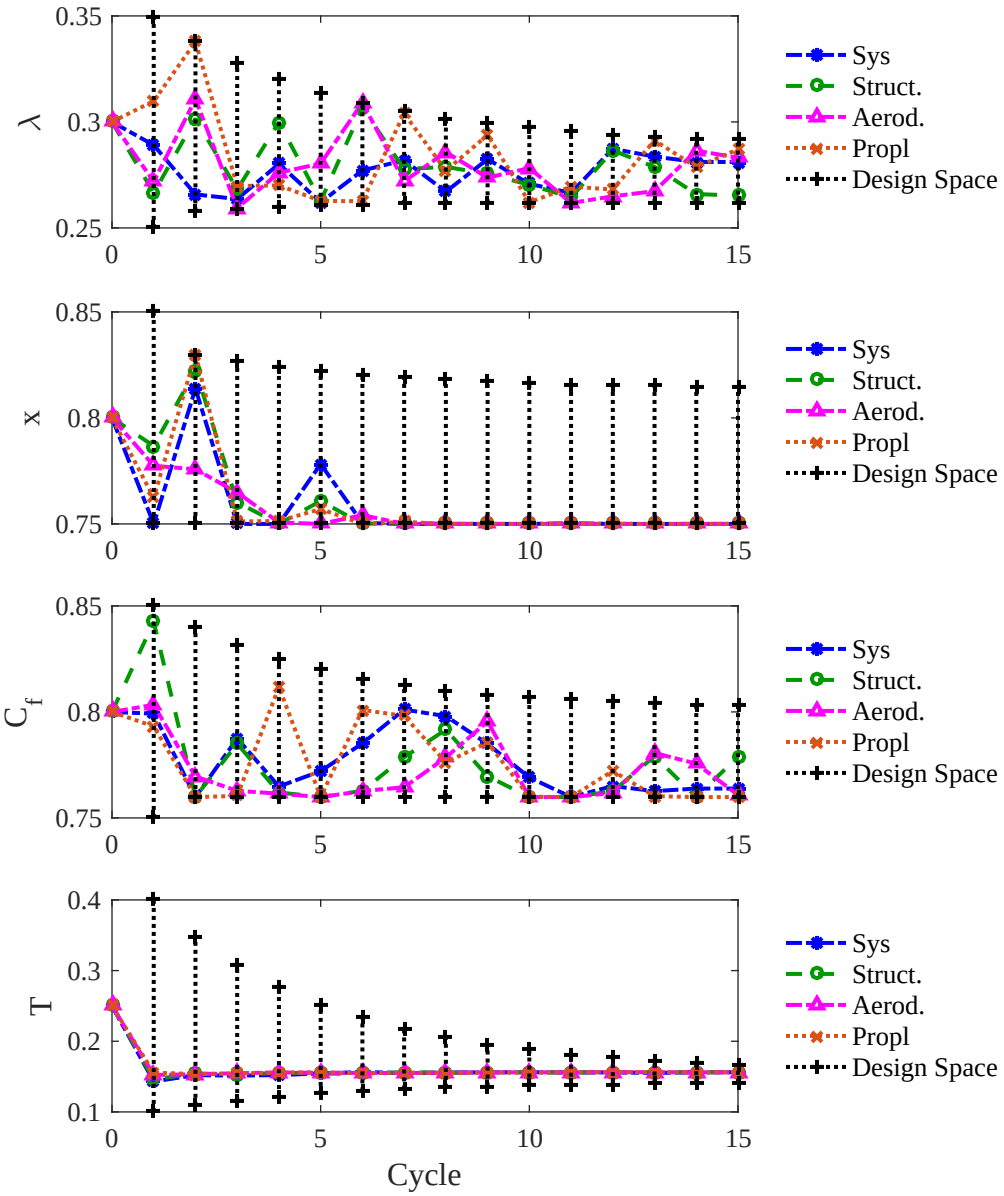

Figure 107: Optimum subsystem design variables estimated by system and subsystem optimizers and design space reduction at the end of each cycle for SST design problem case-1

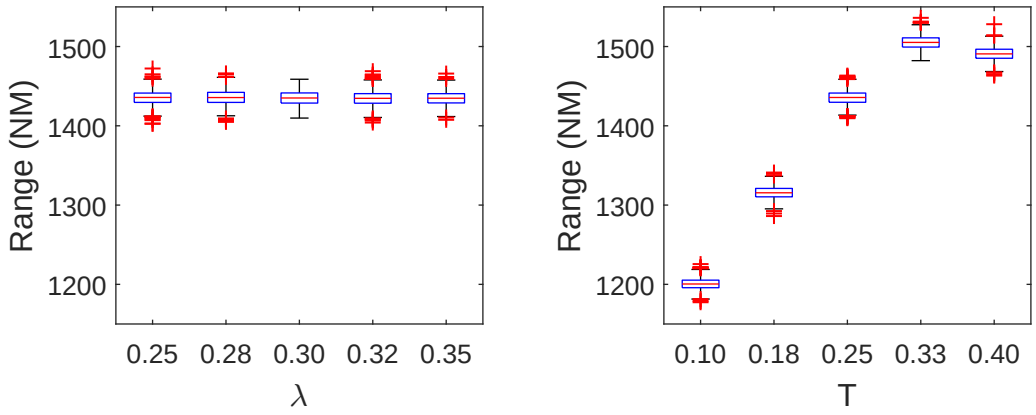

(a) Taper Ratio (b) Throttle Setting

Figure 108: Variation of uncertainty on range (R) with respect to Taper Ratio (λ) and Throttle Setting (T) around the baseline for SST design problem

space reduction strategy to reduce the design space to less than 10% of initial design space for h, M, AR, and Λ. Figure 107 shows the optimum subsystem level design variables evaluated by system and all the subsystem optimizers at the end of each cycle. Compared to system level variables, convergence history of subsystem design variables have not been very smooth. The fluctuations of optimum design variable happens when the system objective function is not very sensitive with respect to that particular variable. For example, system objective in case of the SST problem is not very sensitive to taper ratio λ, which causes considerable fluctuation in convergence history. Whereas, throttle setting has a greater impact on system objective function which leads to a smoother convergence history. The sensitivity of system metric R with respect to λ and T can be observed in Figure 108 where uncertainty on R is plotted for a different setting of λ and T while keeping all the other variables fixed at baseline setting. As observed, uncertainty on range does not change much with λ whereas change in setting of T has a greater impact on range.

Figure 109 and Figure 110 shows histograms of design samples at the end of 1^{st}, 7^{th} and 15^{th} cycle for system and subsystem design variables, respectively. Similar to the analytical problem, it is observed that with each cycle, design samples start

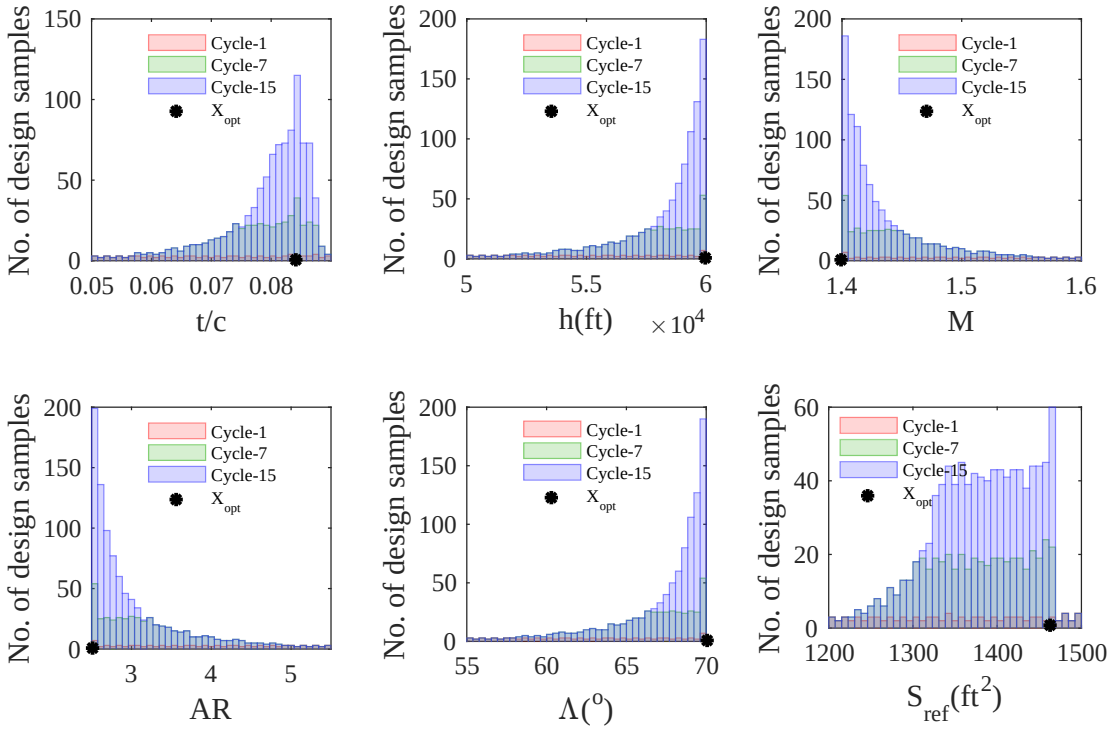

Figure 109: Histogram of design points for system design variables at end of $1^{st}, 7^{th}$ and 15^{th} cycle for SST design problem case-1

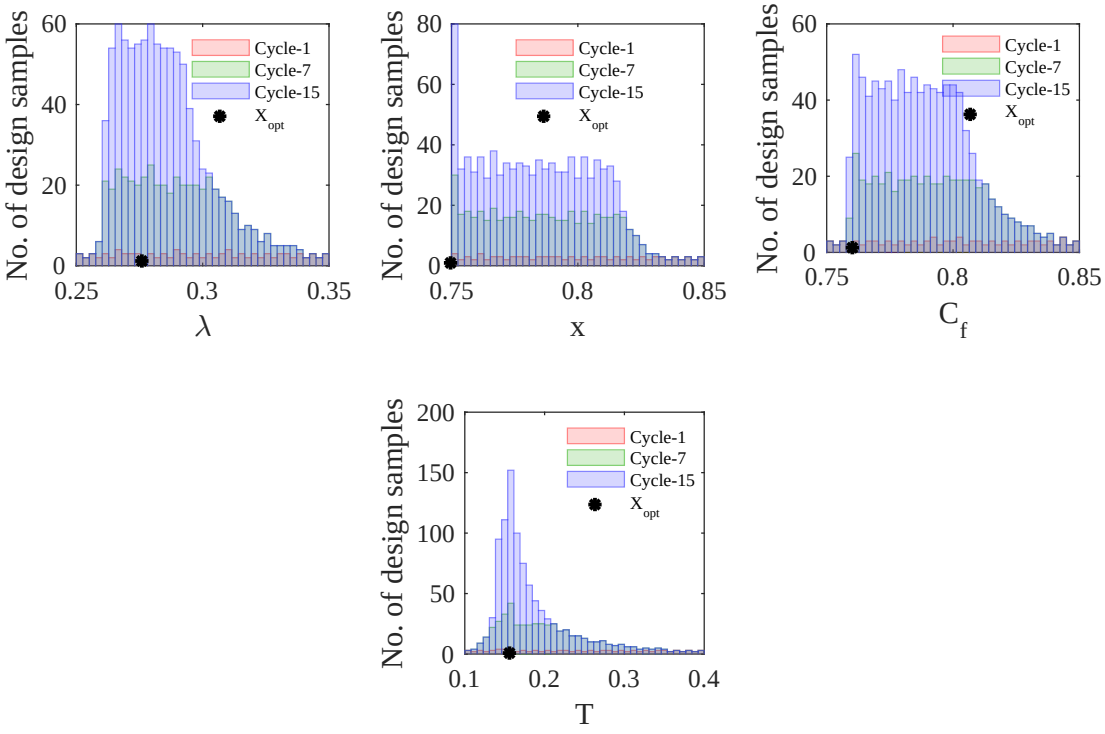

Figure 110: Histogram of design points for subsystem design variables at end of 1^{st}, 7^{th} and 15^{th} cycle for SST design problem case-1

concentrating near the optimum setting of the design variable. Figure 111 shows improvement in accuracy of a quantile copula regression with cycle. The probability density functions of range estimated using quantile copula regression are plotted for cycles $1, 3, 7$ and 15 at the optimum design at the respective cycle and compared with true uncertainty estimated using the SOFPI method. As observed, the quantile copula regression has been able to achieve an accurate estimate of uncertainty from the 7^{th} cycle. It is also observed that with improvement in accuracy of quantile copula regression, the performance of system metric also improved with each cycle which is seen by the shift of probability density function towards higher values of system metric, range (R), with increment of cycle.

Figure 112 shows the scatter plot matrix of coupling and state variables at optimum design of SST design problem case-1 estimated by the CO-PADMA method and compared with the UMDO-SOFPI and MM methods. Almost all the dependencies have been found to be elliptical, similar to a multivariate Gaussian distribution. Very strong statistical dependency has been found among W_T, L and θ, which has been well captured by the CO-PADMA method. Although the MM method has been able to accurately estimate the marginal distributions of coupling variables, it was unable to capture these dependencies because it has been assumed that the coupling variables are independent. Figure 113 compares the contour plot of joint probability density of optimum interdisciplinary compatible solution of W_T and W_E estimated by all the UMDO-SOFPI, MM and CO-PAMDA methods. Although the dependency between W_T and W_E is not very high, the CO-PADMA method has been able to capture the overall trend of joint probability density better than the MM method.

The linear dependencies are quantified with Pearson's correlation matrix in Table 37. Almost all the correlation coefficients estimated by the CO-PADMA process have been found to be within 5% error except the dependency between W_T and W_f, which has an error of 13%. To quantify any underlying non-linear dependency Mutual

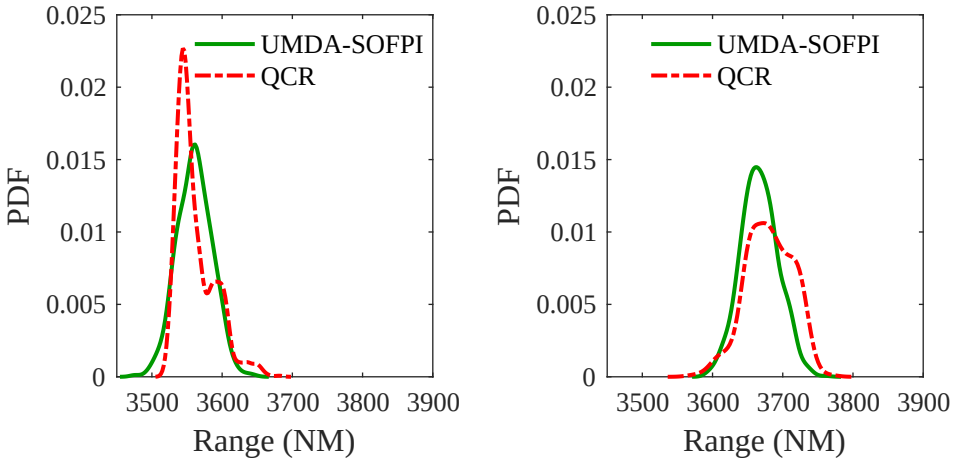

(a) Cycle-1

(b) Cycle-3

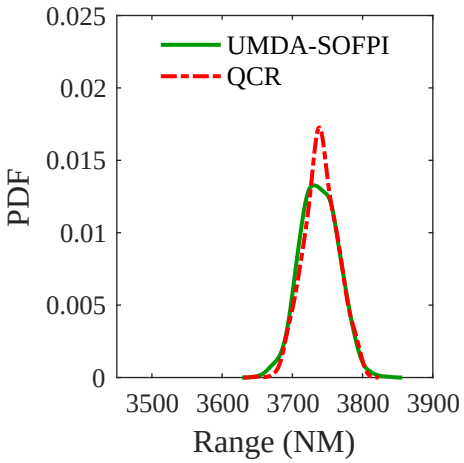

(c) Cycle-7

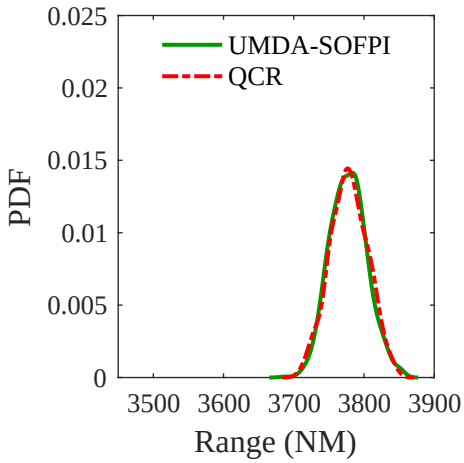

(d) Cycle-15

Figure 111: Improvement in accuracy of quantile copula regression (QCR) with each cycle for SST design problem case-1

Table 37: Comparison of Correlation Matrix of coupling and state variables of SST design problem case-1

Correlation Matrix

		$W_T(lb)$	$W_f(lb)$	θ	$L(lb)$	$D(lb)$	$W_E(lb)$	ESF
UMDO-SOFPI	$W_T(lb)$	1.00	0.08	-1.00	1.00	0.25	0.49	0.25
	$W_f(lb)$	0.08	1.00	-0.08	0.08	-0.03	-0.08	-0.03
	θ	-1.00	-0.08	1.00	-1.00	-0.24	-0.49	-0.24
	$L(lb)$	1.00	0.08	-1.00	1.00	0.25	0.49	0.25
	$D(lb)$	0.25	-0.03	-0.24	0.25	1.00	0.57	1.00
	$W_E(lb)$	0.49	-0.08	-0.49	0.49	0.57	1.00	0.57
	ESF	0.25	-0.03	-0.24	0.25	1.00	0.57	1.00
		$W_T(lb)$	$W_f(lb)$	θ	$L(lb)$	$D(lb)$	$W_E(lb)$	ESF
CO-PADMA	$W_T(lb)$	1.00	-0.04	-1.00	1.00	0.29	0.53	0.29
	$W_f(lb)$	-0.04	1.00	0.04	-0.04	-0.01	-0.05	-0.01
	θ	-1.00	0.04	1.00	-1.00	-0.29	-0.53	-0.29
	$L(lb)$	1.00	-0.04	-1.00	1.00	0.29	0.53	0.29
	$D(lb)$	0.29	-0.01	-0.29	0.29	1.00	0.58	1.00
	$W_E(lb)$	0.53	-0.05	-0.53	0.53	0.58	1.00	0.58
	ESF	0.29	-0.01	-0.29	0.29	1.00	0.58	1.00
		$W_T(lb)$	$W_f(lb)$	θ	$L(lb)$	$D(lb)$	$W_E(lb)$	ESF
$\Delta\rho$ error	$W_T(lb)$	0.00	0.13	0.00	0.00	0.04	0.04	0.04
	$W_f(lb)$	0.13	0.00	0.13	0.13	0.02	0.02	0.02
	θ	0.00	0.13	0.00	0.00	0.05	0.04	0.05
	$L(lb)$	0.00	0.13	0.00	0.00	0.04	0.04	0.04
	$D(lb)$	0.04	0.02	0.05	0.04	0.00	0.01	0.00
	$W_E(lb)$	0.04	0.02	0.04	0.04	0.01	0.00	0.01
	ESF	0.04	0.02	0.05	0.04	0.00	0.01	0.00

Information is computed and compared in Table 38. CO-PADMA has been able to estimate the Mutual Information among the coupling variables within 5% error.

Convergence history of optimum objective function with respect to disciplinary uncertainty quantification and propagation (UQP) function calls are plotted and compared in Figure 114. Convergence history trend with respect to UQP function calls for the UMDO-SOFPI and CO-PADMA methods has been found to be very similar. The convergence history of optimum objective function is plotted against time in Figure 126, where t_{avg} is the average time for each disciplinary UQP call. While the optimization routine could have been stopped by around $4,000t_{avg}$ ($4,000$ UQP calls

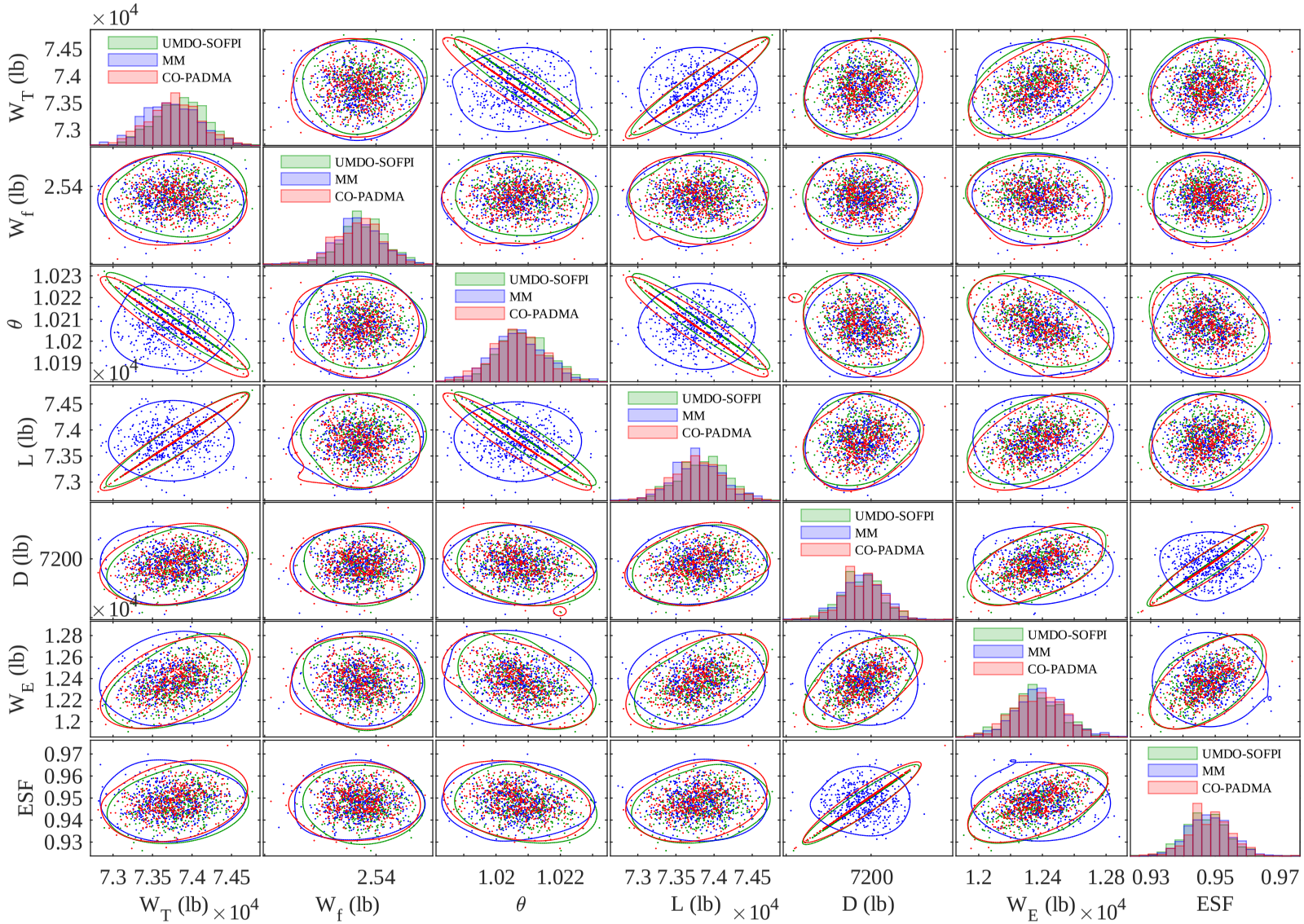

Figure 112: Scatter plot matrix of coupling and state variables at optimum design of SST design problem case-1

Table 38: Comparison of Mutual Information (MI) matrix of coupling and state variables of SST design problem case-1

Mutual Information Matrix

		$W_T(lb)$	$W_f(lb)$	θ	$L(lb)$	$D(lb)$	$W_E(lb)$	ESF
UMDO-SOFPI	$W_T(lb)$	1.17	0.03	1.17	1.17	0.05	0.16	0.05
	$W_f(lb)$	0.03	1.20	0.03	0.03	0.03	0.04	0.03
	θ	1.17	0.03	1.17	1.17	0.05	0.15	0.05
	$L(lb)$	1.17	0.03	1.17	1.17	0.05	0.16	0.05
	$D(lb)$	0.05	0.03	0.05	0.05	1.18	0.20	1.18
	$W_E(lb)$	0.16	0.04	0.15	0.16	0.20	1.19	0.20
	ESF	0.05	0.03	0.05	0.05	1.18	0.20	1.18
		$W_T(lb)$	$W_f(lb)$	θ	$L(lb)$	$D(lb)$	$W_E(lb)$	ESF
CO-PADMA	$W_T(lb)$	1.19	0.04	1.19	1.19	0.08	0.18	0.08
	$W_f(lb)$	0.04	1.15	0.04	0.04	0.04	0.03	0.04
	θ	1.19	0.04	1.19	1.19	0.08	0.18	0.08
	$L(lb)$	1.19	0.04	1.19	1.19	0.08	0.18	0.08
	$D(lb)$	0.08	0.04	0.08	0.08	1.18	0.22	1.18
	$W_E(lb)$	0.18	0.03	0.18	0.18	0.22	1.15	0.22
	ESF	0.08	0.04	0.08	0.08	1.18	0.22	1.18
		$W_T(lb)$	$W_f(lb)$	θ	$L(lb)$	$D(lb)$	$W_E(lb)$	ESF
ΔMI **error**	$W_T(lb)$	0.02	0.01	0.02	0.02	0.02	0.02	0.02
	$W_f(lb)$	0.01	0.05	0.01	0.01	0.01	0.01	0.01
	θ	0.02	0.01	0.02	0.02	0.03	0.02	0.03
	$L(lb)$	0.02	0.01	0.02	0.02	0.02	0.02	0.02
	$D(lb)$	0.02	0.01	0.03	0.02	0.00	0.01	0.00
	$W_E(lb)$	0.02	0.01	0.02	0.02	0.01	0.04	0.01
	ESF	0.02	0.01	0.03	0.02	0.00	0.01	0.00

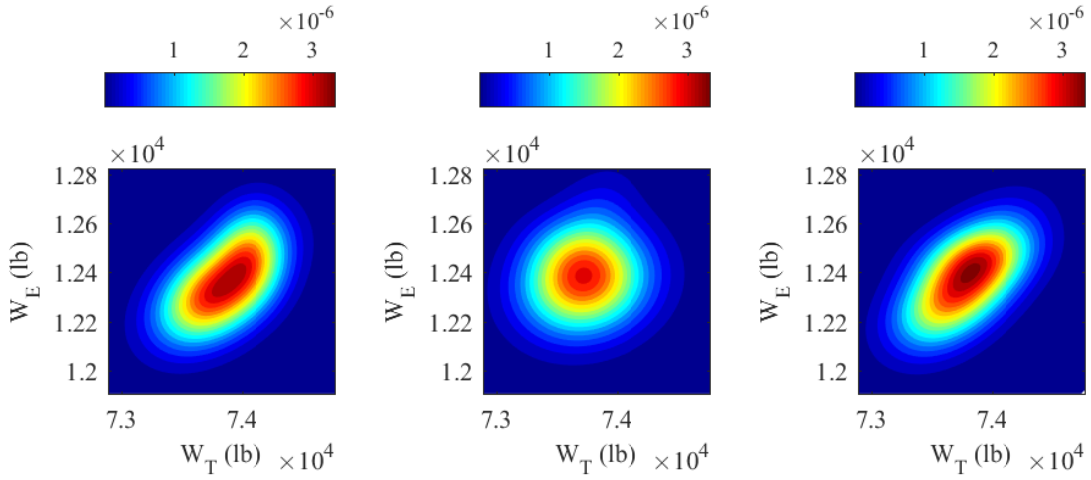

(a) UMDO-SOFPI (b) MM (c) CO-PADMA

Figure 113: Contour plot of joint probability density of optimum interdisciplinary compatible solution of W_T and W_E for SST design problem case-1

for UMDO-SOFPI and cycle 3 for CO-PADMA method), the optimization routine has been continued to ensure overall convergence. Both the UDMO-SOFPI and CO-PADMA methods took almost similar time to achieve overall convergence, but it is observed that the first near-optimum solution achieved by the CO-PADMA method (end of cycle-1) has been achieved in around one-third the time of the UMDO-SOFPI method (required around $2,000$ UQP calls). This is mainly due to the fact that there are three disciplines which have been analyzed concurrently in the CO-PADMA process.

6.4.5.3 Results: SST design problem Case-2

In the case-2 of SST design problem some of the uncertain parameters (W_O, C_{DMIN} and W_{BE}) are assumed to have non-Gaussian distribution. Similar to case-1, 15 cycles of CO-PADMA have been carried to evaluate the optimum solution. The system level optimum design variables are listed in Table 39 and subsystem level optimum design variables are listed in Table 40. The tables also compare the results

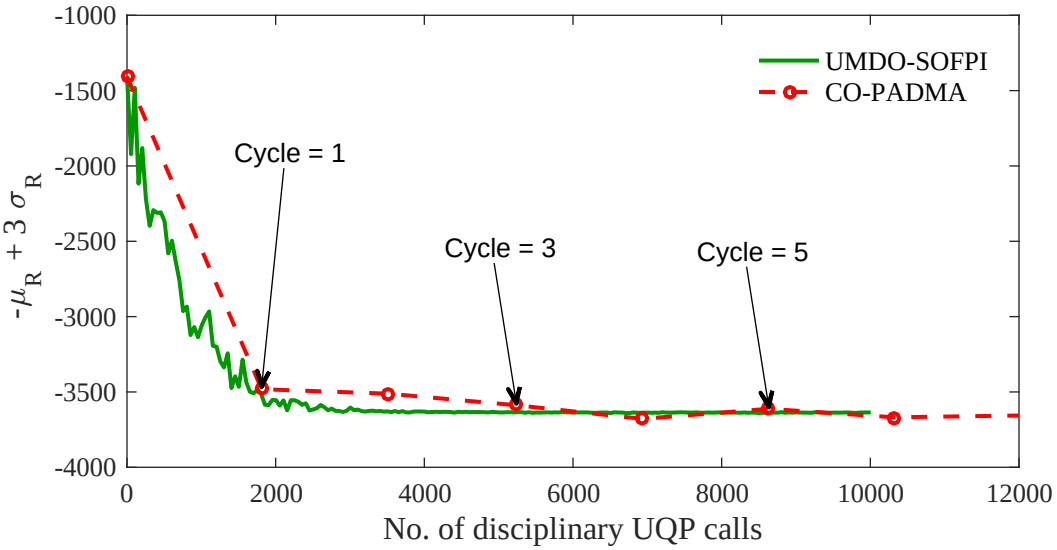

Figure 114: Comparison of convergence characteristics of optimum objective function with respect to disciplinary uncertainty quantification and propagation function calls for SST design problem case-1

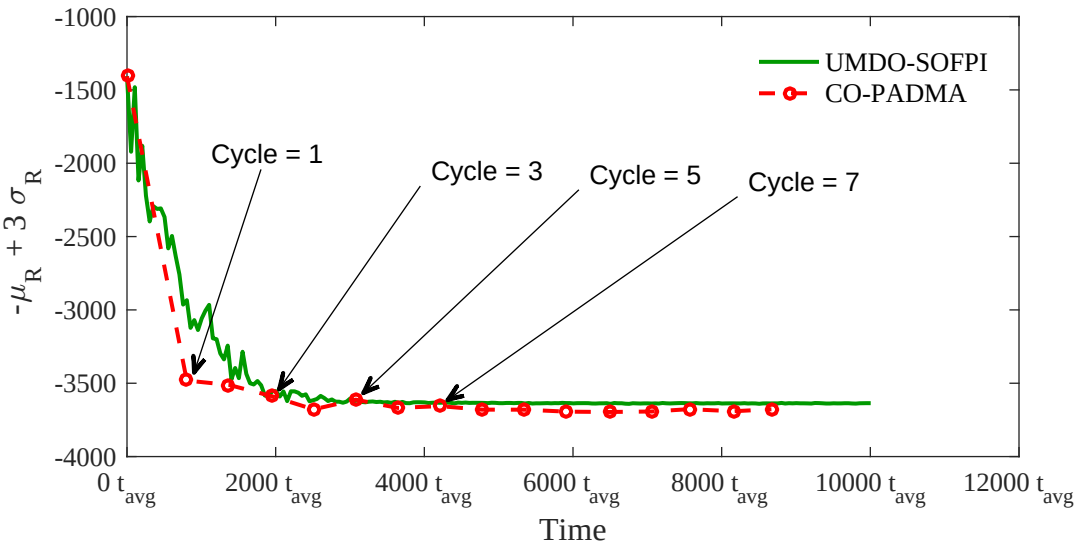

Figure 115: Comparison of convergence characteristics of optimum objective function with respect to time for SST design problem case-1, where t_{avg} is the average time for each disciplinary UQP call

of the CO-PADMA process with true optimum results evaluated using the UMDO-SOFPI method. All the system level design variables have been found to converge with 1.2% error. The optimum design evaluated in case-2 has been found to be very similar to the case-1 problem. Except for t/c, all the other system design variables have converged at the boundary of design space. The subsystem design variables also converged to a value very close to a true solution with the worst cases being λ (3.8% error) and x (1.4% error).

The probability density function and cumulative density function of optimum system metric range (R) evaluated by the CO-PADMA process is plotted in Figure 116. Results are compared with probability density function and cumulative density function estimated by the UMDO-SOFPI and MM methods estimated at true optimum obtained by the UMDO-SOFPI method. Unlike case-1, the probability density function of range has been found to be negatively skewed. The skewness of the probability density function is well captured by the CO-PADMA method whereas the MM method predicted a symmetrical distribution. The statistical metrics of range is listed and compared in Table 41. Both the CO-PADMA and MM methods have been able to predict the statistical mean accurately. However, as predicted by the probability density plot the standard deviation of the MM method is off by 14.3% when compared to the CO-PADMA method which is off by only 6.9%. Skewness estimated by the CO-PADMA process has been found to be very close to the UMDO-SOFPI method, whereas the MM method predicted a very low value of skewness. In terms of closeness of overall distribution measured by K-L divergence, CO-PAMDA method with K-L div. = 0.01 has been able to find better solution when compared to the MM method with K-L div. = 0.14.

Figure 117 shows the optimum system level design variables evaluated by system and all the subsystem optimizers at the end of each cycle. Similar to case-1, all the optimizers have been found to be very consistent for all the system design variables

Table 39: Comparison of optimum system level design variables for SST design problem case-2

	t/c	$h(ft)$	M	AR	$\Lambda(^o)$	$S_{ref}(ft^2)$
UMDO-SOFPI	0.085	60000	1.4	2.5	70.0	1492.766
CO-PADMA	0.084	60000	1.4	2.5	70.0	1498.286
$\Delta \mathbf{x}^*_{norm}$	0.012	0.0	0.0	0.0	0.0	0.004

Table 40: Comparison of optimum subsystem level design variables for SST design problem case-2

	λ	x	C_f	T
UMDO-SOFPI	0.278	0.781	0.755	0.156
CO-PADMA	0.289	0.770	0.758	0.156
$\Delta \mathbf{x}^*_{norm}$	0.038	0.014	0.005	0.000

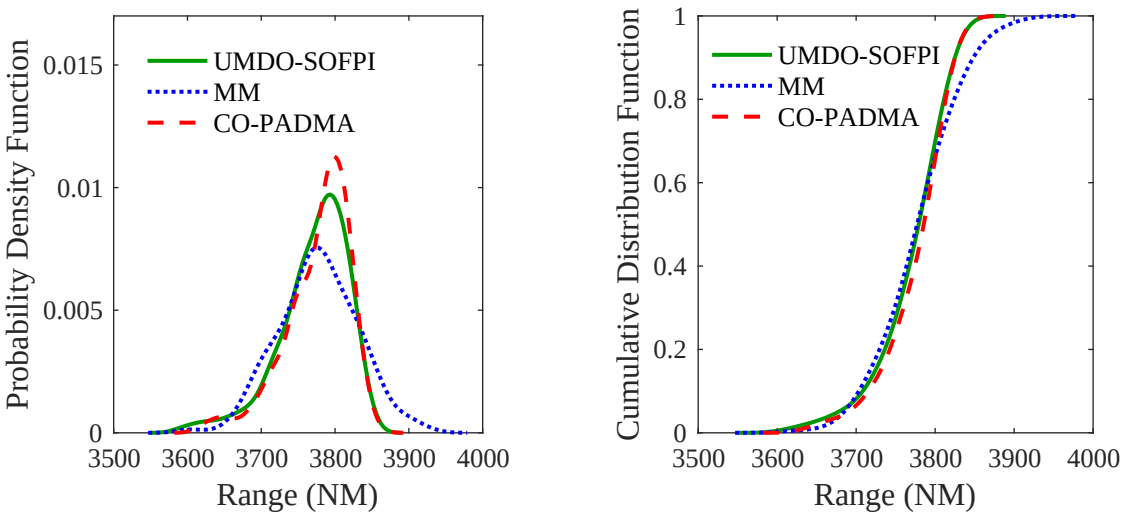

(a) Probability density function

(b) Cumulative distribution function

Figure 116: Comparison of probability density function and cumulative distribution function of system metric range (R) at optimum design estimated using benchmark UMDO-SOFPI method, Moment Matching method (MM) and CO-PADMA method for SST design problem case-2

Table 41: Comparison of statistical metrics of system metric range (R) for SST design problem case-2

	UMDO-SOFPI	**MM**	**CO-PADMA**
Mean(μ_R)	3771.09	3776.86	3776.31
Std. Dev.(σ_R)	47.16	53.93	43.90
Skewness (γ_R)	-1.13	-0.06	-1.12
K-L div.	-	0.14	0.01

which allow design space reduction strategy to reduce the design space to less than 10% of initial design space for h, M, AR, and Λ. Figure 118 shows the optimum subsystem level design variables evaluated by system and all the subsystem optimizers at the end of each cycle. As in case-1, optimum value of λ varies a lot with each cycle compared to the other variables.

Figure 119 and Figure 120 shows histogram of design samples at the end of the 1^{st}, 7^{th} and 15^{th} cycles for system and subsystem design variables, respectively. Similar to case-1, it is observed that the with each cycle, design samples start concentrating near the optimum setting of system design variable. However, due to a large variation in the optimum solution of subsystem design variables, the design samples were uniformly distributed in the reduced space. This is particularly seen in λ, x, and C_f. Figure 121 shows improvement in accuracy of quantile copula regression with cycle. The probability density functions of range estimated using quantile copula regression are plotted for cycles $1, 3, 7$ and 15 at the optimum design at the respective cycle and compared with true uncertainty estimated using the SOFPI method. The quantile copula regression has been found to be have very high inaccuracy in the 1^{st} cycle, but accuracy improved significantly after the 3^{rd} cycle. It is also observed that with improvement in the accuracy of quantile copula regression, the performance of system metric also improved with each cycle, which is seen by the shift of probability density function toward the higher value of system metric, range (R), with each cycle.

Figure 122 shows the scatter plot matrix of coupling and state variables at optimum design as estimated by the CO-PADMA method and compared with the UMDO-SOFPI and MM methods. Unlike case-1, dependencies among only few variables have been found to be elliptical. Most of the dependencies with respect to D, W_E and ESF have been found to be non-elliptical, which has been well captured by the CO-PADMA method. Very strong statistical dependency has been found among W_T, L and θ, similar to case-1, which has been well estimated by the CO-PADMA method. Figure 123

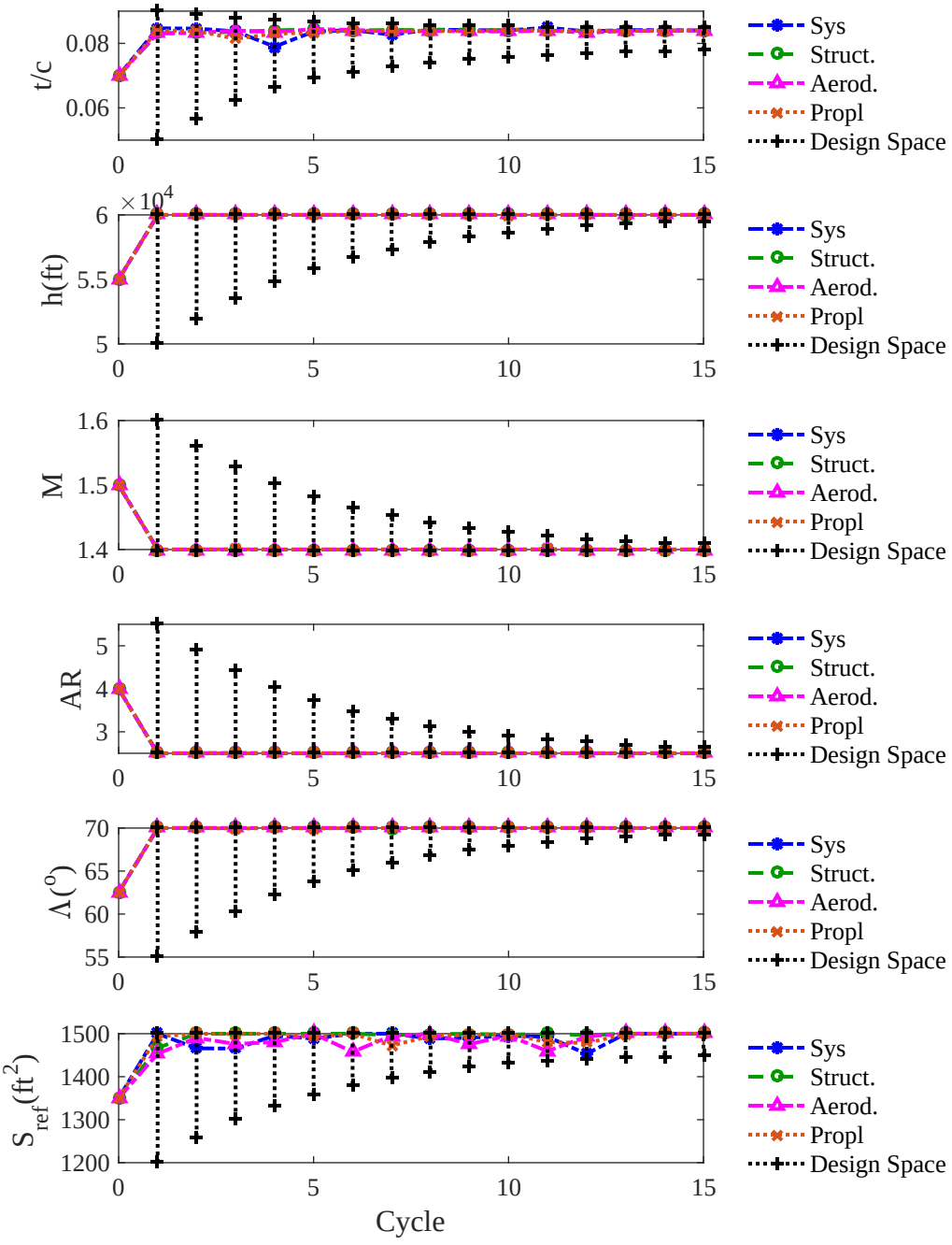

Figure 117: Optimum system design variables estimated by system and subsystem optimizers and design space reduction at the end of each cycle for SST design problem case-2

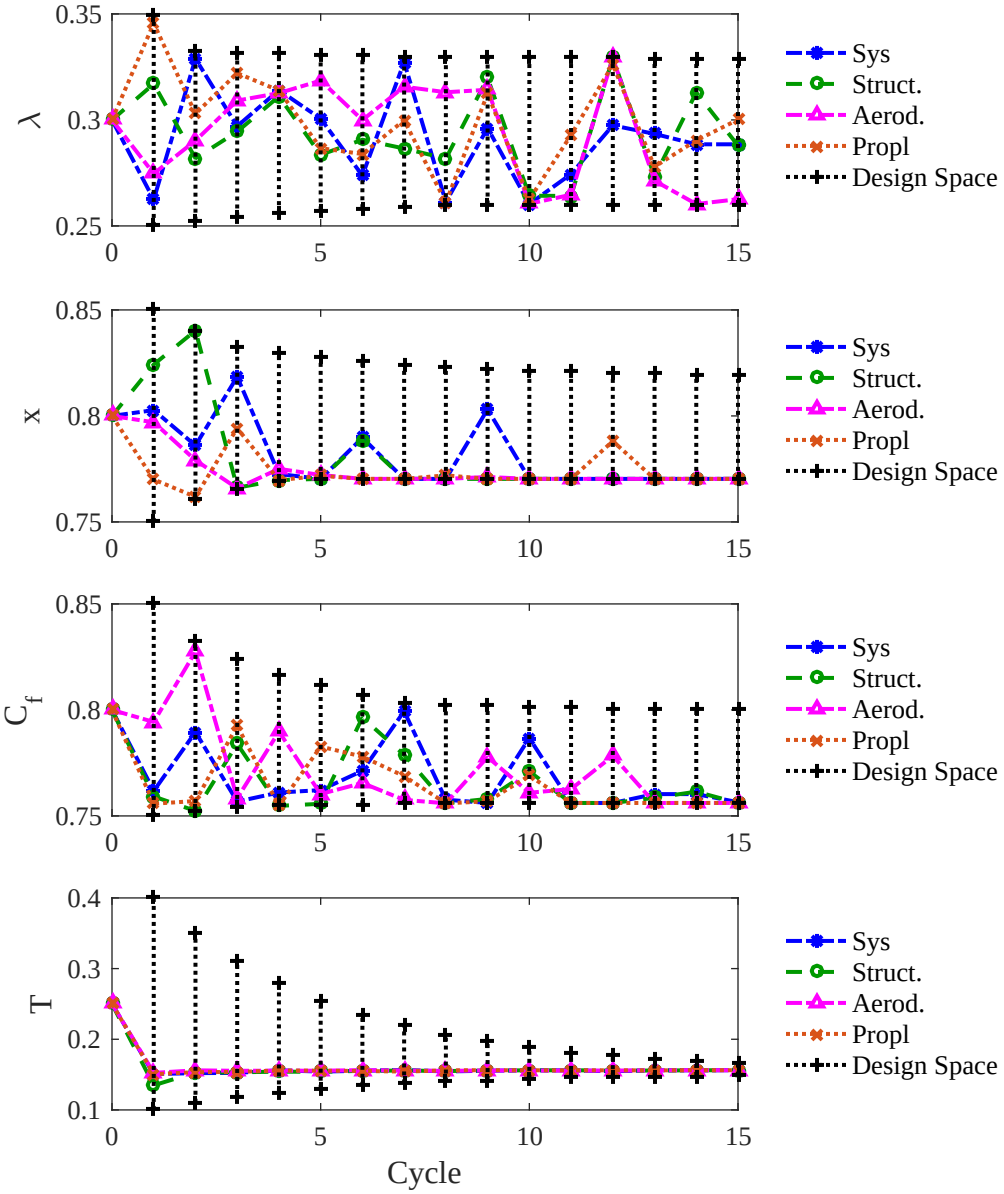

Figure 118: Optimum subsystem design variables estimated by system and subsystem optimizers and design space reduction at the end of each cycle for SST design problem case-2

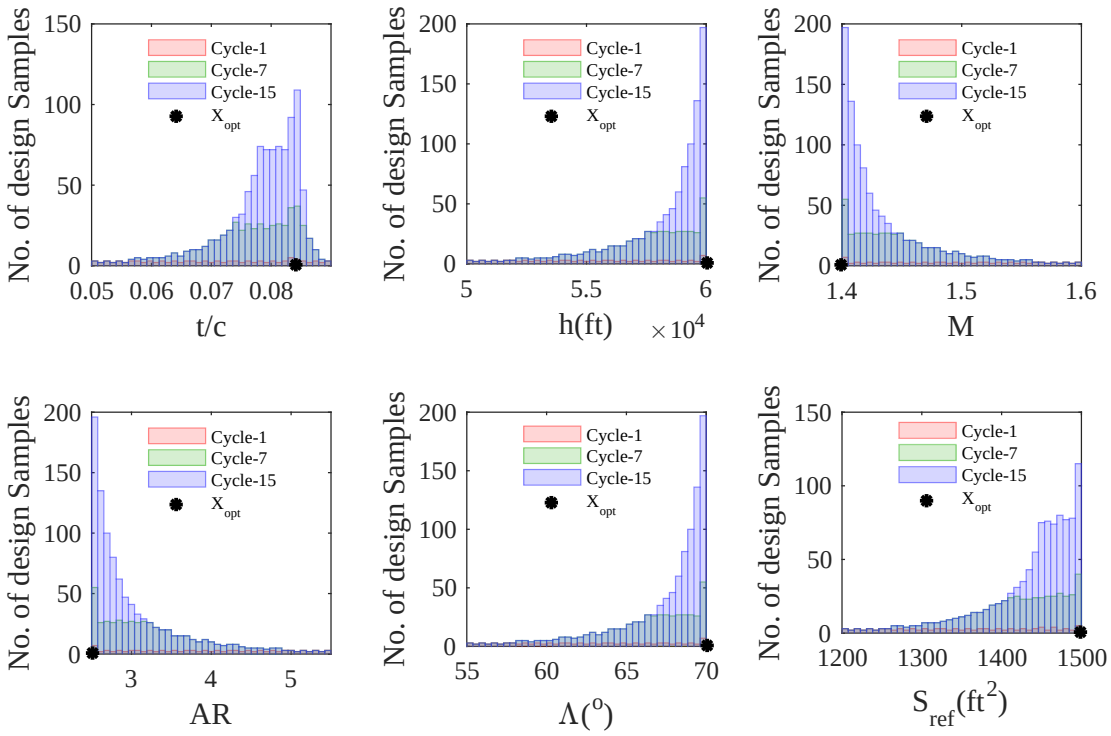

Figure 119: Histogram of design points for system design variables at end of $1^{st}, 7^{th}$ and 15^{th} cycle for SST design problem case-2

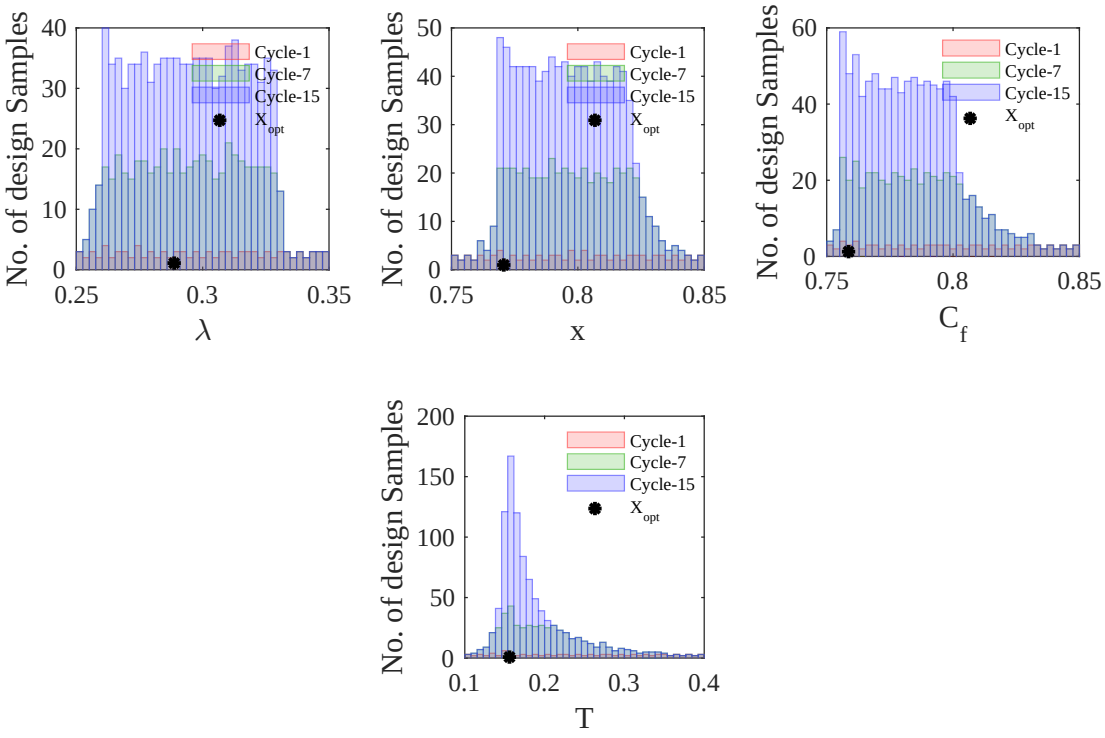

Figure 120: Histogram of design points for subsystem design variables at end of 1^{st}, 7^{th} and 15^{th} cycle for SST design problem case-2

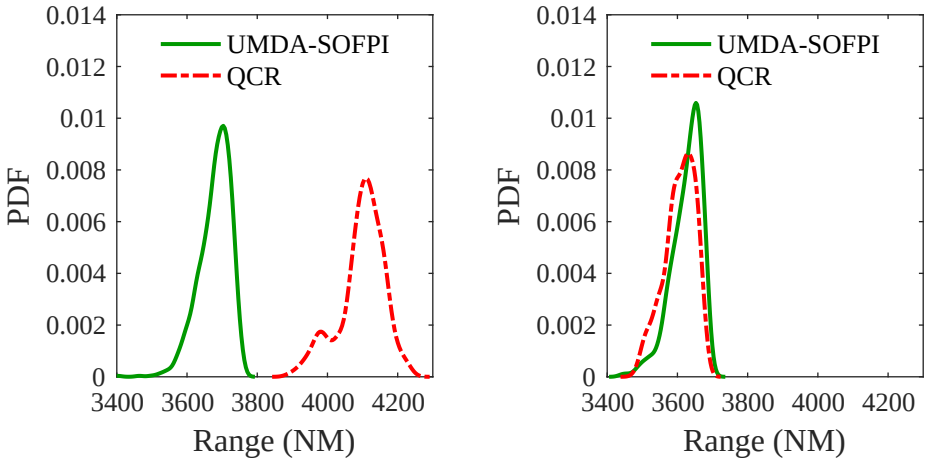

(a) Cycle-1 (b) Cycle-3

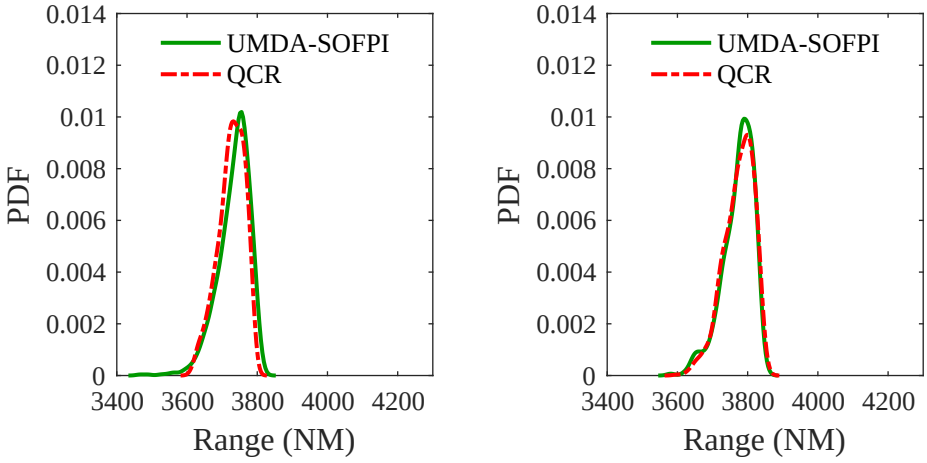

(c) Cycle-7 (d) Cycle-15

Figure 121: Improvement in accuracy of quantile copula regression (QCR) with each cycle for SST design problem case-2

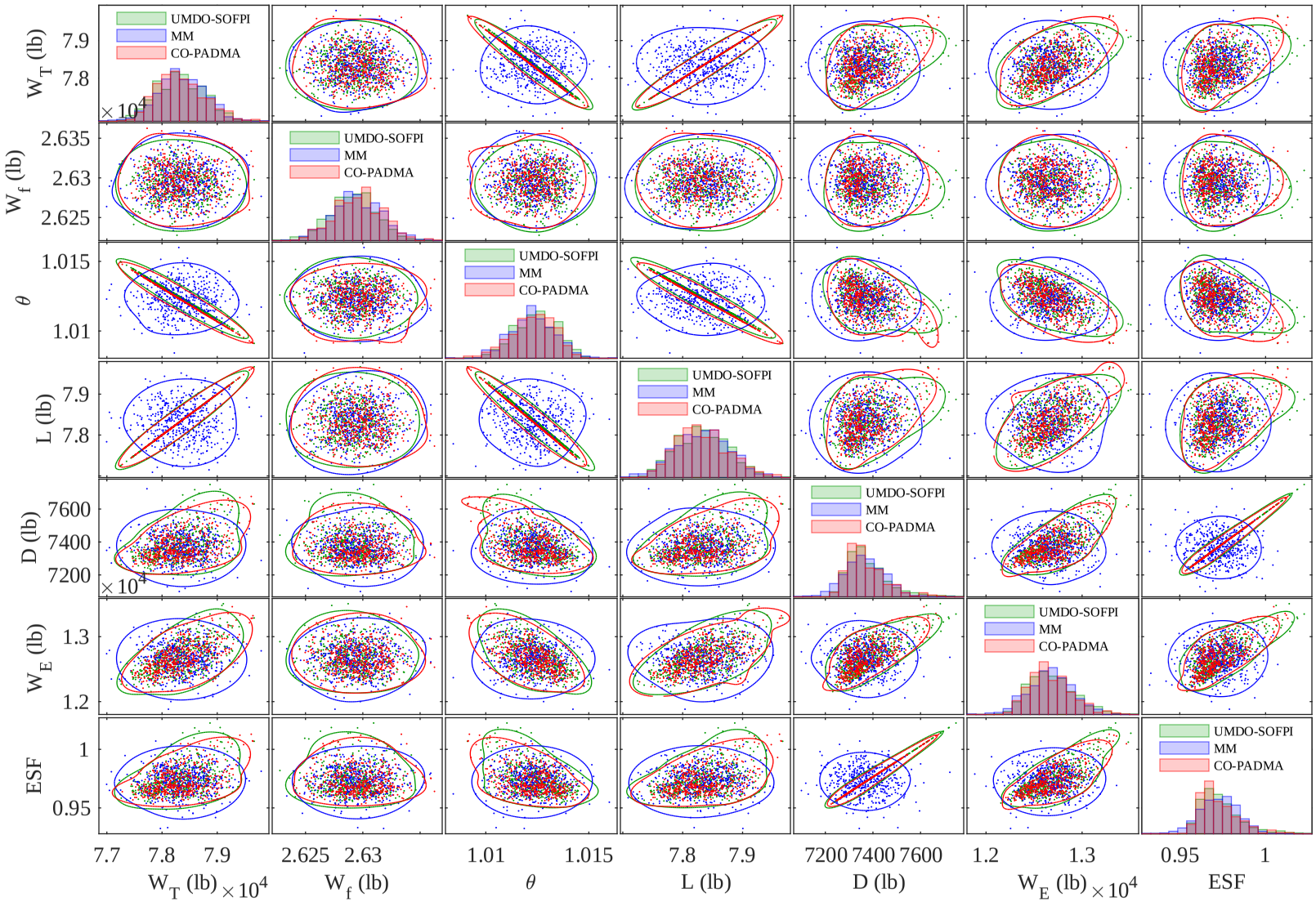

Figure 122: Scatter plot matrix of coupling and state variables at optimum design of SST design problem case-2

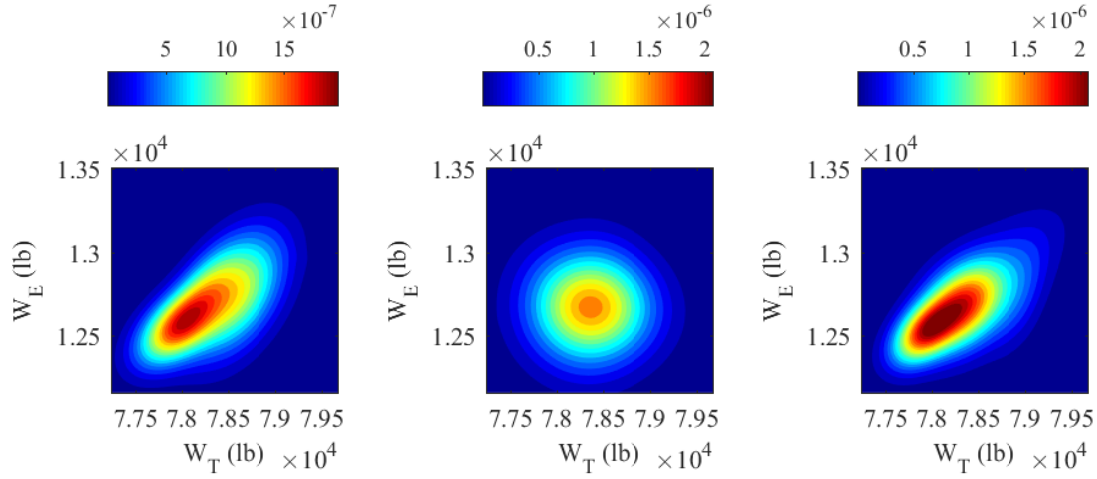

(a) UMDO-SOFPI (b) MM (c) CO-PADMA

Figure 123: Contour plot of joint probability density of optimum interdisciplinary compatible solution of W_T and W_E for SST design problem case-2

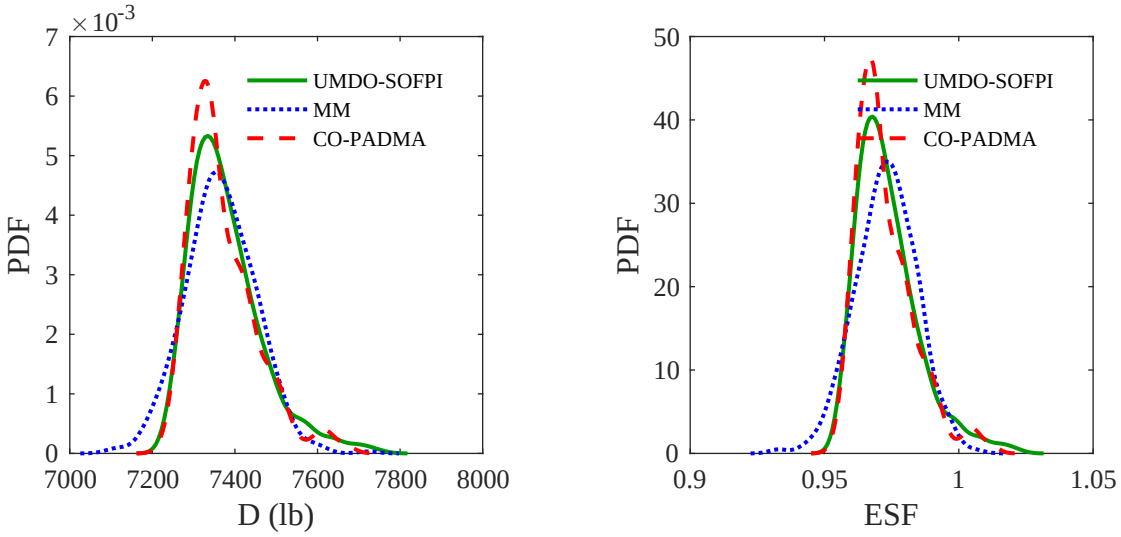

(a) Probability density function of Drag (D)

(b) Probability density function of Engine Scale Factor (ESF)

Figure 124: Comparison of probability density function of Drag (D) and Engine Scale Factor (ESF) at optimum design estimated using benchmark UMDO-SOFPI method, Moment Matching method (MM) and CO-PADMA method for SST design problem case-2

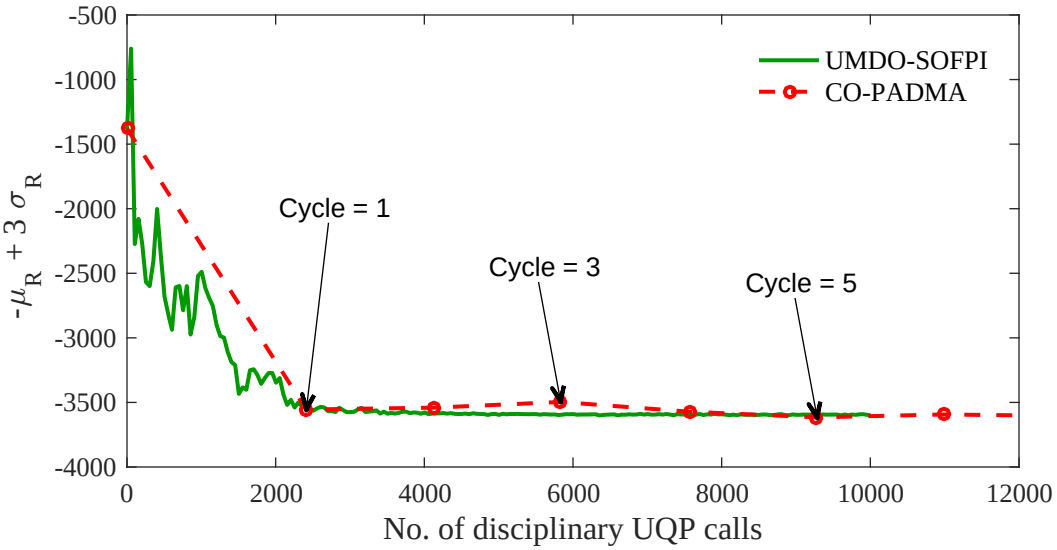

Figure 125: Comparison of convergence characteristics of optimum objective function with respect to disciplinary uncertainty quantification and propagation function calls for SST design problem case-2

compares the contour plot of joint probability density of optimum interdisciplinary compatible solution of W_T and W_E estimated by all the UMDO-SOFPI, MM and CO-PAMDA methods. Similar to case-1, the CO-PADMA method has been able to capture the overall trend of joint probability density better than the MM method. In addition to not capturing these dependencies, the MM method has not been able to accurately estimate the marginal distribution of D, W_E, and ESF. The true probability density functions of D and ESF are skewed whereas the MM method assumed a symmetrical Gaussian distribution for these variables as shown in Figure 124.

The linear dependencies are quantified with Pearson's correlation matrix in Table 42. Almost all the correlation coefficients estimated by the CO-PADMA process has been found to be within 5% error. To quantify any underlying non-linear dependency Mutual Information is computed and compared in Table 43. Most of the Mutual Information among state variables has been captured by the CO-PADMA method with 4% error, except for Mutual Information between W_T, L and θ.

Table 42: Comparison of Correlation Matrix of coupling and state variables of SST design problem case-2

Correlation Matrix

		$W_T(lb)$	$W_f(lb)$	θ	$L(lb)$	$D(lb)$	$W_E(lb)$	ESF
UMDO-SOFPI	$W_T(lb)$	1.00	-0.02	-1.00	1.00	0.42	0.60	0.42
	$W_f(lb)$	-0.02	1.00	0.02	-0.02	-0.03	-0.08	-0.03
	θ	-1.00	0.02	1.00	-1.00	-0.42	-0.60	-0.42
	$L(lb)$	1.00	-0.02	-1.00	1.00	0.42	0.60	0.42
	$D(lb)$	0.42	-0.03	-0.42	0.42	1.00	0.73	1.00
	$W_E(lb)$	0.60	-0.08	-0.60	0.60	0.73	1.00	0.73
	ESF	0.42	-0.03	-0.42	0.42	1.00	0.73	1.00
		$W_T(lb)$	$W_f(lb)$	θ	$L(lb)$	$D(lb)$	$W_E(lb)$	ESF
CO-PADMA	$W_T(lb)$	1.00	-0.04	-1.00	1.00	0.43	0.63	0.43
	$W_f(lb)$	-0.04	1.00	0.04	-0.04	-0.02	-0.03	-0.02
	θ	-1.00	0.04	1.00	-1.00	-0.43	-0.63	-0.43
	$L(lb)$	1.00	-0.04	-1.00	1.00	0.43	0.63	0.43
	$D(lb)$	0.43	-0.02	-0.43	0.43	1.00	0.69	1.00
	$W_E(lb)$	0.63	-0.03	-0.63	0.63	0.69	1.00	0.69
	ESF	0.43	-0.02	-0.43	0.43	1.00	0.69	1.00
		$W_T(lb)$	$W_f(lb)$	θ	$L(lb)$	$D(lb)$	$W_E(lb)$	ESF
$\Delta\rho$ error	$W_T(lb)$	0.00	0.02	0.00	0.00	0.01	0.03	0.01
	$W_f(lb)$	0.02	0.00	0.02	0.02	0.01	0.05	0.01
	θ	0.00	0.02	0.00	0.00	0.00	0.03	0.00
	$L(lb)$	0.00	0.02	0.00	0.00	0.01	0.03	0.01
	$D(lb)$	0.01	0.01	0.00	0.01	0.00	0.03	0.00
	$W_E(lb)$	0.03	0.05	0.03	0.03	0.03	0.00	0.03
	ESF	0.01	0.01	0.00	0.01	0.00	0.03	0.00

Table 43: Comparison of Mutual Information (MI) matrix of coupling and state variables of SST design problem case-2

Mutual Information Matrix

		$W_T(lb)$	$W_f(lb)$	θ	$L(lb)$	$D(lb)$	$W_E(lb)$	ESF
UMDO-SOFPI	$W_T(lb)$	1.06	0.04	1.06	1.06	0.11	0.22	0.11
	$W_f(lb)$	0.04	1.22	0.04	0.04	0.04	0.03	0.04
	θ	1.06	0.04	1.07	1.06	0.12	0.22	0.12
	$L(lb)$	1.06	0.04	1.06	1.06	0.11	0.22	0.11
	$D(lb)$	0.11	0.04	0.12	0.11	1.23	0.36	1.23
	$W_E(lb)$	0.22	0.03	0.22	0.22	0.36	1.11	0.36
	ESF	0.11	0.04	0.12	0.11	1.23	0.36	1.23
		$W_T(lb)$	$W_f(lb)$	θ	$L(lb)$	$D(lb)$	$W_E(lb)$	ESF
CO-PADMA	$W_T(lb)$	1.20	0.02	1.20	1.20	0.13	0.26	0.13
	$W_f(lb)$	0.02	1.11	0.02	0.02	0.03	0.03	0.03
	θ	1.20	0.02	1.20	1.20	0.13	0.26	0.13
	$L(lb)$	1.20	0.02	1.20	1.20	0.13	0.26	0.13
	$D(lb)$	0.13	0.03	0.13	0.13	1.22	0.33	1.22
	$W_E(lb)$	0.26	0.03	0.26	0.26	0.33	1.15	0.33
	ESF	0.13	0.03	0.13	0.13	1.22	0.33	1.22
		$W_T(lb)$	$W_f(lb)$	θ	$L(lb)$	$D(lb)$	$W_E(lb)$	ESF
ΔMI **error**	$W_T(lb)$	0.14	0.02	0.14	0.14	0.01	0.04	0.01
	$W_f(lb)$	0.02	0.12	0.02	0.02	0.02	0.00	0.02
	θ	0.14	0.02	0.13	0.14	0.01	0.04	0.01
	$L(lb)$	0.14	0.02	0.14	0.14	0.01	0.04	0.01
	$D(lb)$	0.01	0.02	0.01	0.01	0.01	0.03	0.01
	$W_E(lb)$	0.04	0.00	0.04	0.04	0.03	0.04	0.03
	ESF	0.01	0.02	0.01	0.01	0.01	0.03	0.01

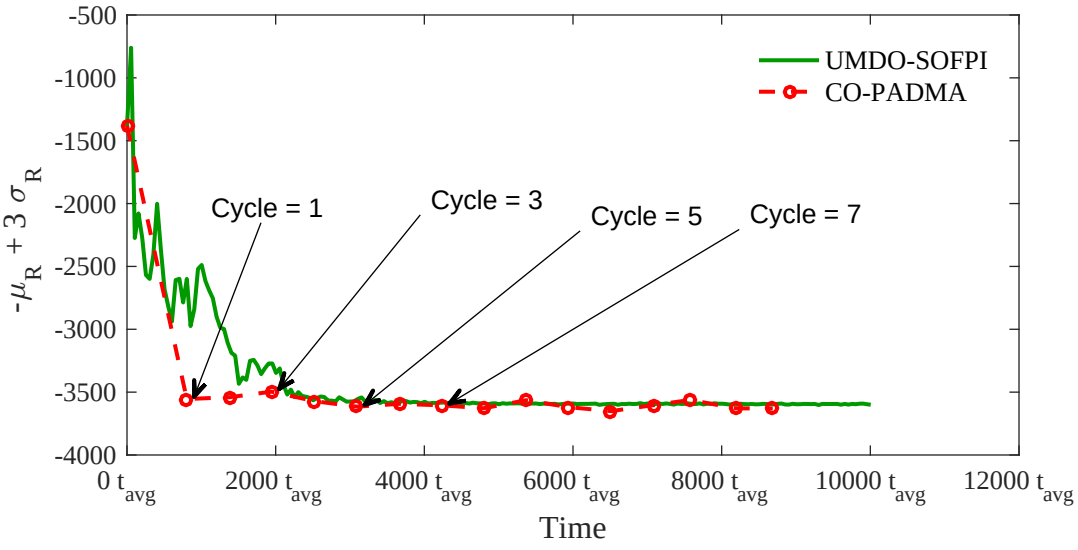

Figure 126: Comparison of convergence characteristics of optimum objective function with respect to time for SST design problem case-2, where t_{avg} is the average time for each disciplinary UQP call

The convergence history of the optimum objective function with respect to disciplinary uncertainty quantification and propagation (UQP) function calls are plotted and compared in Figure 125. Similar to case-1, the convergence history trend with respect to the UQP function calls for both the UMDO-SOFPI and CO-PADMA methods has been found to be very similar. The convergence history of the optimum objective function is plotted against time in Figure 126, where t_{avg} is the average time for each disciplinary UQP call. Although both the UDMO-SOFPI and CO-PADMA methods took almost similar time to achieve overall convergence, it is observed that the first close to optimum solution achieved by the CO-PADMA method (end of cycle-1) has been achieved in around one-third of the time of the UMDO-SOFPI method (required around $2,500$ UQP calls). This is mainly due to the fact that there are three disciplines which were concurrently analyzed in the CO-PADMA process.

6.5 Chapter Summary

The chapter presents the Concurrent Optimization using Probabilistic Analysis of Distributed Multidisciplinary Architectures (CO-PADMA) method, to carry out distributed multidisciplinary design optimization for non-deterministic disciplines. In the CO-PADMA method top level or the system level is mainly responsible for interdisciplinary compatibility and system level optimization using the PADMA method. At the subsystem or discipline level, uncertainty propagation and optimization is carried out using their respective high-fidelity disciplinary analyses and using quantile copula regression for non-local variables.

The CO-PAMDA method is based on model sharing strategy, where quantile copula regressions are used to coordinate the information of non-local variables among the discipline. The accuracy of the method depends on the accuracy of quantile copula regressions. To improve the accuracy of the models, CO-PADMA is iterated through multiple cycles and in each consecutive cycle the domain of the models is reduced based on the information of optimum solution from the previous cycles. Also, at the end of each cycle additional samples of interdisciplinary compatible solutions are added to the database which is used to further improve the accuracy of quantile copula regressions.

The main goal of subsystem optimization is to find high-fidelity optimum based on high-fidelity disciplinary analysis. The interdisciplinary compatible solutions of high-fidelity disciplinary optimum is also added to the database, which helps in improving the accuracy of quantile copula regression near the possible optimum solution for the following cycle.

To test the hypothesis 3.0, the CO-PADMA method is used to carry out distributed optimization for two problems; an analytical problem and a Supersonic Transport (SST) aircraft design problem. To test the robustness of the CO-PADMA

method, two cases in each problem has been tested, one with uncertainties with Gaussian distribution and the other with non-Gaussian distributions. In all the cases, the CO-PADMA method has been able to accurately estimate the optimum solution and accurately quantify the dependence and uncertainty on coupling variables and system metric. The CO-PADMA method has been able to out perform the state of the art, Moment-Matching method, when the uncertainties are non-Gaussian and where the system metric has a significant effect on the dependence of coupling variables.

The main assumption of the CO-PADMA method is the assumption associated with quantile copula regression. In the current work, a quadratic model has been used to model the quantiles of disciplinary metric as well the parameters of copula function. Although CO-PADMA allows improvement in accuracy of quantile copula regression in each cycle, high order or non-linear models are recommended when the design space has high non-linearity or multi-modality. Also, the quantile copula regression used in this work has assumed dependence based on Gaussian copula. In a scenario, where there is tail dependence or non-monotonic dependence, an assumption of Gaussian copula may not be valid.

CHAPTER VII

CONCLUSION

An inherent property of complex system design is uncertainty. One such complex system is aircraft. Design of aircraft without considering uncertainty may lead to over-design or under-design. Therefore, it is important to consider uncertainty in the aircraft design process to avoid an expensive redesign process or performance penalty. To quantify the uncertainties on the system level metric accurately, it is important to capture the interaction of coupling variables among the disciplines in addition to quantifying uncertainties in each discipline independently. Uncertainty-based Multidisciplinary Optimization (UMDO) is a procedure which relies on propagation of uncertainties across several disciplines to quantify the uncertainty of system performance while handling the interdisciplinary interactions. However, in an industrial setting, all the disciplines and subsystems cannot be integrated into a single workbench to carry out uncertainty analysis using an integrated or single level UMDO method.

A distributed or decomposition-based UMDO, is an alternative to integrated UMDO which allows each discipline to carry out uncertainty analysis and design optimization independently and concurrently in a distributed fashion. Nevertheless, there are some shortcomings to the current state of the art of distributed UMDO methods. One of the main challenges in the distributed UMDO process is handling of dependencies and interdisciplinary compatibilities. Most of the current state of the art methods assume that the coupling variables are independent of each other. The assumption of independence may lead to inaccurate quantification of uncertainty when the system level metric is sensitive to the dependence of coupling variables. Also,

interdisciplinary compatibility is generally handled by matching the statistics, such as statistical moments of coupling variables. This does not ensure that the interdisciplinary compatibility is satisfied for each instance or sample of coupling variables and can also lead to inaccurate quantification of system level metric. To overcome some of these challenges, distributed UMDO methods based on approximate model sharing strategy uses approximate models of disciplinary analysis to handle the dependencies and interdisciplinary compatibility. The methods are based on deterministic approximate models which are only applicable for deterministic disciplines with parametric or epistemic uncertainty, such that the disciplinary metric can be modeled explicitly as a function of uncertain variables. However, in many scenarios disciplines are non-deterministic and have aleatory or inherent uncertainty due to numerical error, structural uncertainty, experimental uncertainty, interpolation uncertainty, expert judgment, etc. For non-deterministic disciplines, probabilistic models of disciplinary state variables can capture the inherent uncertainties in the discipline. Nonetheless, there are limitations in the existing probabilistic models in literature to handle non-Gaussian noises or uncertainties, heteroskedasticity and dependence among the multivariate responses.

The research presented in this dissertation comprises methodologies to overcome the limitations in distributed UMDO methods and are summarized in this chapter.

7.1 Research Question 1.0 and Hypothesis

Research Question 1.0: *What is an appropriate method to accurately quantify the uncertainty on system metric and joint distribution of coupling variables while handling the dependency and interdisciplinary compatibility in a distributed multidisciplinary analysis under uncertainty?*

Hypothesis 1.0: *In a distributed multidisciplinary analysis under uncertainty, if accurate conditional probability density functions of disciplinary metrics are available from each discipline, then Probabilistic Analysis of Distributed Multidisciplinary Architectures (PADMA) can accurately quantify the uncertainty on system metric and joint distribution of coupling variables by evaluating probability of Event of Interdisciplinary Compatibility (EIC).*

Probabilistic Analysis of Distributed Multidisciplinary Architectures (PADMA) is a distributed UMDA method, that quantifies the uncertainty on system metric and joint distribution of coupling variables by evaluating the probability of Event of Interdisciplinary Compatibility (EIC). The probability of EIC is evaluated by conditional probability models built by each discipline by carrying out uncertainty quantification and propagation independently and concurrently. To carry out uncertainty propagation in each discipline, the converged or interdisciplinary compatible distributions of input coupling variables are not required. One can use guessed probability distributions with any functional form for the input coupling variables and use that to carry out uncertainty propagation in each discipline concurrently and independently. However, the domain of the guessed probability distributions should be large enough such that it can encompass the true interdisciplinary compatible solutions. The only assumption in the PADMA method is that accurate models of conditional probability density functions of disciplinary metrics be available from each discipline. In this work, quantile copula regression has been used to model these conditional probability functions.

The hypothesis has been tested on two numerical problems with both Gaussian and non-Gaussian cases. In all the test cases, the PADMA method has captured the dependency structure as well as accurately estimating the correlation coefficient and mutual information among coupling variables. The PADMA method has also accurately quantified the uncertainty on system metric as compared to the state of

art Moment-Matching method for distributed UMDO.

7.2 Research Question 2.0 and Hypothesis

Research Question 2.0: *What is an appropriate probabilistic modeling technique to comprehensively model conditional probability of multivariate disciplinary responses with heteroskedasticity and statistical dependence ?*

Hypothesis 2.0: *If the disciplinary responses are continuous variables and if the dependencies among responses are monotonic, then quantile copula regression is an appropriate method to comprehensively model the conditional probability density functions of disciplinary metrics using quantile regressions and model dependencies among them using copula.*

A quantile copula regression method has been developed in the current work to comprehensively model the conditional probability distributions of multivariate responses, and model the dependencies with copula. Quantile copula regression does not assume any functional form of probability densities and instead models different level of quantiles which provides a comprehensive information of the true probability densities. The copula function decouples the marginal distributions from the dependence structure and allows independent modeling of any arbitrary marginal distributions using quantile regression.

In the current work a quadratic response surface model has been used to model both quantiles of responses and copula parameters. Also, the Gaussian copula function has been used in the current work to model the dependencies. The hypothesis has been tested with a simple beam problem with both Gaussian and non-Gaussian responses and non-linear dependencies

7.3 Research Question 3.0 and Hypothesis

Research Question 3.0: *What is an appropriate procedure to carry out distributed optimization of multidisciplinary system under uncertainty to accurately quantify the dependency and uncertainty on coupling variables and system metric for non-deterministic disciplinary analyses ?*

Hypothesis 3.0: *If accurate models of conditional probability densities of disciplinary metrics can be built, then Concurrent Optimization using Probabilistic Analysis of Distributed Multidisciplinary Architectures (CO-PADMA) can find the optimum design and estimate the uncertainty and dependence of system metrics and state variables accurately, while allowing distributed optimization and uncertainty analysis for a multidisciplinary system.*

Concurrent Optimization using Probabilistic Analysis of Distributed Multidisciplinary Architectures (CO-PADMA) method has been developed to carry out distributed multidisciplinary design optimization for non-deterministic disciplines. In the CO-PADMA method the top level or the system level is mainly responsible for interdisciplinary compatibility and system level optimization by applying the PADMA method and using quantile copula regression models of disciplinary metrics. At subsystem or discipline level, uncertainty propagation and optimization is carried out using their respective high-fidelity disciplinary analyses and using quantile copula regression for non-local variables.

To improve the accuracy of the quantile copula regression model, CO-PADMA iterates through multiple cycle and in each consecutive cycle the domain of the models is reduced based on the information of optimum solution from the previous cycles. Also, at the end of each cycle additional samples of interdisciplinary compatible solutions are used to update and improve the accuracy of quantile copula regressions.

The hypothesis has been tested on an analytical problem and a Supersonic Transport (SST) aircraft design problem for both Gaussian and non-Gaussian uncertainties. In all the cases, the CO-PADMA method has been able to accurately estimate the optimum solution and accurately quantify the dependence and uncertainty on coupling variables and system metric. The CO-PADMA method has also been able to out perform the state of the art, Moment-Matching method, when the uncertainties are non-Gaussian and when the system metric has a significant effect on the dependence of coupling variables.

7.4 Limitations

Accuracy of both the PADMA and CO-PADMA methods developed in the current work is limited by the accuracy of conditional probability models, for which quantile copula regression has been used. There are mainly three critical aspects which affect the accuracy of quantile copula regression.

- **Number of samples:** Similar to deterministic regression model, accuracy of quantile copula regression is also affected by the number of samples to train it. Quantile regressions of multiple quantiles are required to comprehensively estimate the conditional probability densities. This is particularly important for capturing the tail probabilities, where the inaccuracy of the quantile regression increases due to relatively fewer samples around that region. As the number of quantile levels increase, the required number of samples to model these quantiles also needs to be increased to maintain accuracy. Also, the accuracy of copula parameters estimation improves with the increase in number of samples.

- **Model of quantile and copula function:** The quadratic response surface model has been used in the current work to model both the quantiles of responses and the copula parameters. However, for non-linear problems or problems with

multi-modality, higher order models or non-linear methods like spline, Artificial Neural Network, etc might be required.

- **Copula function:** One of the main assumptions in this work is use of the Gaussian copula to model the dependencies. Although the Gaussian copula is very robust and easily applicable for a variety of problems, it also has some limitations. For example, the Gaussian copula is an elliptical copula and cannot model the tail dependence accurately. Although the Gaussian copula can handle certain non-linear dependencies, it cannot capture the non-monotonic dependencies.

7.5 Recommendation for Future Work

Although all the hypothesis tested in the current work have been able to fulfill the research objective under certain conditions, some of the possible extensions of the presented research work are:

- **Application of the PADMA and CO-PADMA methods on coupled high-fidelity multidisciplinary problems:** In the current work, low to mid-fidelity problems have been used to demonstrate the PADMA and CO-PADMA methods with the purpose of validating the hypothesis. A recommendation for the future work is to study the applicability and behavior of these methods on high-fidelity coupled multidisciplinary problems.

- **Multi-objective distributed UMDO:** The CO-PADMA method developed in current work has only been formulated for single objective optimization problems. However, many industrial level engineering problems are multi-objective in nature. A recommendation for future work is to extend the formulation of CO-PADMA method for multi-objective problems.

- **Discrete uncertainty variables:** In the current work all the uncertain variables are assumed to be continuous. Although, the PADMA and CO-PADMA procedure can be extended for discrete uncertain variables in a straightforward way, a new formulation is required for probabilistic modeling using quantile copula regression to handle both continuous and discrete uncertainties simultaneously.

- **Trust-region methods for optimization:** In the CO-PADMA method, design space reduction technique has been used to improve the accuracy of the probabilistic models near the optimum region, by reducing the size of design space at the end of each cycle. However, only reduction of design space may not guarantee capturing an optimum solution, particularly for a highly nonlinear problem. An extension of design space reduction technique is to apply trust-region based methods [217] which allows more flexibility in terms of improving the model as well handing the optimization process.

- **Non-linear quantile copula regression model:** As discussed previously, for a non-linear and multi-modal problems, assumption of quadratic response surface will generate inaccuracy in quantile copula regression. A recommendation for future work is to extend quantile copula regression using non-linear models such as spline, Artificial Neural Network, etc.

- **Generalized copula function modeling:** In the current work, Gaussian copula function has been used to model the dependencies. An extension to this assumption is to formulate a generalized copula function modeling in which the best possible copula functions can be selected based on the information from the data.

- **Quantifying model form uncertainty quantification of quantile copula regression model:** In the current work only the uncertainties associated

with the disciplinary analyses have been quantified. However, assumptions used in building the conditional probability model using quantile copula regression introduce model form uncertainty. It might be necessary to quantify the uncertainty associated with the quantile copula regression when they are built with sparse data with non-linear trend and the possible uncertainty due to the model form is high.

7.6 Overall Contribution

There are three main contributions in this work:

1. **Probabilistic Analysis of Distributed Multidisciplinary Architectures (PADMA)** method to accurately quantify the uncertainty on system metric and joint distribution of coupling variables in a distributed multidisciplinary analysis under uncertainty.

2. **Quantile Copula Regression** technique to comprehensively model the conditional probability density functions and dependencies for multivariate disciplinary responses.

3. **Concurrent Optimization using Probabilistic Analysis of Distributed Multidisciplinary Architectures (CO-PADMA)** method to carry out UMDO to find optimum design and estimate the uncertainty and dependence of system metrics and state variables accurately, while allowing distributed optimization and uncertainty analysis for a multidisciplinary system.

Appendices

APPENDIX I

DISTRIBUTED MDO METHODS

A.1 Collaborative Optmization

Collaborative Optimization (CO) introduced by Braun and Kroo [218] is a bi-level MDO process. In CO, the overall optimization process is decomposed into disciplinary subproblems. To handle the coupling between disciplines, each discipline uses copies of shared variables and coupling variables from other disciplines, which are also called auxiliary variables. These copies of shared variables and auxiliary variables are shared between all the disciplines and are set as a target. At each iteration, all the the subsystems minimize the discrepancy between the target set up by system level and disciplinary outputs, while satisfying the local constraints by optimizing the local design variables. After each disciplinary optimization, optimum disciplinary state variables are passed on to the system level optimizer. The system level optimizer carries out optimization using shared design variables and auxiliary design variables to minimize the system objective, while maintaining the disciplinary compatibility constraints. Disciplinary compatibility constraints are enforced by matching the auxiliary design variables to the real coupling state variables passed on from subsystem optimization. The system optimization problem is given as

System Optimizer

$$\begin{aligned} \text{minimize} \quad & f_0(x_0, \hat{x}_1, \ldots, \hat{x}_N, \hat{y}) && \text{(165a)} \\ \text{with respect to} \quad & x_0, \hat{x}_1, \ldots, \hat{x}_N, \hat{y} \\ \text{such that} \quad & c_0(x_0, \hat{x}_1, \ldots, \hat{x}_N, \hat{y}) \geq 0 && \text{(165b)} \\ & J_i^* = ||\hat{x}_{0i} - x_0||^2 + ||\hat{x}_i - x_i||^2 + \\ & \qquad ||\hat{y} - y_i(\hat{x}_{0i}, x_i, \hat{y}_{j \neq i})||^2 = 0 \qquad \text{for } i = 1, \ldots, N && \text{(165c)} \end{aligned}$$

and i^{th} subsystem optimization is given as

i^{th} Subsystem Optimizer

$$\begin{aligned} \text{minimize} \quad & J_i(\hat{x}_{0i}, x_i, y_i(\hat{x}_{0i}, x_i, \hat{y}_{j \neq i})) && \text{(166a)} \\ \text{with respect to} \quad & \hat{x}_{0i}, x_i \\ \text{such that} \quad & c_i(\hat{x}_{0i}, x_i, y_i(\hat{x}_{0i}, x_i, \hat{y}_{j \neq i})) \geq 0 && \text{(166b)} \end{aligned}$$

where x is a vector of design variable, y are coupling variables, f is the objective function, c is the design constraints, and N is the number of disciplines. Subscript $()_i$ specifies variables that apply to discipline i, Subscript $()_0$ specifies variables that are shared between more that one discipline, superscript $()^*$ specifies the variable at optimum values, and circumflex $\hat{()}$ specifies independent copies distributed to other disciplines.

A.2 Concurrent SubSpace Optimization

Concurrent Subspace Optimization (CSSO) [219]is also a bi-level MDO process which decomposes the MDO problem into independent subspace problems. The subspace optimizer carries out the optimization process concurrently using its local design variables while the non-local coupled state variables are approximated using global sensitivity equations (GSE). At the system level, in addition to system level optimization using all the design variables, a coordination problem is solved to compute the

"responsibility" coefficients which are assigned to each discipline. These coefficients provide information on the design variables preferences for non-local constraint satisfaction and allows disciplines to have certain degrees of autonomy within the system as a whole. Surrogate-based CSSO [220] is another version where surrogates are built for state variables from each discipline. These surrogates are used to approximate non-local coupled variables in each discipline instead of using GSE. To improve the computational efficiency, disciplinary surrogates are used to model multidisciplinary interaction at system level. The system optimization problem is given as

System Optimizer

$$\begin{aligned} \text{minimize} \quad & f_0(x, \tilde{y}(x, \tilde{y})) && \text{(167a)} \\ \text{with respect to} \quad & x \\ \text{such that} \quad & c_0(x, \tilde{y}(x, \tilde{y})) \geq 0 && \text{(167b)} \\ & c_i(x_0, x_i, \tilde{y}(x_0, x_i, \tilde{y}_{j\neq i})) \geq 0 \qquad \text{for } i = 1, \ldots, N && \text{(167c)} \end{aligned}$$

and i^{th} subsystem optimization is given as

i^{th} Subsystem Optimizer

$$\begin{aligned} \text{minimize} \quad & f_0(x, y_i(x_i, \tilde{y}_{j\neq i}), \tilde{y}_{j\neq i}) && \text{(168a)} \\ \text{with respect to} \quad & x_0, x_i \\ \text{such that} \quad & c_0(x, \tilde{y}(x, \tilde{y})) \geq 0 && \text{(168b)} \\ & c_i(x_0, x_i, \tilde{y}(x_0, x_i, \tilde{y}_{j\neq i})) \geq 0 && \text{(168c)} \\ & c_j(x_0, \tilde{y}_j(x_0, \tilde{y})) \geq 0 \qquad \text{for } i = 1, \ldots, i-1, i+1, \ldots N && \text{(168d)} \end{aligned}$$

where tilde $\tilde{()}$ specifies an approximation of the variables and other notations are similar to the one used in CO.

A.3 Bilevel System Integrated System Synthesis

Similar to CO and CSSO, Bilevel system integrated system synthesis(BLISS) [221] is bi-level architecture which decomposes the overall MDO problems into disciplinary subproblems. However, unlike CSSO, local design variables are optimized at discipline level while shared variables are optimized at system level. Information transfer among disciplines is done by building a series of approximation models within the user-defined boundaries of design variables. The original BLISS formulation builds these model through linear approximation by using coupled sensitivity information. In a different formulation called BLISS-2000 [216], information exchange between system and discipline subproblems occurs through surrogate models of the discipline optima and copies of coupling variables are used to enforce consistency at the optimum.

The system optimization problem is given as

System Optimizer

$$\begin{aligned} \text{minimize} \quad & f_0(x, \tilde{y}(x, \hat{y})) && \text{(169a)} \\ \text{with respect to} \quad & x_0, \hat{y}, w \\ \text{such that} \quad & c_0(x, \tilde{y}(x, \tilde{y}, w)) \geq 0 && \text{(169b)} \\ & \hat{y}_i - \tilde{y}_i(x_0, x_i, \hat{y}_{j\neq i}, w_i)) = 0 \qquad \text{for } i = 1, \ldots, N && \text{(169c)} \end{aligned}$$

and i^{th} subsystem optimization is given as

i^{th} **Subsystem Optimizer**

$$\begin{aligned} \text{minimize} \quad & w_i^T y_i && \text{(170a)} \\ \text{with respect to} \quad & x_i \\ \text{such that} \quad & c_0(x, \tilde{y}(x, \tilde{y})) \geq 0 && \text{(170b)} \\ & c_i(x_0, x_i, y_i(x_0, x_i, y_i(x_0, x_i, \hat{y}_{j\neq i}))) \geq 0 && \text{(170c)} \end{aligned}$$

where w_i are weighing coefficients attached to the discipline states which represent sensitivity of system level metric with respect to disciplinary metric.

A.4 Analytical Target Cascading

Analytical Target Cascading (ATC) is a hierarchical target cascading method which has been developed to propagate targets through a hierarchical system to achieve a feasible design satisfying these targets [222]. In an MDO formulation of ATC [223], system level optimizes system level objective function with a penalty function using the system level design variables and auxiliary variables. The penalty function consists of discrepancy of system target and optimum solution from elements next in the hierarchy.

Let's say the system is decomposed into N levels and M elements. The subscript $()_{ij}$ denotes the j^{th} element of the system in the i^{th} level. f_{ij}, $g_{ij} \leq 0$, and $h_{ij} = 0$ denotes the objective function, the inequality and the equality constraints, respectively. The local variables of element j are denoted by x_{ij} and r_{ij} is the output of j^{th} element's analysis model a_{ij} and $\mathcal{C}_{ij}$ is the set of children of element j. Let π represent a consistency constraint relaxation function, then the optimization problem of j^{th} element is given as

$$\begin{aligned}
\text{minimize} \quad & f_{ij}(\overline{x}_{ij}) + \pi(t_{ij} - r_{ij}) + \sum_{k \in \mathcal{C}_{ij}} \pi(t_{(i+1)k} - r_{(i+1)k}) && \text{(171a)} \\
\text{with respect to} \quad & \overline{x}_{ij} \\
\text{such that} \quad & g_{ij}(\overline{x}_{ij}) \leq 0 && \text{(171b)} \\
& h_{ij}(\overline{x}_{ij}) = 0 && \text{(171c)} \\
\text{where} \quad & \overline{x}_{ij} = [x_{ij}, t_{(i+1)k}] \qquad \forall k \in \mathcal{C}_{ij}
\end{aligned}$$

where t_{ij} is the target for j^{th} element of i^{th} level and variables t_{ij} and $r_{(i+1)k}$ for $k \in \mathcal{C}_{ij}$ are constants with respect to element j.

APPENDIX II

PROBABILISTIC MODELING: PARAMETER ESTIMATION

The main goal of a discriminative probabilistic model is to predict the uncertainty on output variables y, given some new value of input variable x on the basis of an available set of N training data $\mathbf{X} = (\mathbf{x}_1, \mathbf{x}_2, \ldots, \mathbf{x}_N)^T$ and their corresponding outputs $\mathbf{y} = (y_1, y_2, \ldots, y_N)^T$, where each input training data consists of D predictor variables $\mathbf{x} = (x_1, x_2, \ldots, x_D)^T$. The uncertainty over the output variables are expressed using some probability distribution. Generally, it is assumed that for a given value of $\mathbf{x}$, y follows some fixed parametric probability distribution family like Gaussian distribution as

$$\mathrm{P}(y|\mathbf{x}, \mathbf{w}) = \mathcal{N}(y|\mu(\mathbf{x}, \mathbf{w}), \beta^{-1}) \tag{172}$$

where $\mu(\mathbf{x}, \mathbf{w})$ is the function determining the mean for a given value of $\mathbf{x}$, $\mathbf{w}$ are the unknown parameters of mean function, β is the unknown precision or inverse of variance. Typically homoscedasticity is assumed, i.e. dependent variables have constant variance across the range of input variables, therefore β is independent of $\mathbf{x}$.

One of the criteria for determining the unknown parameters $\mathbf{w}$ and β is by using the training data to find the parameter values which maximize the likelihood function, which is also known as *maximum likelihood (ML) approach*. If the data are assumed to be drawn independently from the distribution given in Equation 73, then the likelihood function is given as

$$\mathrm{P}(\mathbf{y}|\mathbf{X}, \mathbf{w}, \beta) = \prod_{n=1}^{N} \mathcal{N}(y_n|\mu(\mathbf{x}_n, \mathbf{w}), \beta^{-1}) \tag{173}$$

In machine learning and statistics, instead of maximizing the likelihood function, the log likelihood function is maximized for convenience. Using the functional form

of Gaussian distribution, the log likelihood function is given as

$$\ln \mathrm{P}(\mathbf{y}|\mathbf{X}, \mathbf{w}, \beta) = -\frac{\beta}{2}\sum_{n=1}^{N}\{\mu(\mathbf{x}_n, \mathbf{w}) - y_n\}^2 + \frac{N}{2}\ln \beta - \frac{N}{2}\ln 2(\pi) \tag{174}$$

Generally as the first step, the log likelihood function is only maximized with respect to $\mathbf{w}$. The solution is denoted as $\mathbf{w}_{ML}$. The last two term in Equation 174 are constant with respect to $\mathbf{w}$, therefore maximizing log likelihood function with respect to $\mathbf{w}$ is equivalent to minimizing *the sum-of-squares error function.*

Next, the log likelihood function is used to evaluate the precision parameter β to evaluate β_{ML}, which is given as

$$\frac{1}{\beta_{ML}} = \frac{1}{N}\sum_{n=1}^{N}\{\mu(\mathbf{x}_n, \mathbf{w}_{ML}) - y_n\}^2 \tag{175}$$

Once the parameters are estimated, the *predictive distribution* of y for any new value of $\mathbf{x}$ is given by substituting maximum likelihood parameters in Equation 73 and is given as

$$\mathrm{P}(y|\mathbf{x}, \mathbf{w}) = \mathcal{N}(y|\mu(\mathbf{x}, \mathbf{w}_{ML}), \beta_{ML}^{-1}) \tag{176}$$

In addition to *maximum likelihood approach* two other commonly used approaches are *maximum posterior (MAP) approach* and *full Bayesian treatment.* In MAP approach, a prior distribution is introduced over the unknown $\mathbf{w}$. For example, a prior in the form of Gaussian distribution can be assumed as

$$\mathrm{P}(\mathbf{w}|\alpha) = \mathcal{N}(\mathbf{w}|\mathbf{0}, \alpha^{-1}\mathbf{I}) \tag{177}$$

where α is the precision of the distribution (also known as *hyperparameters*) and $\mathbf{I}$ is the identity matrix. Using the Bayes' theorem, the posterior distribution of $\mathbf{w}$ is proportional to the product of prior distribution and the likelihood function as

$$\mathrm{P}(\mathbf{w}|\mathbf{X}, \mathbf{y}, \alpha, \beta) \propto \mathrm{P}(\mathbf{y}|\mathbf{X}, \mathbf{w}, \beta)\mathrm{P}(\mathbf{w}|\alpha) \tag{178}$$

The parameter $\mathbf{w}$ is then evaluated by finding the value $\mathbf{w}_{MAP}$ which maximizes the posterior distribution which is equivalent to minimizing

$$\frac{\beta}{2}\sum_{n=1}^{N}\{\mu(\mathbf{x}_n, \mathbf{w}) - y_n\}^2 + \frac{\alpha}{2}\mathbf{w}^T\mathbf{w}. \tag{179}$$

Unlike ML and MAP approaches where a fixed value of $\mathbf{w}$, i.e. $\mathbf{w}_{ML}$ and $\mathbf{w}_{MAP}$, is used to evaluate predictive distribution, full Bayesian approach uses the posterior distribution of $\mathbf{w}$ to evaluate the predictive distribution. The posterior distribution of $\mathbf{w}$ is evaluated in the similar way as in MAP approach. Assuming that the parameters α and β are fixed (although in full Bayesian treatment distribution of these parameters are also inferred [108]), the predictive distribution is given as

$$\mathrm{P}(y|\mathbf{x}, \mathbf{X}, \mathbf{y}) = \int \mathrm{P}(y|\mathbf{x}, \mathbf{w})\mathrm{P}(\mathbf{w}|\mathbf{X}, \mathbf{y})\ \mathrm{d}\mathbf{w}. \tag{180}$$

where $\mathrm{P}(y|\mathbf{x}, \mathbf{w})$ is given by Equation 73 and $\mathrm{P}(\mathbf{w}|\mathbf{X}, \mathbf{y})$ is evaluated by normalizing the right hand side of Equation 178. Please note that α and β notations are omitted to simplify the notation. If the likelihood function is a Gaussian function and prior distribution is a Gaussian distribution in Equation 178, then the posterior distribution also follows Gaussian distribution. Additionally, if the mean function is given as the polynomial function $\mu(\mathbf{X}, \mathbf{w}) = \mathbf{w}^T\boldsymbol{\phi}(\mathbf{X})$, where $\phi_i(\mathbf{X})$ are some basis functions such as polynomial function $\phi_i(\mathbf{X}) = \mathbf{x}^i$, then integration in Equation 180 can be performed analytically and the predictive distribution is given by a Gaussian distribution as

$$\mathrm{P}(y|\mathbf{x}, \mathbf{X}, \mathbf{y}) = \mathcal{N}(y|m(\mathbf{x}), s^2(\mathbf{x})) \tag{181}$$

where the mean and variance are given by

$$m(\mathbf{x}) = \beta\boldsymbol{\phi}(\mathbf{x})^T\mathbf{S}\sum_{n=1}^{N}\boldsymbol{\phi}(\mathbf{x}_n)y_n \tag{182a}$$

$$s^2(\mathbf{x}) = \beta^{-1} + \boldsymbol{\phi}(\mathbf{x})^T\mathbf{S}\boldsymbol{\phi}(\mathbf{x}) \tag{182b}$$

where matrix $\mathbf{S}$ is given as

$$\mathbf{S}^{-1} = \alpha\mathbf{I} + \beta\sum_{n=1}^{N}\boldsymbol{\phi}(\mathbf{x}_n)\boldsymbol{\phi}(\mathbf{x}_n)^T \tag{183}$$

As seen in Equation 180, in full Bayesian approach, mean as well as variance of the predictive distribution depends on $\mathbf{x}$. The first term in Equation 182b captures

the uncertainty due to noise on output which is similar to β_{ML}^{-1} and β_{MAP}^{-1}. In addition to that, the second term captures the uncertainty in the parameters $\mathbf{w}$ due to full Bayesian treatment, which allows the capture of *model form uncertainty*.

APPENDIX III

TUTORIAL: QUANTILE COPULA REGRESSION

Quantile Copula Regression is a probabilistic modeling technique to model the joint distribution of multiple responses of a discipline, model, subsystem or even a multidisciplinary system, as a function of predictor or input variables. Let $\mathbf{y} = [y_1, y_2, \ldots, y_p]$ be the p output variables of a stochastic or non-deterministic system and $\mathbf{x}$ be the vector of input variables, then according to quantile copula regression, joint distribution of outputs at a given predictor $\mathbf{x}$ is given as

$$F(\mathbf{y}|\mathbf{x}, \boldsymbol{\beta_1}, \ldots, \boldsymbol{\beta_p}, \boldsymbol{\alpha}) = C\left(F_1(y_1|\mathbf{x}, \boldsymbol{\beta_1}), \ldots, F_p(y_p|\mathbf{x}, \boldsymbol{\beta_p})|\mathbf{x}, \boldsymbol{\alpha}\right) \tag{184}$$

where $\boldsymbol{\beta_1}, \ldots, \boldsymbol{\beta_p}$ are the matrices of parameters associated with quantile regressions of p responses such that $F_i(y_i|\mathbf{x}) = Q^{-1}_{Y_i|\mathbf{x}}(y_i|\mathbf{x}, \boldsymbol{\beta_i})$ and $Q_{Y_i|\mathbf{x}}(\tau|\mathbf{x}, \boldsymbol{\beta_i})$ is conditional quantile functions of y_i estimated using the quantile regression models for i^{th} response. C is a copula function which models the dependency among the disciplinary responses. The copula function is selected either qualitatively by the expert judgment or quantitatively by using methods like Akaike Information Criterion (AIC) [205], the Bayesian Information Criterion (BIC) [206], the Deviance Information Criterion (DIC) [207], etc. In the current work the Gaussian copula function has been used to model the dependencies and is given as

$$C(u_1, \ldots, u_p; \Sigma) = \Phi_\Sigma\left[\Phi^{-1}(u_1), \ldots, \Phi^{-1}(u_p)\right] \tag{185}$$

where Φ is the cumulative distribution function of a standard Gaussian distribution with zero mean and unit standard deviation and Φ_Σ is the joint cumulative distribution function of a multivariate Gaussian distribution with correlation matrix Σ. Σ is a symmetric matrix and has $p(p+1)/2$ elements. The elements of correlation matrix

$\boldsymbol{\theta} = [\rho_1, \ldots, \rho_{p(p+1)/2}]$ are Gaussian copula parameters and are modeled as a function of input variables $\mathbf{x}$ as $\boldsymbol{\theta} = f_\theta(\mathbf{x}, \boldsymbol{\alpha})$, where $\boldsymbol{\alpha}$ is the vector or matrix of regression coefficients.

In the current work, modified Inference Function for Margins (IFM) method is used to estimate the quantile copula parameters $\boldsymbol{\beta_1}, \ldots, \boldsymbol{\beta_p}$ and $\boldsymbol{\alpha}$. Modified IFM is a two stage process in which the first stage estimates the parameters of the marginal distribution, i.e. the matrices of regression coefficients of quantile regressions $\boldsymbol{\beta_1}, \ldots, \boldsymbol{\beta_p}$ and the second stage estimates the regression coefficients of copula parameters, i.e. $\boldsymbol{\alpha}$.

To demonstrate the parameter estimation of quantile copula regression the beam model shown in Figure 68 has been selected where vertical load Y (lbf) and horizontal load X (lbf) are the inputs. The outputs of the discipline are maximum stress s (lbf/in^2), maximum displacement d (in), and beam volume v (in^3). The uncertainty variables are beam width w $(in) \sim Unif(3.2, 4.8)$ and beam thickness t (in) $\sim Triangular(3.0, 4.3, 4.5)$, which are assumed to be embedded in the discipline such that the discipline acts like a non-deterministic function. Deterministic parameters are beam length $L = 100(in)$ and Modulus of Elasticity $E = 2.9 \times 10^6 (lbf/in^2)$. The beam model is given as

$$s = \frac{600}{wt^2}Y + \frac{600}{w^2t}X \tag{186a}$$

$$d = \frac{4L^3}{Ewt}\sqrt{\frac{Y}{t^2}^2 + \frac{X}{w^2}^2} \tag{186b}$$

$$v = Lwt \tag{186c}$$

In the current work, the computer program for quantile copula regression modeling is built using two softwares, MATLAB® [164] and statistical software package, R [224]. 10,000 samples are generate in the input space given by $X \in [500, 1500]$ and $Y \in [1500, 2500]$ and stored in a MATLAB matrix variable `x` of size 10000×2. The the random outputs s, d and v are evaluated for each sample of input and stored in a

MATLAB matrix variable y of size 10000×3. The MATLAB script to generate the data is given as

```
n= 10000;
pd = makedist('Triangular','a',3,'b',4.3,'c',4.5);
t =random(pd,n,1);
w= unifrnd(repmat([3.2],n,1),repmat([4.8],n,1));
X= 500 + rand(n,1)*1000;
Y = 1500 + rand(n,1)*1000;
[s,d,v] = beam(X,Y,w,t);
x = [X,Y];
y = [s,d,v]
```

The MATLAB function `[s,d,v] = beam(X,Y,w,t)` is given as

```
function [s,d,v] = beam(X,Y,w,t)
L =100; % beam length
E =2.9e6; % Modulus of Elasticity
s = 600./(w.*t.^2) .*Y + 600./(w.^2.*t).*X;
d = 4*L.^3./(E*w.*t).*sqrt((Y./(t.^2)).^2 + (X./(w.^2)).^2);
v = L*w.*t;
```

To model and estimate the parameters of quantile copula regression for the beam model, steps of IFM process is given as follows.

C.1 Modified IFM Stage-1: Quantile Regression Modeling

The first stage of modified IFM method is to model the marginal distribution of responses with quantile copula regression. The first step to model quantile regression is to normalize the input variables and built the *design matrix* of input variables, which depends on the polynomial model of quantile regression. In this example, quantile regression models are built for 20 quantiles for τ equally spaced between 0.02 and 0.98. Each quantile regression is modeled using quadratic polynomial model. Following MATLAB script is used to build quantile regression models of each response, and all the information are stored in a *structure array* `QCRmdl`

```
RScriptPath = 'C:\Program Files\R\R-3.2.3\bin\x64\Rscript'; % ...
    Path of R script
```

```
srcPath = '../src/QR'; % Path of all the source file quantile ...
    copula regression
xmin = [500,1500]; % minimum of design space
xmax = [1500,2500]; % maximum of design space
QCRmdl.xmin = xmin;
QCRmdl.xmax = xmax;
ny = size(y,2); % Number of responses
varname = {'d';'s';'v'}; % Name of response variables
QCRmdl.varname = varname; % Store infomration in QCRmdl
% Save normalize predictors in QCRmdl
dx = xmax - xmin;
xnorm = (x - repmat(xmin,size(x,1),1)) ./ repmat(dx,size(x,1),1);
% Build quantile regression for each response
QRmodel = 'quadratic'; % polynomial model for quantile regression
for i = 1:ny
    QCRmdl.QRmdl(i) = ...
        BuildQR(xnorm,y(:,i),srcPath,RScriptPath,xmin,xmax,...
    QRmodel,linspace(0.02,0.98,20));
end
QCRmdl.QRmodel = QRmodel;
```

The quantile regression coefficients are evaluated in R software, which is called by the MATLAB function `BuildQR` using the `Rscript` file stored in the location specified by `RScriptPath`. `Rscript` is the batch file of R software which comes with the installation package of R and is used to run R software in batch mode. The MATLAB function `BuildQR` is given below.

```
function[mdl] = BuildQR(xnorm,y,srcPath,Rpath,xmin,xmax,varargin)
reg_model  = varargin{1};
quant_list = varargin{2};
% Create design matrix
X = x2fx(xnorm,reg_model);
X = X(:,2:end);
% Format quat_list for R software
[m,n] = size(quant_list);
if n > m
    quant_list = quant_list';
end
% Store data for quantreg library in R software
csvwrite('data.csv',[X,y]);
csvwrite('quantiles.csv',quant_list);
% Format path naming
RScriptPath = ['"',strrep(Rpath,'\','/'),'"'];
CurrentDirectory=strrep(srcPath,'\','/');
% Call R software in batch mode
system([RScriptPath,' ','"',CurrentDirectory,'\R_Scrip_QuantReg.R"'])
% Import quantile regression coefficients into MATLAB
Coeff = csvread('Rquantreg_out.csv',1,1);
```

```
% Store information in model struture
mdl.xmin = xmin;
mdl.xmax = xmax;
mdl.reg_mdl = reg_model;
mdl.quant_list = quant_list;
mdl.coeff = Coeff;
```

To evaluate the quantile regression coefficients, *Quantreg* [225] library in R software is used. MATLAB function `BuildQR` runs script `R_Scrip_QuantReg.R` in R software package in a batch mode to evaluate the quantile regression coefficients. The script `R_Scrip_QuantReg.R` is given below.

```
library("quantreg")
rawdat <- read.csv('data.csv',header=FALSE)
quant_list <- read.csv('quantiles.csv',header=FALSE)
q <- data.matrix(quant_list)
y <- data.matrix(rawdat[ncol(rawdat)])
x <- data.matrix(rawdat[,1:ncol(rawdat)-1])
rq_mdl <- rq(y ~ x,q)
write.csv(rq_mdl$coefficients,file='Rquantreg_out.csv')
```

At the end of modified IFM stage-1, all the information regarding quantile regression of i^{th} response is stored in `QCRmdl.QRmdl(i)`. The matrix of quantile regression coefficients for i^{th} variables, $\hat{\boldsymbol{\beta}}_i$, is stored as matrix `QCRmdl.QRmdl(i).coeff`, where j^{th} column of the matrix contains the quantile regression coefficient of τ_j^{th} quantile. For the beam problem with quadratic polynomial model for the quantile regression, size of the matrix `QCRmdl.QRmdl(i).coeff` is 6×20.

C.2 Modified IFM Stage-2: Copula Parameter Regression Modeling

In the second stage of modified IFM method, the regression coefficients of copula parameters are evaluated. At first, the samples of all the response variables are transformed into uniform distribution by carrying out *inverse probability transform* using quantile regression built in stage-1. Probability inverse transform of j^{th} sample of i^{th} variable is carried out by evaluating the value of conditional cumulative distribution function of `y(j,i)` at input value of `x(j,:)`. The MATLAB script is given

below

```
ynorm = zeros(size(y,1),ny);
for i = 1:ny
    for j = 1:size(y,1)
        ynorm(j,i) = condStats(x(j,:),y(j,i),QCRmdl.QRmdl(i),'cdf');
    end
end
```

The MATLAB function `condStats` evaluates the conditional statistics of a sample of `y(j,i)` at input `x(j,:)`, where probability density function is evaluated using the Equations 94, 95, and 96, cumulative distribution function is evaluated using the Equations 97, 98, and 99, and quantile is evaluated using Equations 103, 104, and 105. The MATLAB code is given below

```
function [stats] = condStats(x,y,mdl,type)
% type: type of statistics: 'pdf', 'cdf' or 'quantile'
% mdl: Quantile regression model struture
% Note for quantile estimation variable y represents tau

% Normalize input for quantile estimations
dx = mdl.xmax - mdl.xmin;
xnorm = (x - mdl.xmin) ./dx;
% Evaluate the terms of quantile regression polynomilas
X = x2fx(xnorm,mdl.reg_mdl);

% Evaluate each quantiles
ytau = X * mdl.coeff;
tau = mdl.quant_list;

% Estimate the terms for interpolations
alpha1 = (tau(2) - tau(1))/(ytau(2) - ytau(1));
beta1 = tau(1)/alpha1;
alphaN = (tau(end) - tau(end-1))/(ytau(end)-ytau(end-1));
betaN = (1-tau(end))/alphaN;

% Estimate the ranges of tau
mintau = min(tau);
maxtau = max(tau);
% Estimate the ranges of quantiles
miny = min(ytau);
maxy = max(ytau);
% Define interpolation function
interp_mdl = 'linear';

if strcmp(type,'cdf')
    for i = 1:length(y)
```

```
        if y(i) < miny
            stats(i,1) = alpha1*beta1*exp((y(i)-miny)/beta1);
        elseif y(i) > maxy
            stats(i,1) = 1- alphaN*betaN*exp((maxy-y(i))/betaN);
        else
            stats(i,1) = interp1(ytau,tau,y(i),interp_mdl,'extrap');
        end
    end
elseif strcmp(type,'pdf')
    for i = 1:length(y)
        if y(i) < miny
            stats(i,1) = alpha1 *exp(-abs(y(i)-miny)/beta1);
        elseif y(i) > maxy
            stats(i,1) = alphaN *exp(-abs(y(i)-maxy)/betaN);
        else
            stats(i,1) = (tau(idx+1)-tau(idx))/(ytau(idx+1) - ...
                ytau(idx));
        end
    end
elseif strcmp(type,'quantile')
    for i = 1:length(y)
        if y(i) < mintau
            stats(i,1) = ytau(1) + beta1 * log(y(i)/alpha1/beta1);
        elseif y(i) > maxtau
            stats(i,1) =  ytau(end) - betaN*log( (1 - ...
                y(i))/alphaN/betaN);
        else
            stats(i,1) = interp1(tau,ytau,y(i),interp_mdl,'extrap');
        end
    end
end
```

After carrying out probability inverse transform, the regression coefficients of each copula parameter are estimated by maximizing the log-likelihood or minimizing the negative of log-likelihood of all the samples with respect to regression coefficients of Gaussian copula parameters and stored in `QCRmdl.Cmodel` as

```
Cmodel = 'quadratic'; % polynomial model for copula parameter ...
    regression
for i = 1:ny-1
    for j = i+1:ny
        QCRmdl.Cmdl(i,j).p = GaussCopulaCorrFuncFit(xnorm,...
        [ynorm(:,i),ynorm(:,j)],Cmodel);
    end
end
for j = 1:ny-1
    for i = j+1:ny
        QCRmdl.Cmdl(i,j) = QCRmdl.Cmdl(j,i);
    end
```

```
12 end
13 QCRmdl.Cmodel = Cmodel;
```

GaussCopulaCorrFuncFit function carries out optimization to minimize the negative of log-likelihood as

```
1 function pmin = GaussCopulaCorrFuncFit(x,u,model)
2 v = norminv(u);
3 d = size(x,2);
4 p0 = zeros(1 + d + d*(d-1)/2,1);
5 options = optimset('Display','iter','TolCon',10^-12,...
6 'TolFun',10^-4,'TolX',10^-6);
7 A = [];
8 b = [];
9 [pmin,fval] = fmincon(@(p)evalCorrRegLikelihood(p,x,v,model),p0,A,b);
```

The negative log-likelihood with respect to regression coefficients p is evaluated by function evalCorrRegLikelihood as

```
1 function nlogl = evalCorrRegLikelihood(p,x,y,model)
2 r = evalCorr(x,p,model); % evaluate correlation at different ...
     value of x
3 maxr = max(abs(r)); % evaluate absolute maximum value of ...
     correlation coefficient
4 if maxr >= 1
5     nlogl = 10^50; % Impose penalty if abs(correlation) >1
6 else
7     nlogl = nLogLGaussCopulaReg(y,r);
8 end
```

The function evalCorr estimate the correlation at given predictor value for the specified polynomial model, model and regression coefficient, p.

```
1     function r = evalCorr(x,p,model)
2     % evaluate correlation at different value of x for givem ...
        model and
3     % parameter p
4     d = size(x,2);
5     xmat = x2fx(x,model);
6     r = xmat*p;
```

The function nLogLGaussCopulaReg evaluate the negative log-likelihood of samples y with respect to regression coefficients p for a Gaussian copula.

```
function nlogl_GC = nLogLGaussCopulaReg(y,R)
% evalaute negative likeliood of gaussian copula for ...
    copula-quantile
% regression
% Note: this evaluates bivariate copula. For multivariate, ...
    loop through all
% pairwise varaible for each combinations
nlogl_GC = -log((1-R.^2).^(-0.5)) + (y(:,1).^2 + y(:,2).^2 - ...
    2.*R.*y(:,1).*y(:,2))./(1-R.^2)./2;
nlogl_GC = sum(nlogl);
```

The coefficients of copula parameter regressions between i^{th} and j^{th} variables are stored in the $(\text{i,j})^{th}$ element of cell matrix `QCRmdl.Cmd`. For the beam problem, size of `QCRmdl.Cmd` matrix is 3×3 and each element of the cell matrix contains a vector of regression coefficients of size 6×1.

C.3 Model Prediction

Once the quantile copula regression is built, it can be used to evaluate the joint probability densities or generate samples of multivariate responses for any given value of predictor within the domain which has been used to build the models.

C.3.1 Joint Probability Density Estimation

The joint probability density is estimated using `QCRmdlPDF(QCRmdl,x,y,var)` function by specifying the the quantile copula regression model `QCRmdl`, value of predictor variables `x`, value of response variables `y`, and variable name `var`.

```
function stats = QCRmdlPDF(QCRmdl,x,y,var)
% Evaluate joint PDF of variable(s) given in var using the QCR model
% conditioned at x
% var is the cell carry containting the variable name

ny = size(var,1);

% Find the id of variables in var
for i = 1:ny
    idx(i) = find(strcmp(QCRmdl.varname,var{i}));
end

% Normalize predictor variable
dx = QCRmdl.xmax - QCRmdl.xmin;
```

```
xnorm = (x - QCRmdl.xmin)./dx;

% Evaluate correlation matrix
c = zeros(ny,ny);
for i = 1:ny-1
    for j = i+1:ny
        p = QCRmdl.Cmdl(idx(i),idx(j)).p;
        c(i,j) = evalCorr(xnorm,p,QCRmdl.Cmodel);
    end
end
c = c + c';
c = c + eye(ny);

% Check for positive definiteness
eigen = eig(c);
if min(eigen) < 0
    c = nearestSPD(c);
    c = corrcov(c);
end

% Evaluate joint PDF
for i = 1:ny
    u(:,i) = condStats(x,y(:,i),QCRmdl.QRmdl(idx(i)),'cdf');
    u(:,i) = norminv(u(:,i));
    pdfy(:,1) = condStats(x,y(:,i),QCRmdl.QRmdl(idx(i)),'pdf');
end

cpdf = mvnpdf(u,zeros(1,ny),c);
stats = prod(pdfy,2).*cpdf;
```

Since each correlation coefficients are evaluated independently, there is a possibility that correlation matrix is not a positive semidefinite matrix due to error associated with copula parameter regression models. The MATLAB function `nearestSPD(c)` is used to estimate the nearest positive semidefinite matrix in case `c` is not positive semidefinite. The method used in `nearestSPD(c)` is developed by Higham [226] and is available at MATLAB's file exchange server (**`www.mathworks.com/matlabcentral/fileexchange`**).

For example, quantile copula regression model built for the beam model can be used to estimate joint probability density of d and s at $X = 800$ and $Y = 2000$ by executing the following script.

```
varname = {'d';'s'};
xin = [800,2000];
```

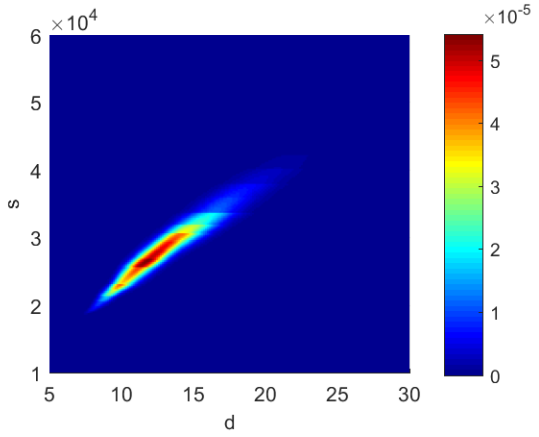

Figure 127: Contour of joint probability density of d and s estimated at $X = 800$ and $Y = 2000$ using quantile copula regression

```
y1 = linspace(5,30,100);
y2 = linspace(1e4,6e4,100);
[Y1,Y2] = meshgrid(y1,y2);
for i = 1:100
    for j = 1:100
        pdf(i,j)=CQRmdlPDF(CQRmdl,xin,[Y1(i,j),Y2(i,j)],varname);
    end
end
contourf(Y1,Y2,pdf);
```

Figure 127 shows the joint probability density contour estimated by quantile copula regression.

C.3.2 Sampling of Multivariate Responses

The samples are generate using `QCRmdlSample(QCRmdl,x,var,ns)` function by specifying the the quantile copula regression model `QCRmdl`, value of predictor variables `x`, variable names of the responses specified using cell array `var`, and number of samples required, `ns`.

```
function ys = QCRmdlSample(QCRmdl,x,var,ns)
% generate sample of variable(s) given in var using the QCR model
% conditioned at x
% var is the cell carry containting the variable name
% ns is the number of samples to be generated

ny = size(var,1);

```

```
% Find the id of variables in var
for i = 1:ny
    idx(i) = find(strcmp(QCRmdl.varname,var{i}));
end

% Normalize predictor variable
dx = QCRmdl.xmax - QCRmdl.xmin;
xnorm = (x - QCRmdl.xmin)./dx;

% Evaluate correlation matrix
c = zeros(ny,ny);
for i = 1:ny-1
    for j = i+1:ny
        p = QCRmdl.Cmdl(idx(i),idx(j)).p;
        c(i,j) = evalCorr(xnorm,p,QCRmdl.Cmodel);
    end
end
c = c + c';
c = c + eye(ny);

% Check for positive definiteness
eigen = eig(c);
if min(eigen) < 0
    disp(['x =',num2str(x)]);
    c = nearestSPD(c); % Find the nearest positive semidefinite ...
       matrix
    c = corrcov(c);
end

% Generate uniform samples by probability inverse transform of
% multivariate standard normal with correlation matrx c
u = normcdf(mvnrnd(zeros(1,ny),c,ns));

% Generate samples by estimating the quantiles using quantile ...
   copula regression
for i = 1:ny
    ys(:,i) = condStats(x,u(:,i),QCRmdl.QRmdl(idx(i)),'quantile');
end
```

For example, quantile copula regression model built for the beam model can be used to generate 500 samples of d and s at $X = 800$ and $Y = 2000$ by executing the following script.

```
varname = {'d';'s'};
xin = [800,2000];
ns = 500;
ys = QCRmdlSample(QCRmdl,xin,varname,ns);
h=scatterhist(ys(:,1),ys(:,2));
```

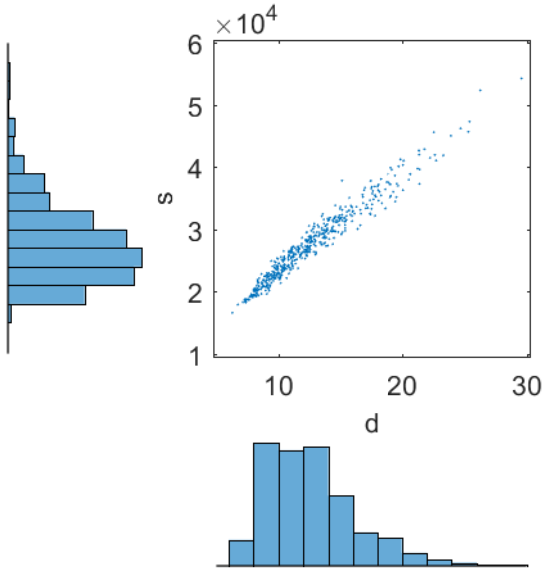

Figure 128: Scatter plot of samples of d and s generated at $X = 800$ and $Y = 2000$ using quantile copula regression

Figure 128 shows the scatter plot of the samples generated by quantile copula regression.

REFERENCES

[1] Rowe, W., "Understanding uncertainty," *Risk analysis*, Vol. 14, No. 5, 1994, pp. 743–750.

[2] Martins, J. and Lambe, A., "Multidisciplinary design optimization: a survey of architectures," *AIAA journal*, Vol. 51, No. 9, 2013, pp. 2049–2075.

[3] Zang, T. A., Hemsch, M. J., Hilburger, M. W., Kenny, S. P., Luckring, J. M., Maghami, P., Padula, S. L., Strout, W. J., Hilburger, W., Padula, L., and Jefferson, W., "Needs Based and Opportunities Multidisciplinary Vehicles for Uncertainty Design Methods for Aerospace Vehicles," Tech. rep., NASA, 2002.

[4] Deshmukh, A. and Collopy, P., "Fundamental Research into the Design of Large-Scale Complex Systems," *13th AIAA/ISSMO Multidisciplinary Analysis Optimization Conference, Fort Worth, Texas*, 2010.

[5] Becz, S., Pinto, A., Zeidner, L., Khire, R., Banaszuk, A., and Reeve, H., "Design system for managing complexity in aerospace systems," *10th AIAA Aviation Technology, Integration, and Operations (ATIO) Conference,Fort Worth, Texas*, 2010.

[6] Schofield, A., "End of Year Is New Goal for 787 First Flight," *Aviation Week*, Aug 2009.

[7] Beelaerts van Blokland, W. W. A., Verhagen, W. J. C., and Santema, S. C., "The Effects of Co-Innovation on the Value-time Curve: Quantitative Study on Product Level," *Journal of business market management*, Vol. 2, No. 1, 2008, pp. 5–24.

[8] Hellemans, A., "Manufacturing Mayday," *IEEE Spectrum*, Vol. 44, No. 1, Jan 2007, pp. 10–13.

[9] "Facts & Figures - Air Transport Action Group (ATAG)," www.atag.org/facts-and-figures.html, accessed September 5, 2015.

[10] "Current Market Outlook: 2015 - 2034," *Boeing Commercial Airplane*, 2015.

[11] "ICAO Environmental Report 2010: Aviation Outlook," *International Civil Aviation Organization (ICAO)*, 2010.

[12] Guynn, M. D., Berton, J. J., Tong, M. J., and Haller, W. J., "Advanced Single-Aisle Transport Propulsion Design Options Revisited," *2013 Aviation Technology, Integration, and Operations Conference*, AIAA Aviation, American Institute of Aeronautics and Astronautics, 2013.

[13] Wagner, R. D. and Fischer, M. C., "Developments in the NASA transport aircraft laminar flow program," *AIAA Paper*, No. 83-0090, 1983.

[14] Anders, S. G., Sellers, W. L., and Washburn, A. E., "Active flow control activities at NASA Langley," *2nd AIAA Flow Control Conference*, 2004.

[15] Van Zante, D. E., Collier, F., Orton, A., Khalid, S. A., Wojno, J. P., and Wood, T. H., "Progress in open rotor propulsors: The FAA/GE/NASA open rotor test campaign," *The Aeronautical Journal*, Vol. 118, 2014, pp. 1181–1213.

[16] Hughes, C., "Geared turbofan technology," *NASA Environmentally Responsible Aviation Project. Green Aviation Summit. NASA Ames Research Center*, 2010.

[17] Liebeck, R., Page, M., and Rawdon, B., "Blended-wing-body subsonic commercial transport," *AIAA paper*, Vol. 438, 1998.

[18] Gundlach, J. F., Philippe-André, Té, trault, Gern, F. H., Nagshineh-Pour, A. H., Ko, A., Schetz, J. A., Mason, W. H., Kapania, R. K., et al., "Conceptual design studies of a strut-braced wing transonic transport," *Journal of aircraft*, Vol. 37, No. 6, 2000, pp. 976–983.

[19] Gur, O., Bhatia, M., Mason, W. H., Schetz, J. A., Kapania, R. K., and Nam, T., "Development of a framework for truss-braced wing conceptual MDO," *Structural and Multidisciplinary Optimization*, Vol. 44, No. 2, 2011, pp. 277–298.

[20] Mavris, D. N., Delaurentis, D. A., Bandte, O., and Hale, M. A., "A Stochastic Approach to Multi-disciplinary Aircraft Analysis and Design 36th Aerospace Sciences Meeting & Exhibit," *36th AIAA Aerospace Sciences Meeting*, American Institute of Aeronautics and Astronautics, 1998.

[21] Roskam, J., *Airplane Design Part VIII: Airplane Cost Estimation Design Development and Manufacturing and Operating*, Design Analysis & Research, 2002.

[22] Raymer, D. P., *Aircraft design: a conceptual approach*, American Institute of Aeronautics and Astronautics, 1989.

[23] Forrester, A., Sobester, D. A., and Keane, A., *Engineering Design via Surrogate Modelling: A Practical Guide*, John Wiley & Sons, 2008.

[24] Shah, J. and Hazelrigg, H., "Research opportunities in engineering design," *NSF Strategic Planning Workshop, Final Report*, 1996.

[25] Booker, J. and Ross, T., "An evolution of uncertainty assessment and quantification," *Scientia Iranica*, Vol. 18, No. 3, Jun 2011, pp. 669–676.

[26] Nikolaidis, E., Ghiocel, D. M., and Singhal, S., *Engineering Design Reliability Handbook*, CRC Press, 2004.

[27] de Rocquigny, E., Devictor, N., and Tarantola, S., *Uncertainty in Industrial Practice: A Guide to Quantitative Uncertainty Management*, John Wiley & Sons, 2008.

[28] Thunnissen, D., "Uncertainty classification for the design and development of complex systems," *Proceedings of the 3rd Annual Predictive Methods Conference, Veros Software*, 2003.

[29] Kirby, M. R. and Mavris, D. N., "Forecasting Technology Uncertainty in Preliminary Aircraft Design," *SAE Technical Paper*, Oct 1999.

[30] Kirby, M. R., *A methodology for technology identification, evaluation, and selection in conceptual and preliminary aircraft design.*, Doctoral dissertation, Georgia Institute of Technology, 2001.

[31] Oberkampf, W. and DeLand, S., "Error and uncertainty in modeling and simulation," *Reliability Engineering & System Safety*, Vol. 75, 2002, pp. 333–357.

[32] Soban, D. S. and Mavris, D. N., "Assessing the Impact of Technology on Aircraft Systems Using Technology Impact Forecasting," *Journal of Aircraft*, Vol. 50, No. 5, sep 2013, pp. 1380–1393.

[33] de Weck, O. L., "Feasibility of a 5x speedup in system development due to meta design," *ASME 2012 International Design Engineering Technical Conferences and Computers and Information in Engineering Conference*, American Society of Mechanical Engineers, 2012, pp. 1105–1110.

[34] Van der Velden, A., Koch, P., Devanathan, S., Haan, J., Naehring, D., and Fox, D., "Probabilistic certificate of correctness for cyber physical systems," *ASME 2012 International Design Engineering Technical Conferences and Computers and Information in Engineering Conference*, American Society of Mechanical Engineers, 2012, pp. 1043–1054.

[35] Van der Velden, A., Malik, K., Hortig, N., and Naehring, D., "The probabilistic certificate of correctness metric for early stage virtual prototype verification and validation," *NAFEMS 2013 World Congress, Salzburg, Austria*, 2013.

[36] Forsberg, K. and Mooz, H., "Proceedings of the First Annual NCOSE Conference," 2000.

[37] Ross, T., Booker, J., and Montoya, A., "New developments in uncertainty assessment and uncertainty management," *Expert Systems with Applications*, Vol. 40, No. 3, Feb 2013, pp. 964–974.

[38] Montgomery, D. C. and Runger, G. C., *Applied statistics and probability for engineers*, John Wiley & Sons, 6th ed., 2010.

[39] Dubois, D. and Prade, H., *Possibility theory*, John Wiley & Sons, Inc., 1999.

[40] Dempster, A. P., "Upper and lower probabilities induced by a multivalued mapping," *The annals of mathematical statistics*, 1967, pp. 325–339.

[41] Joslyn, C. and Booker, J. M., "Generalized information theory for engineering modeling and simulation," *Engineering Design Reliability Handbook*, Vol. 9, 2004, pp. 1–40.

[42] Kurowicka, D. and Cooke, R. M., *Uncertainty analysis with high dimensional dependence modelling*, John Wiley & Sons, 2006.

[43] Tarantola, A., *Inverse problem theory and methods for model parameter estimation*, SIAM, 2005.

[44] Saltelli, A., Ratto, M., Andres, T., Campolongo, F., Cariboni, J., Gatelli, D., Saisana, M., and Tarantola, S., *Global Sensitivity Analysis: The Primer*, John Wiley & Sons, 2008.

[45] Cacuci, D. G., *Sensitivity & Uncertainty Analysis, Volume 1: Theory, Volume 1*, CRC Press, 2003.

[46] Dantzig, G. B., "Linear Programming under Uncertainty," *Management Science*, apr 1955.

[47] Freund, R. J., "The Introduction of Risk into a Programming Model," *Econometrica*, Vol. 24, No. 3, jul 1956, pp. 253–263.

[48] Tong, Y., "Literature review on aircraft structural risk and reliability analysis," Tech. rep., DSTO Aeronautical and Maritime Research Laboratory, 2001.

[49] Frangopol, D. M. and Maute, K., "Life-cycle reliability-based optimization of civil and aerospace structures," *Computers & Structures*, Vol. 81, No. 7, apr 2003, pp. 397–410.

[50] Padula, S. L., Gumbert, C. R., and Li, W., "Aerospace applications of optimization under uncertainty," *Optimization and Engineering*, Vol. 7, No. 3, sep 2006, pp. 317–328.

[51] Long, M. W. and Narciso, J. D., "Probabilistic Design Methodology for Composite Aircraft Structures." Tech. rep., DTIC Document, jun 1999.

[52] Dodson, M. and Parks, G. T., "Robust aerodynamic design optimization using polynomial chaos," *Journal of Aircraft*, Vol. 46, No. 2, 2009, pp. 635–646.

[53] Padulo, M., Campobasso, M. S., and Guenov, M. D., "Novel Uncertainty Propagation Method for Robust Aerodynamic Design," *AIAA Journal*, Vol. 49, No. 3, mar 2011, pp. 530–543.

[54] Pettit, C., "Uncertainty quantification in aeroelasticity: recent results and research challenges," *Journal of Aircraft*, Vol. 41, No. 5, 2004.

[55] Lew, J.-S. and Juang, J.-N., "Robust Generalized Predictive Control with Uncertainty Quantification," *Journal of Guidance, Control, and Dynamics*, Vol. 35, No. 3, may 2012, pp. 930–937.

[56] Yeh, H. H., Banda, S. S., Heise, S. A., and Bartlett, A. C., "Robust control design with real-parameter uncertainty and unmodeled dynamics," *Journal of Guidance, Control, and Dynamics*, Vol. 13, No. 6, nov 1990, pp. 1117–1125.

[57] DeLaurentis, D. A. and Mavris, D. N., "Uncertainty modeling and management in multidisciplinary analysis and synthesis," *AIAA Aerospace Sciences Meeting, Paper No. AIAA-2000–422*, 2000.

[58] Allaire, D. and Willcox, K., "Surrogate Modeling for Uncertainty Assessment with Application to Aviation Environmental System Models," *AIAA Journal*, Vol. 48, No. 8, aug 2010, pp. 1791–1803.

[59] Thunnissen, D., *Propagating and mitigating uncertainty in the design of complex multidisciplinary systems*, Ph.D. thesis, California Institute of Technology, 2005.

[60] Yao, W., Guo, J., Chen, X., and Van Tooren, M., "Utilizing uncertainty multidisciplinary design optimization for conceptual design of space systems," *8th Annual Conference on Systems Engineering Research, CSER 2010, Hoboken, NJ, USA*, 2010.

[61] Yao, W., Chen, X., Luo, W., van Tooren, M., and Guo, J., "Review of uncertainty-based multidisciplinary design optimization methods for aerospace vehicles," *Progress in Aerospace Sciences*, Vol. 47, No. 6, aug 2011, pp. 450–479.

[62] Lu, S., Elmaraghy, W., Schuh, G., and Wilhelm, R., "A scientific foundation of collaborative engineering," *CIRP Annals - Manufacturing Technology*, Vol. 56, No. 1, 2007, pp. 605–634.

[63] Tseng, M. M., Kjellberg, T., and Lu, S. C.-Y., "Design in the New e-Commerce Era," *CIRP Annals - Manufacturing Technology*, Vol. 52, No. 2, jan 2003, pp. 509–519.

[64] "Management Idea: Outsourcing," The Economist, March 19, 2009.

[65] Monell, D. W. and Piland, W. M., "Aerospace systems design in NASA's collaborative engineering environment," *Acta Astronautica*, Vol. 47, No. 2, 2000, pp. 255–264.

[66] Rumsey, C. L., Gatski, T., Sellers III, W., Vasta, V., and Viken, S., "Summary of the 2004 computational fluid dynamics validation workshop on synthetic jets," *AIAA Journal*, Vol. 44, No. 2, 2006, pp. 194–207.

[67] Keane, A. and Nair, P., *Computational Approaches for Aerospace Design: The Pursuit of Excellence*, John Wiley & Sons, 2005.

[68] Ackoff, R. L., *Redesigning the Future: Systems Approach to Societal Problems*, John Wiley & Sons Inc, 1st ed., 1974.

[69] Sobieszczanski-sobieski, J., "Sensitivity of Complex , Internally Coupled Systems," *AIAA Journal*, Vol. 28, No. 1, 1990, pp. 153–160.

[70] Sobieszczanski-Sobieski, J., "Multidisciplinary design optimization: an emerging new engineering discipline," *Advances in Structural Optimization*, Springer Netherlands, 1995, pp. 483–496.

[71] Nicolai, L. and Carichner, G., *Fundamentals of aircraft and airship design*, American Institute of Aeronautics and Astronautics, Reston VA, 2010.

[72] Moir, I. and Seabridge, A., *Aircraft Systems: Mechanical, Electrical, and Avionics Subsystems Integration*, John Wiley & Sons, Ltd, 3rd ed., 2008.

[73] Schmit, L. A., "Structural synthesis 1959-1969 – A decade of progress," *Recent Advances in Matrix Methods of Structural Analysis and Design Seminar*, Univ. of Alabama Press, United States, 1971.

[74] Schmit, L. A., "Structural synthesis: precursor and catalyst," Tech. rep., NASA. Langley Research Center Recent Experiences in Multidisciplinary Analysis and Optimization, 1984.

[75] Haftka, R. T., "Automated Procedure for Design of Wing Structures to Satisfy Strength and Flutter Requirements," Tech. rep., TN D-7264, NASA Langley Research Center, Hampton, VA, 1973.

[76] Haftka, R. T., "Optimization of flexible wing structures subject to strength and induced drag constraints," *AIAA Journal*, Vol. 15, No. 8, 1977, pp. 1101–1106.

[77] Haftka, R. T. and Shore, C. P., "Approximate Methods for Combined Thermal/Structural Design," Tech. rep., TP-1428, NASA, 1979.

[78] Green, J. A., "Aeroelastic tailoring of aft-swept high-aspect-ratio composite wings," *Journal of Aircraft*, Vol. 24, No. 11, nov 1987, pp. 812–819.

[79] Grossman, B., Haftka, R. T., Sobieszczanski-Sobieski, J., Kao, P.-J., Polen, D. M., and Rais-Rohani, M., "Integrated aerodynamic-structural design of a transport wing," *Journal of Aircraft*, Vol. 27, No. 12, dec 1990, pp. 1050–1056.

[80] Livne, E., "Integrated Aeroservoelastic Optimization: Status and Direction," *Journal of Aircraft*, Vol. 36, No. 1, jan 1999, pp. 122–145.

[81] Kroo, I., Altus, S., Braun, R., Gage, P., and Sobieski, I., "Multidisciplinary optimization methods for aircraft preliminary design," *AIAA paper 4325*, 1994, pp. 1994.

[82] Antoine, N. E. and Kroo, I. M., "Framework for aircraft conceptual design and environmental performance studies," *AIAA journal*, Vol. 43, No. 10, 2005, pp. 2100–2109.

[83] Henderson, R. P., Martins, J., and Perez, R. E., "Aircraft conceptual design for optimal environmental performance," *Aeronautical Journal*, Vol. 116, No. 1175, 2012, pp. 1–22.

[84] Gur, O., Bhatia, M., Schetz, J. A., Mason, W. H., Kapania, R. K., and Mavris, D. N., "Design optimization of a truss-braced-wing transonic transport aircraft," *Journal of aircraft*, Vol. 47, No. 6, 2010, pp. 1907–1917.

[85] Zink, P. S., DeLaurentis, D., Hale, M., Volovoi, V. V., Schrage, D. P., Craig, J., Fulton, R. E., Mistree, F., Mavris, D. N., Chen, W., and Others, "New approaches to high speed civil transport multidisciplinary design and optimization," *Aerospace Conference Proceedings, 2000 IEEE*, Vol. 1, IEEE, 2000, pp. 355–369.

[86] DeLaurentis, D. A., Cesnik, C. E. S., Lee, J.-M., Mavris, D. N., and Schrage, D. P., "A new approach to integrated wing design in conceptual synthesis and optimization," *Proceedings of the 6th AIAA. NASA/ISSMO Symposium on Multidisciplinary Analysis and Optimization*, 1996.

[87] de Weck, O., Agte, J., Sobieszczanski-Sobieski, J., Arendsen, P., Morris, A., and Spieck, M., "State-of-the-Art and Future Trends in Multidisciplinary Design Optimization," *48th AIAA/ASME/ASCE/AHS/ASC Structures, Structural Dynamics, and Materials Conference*, Structures, Structural Dynamics, and Materials and Co-located Conferences, apr 2007.

[88] Gavel, H., Ölvander, J., and Krus, P., "Optimal Conceptual Design of Aircraft Fuel Transfer Systems," *Journal of Aircraft*, Vol. 43, No. 5, sep 2006, pp. 1334–1340.

[89] Antoine, N. E. and Kroo, I. M., "Aircraft Optimization for Minimal Environmental Impact," *Journal of Aircraft*, Vol. 41, No. 4, jul 2004, pp. 790–797.

[90] Rallabhandi, S. K. and Mavris, D. N., "Aircraft Geometry Design and Optimization for Sonic Boom Reduction," *Journal of Aircraft*, Vol. 44, No. 1, jan 2007, pp. 35–47.

[91] Kirby, M. and Mavris, D., "The Environmental Design Space," *26th Congress of International Council of the Aeronautical Sciences*, Anchorage, Alaska, USA, 2008.

[92] Agte, J., Weck, O., Sobieszczanski-Sobieski, J., Arendsen, P., Morris, A., and Spieck, M., "MDO: assessment and direction for advancement – an opinion of one international group," *Structural and Multidisciplinary Optimization*, Vol. 40, No. 1-6, apr 2009, pp. 17–33.

[93] German, B. and Daskilewicz, M., "An MDO-Inspired Systems Engineering Perspective for the "Wicked" Problem of Aircraft Conceptual Design," *9th AIAA Aviation Technology, Integration, and Operations Conference (ATIO)*, Aviation Technology, Integration, and Operations (ATIO) Conferences, sep 2009.

[94] Sobieszczanski-Sobieski, J. and Haftka, R., "Multidisciplinary aerospace design optimization: survey of recent developments," *Structural optimization*, Vol. 14, No. 1, aug 1997, pp. 1–23.

[95] Helton, J. C. and Burmaster, D. E., "Guest editorial: treatment of aleatory and epistemic uncertainty in performance assessments for complex systems," *Reliability Engineering & System Safety*, Vol. 54, No. 2-3, nov 1996, pp. 91–94.

[96] Hoffman, F. O. and Hammonds, J. S., "Propagation of uncertainty in risk assessments: the need to distinguish between uncertainty due to lack of knowledge and uncertainty due to variability." *Risk analysis : an official publication of the Society for Risk Analysis*, Vol. 14, No. 5, oct 1994, pp. 707–12.

[97] Roy, C. J. and Oberkampf, W. L., "A complete framework for verification, validation, and uncertainty quantification in scientific computing," *48th AIAA Aerospace Sciences Meeting Including the New Horizons Forum and Aerospace Exposition*, 2010, pp. 4–7.

[98] Dequech, D., "Fundamental Uncertainty and Ambiguity," *Eastern Economic Journal*, Vol. 26, No. 1, 2000, pp. 41–60.

[99] Luce, R. D. and Raiffa, H., *Games and decisions: Introduction and critical surveys*, Wiley New York, NY., 1957.

[100] Morgan, M. G., Henrion, M., and Small, M., *Uncertainty: a guide to dealing with uncertainty in quantitative risk and policy analysis*, Cambridge University Press, 1st ed., 1992.

[101] Serway, R., Moses, C., and Moyer, C., *Modern physics*, Cengage Learning, 2004.

[102] Zhou, K., Doyle, J. C., Glover, K., and Others, *Robust and optimal control*, Vol. 40, Prentice hall New Jersey, 1996.

[103] Ayyub, B. M., *Uncertainty modeling and analysis in civil engineering*, CRC Press, 1997.

[104] Otto, K. N. and Antonsson, E. K., "Tuning parameters in engineering design," *Journal of Mechanical Design*, Vol. 115, No. 1, 1993, pp. 14–19.

[105] DeLaurentis, D. A., *A probabilistic approach to aircraft design emphasizing stability and control uncertainties*, Doctoral dissertation, Georgia Institute of Technology, 1998.

[106] Kolmogorov, A., *Foundations of the Theory of Probability*, Oxford, England: Chelsea Publishing Co., 1950.

[107] Papoulis, A., "Bayes' theorem in statistics and Bayes' theorem in statistics (reexamined)," *Probability, random variables, and stochastic processes. 2nd ed. New York, NY: McGraw-Hill*, 1984, pp. 38–114.

[108] Bishop, C. M., *Pattern Recognition and Machine Learning*, Springer-Verlag New York, Inc., 1st ed., 2006.

[109] Gelman, A., Carlin, J. B., Stern, H. S., and Rubin, D. B., *Bayesian Data Analysis*, CRC Press, 2003.

[110] Wang, P., Youn, B. D., Xi, Z., and Kloess, A., "Bayesian reliability analysis with evolving, insufficient, and subjective data sets," *Journal of Mechanical Design*, Vol. 131, No. 11, 2009, pp. 111008(1)–111008(11).

[111] Shafer, G. and Others, *A mathematical theory of evidence*, Vol. 1, Princeton university press, 1976.

[112] Zadeh, L., "Fuzzy sets as a basis for a theory of possibility," *Fuzzy sets and systems*, Vol. 1, No. 1, 1978, pp. 3–28.

[113] Rao, S. S. and Berke, L., "Analysis of uncertain structural systems using interval analysis," *AIAA journal*, Vol. 35, No. 4, 1997, pp. 727–735.

[114] Saltelli, A., Tarantola, S., and Campolongo, F., "Sensitivity analysis as an ingredient of modeling," *Statistical Science*, Vol. 15, No. 4, 2000, pp. 377–395.

[115] Sobol', I. M., "On sensitivity estimation for nonlinear mathematical models," *Matematicheskoe Modelirovanie*, Vol. 2, No. 1, 1990, pp. 112–118.

[116] Montgomery, D. C., Peck, E. A., and Vining, G. G., *Introduction to linear regression analysis*, John Wiley & Sons, 5th ed., 2012.

[117] Hastings, W. K., "Monte Carlo sampling methods using Markov chains and their applications," *Biometrika*, Vol. 57, No. 1, apr 1970, pp. 97–109.

[118] Melchers, R., "Importance sampling in structural systems," *Structural Safety*, Vol. 6, No. 1, jul 1989, pp. 3–10.

[119] Bucher, C. G., "Adaptive sampling – an iterative fast Monte Carlo procedure," *Structural Safety*, Vol. 5, No. 2, jun 1988, pp. 119–126.

[120] Haldar, A. and Mahadevan, S., *Probability, reliability, and statistical methods in engineering design*, John Wiley & Sons, Incorporated, 2000.

[121] Rosenblatt, M., "Remarks on a multivariate transformation," *The annals of mathematical statistics*, Vol. 23, No. 3, 1952, pp. 470–472.

[122] Evans, D. H., "An Application of Numerical Integration Techniques to Statistical Tolerancing," *Technometrics*, Vol. 9, No. 3, 1967, pp. 441–456.

[123] Lee, S. H. and Kwak, B. M., "Response surface augmented moment method for efficient reliability analysis," *Structural Safety*, Vol. 28, No. 3, jul 2006, pp. 261–272.

[124] Xiong, F., Greene, S., Chen, W., Xiong, Y., and Yang, S., "A new sparse grid based method for uncertainty propagation," *Structural and Multidisciplinary Optimization*, Vol. 41, No. 3, oct 2009, pp. 335–349.

[125] Eldred, M., "Recent Advances in Non-Intrusive Polynomial Chaos and Stochastic Collocation Methods for Uncertainty Analysis and Design," *50th AIAA/ASME/ASCE/AHS/ASC Structures, Structural Dynamics, and Materials Conference*, 2009.

[126] Mathelin, L. and Hussaini, M. Y., "A Stochastic Collocation Algorithm for Uncertainty Analysis," *NASA Scientific and Technical Information (STI), CR-2003-212153*, 2003.

[127] Myers, R. H., Montgomery, D. C., and Anderson-Cook, C. M., *Response surface methodology: process and product optimization using designed experiments*, John Wiley & Sons, 2009.

[128] Taguchi, G., Elsayed, E. A., and Hsiang, T. C., *Quality engineering in production systems*, McGraw-Hill New York, 1989.

[129] Park, G. J., Lee, T. H., Lee, K. H., and Hwang, K. H., "Robust design: an overview," *AIAA journal*, Vol. 44, No. 1, 2006, pp. 181–191.

[130] Padmanabhan, D., *Reliability-based optimization for multidisciplinary system design*, Doctoral dissertation, University of Notre Dame, 2003.

[131] Agarwal, H., *Reliability based design optimization: formulations and methodologies*, Doctoral dissertation, University of Notre Dame, 2004.

[132] Du, X. and Chen, W., "Sequential optimization and reliability assessment method for efficient probabilistic design," *Journal of Mechanical Design*, Vol. 126, No. 2, 2004, pp. 225–233.

[133] Zou, T. and Mahadevan, S., "A direct decoupling approach for efficient reliability-based design optimization," *Structural and Multidisciplinary Optimization*, Vol. 31, No. 3, 2006, pp. 190–200.

[134] Agarwal, H., Renaud, J. E., Lee, J. C., and Watson, L. T., "A unilevel method for reliability based design optimization," *Proceedings of 45th AIAA/ASME/ASCE/AHS/ASC Structures, Structural Dynamics and Materials Conference*, 2004.

[135] Chen, X., Hasselman, T. K., Neill, D. J., et al., "Reliability based structural design optimization for practical applications," *Proceedings of the 38th AIAA/ASME/ASCE/AHS/ASC structures, structural dynamics, and materials conference*, 1997, pp. 2724–2732.

[136] Agarwal, H. and Renaud, J. E., "New decoupled framework for reliability-based design optimization," *AIAA journal*, Vol. 44, No. 7, 2006, pp. 1524–1531.

[137] Du, X., Guo, J., and Beeram, H., "Sequential optimization and reliability assessment for multidisciplinary systems design," *Structural and Multidisciplinary Optimization*, Vol. 35, No. 2, 2008, pp. 117–130.

[138] McAllister, C. D. and Simpson, T. W., "Multidisciplinary Robust Design Optimization of an Internal Combustion Engine," *Journal of Mechanical Design*, Vol. 125, No. 1, mar 2003, pp. 124.

[139] Gu, X., Renaud, J., and Penninger, C., "Implicit Uncertainty Propagation for Robust Collaborative Optimization," *Journal of Mechanical Design*, Vol. 128, No. 4, 2006, pp. 1001–1013.

[140] Liu, H. and Fan, W., "A robust collaborative optimization method under multidisciplinary uncertainty," *The Sixth International Symposium on Operations Research and Its Applications (ISORA)*, 2006.

[141] Xiong, F., Sun, G., Xiong, Y., and Yang, S., "A moment-matching robust collaborative optimization method," *Journal of Mechanical Science and Technology*, Vol. 28, No. September, 2014, pp. 1365–1372.

[142] Ghosh, S., Lee, C., and Mavris, D. N., "Covariance Matching Collaborative Optimization for Uncertainty-based Multidisciplinary Aircraft Design," *15th AIAA/ISSMO Multidisciplinary Analysis and Optimization Conference*, 2014.

[143] Wang, W., Fan, W., T, C., and Y, Y., "Robust Collaborative Optimization Method Based on Dual-response Surface," *Chinese Journal of Mechanical Engineering*, Vol. 22, No. 2, 2009, pp. 169–176.

[144] Padmanabhan, D. and Batill, S., "Reliability based optimization using approximations with applications to multi-disciplinary system design," *40th AIAA Aerospace Sciences Meeting & Exhibit*, 2002.

[145] Yao, W., Chen, X., Wei, Y., and Gao, S., "A game theory based composite subspace uncertainty multidisciplinary design optimization procedure," *Eighth world congress on structural and multidisciplinary optimization*, 2009.

[146] Kokkolaras, M., Mourelatos, Z. P., and Papalambros, P. Y., "Design optimization of hierarchically decomposed multilevel systems under uncertainty," *Journal of Mechanical Design*, Vol. 128, No. 2, 2005, pp. 503–508.

[147] Liu, H., Chen, W., Kokkolaras, M., Papalambros, P. Y., and Kim, H. M., "Probabilistic Analytical Target Cascading: A Moment Matching Formulation for Multilevel Optimization Under Uncertainty," *Journal of Mechanical Design*, Vol. 128, No. 4, 2006, pp. 991.

[148] Xiong, F., Yin, X., Chen, W., and Yang, S., "Enhanced probabilistic analytical target cascading with application to multiscale design," *Engineering Optimization*, Vol. 42, No. 6, 2010, pp. 581–592.

[149] Koller, D. and Friedman, N., *Probabilistic graphical models: principles and techniques*, MIT press, 2009.

[150] Jensen, F. V., *Introduction to Bayesian Networks*, Springer-Verlag New York, Inc., Secaucus, NJ, USA, 1st ed., 1996.

[151] Dawid, A. P., "Conditional Independence for Statistical Operations," *The Annals of Statistics*, Vol. 8, No. 3, 1980, pp. 598–617.

[152] Sankararaman, S. and Mahadevan, S., "Likelihood-Based Approach to Multidisciplinary Analysis Under Uncertainty," *Journal of Mechanical Design*, Vol. 134, No. 3, 2012, pp. 031008.

[153] Cha, S., "Comprehensive survey on distance/similarity measures between probability density functions," *International Journal of Mathematical Models and Methods in Applied Sciences*, Vol. 1, No. 4, 2007, pp. 300–307.

[154] Hajela, P., Bloebaum, C. L., and Sobieszczanski-Sobieski, J., "Application of global sensitivity equations in multidisciplinary aircraft synthesis," *Journal of Aircraft*, Vol. 27, No. 12, 1990, pp. 1002–1010.

[155] Fung, R. M. and Chang, K.-C., "Weighing and Integrating Evidence for Stochastic Simulation in Bayesian Networks," *Proceedings of the Fifth Annual Conference on Uncertainty in Artificial Intelligence*, North-Holland Publishing Co., 1990, pp. 209–220.

[156] Yuan, C. and Druzdzel, M. J., "Importance sampling algorithms for Bayesian networks: Principles and performance," *Mathematical and Computer Modelling*, Vol. 43, No. 9, 2006, pp. 1189–1207.

[157] Henrion, M., "Propagating Uncertainty in Bayesian Networks by Probabilistic Logic Sampling," *Uncertainty in Artificial Intelligence 2 Annual Conference on Uncertainty in Artificial Intelligence (UAI-86)*, Elsevier Science, Amsterdam, NL, 1986, pp. 149–163.

[158] Stoer, J. and Bulirsch, R., *Introduction to numerical analysis*, Springer Science & Business Media, 2013.

[159] Neal, R. M., "Slice Sampling," *The Annals of Statistics*, Vol. 31, No. 3, 2003, pp. 705–741.

[160] Efraimidis, P. S. and Spirakis, P. G., "Weighted random sampling with a reservoir," *Information Processing Letters*, Vol. 97, No. 5, 2006, pp. 181–185.

[161] Helton, J., Johnson, J., Sallaberry, C., and Storlie, C., "Survey of sampling-based methods for uncertainty and sensitivity analysis," *Reliability Engineering & System Safety*, Vol. 91, No. 10-11, oct 2006, pp. 1175–1209.

[162] Kraskov, A., Stögbauer, H., and Grassberger, P., "Estimating mutual information," *Phys. Rev. E*, Vol. 69, Jun 2004, pp. 066138.

[163] Amaral, S., Allaire, D., and Willcox, K. E., "A Decomposition Approach to Uncertainty Analysis of Multidisciplinary Systems," *12th AIAA Aviation Technology, Integration, and Operations (ATIO) Conference*, 2012.

[164] MATLAB, *9.0.0 (R2016a)*, The MathWorks Inc., Natick, Massachusetts, 2016.

[165] Du, X. and Chen, W., "Efficient uncertainty analysis methods for multidisciplinary robust design," *AIAA journal*, Vol. 40, No. 3, 2002, pp. 545–552.

[166] Liang, C., *Multidisciplinary Analysis and Optimization under Uncertainty*, Ph.D. thesis, Vanderbilt University, 2016.

[167] Scholkopf, B. and Smola, A. J., *Learning with kernels: support vector machines, regularization, optimization, and beyond*, MIT press, 2001.

[168] Dobson, A. J. and Barnett, A., *An introduction to generalized linear models*, CRC press, 2008.

[169] Torenbeek, E., "Airplane weight and balance," *Synthesis of Subsonic Airplane Design: An introduction to the preliminary design of subsonic general aviation and transport aircraft, with emphasis on layout, aerodynamic design, propulsion and performance*, Springer Netherlands, 1982, pp. 263–302.

[170] Gilbert, B. J. and Koenker, R., "Asymptotic Theory of Least Absolute Error Regression," *Journal of the American Statistical Association*, Vol. 73, No. 363, apr 1978, pp. 618–622.

[171] Koenker, R. and Bassett, G., "Regression Quantiles," *Econometrica*, Vol. 46, No. 1, 1978, pp. 33–50.

[172] Koenker, R., *Quantile Regression*, Cambridge University Press, 2005.

[173] Yu, K., Lu, Z., and Stander, J., "Quantile regression: Applications and current research areas," *Journal of the Royal Statistical Society Series D: The Statistician*, Vol. 52, No. 3, 2003, pp. 331–350.

[174] Koenker, R. W. and D'Orey, V., "Algorithm AS 229: Computing Regression Quantiles," *Journal of the Royal Statistical Society. Series C (Applied Statistics)*, Vol. 36, No. 3, 1987, pp. 383–393.

[175] Portnoy, S. and Koenker, R., "The Gaussian hare and the Laplacian tortoise: computability of squared-error versus absolute-error estimators," *Statistical Science*, Vol. 12, No. 4, nov 1997, pp. 279–300.

[176] Sánchez, L. B. and Lachos, V. H., "Likelihood Based Inference for Quantile Regression Using the Asymmetric Laplace Distribution," *Journal of Statistical Computation and Simulation*, Vol. 81, 2013, pp. 1565–1578.

[177] Kottas, A. and Krnjajic, M., "Bayesian Semiparametric Modelling in Quantile Regression," *Scandinavian Journal of Statistics*, Vol. 36, No. 2, jun 2009, pp. 297–319.

[178] Kozumi, H. and Kobayashi, G., "Gibbs sampling methods for Bayesian quantile regression," *Journal of Statistical Computation and Simulation*, Vol. 81, No. 11, nov 2011, pp. 1565–1578.

[179] Yu, K. and Moyeed, R. A., "Bayesian quantile regression," *Statistics & Probability Letters*, Vol. 54, No. 4, oct 2001, pp. 437–447.

[180] Kottas, A. and Gelfand, A. E., "Bayesian Semiparametric Median Regression Modeling," *Journal of the American Statistical Association*, Vol. 96, No. 456, 2001, pp. 1458–1468.

[181] Cannon, A. J., "Quantile regression neural networks: Implementation in R and application to precipitation downscaling," *Computers & Geosciences*, Vol. 37, No. 9, sep 2011, pp. 1277–1284.

[182] Boukouvalas, A., Barillec, R., and Cornford, D., "Gaussian Process Quantile Regression using Expectation Propagation," *29th International Conference on Machine Learning (ICML 2012)*, jun 2012.

[183] Thompson, P., Cai, Y., Moyeed, R., Reeve, D., and Stander, J., "Bayesian nonparametric quantile regression using splines," *Computational Statistics & Data Analysis*, Vol. 54, No. 4, apr 2010, pp. 1138–1150.

[184] Roger Koenker, P. N., "Inequality Constrained Quantile Regression," *Sankhyā: The Indian Journal of Statistics (2003-2007)*, Vol. 67, No. 2, 2005, pp. 418–440.

[185] Chernozhukov, V., Fernández-Val, I., and Galichon, A., "Quantile and probability curves without crossing," *Econometrica*, Vol. 78, No. 3, 2010, pp. 1093–1125.

[186] Quiñonero-Candela, J., Rasmussen, C. E., Sinz, F., Bousquet, O., and Schölkopf, B., "Evaluating predictive uncertainty challenge," *Machine Learning Challenges. Evaluating Predictive Uncertainty, Visual Object Classification, and Recognising Tectual Entailment*, Springer, 2006, pp. 1–27.

[187] Cook, J. D., "Determining distribution parameters from quantiles," *UT MD Anderson Cancer Center Department of Biostatistics Working Paper Series - Working Paper 55, Houston, TX*, 2010.

[188] Bouyé, E., Durrleman, V., Nikeghbali, A., Riboulet, G., and Roncalli, T., "Copulas for finance- A reading guide and some applications," *Goupe de Recherche Opérationnelle, Crédit Lyonnais, Lyon, Available at SSRN: https://ssrn.com*, 2000.

[189] Cherubini, U., Luciano, E., and Vecchiato, W., *Copula methods in finance*, John Wiley & Sons, 2004.

[190] Rui, C. and Pu, G., "Convertible bond pricing model based on copula approach," *International Conference on Management Science & Engineering 18th Annual Conference Proceedings*, IEEE, 2011.

[191] Frees, E. W. and Valdez, E. A., "Understanding relationships using copulas," *North American Actuarial Journal*, Vol. 2, No. 1, 1998, pp. 1–25.

[192] Frees, E. W. and Wang, P., "Credibility using copulas," *North American Actuarial Journal*, Vol. 9, No. 2, 2005, pp. 31–48.

[193] Wang, W. and Wells, M. T., "Model selection and semiparametric inference for bivariate failure-time data," *Journal of the American Statistical Association*, Vol. 95, No. 449, 2000, pp. 62–72.

[194] Escarela, G. and Carriere, J. F., "Fitting competing risks with an assumed copula," *Statistical Methods in Medical Research*, Vol. 12, No. 4, 2003, pp. 333–349.

[195] Huang, M., Wang, Q., Li, Y., and Ao, L., "An approach for improvement of avionics reliability assessment based on copula theory," *9th International Conference on Reliability, Maintainability and Safety (ICRMS)*, IEEE, 2011.

[196] Noh, Y., Choi, K. K., and Du, L., "Reliability-based design optimization of problems with correlated input variables using a Gaussian Copula," *Structural and Multidisciplinary Optimization*, Vol. 38, No. 1, jun 2008, pp. 1–16.

[197] Zhang, Y. and Lam, J. S. L., "A Copula Approach in the Point Estimate Method for Reliability Engineering," *Quality and Reliability Engineering International*, Vol. 32, No. 4, 2016, pp. 1501–1508.

[198] Sklar, A. W., *Fonctions de répartition à n dimensions et leurs marges*, Vol. 8, Universit{é} Paris 8, 1959.

[199] Nelsen, R. B., *An Introduction to Copulas*, Springer-Verlag New York, 2006.

[200] Sklar, A., "Random variables, distribution functions, and copulas: a personal look backward and forward," *Distributions with Fixed Marginals and Related Topics, IMS Lecture Notes Monogr. Ser.*, Vol. 28, 1996, pp. 1–14.

[201] Cambanis, S., Huang, S., and Simons, G., "On the theory of elliptically contoured distributions," *Journal of Multivariate Analysis*, Vol. 11, No. 3, 1981, pp. 368–385.

[202] Fang, K.-T., Kotz, S., and Ng, K. W., *Symmetric multivariate and related distributions*, Chapman and Hall, 1990.

[203] Joe, H. and Xu, J. J., "The Estimation Method of Inference Functions for Margins for Multivariate Models," *Technical Report no. 166, Department of Statistics, University of British Columbia*, 1996, pp. 1–21.

[204] Choroś, B., Ibragimov, R., and Permiakova, E., "Copula estimation," *Copula theory and its applications*, Springer, 2010, pp. 77–91.

[205] Akaike, H., "Akaike's Information Criterion," *International Encyclopedia of Statistical Science*, Springer, 2011, pp. 25–25.

[206] Huard, D., Evin, G., and Favre, A.-C., "Bayesian copula selection," *Computational Statistics & Data Analysis*, Vol. 51, No. 2, 2006, pp. 809–822.

[207] Spiegelhalter, D. J., Best, N. G., Carlin, B. P., and Linde, A., "The deviance information criterion: 12 years on," *Journal of the Royal Statistical Society: Series B (Statistical Methodology)*, Vol. 76, No. 3, 2014, pp. 485–493.

[208] Silva, R. D. S. and Lopes, H. F., "Copula, marginal distributions and model selection: A Bayesian note," *Statistics and Computing*, Vol. 18, No. 3, 2008, pp. 313–320.

[209] Spiegelhalter, D. J., Best, N. G., Carlin, B. P., and Van Der Linde, A., "Bayesian measures of model complexity and fit," *Journal of the Royal Statistical Society: Series B (Statistical Methodology)*, Vol. 64, No. 4, 2002, pp. 583–639.

[210] Cleveland, W., *The Elements of Graphing Data*, Hobart Press, 2nd ed., 1994.

[211] Genest, C. and Boies, J.-C., "Detecting Dependence With Kendall Plots," *The American Statistician*, Vol. 57, No. 4, nov 2003, pp. 275–284.

[212] Li, D., Tang, X., Zhou, C., and Phoon, K.-K., "Uncertainty analysis of correlated non-normal geotechnical parameters using Gaussian copula," *Science China Technological Sciences*, Vol. 55, No. 11, 2012, pp. 3081–3089.

[213] Phoon, K.-K. and Ching, J., *Risk and reliability in geotechnical engineering*, CRC Press, 2014.

[214] Altus, T. D., "A response surface methodology for bi-level integrated system synthesis (BLISS)," *Tech. Report, NASA/CR-2002-211652*, 2002.

[215] Hansen, N., "The CMA evolution strategy: a comparing review," *Towards a new evolutionary computation*, Springer, 2006, pp. 75–102.

[216] Sobieszczanski, J., Agte, J. S., and Jr Robert R., S., "Bi-Level Integrated System Synthesis (BLISS)," *AIAA journal*, Vol. 38, No. 1, 2000, pp. 164–172.

[217] Byrd, R. H., Schnabel, R. B., and Shultz, G. A., "A trust region algorithm for nonlinearly constrained optimization," *SIAM Journal on Numerical Analysis*, Vol. 24, No. 5, 1987, pp. 1152–1170.

[218] Braun, R. D. and Kroo, I. M., "Development and application of the collaborative optimization architecture in a multidisciplinary design environment," *ICASE/NADA Langley Workshop on Multidisciplinary Design Optimization: State of the Art*, 1995, pp. 98–116.

[219] L., B. C., Hajela, P., and Sobieszczanski-Sobieski, J., "Non-hierarchic system decomposition in structural optimization," *Engineering Optimization*, Vol. 19, No. 3, may 1992, pp. 171–186.

[220] Sellar, R. S., Batill, S. M., and Renaud, J. E., "Response Surface Based, Concurrent Subspace Optimization For Multidisciplinary System Design," *34th AIAA Aerospace Sciences Meeting and Exhibit*, Vol. 0, 1996, pp. 96–714.

[221] Sobieszczanski -Sobieski, J., Agte, J. S., and Sandusky, R., "Bi-Level Integrated System Synthesis," *AIAA journal*, Vol. 38, No. 1, 2000, pp. 164–172.

[222] Kim, H. M., Michelena, N. F., Papalambros, P. Y., and Jiang, T., "Target Cascading in Optimal System Design," *Journal of Mechanical Design*, Vol. 125, No. 3, 2003, pp. 474.

[223] Tosserams, S., Etman, L. F. P., and Rooda, J. E., "Augmented Lagrangian coordination for distributed optimal design in MDO," *International Journal for Numerical Methods in Engineering*, Vol. 73, No. 13, mar 2008, pp. 1885–1910.

[224] R Core Team, *R: A Language and Environment for Statistical Computing*, R Foundation for Statistical Computing, Vienna, Austria, 2016.

[225] Koenker, R., "Quantreg: quantile regression," *R package version*, Vol. 5, No. 05, 2013.

[226] Higham, N. J., "Computing a nearest symmetric positive semidefinite matrix," *Linear algebra and its applications*, Vol. 103, 1988, pp. 103–118.

VITA

Sayan Ghosh was born and raised in Patna, Bihar, India. He attended his undergraduate school at Indian Institute of Technology, Khargapur, India and received a Bachelor of Technology (B.Tech) degree in Aerospace Engineering in 2007. Thereafter, he worked for General Motors (GM) Technical Center, Bangalore, India as an Aerodynamic Analyst for one year, where he conducted high-fidelity aerodynamics analysis and optimization using Computational Fluid Dynamics (CFD) on new road vehicle concepts. In 2008, he joined the graduate program in Aerospace Engineering at Iowa State University. As a graduate research assistant he conducted research on developing CFD tools to support Multi-University Research Initiative (MURI) on Rotorcraft Brownout. After earning his Master of Science (M.S.) degree in aerospace engineering, he joined Aerospace Systems Design Laboratory (ASDL) at Georgia Tech to continue his graduate studies. As a graduate researcher he conducted research with various sponsors including NASA, Boeing, and Airbus in the area of systems engineering, probabilistic design, and uncertainty quantification and management. He graduated with a Ph.D. in aerospace engineering, with a minor in mathematics, from Georgia Tech in December 2016.